Reversible Addition Fragmentation Chain Transfer (RAFT) of a New Class of pH-Sensitive Monomers and Polymerization Induced Self-Assembly (PISA) in Supercritical Carbon Dioxide

Abdullah Yahya Abdullah Alzahrani, M.Sc. (Hons)

Thesis presented for the qualification of Ph.D. degree
To the National University of Ireland Galway

School of Chemistry

National University of Ireland, Galway
September 2018

Supervisors: Prof. Fawaz Aldabbagh
Dr. Yury Rochev
Head of School: Dr. Patrick O'Leary

Table of Contents

Declaration

I hereby declare that this thesis is my original work, except the solving of X-ray crystal structure of *N*-(hydroxymethyl)azocan-1-ium chloride and *N*-[(azocan-1-yl)methyl]prop-2-enamide hydrochloride by Prof. Patrick McArdle and Dr. Styliana I. Mirallai for preparing crystals of the latter compound for X-ray analysis, and it has been written by me in its entirety. I have duly acknowledged all the sources of information which have been used in the thesis. This thesis has also not been submitted for any degree in any university previously.

Abdullah Yahya Alzahrani

October 2018

Acknowledgments

Firstly, I must thank my supervisor Prof. Fawaz Aldabbagh for giving me the opportunity of doing this PhD and for all his advices and guidance throughout the course of my research: Without his trust and encouragement, none of this would be possible. I wish to thank Dr. Yury Rochev for taking over as official supervisor at NUIG.

I would also like to acknowledge and thank Prof. Per B. Zetterlund (CAMD, UNSW, Australia) for his advice and contribution on future analysis on polymer samples in chapter 3.

I acknowledge the solving of X-ray crystal structure of *N*-(hydroxymethyl)azocan-1-ium chloride and *N*-[(azocan-1-yl)methyl]prop-2-enamide hydrochloride by Prof. Patrick McArdle. I thank Dr. Styliana I. Mirallai for preparing crystals of the latter compound for X-ray analysis. I thank Dr. Benjamin Chalmers and Dr. Styliana I. Mirallai for their advises on the preparations in chapter 1. I thank Gerard Hawkins and Dr. Benjamin A. Chalmers for their advises on polymerization reactions, and other members of the Aldabbagh research group for their friendship.

I wish to thank the Ministry of Education of the Kingdom of Saudi Arabia for financial supporting my PhD.

Finally, I must thank my family, my parents, my brothers and sisters for their continuous support and encouragement.

Abstract

Chapter 1 The traditional thermal Mannich reaction is unsuitable for preparing polymerizable *N*-methylene amino substituted acrylamides and methacrylamides. Herein we provide a facile multi-gram high yield synthesis of these monomeric precursors to stimuli-responsive polymers by addition of acrylamide and methacrylamide onto *in situ* generated or freshly isolated methylene Schiff base (iminium) salts. The synthetic methodology developed in synthesizing building blocks for smart polymers is described in context with the chemical literature. An Experimental section describes gram-scale syntheses of monomers. Parts of this chapter were published in *Organic & Biomolecular Chemistry*, **2018**, *16*, 4108–4116.

Chapter 2 Begins with an introduction to Reversible Addition Fragmentation Chain Transfer (RAFT). The previously elusive *N*-[cycloamino)methyl]acrylamides monomer class prepared in Chapter 1 is subjected to the first controlled/living polymerizations, which gave water-soluble well-defined polyacrylamide triblock copolymers. . An Experimental section describes the RAFT procedures in detail from poly(*N*,*N*-dimethylacrylamide) macro-RAFT. Parts of this chapter were published were published in *J. Polym. Sci., Part A: Polym Chem*. **2017**, *55*, 2123–2128.

Chapter 3 Begins with an introduction to Atom Transfer Radical Polymerization (ATRP) and an overview of the literature on Polymerization Induced Self-Assembly (PISA), and controlled/living dispersion polymerizations in the benign polymerization medium, supercritical carbon dioxide ($scCO_2$). The results and discussion presented are yet to be published; describing the first PISA in $scCO_2$ to give higher order non-spherical objects, namely rods and vesicles. PISA in $scCO_2$ was implemented using ATRP of benzyl methacrylate (BzMA) using a dispersion polymerization from poly(dimethylsiloxane, DMS) bromide macroinitiator. Giant rods and vesicles up to 30 μm in length were produced at the highest degrees of polymerization and the highest solids content.

Abbreviations

AIBN	2,2′-azobis(isobutyronitrile)
ATRP	atom transfer radical polymerization
ARGET	activator regenerated by electron transfer
aq	aqueous
α	fractional monomer conversion
b	block
br	broad
b.p	boiling point
BzMA	Benzyl methacrylate
BMA	*n*-butyl methacrylate
Cl^-	chloride
CP	conventional preparation
Conv.	conversion
CTA	chain transfer agent
CPDB	2-cyanoprop-2-yl dithiobenzoate
CDTPA	4-cyano-4-[(dodecylsulfanylthiocarbonyl)sulfanyl]pentanoic acid
CPDTTC	2-cyano-2-propyldodecyltrithiocarbonate
M	concentration
CRP	controlled radical polymerization
J	coupling constant
J_{crit}	critical degree of polymerization
δ	chemical shift (ppm)
cm	centimeter
^{13}C NMR	carbon- 13 nuclear magnetic resonance
DCM	dichloromethane
DDMAT	2-(dodecylthiocarbonothioylthio)-2-methylpropionic acid
DMA	*N,N*-dimethylacrylamide
DMF	*N,N*-dimethylformamide
DP	degree of polymerization
^oC	degrees centigrade
Dept	distortionless enhancement by polarization transfer

D_2O	deuterium oxide
DMSO	dimethyl sulfoxide
DLS	dynamic light scattering
$CDCl_3$	deuterated chloroform
d	doublet
dd	doublet of doublets
equiv	equivalent
etc	et cetera
Et	ethyl group
e.g.	for example
f	initiator efficiency
g	gram
GPC	gel permeation chromatography
Hz	hertz
HMTETA	1,1,4,7,10,10-Hexamethyltriethylenetetramine
HEMA	2-hydroxyethyl methacrylate
HRMS	High-resolution mass spectrometry
HPMA	2-hydroxypropyl methacrylate
I	initiator
[I]	initiator concentration
$I^{\bullet}$	initiator radical
IR	infrared radiation
inistab	macroinitiator and stabilizer combined
L	liter
LCST	lower critical solution temperature
LDA	lithium diisopropylamide
M	monomer
$[M]_0$	initial concentration of monomer at time = 0
$[M]_t$	monomer concentration at time = t
Me	methyl
MEA	*N*-(2-morpholin-4-ylethyl)acrylamide
mg	milligram
mL	milliliter

μm	micrometer
mm	millimeter
mmol	millimole
M_n	number-average molecular weight
M_n(GPC)	number average molecular weight estimated by GPC
M_n(NMR)	number average molecular weight estimated by NMR
$M_{n,th}$	theoretical number average molecular weight
mol	mole
m.p.	melting point
MPa	megapascal
M	molar
MW	molecular weight
M_W	weight average molecular weight
MWD	molecular weight distribution
MHz	megahertz
M_w/M_n	polydispersity
$Đ$	polydispersity
m	multiple
μg	microgram
m/z	Mass/charge ratio
min	minute
nm	nanometer
NMR	nuclear magnetic resonance
NMP	nitroxide-mediated radical polymerization
NIPAM	*N*-isopropylacrylamide
PDI	polydispersity index
P•	propagating polymer radical
PDMA	poly(dimethyl acrylamide)
PDMS	poly(dimethylsiloxane)
PNIPAM	poly(*N*-isopropylacrylamide)
PNEMAM	poly(*N*-ethylmethacrylamide)
PISA	polymerization induced self-assembly
PMDETA	*N*,*N*,*N'*,*N''*,*N''*-pentamethyldiethylenetriamine

ppm	parts per million
P(St)	poly(styrene)
PEOMA	poly(ethyleneoxide) methyl ether methacrylate macromonomers
PTFE	polytetrafluoroethylene
%	percent or yield
q	quartet
quint	quintet
$R^{\bullet}$	radical
RAFT	reversible addition fragmentation transfer
RDRP	reversible deactivation radical polymerization
R_p	rate of polymerization
R-X	alkyl halide
s	singlet
$scCO_2$	supercritical carbon dioxide
SG1	*N*-*tert*-butyl-*N*-(1-diethylphosphono-2,2-dimethylpropyl) nitroxide
St	styrene
SEM	scanning electron microscopy
SNH	saturated nitrogen heterocycle
T	time
TMS	tetramethylsilane $(CH_3)_4Si$
TEM	transmission electron microscopy
T_g	glass transition temperature
t-BA	*tert*-butyl acrylate
TBAM	*tert*-butyl acrylamide
THF	tetrahydrofuran
TMSI	trimethylsilyl iodide
VA-044	2,2'-azobis[2-(2-dimidazolin-2-yl)propane] dihydrochloride
wt.%	weight percentage
v/v	volume per volume
w/v	weight per volume

Chapter 1

Synthesis of *N*-[(dialkylamino)methyl)]acrylamides and *N*-[(dialkylamino)methyl)]methacrylamides from Schiff Base Salts: Useful building blocks for smart polymers

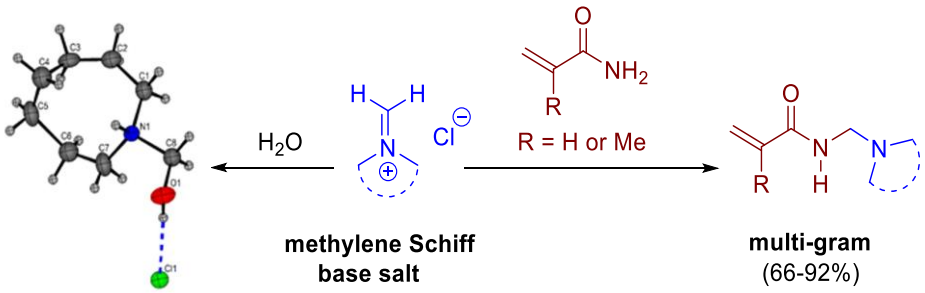

Parts of this chapter have been taken from the publication listed below (this publication is also appended to the end of this thesis); published in A. Alzahrani, S. I. Mirallai, B. A. Chalmers, P. McArdle and F. Aldabbagh. *Org. Biomol. Chem.*, **2018**, *16*, 4108–4116.

1.1 Introduction

The three-component Mannich reaction is fundamental allowing access to β-amino methylated carbonyl compounds.[1-2] *N*-[(Dialkylamino)-methyl)]acrylamide and methacrylamide derivatives are valuable monomeric precursors to smart polymers, with functionality capable of dual temperature and pH-responsiveness (Figure 1.1), however potential applications have not been realized due to problems with their synthesis.

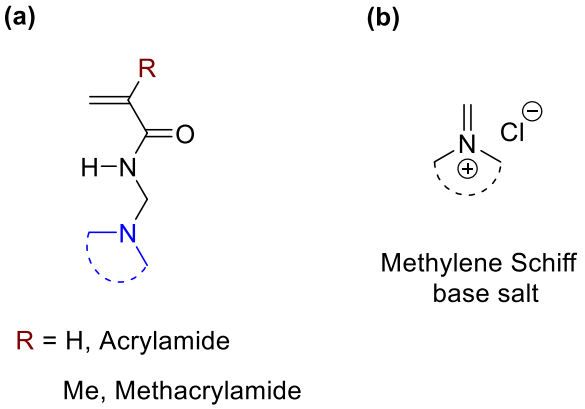

Figure 1.1: (a) Synthetic targets and **(b)** precursors.

Literature routes have used one-pot aza-Mannich condensation of (meth)acrylamide with formaldehyde to generate the Schiff base followed by secondary amine addition (Scheme 1.1).[3-6] The reaction operates thermally (at ~80 °C) and is inefficient in forming the Schiff base *in situ*, with the elevated temperature resulting in premature polymerization of the monomer and intermediates. The reaction has the added difficulty of monomer isolation, which requires vacuum distillation from the aqueous reaction mixture.

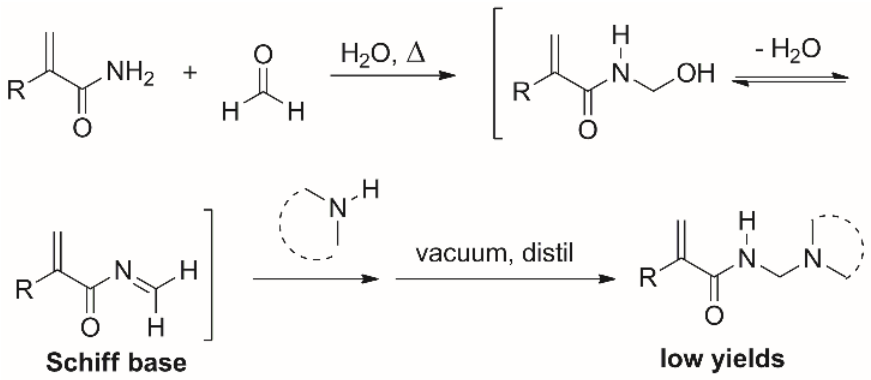

Scheme 1.1: One-pot thermal Mannich reaction.

The most widely studied temperature-responsive polymers are those with lower critical solution temperature (LCST) close to physiological temperature, such as poly(*N*-isopropylacrylamide) and poly(*N*,*N*-diethylacrylamide) with LCST of 32–33 °C in water.[7-9] The reverse solubility transition is called upper critical solution temperature (UCST), i.e. the polymer is insoluble at low temperatures and dissolves upon heating, such as poly(methyl methacrylate) (PMMA) in EtOH/H_2O mixtures.[55] The *N*-dialkyl amino (including saturated nitrogen heterocycle) of substituted acrylamides and methacrylamides can be reversibly ionized allowing pH-response that alters polymer hydrophobicity.[9-15] Amphiphilic block copolymers comprising of such monomers can self-assemble into a variety of nano-objects for use as stimuli-responsive polymersomes for targeted delivery of therapeutics.[11-13] In a recent communication, the synthesis of selected acrylamides containing an *N*-methylene saturated nitrogen heterocycles {*N*-[(morpholin-4-yl)methyl]prop-2-enamide(**1a**), *N*-[(pyrrolidin-1-yl)methyl]prop-2-enamide (**2a**) and *N*-[(piperidin-1-yl)methyl]prop-2-enamide (**3a**)}, and their incorporation into well-defined water-soluble block copolymer polyacrylamides was realized (Scheme 1.2).[14] In this chapter, we expand on the monomer synthesis by providing efficient multi-gram routes to acrylamides and methacrylamides, including those with dialkyl acyclic and large saturated nitrogen heterocyclic rings. The synthesis involves efficient generation of the methylene Schiff base salt, which was characterized in the hydrated form.

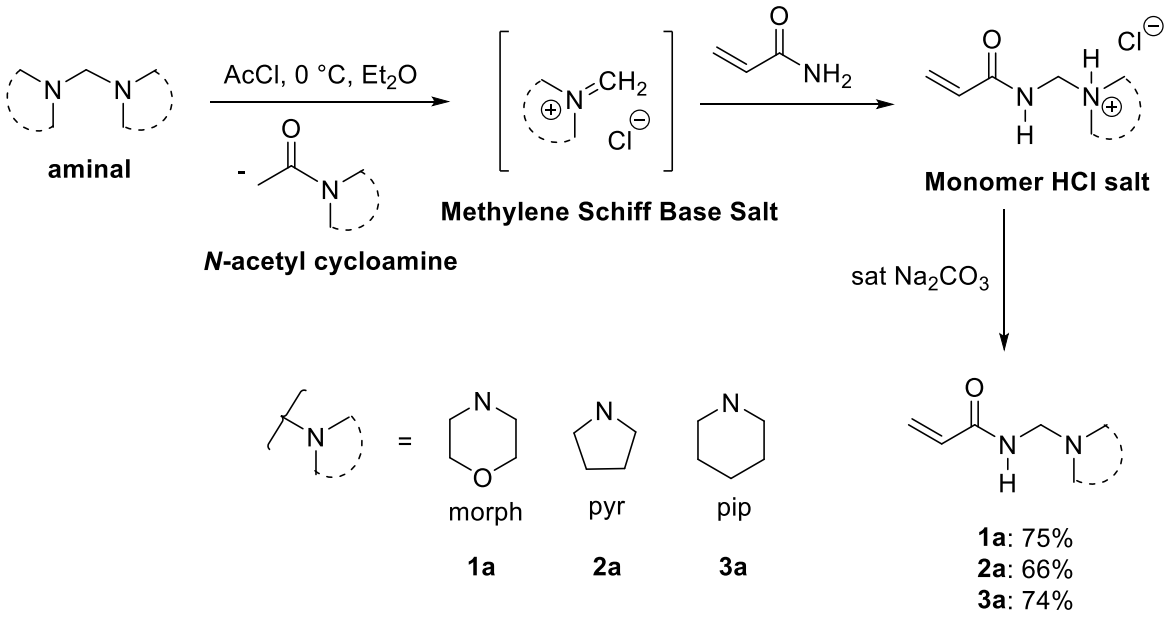

Scheme 1.2: Approaches to *N*-[(cycloalkylamino)methyl]acrylamides.

1.2 Aims and Objectives

- Our first objective was to prepare methacrylamides substituted at the nitrogen with *N*-methylene saturated nitrogen heterocycles. These were 2-methyl-*N*-[(morpholin-4-yl)methyl]prop-2-enamide (**1b**), 2-methyl-*N*-[(pyrrolidin-1-yl)methyl]prop-2-enamide (**2b**) and 2-methyl-*N*-[(piperidin-1-yl)methyl]prop-2-enamide (**3b**) via their HCl salts for use as macro-RAFT agents in future block copolymer synthesis in (Figure 1.2a).

- Our second objective was to prepare acrylamides and methacrylamides substituted at the nitrogen with saturated nitrogen heterocycles of larger ring sizes. These were *N*-[(azepan-1-yl)methyl]prop-2-enamide hydrochloride (**4a.HCl**), *N*-[(azepan-1-yl)methyl]prop-2-enamide (**4a**), *N*-[(azepan-1-yl)methyl]-2-methylprop-2-enamide hydrochloride (**4b.HCl**), *N*-[(azepan-1-yl)methyl]-2-methylprop-2-enamide (**4b**), *N*-[(azocan-1-yl)methyl]prop-2-enamide hydrochloride (**5a.HCl**), *N*-[(azocan-1-yl)methyl]prop-2-enamide (**5a**), *N*-[(azocan-1-yl)methyl]-2-methylprop-2-enamide hydrochloride (**5b.HCl**) and *N*-[(azocan-1-yl)methyl]-2-methylprop-2-enamide (**5b**) in (Figure 1.2b). The seven- and eight-membered containing polyacrylamide blocks will be more hydrophobic with unique sensitivities to pH and CO_2 in future amphiliphilic block copolymers.

- The third objective was to prepare acrylamides and methacrylamides substituted at the nitrogen with *N*-methylene *N*,*N*-dialkyl acyclic substituents, which are known to have greater water solubility as polymers (see later discussion). The monomers to be synthesized were *N*-[(dimethylamino)methyl]prop-2-enamide (**6a**), *N*-[(dimethylamino)methyl]-2-methylprop-2-enamide (**6b**), *N*-[(diethylamino)methyl]prop-2-enamide (**7a**), *N*-[(diethylamino)methyl]-2-methylprop-2-enamide (**7b**), *N*-[(dipropylamino)methyl]prop-2-enamide (**8a**), *N*-[(dipropylamino)methyl]-2-methylprop-2-ena-mide (**8b**), *N*-[(dibutylamino)methyl]prop-2-enamide (**9a**) and *N*-[(dibutylamino)methyl]-2-methylprop-2-enamide (**9b**) in (Figure 1.2c).

(a)

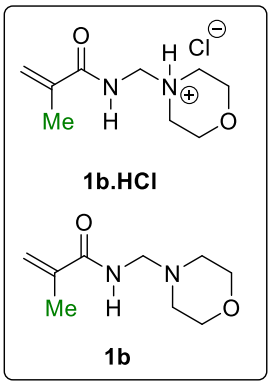

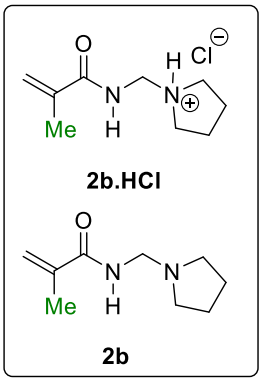

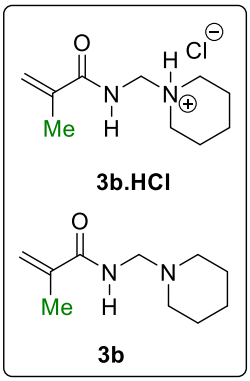

(b)

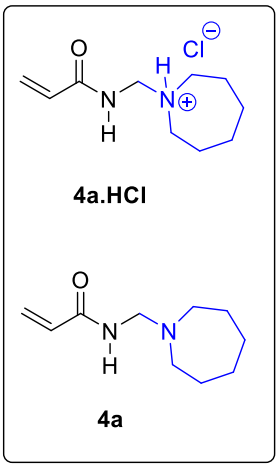

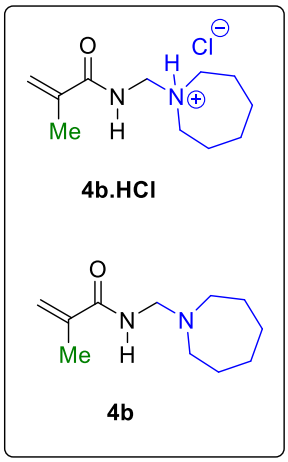

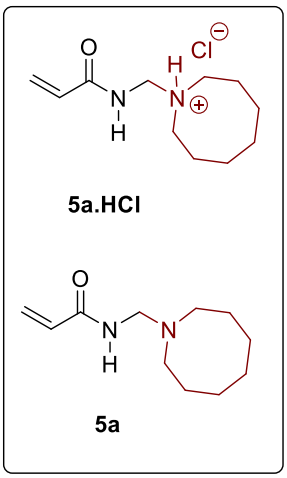

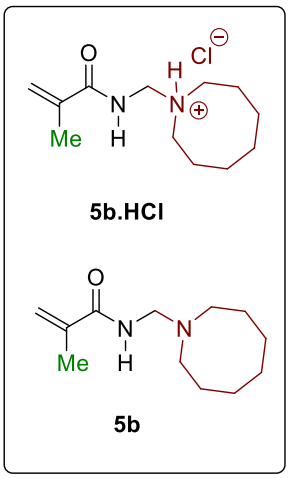

(c)

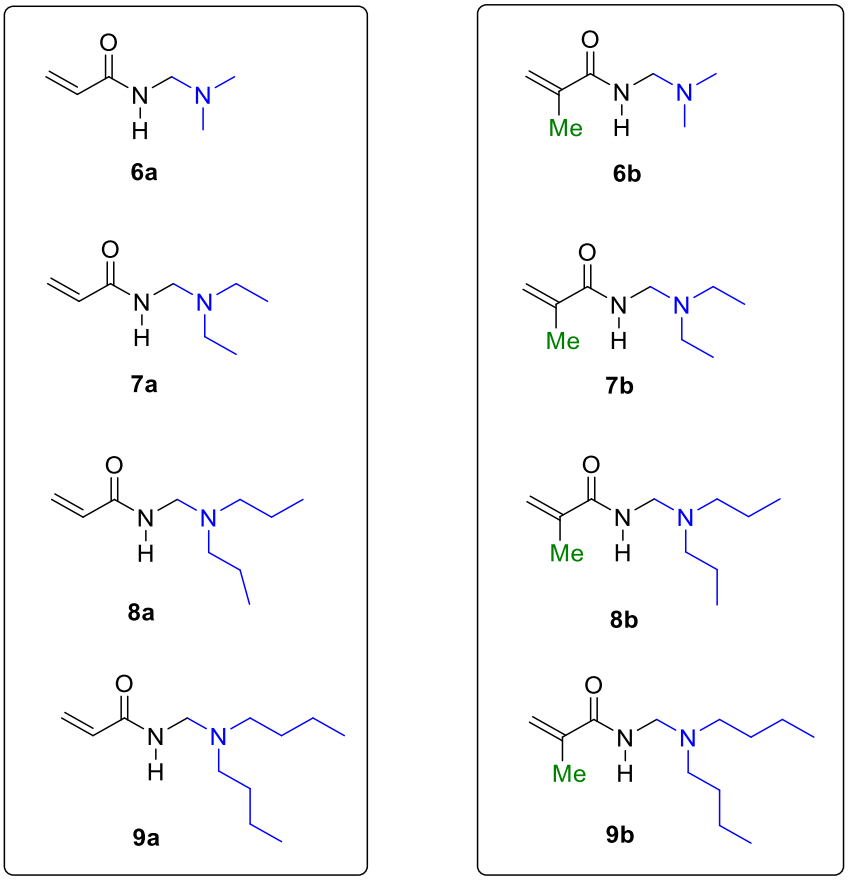

Figure 1.2: Target novel monomers to be prepared in this chapter.

The synthesis of the novel acrylamides **4a–9a** and methacrylamides **1b–9b** will be discussed in context with the literature in the following sections of this chapter.

1.3 Results and Discussion

1.3.1 Preparation of aminals

In contrast to the one-pot thermal Mannich condensation reaction in Scheme 1.1, our synthesis uses readily accessible aminals **10a–10i** made from the condensation of formaldehyde with secondary amines; morpholine, pyrrolidine, piperidine, azepane, azocane, dimethylamine, diethylamine, dipropylamine and dibutylamine (Table 1.1).[16-17] For the synthesis of aminals in entries 4–9, isolation of the product required the addition of KOH pellets to help remove water. All aminals **10a–10i** were obtained in high yields of 83–98% in comparable yields to literature reports by reduced pressure distillation, except **10f** and **10g** aminals, which did not require a vacuum (at 760 mmHg) for distillation. *N*,*N*,*N'*,*N'*-Tetrabutylmethanediamine (**10i**) was obtained in 85% isolated yield, however repeated fractional distillations did not remove contamination by approximately 10% of the *N*,*N*-dibutylaminomethanol (Scheme 1.3).

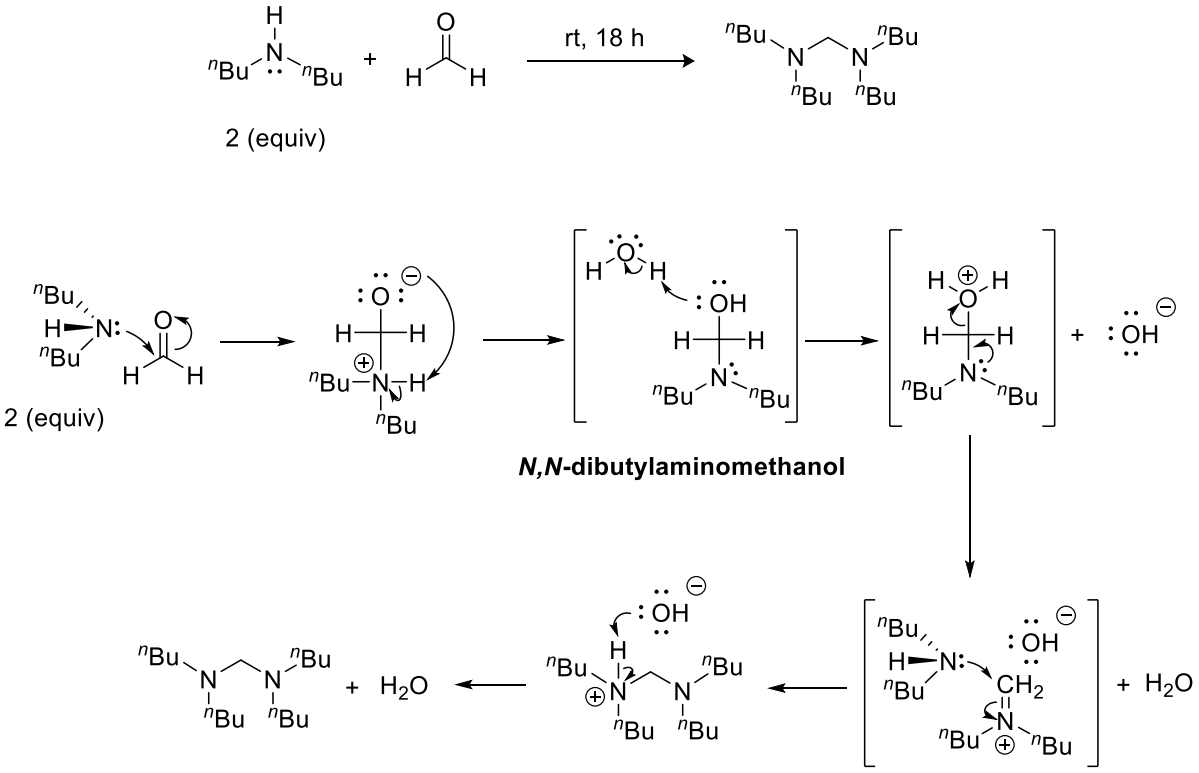

Scheme 1.3: Synthesis and mechanism for *N*,*N*,*N*′,*N*′-tetrabutylmethanediamine.

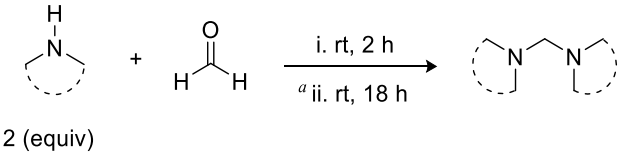

Entry	Amines	Aminals	Yields %	B.p °C at 0.25 mmHg	B.p °C in *Lit*- (mmHg)
1	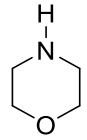	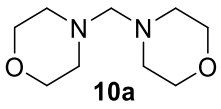 **10a**	98, (92)[17]	66–68	65 (0.1)[17]
2	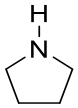	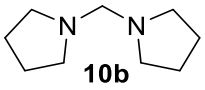 **10b**	83, (85)[16]	62–64	70 (7)[16]
3	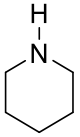	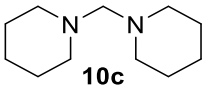 **10c**	93, (90)[17]	50–52	60 (0.1)[17]
[a] 4	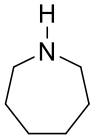	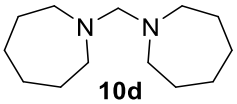 **10d**	90, -	83–85	-
[a] 5	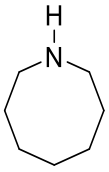	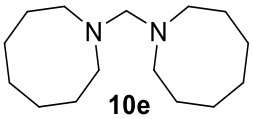 **10e**	88	138–140	new
[a] 6	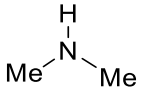	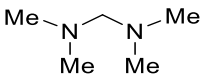 **10f**	94, (92)[16]	[c] 81–83	[c] 82–83
[a] 7	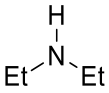	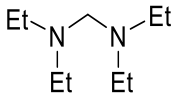 **10g**	98, (90)[16]	[c] 47–48	[c] 47–48
[a] 8	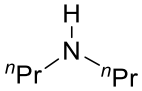	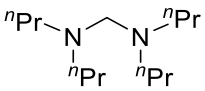 **10h**	91, (73)[18]	86–88	77–78 (2)[18]
[a] 9	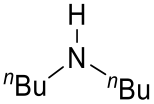	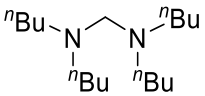 **10i**	[b] 85, -	112–114	-

Table 1.1: Preparation of aminals, [a] KOH used on work up, [b] contains 10% of the *N*,*N*-dibutylaminomethanol, [c] at 760 mmHg. Literature yields are within the brackets.

1.3.2 Preparation of methylene Schiff base salts

Böhme pioneered the quaternization of the aminal to generate the methylene Schiff base (iminium) salt using acetyl chloride. Acetyl chloride was our preferred method for activating aminals, because of its low molecular weight, low cost and high atom economy in comparison to alternative literature reagents (e.g. trichloromethylsilane), and this methodology was adopted for this PhD (Scheme 1.4).[17,19-21]

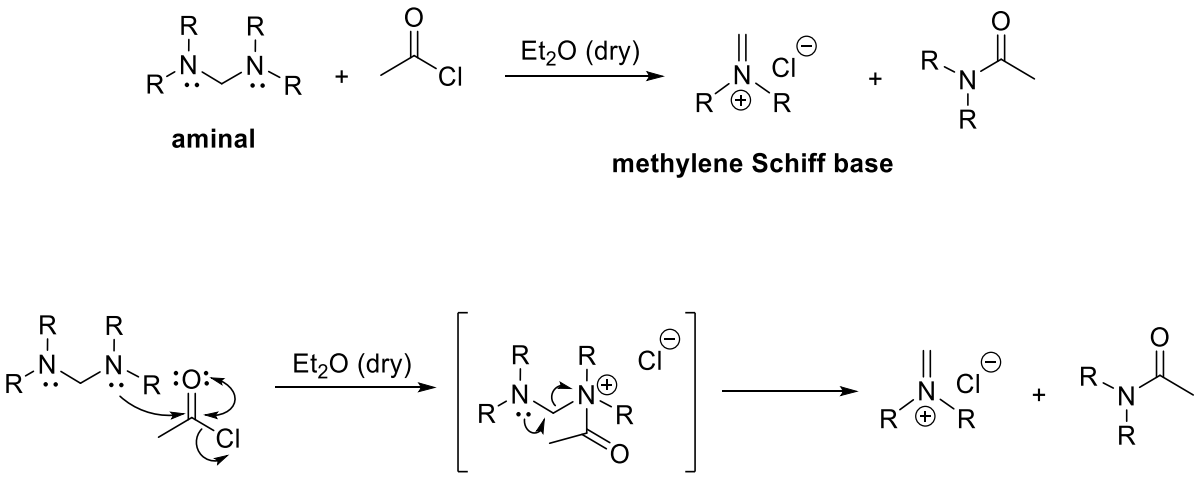

Scheme 1.4: Synthesis and mechanism for methylene Schiff base chloride using AcCl.

Rochin *et al*, generated methylene Schiff base salt chloride in high yield from *gem*-aminoether reagent as an alternative to aminals, by reaction with trichloromethylsilane ($MeSiCl_3$) in acetonitrile at room temperature (Scheme 1.5).[22]

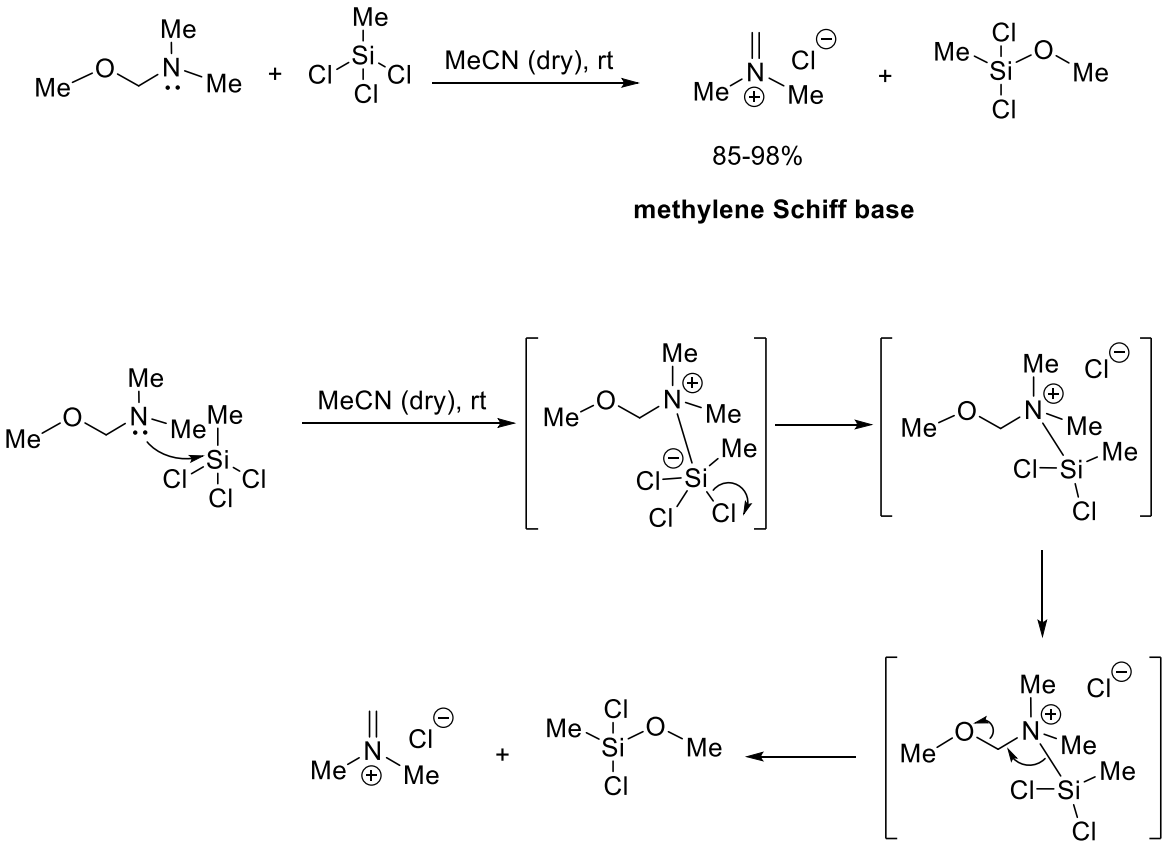

Scheme 1.5: Synthesis and mechanism for methylene Schiff base chloride using *gem*-aminoether reagent with $MeSiCl_3$.

Heaney *et al*, generated methylene Schiff base salt chloride from aminal reaction with trichloromethylsilane ($MeSiCl_3$) in acetonitrile at room temperature (Scheme 1.6).[16]

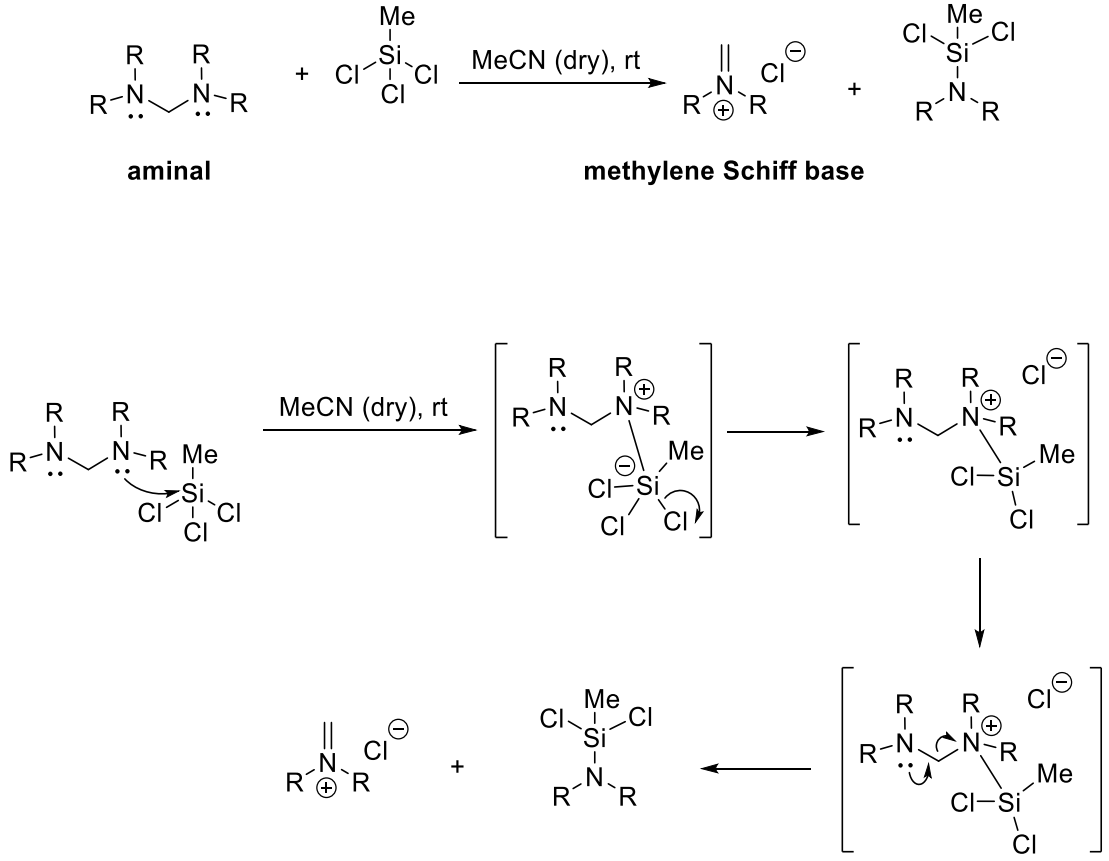

Scheme 1.6: Synthesis and mechanism for methylene Schiff base chloride using $MeSiCl_3$.

The most utilised Schiff base salt is commercial *N*,*N*-dimethylmethyleneiminium iodide or Eschenmoser's salt.[23-24] The original synthesis uses the reaction of trimethylamine with diiodomethane (CH_2I_2) as the by-product (Scheme 1.7).[23] The difference in making the Eschenmoser's salt is the circumvention of the requirement for aminal in the synthesis of methylene Schiff base, although a later procedure uses trimethylsilyl iodide (TMSI) and aminals.[24]

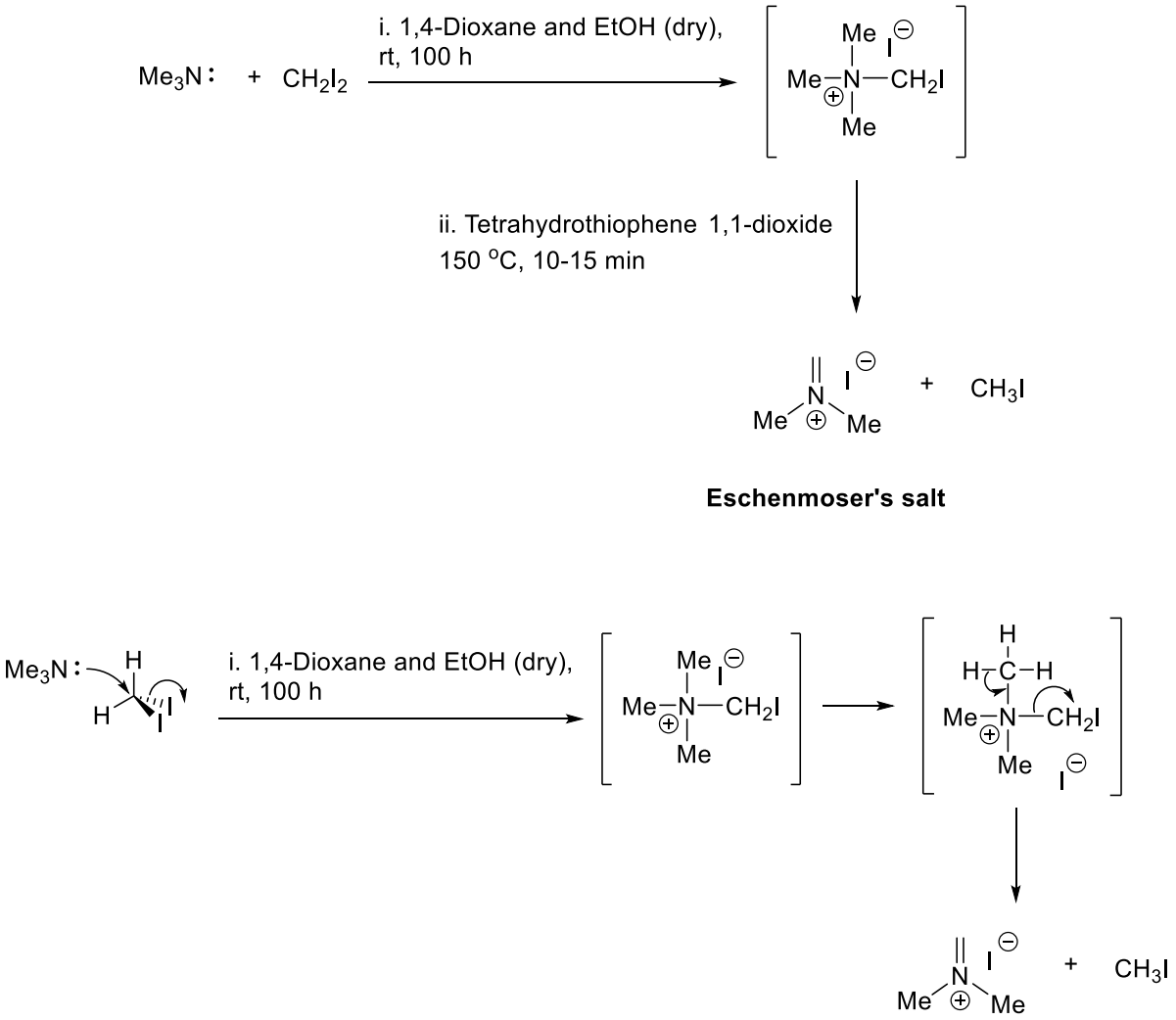

Scheme 1.7: Synthesis of Eschenmoser's salt (*N*,*N*-dimethylmethyleneiminium iodide).

In our case, treatment of aminals **10d–10i** with acetyl chloride in diethyl ether at 0 °C allowed access to both larger heterocyclic and acyclic Schiff base salts **11a–11f**, which were more conveniently characterized as *N*-hydroxymethyl salt derivatives **12a–12f** (Scheme 1.8).

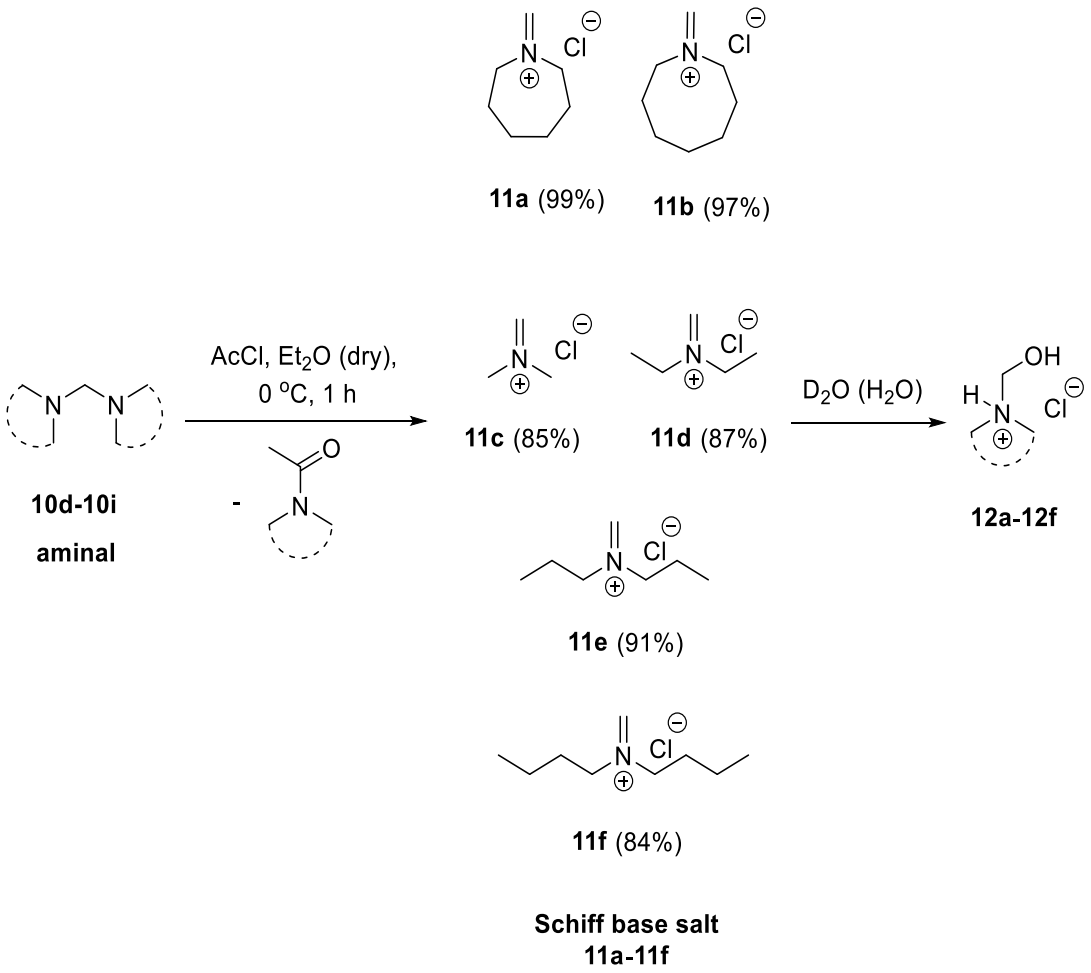

Scheme 1.8: Synthesis of Schiff base salts **11a–11f** characterized by ^{1}H NMR as hydrated derivatives **12a–12f**.

NMR spectra of iminium salts **11a–11f** showed mixtures with their respective hydrated hydrochloride salts **12a–12f**. For example, the ^{1}H-NMR spectrum in CD_2Cl_2 gave similar intensity signals for the *exo*-methylene at 8.87 ppm of *N*-methylideneazocan-1-ium chloride (**11b**) and its *N*-hydroxymethyl derivative **12b** *exo*-methylene at 4.74 ppm (Figure 1.3a). Upon recrystallization from acetonitrile, the more stable *N*-(hydroxymethyl)azocan-1-ium chloride **12b** was obtained (Figure 1.3b). It was thus more convenient to characterize methylene Schiff base salts **11a–11f** using NMR in D_2O, as **12a–12f** (Figure 1.3c). An exception was *N*,*N*-dibutylmethaniminium chloride (**11f**), which appeared less hygroscopic, The NMR spectrum in CD_2Cl_2, containing only trace amounts of hydrated adduct **12f** (Figure 1.4a). The *exo*-methylene at 8.58 ppm in CD_2Cl_2 for the methylene Schiff base was replaced by the *exo*-methylene at 4.83 ppm in D_2O for *N*-butyl-*N*-(hydroxymethyl)butan-1-iminium chloride (**12f**) (Figure 1.4b).

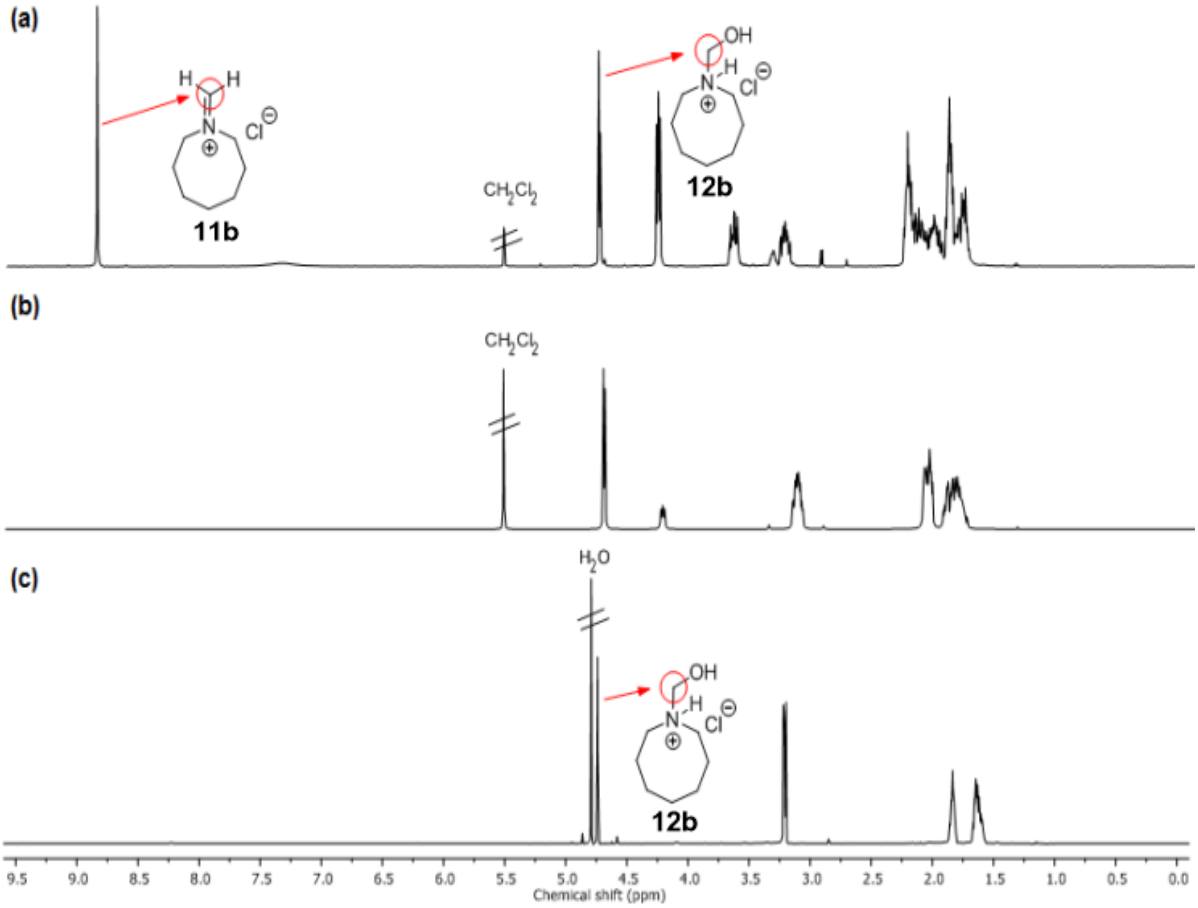

Figure 1.3: ^{1}H-NMR Spectrum: **(a)** of the initially isolated mixture containing *N*-methylideneazocan-1-ium chloride (**11b**) and *N*-(hydroxymethyl)azocan-1-ium chloride (**12b**) in CD_2Cl_2, and spectra of **12b** after recrystallization from MeCN in **(b)** CD_2Cl_2, and **(c)** D_2O.

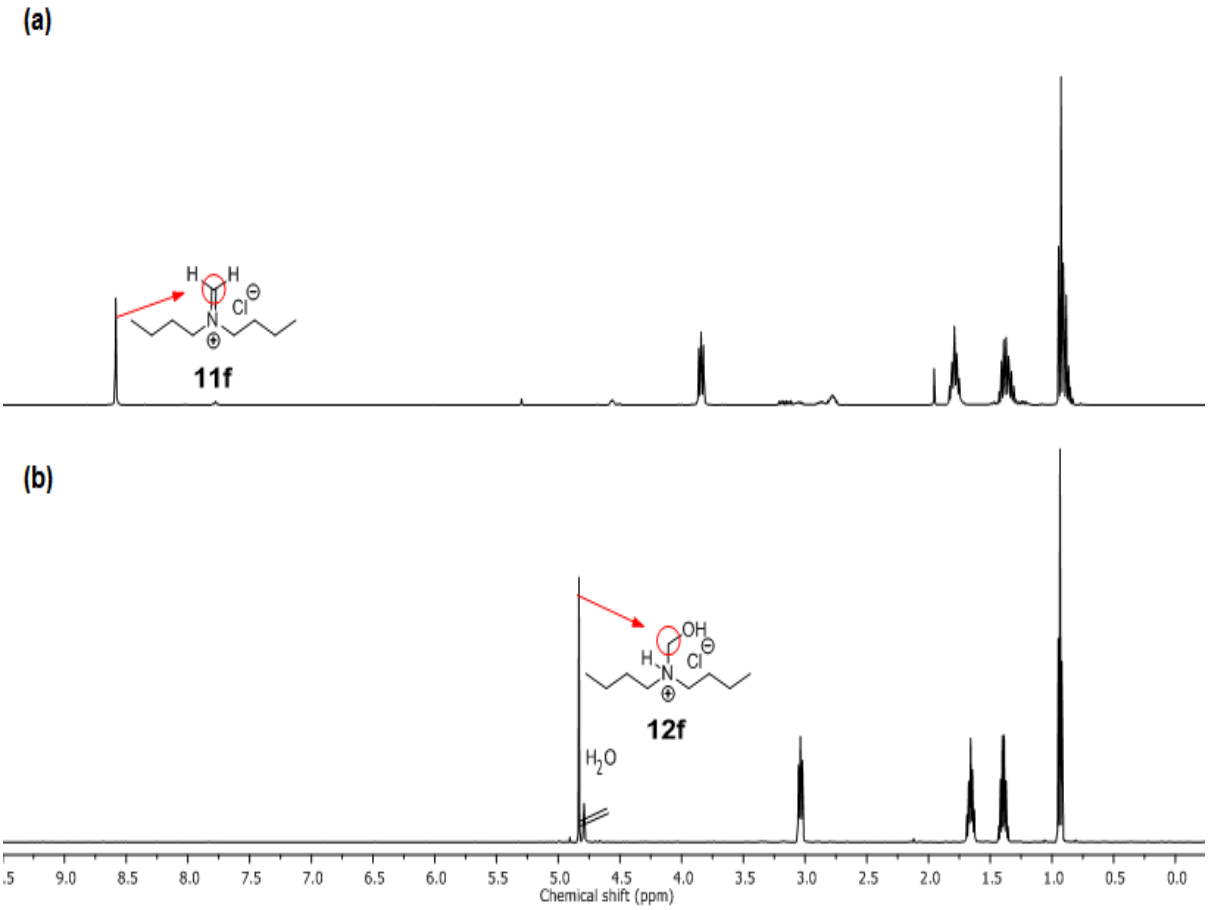

Figure 1.4: ^{1}H-NMR Spectrum: **(a)** of *N*,*N*-dibutylmethaniminium chloride (**11f**) in CD_2Cl_2, and **(b)** of *N*-butyl-*N*-(hydroxymethyl)butan-1-iminium chloride (**12f**) in D_2O.

The X-ray crystal structure of *N*-(hydroxymethyl)azocan-1-ium chloride (**12b**) was obtained (Figure 1.5a and Table 1.2). The large eight membered ring of **12b** was found to be disordered over two equally populated sites with both the N-H and O-H bonds found to be involved in H-bonding to the chloride counter ion (Figure 1.5b). Interestingly, a search of the CCDC data base for the $R_2NH\text{-}CH_2\text{-}OH$ moiety gave only one hit, CSD code DIVDET, which was for a pyrimidine salt of *tris*(hydroxymethyl)ammonium chloride (2/1) in (Figure 1.6).[25] The hydroxymethyl hydrochlorides **12a–12f** were however difficult to isolate cleanly due to their susceptibility to decomposition to formaldehyde.

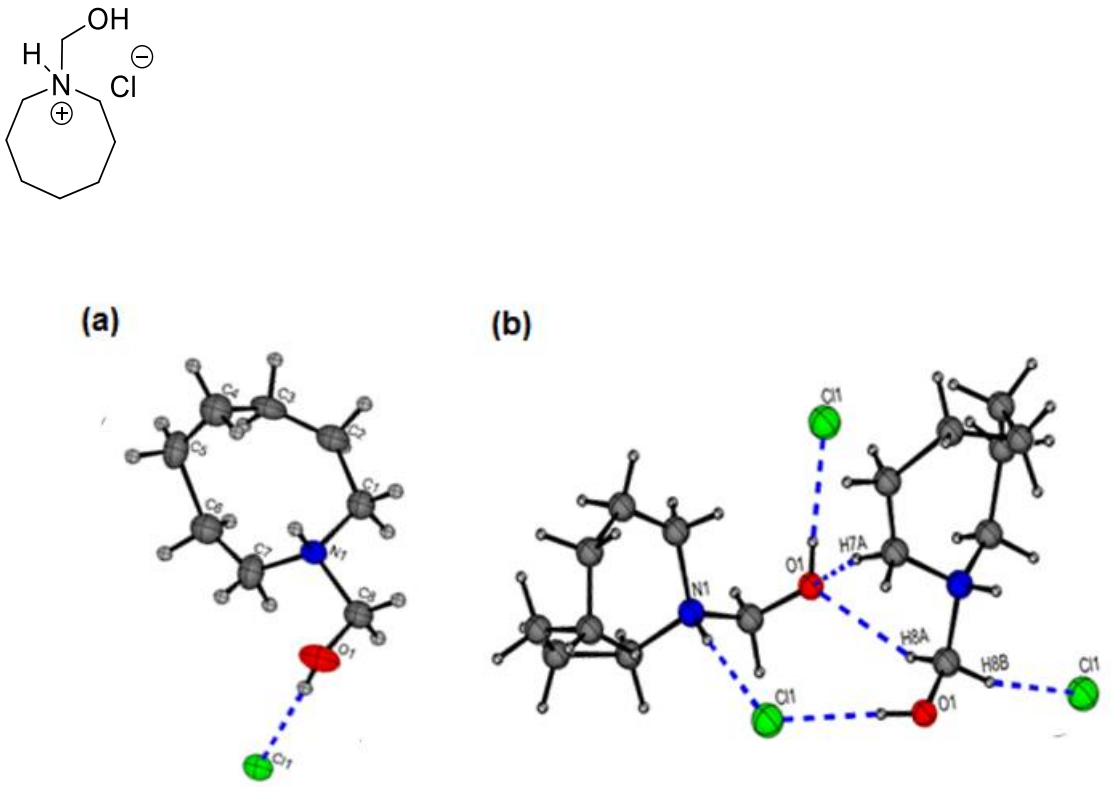

Figure 1.5: The X-ray crystal structure of *N*-(hydroxymethyl)azocan-1-ium chloride (**12b**): **(a)** only one component of the ring disorder shown for clarity, and **(b)** H-bonding interactions (Table 1.2).

D-H...A	d(D-H)	d(H...A)	d(D...A)	<(DHA)
O(1)-H(1O1)...Cl(1)	0.82	2.17	2.984(4)	174.2
N(1)-H(1)...Cl(1)#1	0.98	2.21	3.150(4)	160.3
C(7)-H(7A)...O(1)#2	0.97	2.35	3.247(7)	152.9
C(8)-H(8A)...O(1)#2	0.97	2.38	3.229(6)	146.3
C(8)-H(8B)...Cl(1)#3	0.97	2.78	3.667(5)	151.6

Table 1.2: Hydrogen bonds for 1-(hydroxymethyl)azocan-1-ium chloride (**12b**) [Å (**d** = distance) and ° (< for angle)].

Symmetry transformations used to generate equivalent atoms:

#1 x,-y+3/2,z-1/2 #2 x,-y+3/2,z+1/2 #3 -x+2,y-1/2,-z+3/2

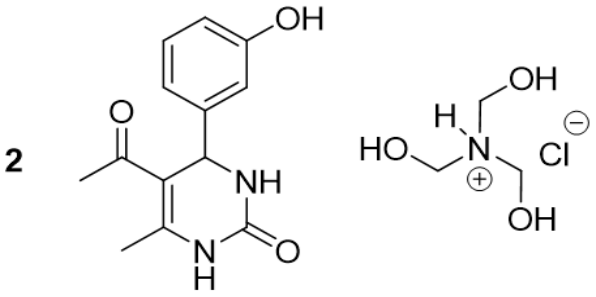

Figure 1.6: Structure of 5-acetyl-4-(3-hydroxyphenyl)-6-methyl-1,2,3,4-tetrahydropyrimidin-2-one-*tris*-(hydroxymethyl)ammonium chloride (2/1).

1.3.3 Reactions of methylene Schiff base salts

There are numerous accounts of alkylation and nucleophilic addition onto methylene Schiff base salts.[16-34] In 1975, by Böhme and Backhaus carried out the reaction of methylene Schiff base salt such as *N*,*N*-dimethylmethaniminium chloride with sodium salt of carboxylic acid in dichloromethane to give the carboxylic ester (dimethylamino)methyl acetate (Scheme 1.9).[20]

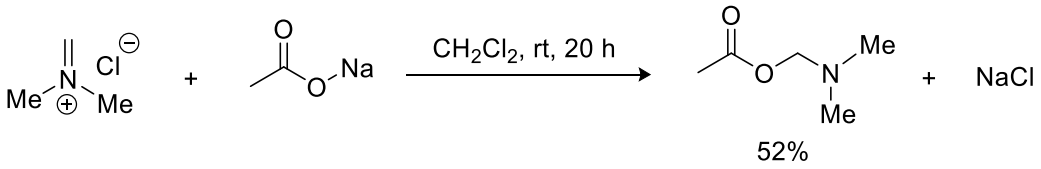

Scheme 1.9: Reaction of methylene Schiff base chloride with sodium acetate.

Heaney used methylene Schiff base salt chlorides as electrophiles in substitution reactions with aromatic heterocycle compounds, such as 2-methylfuran and indole (Scheme 1.10).[16]

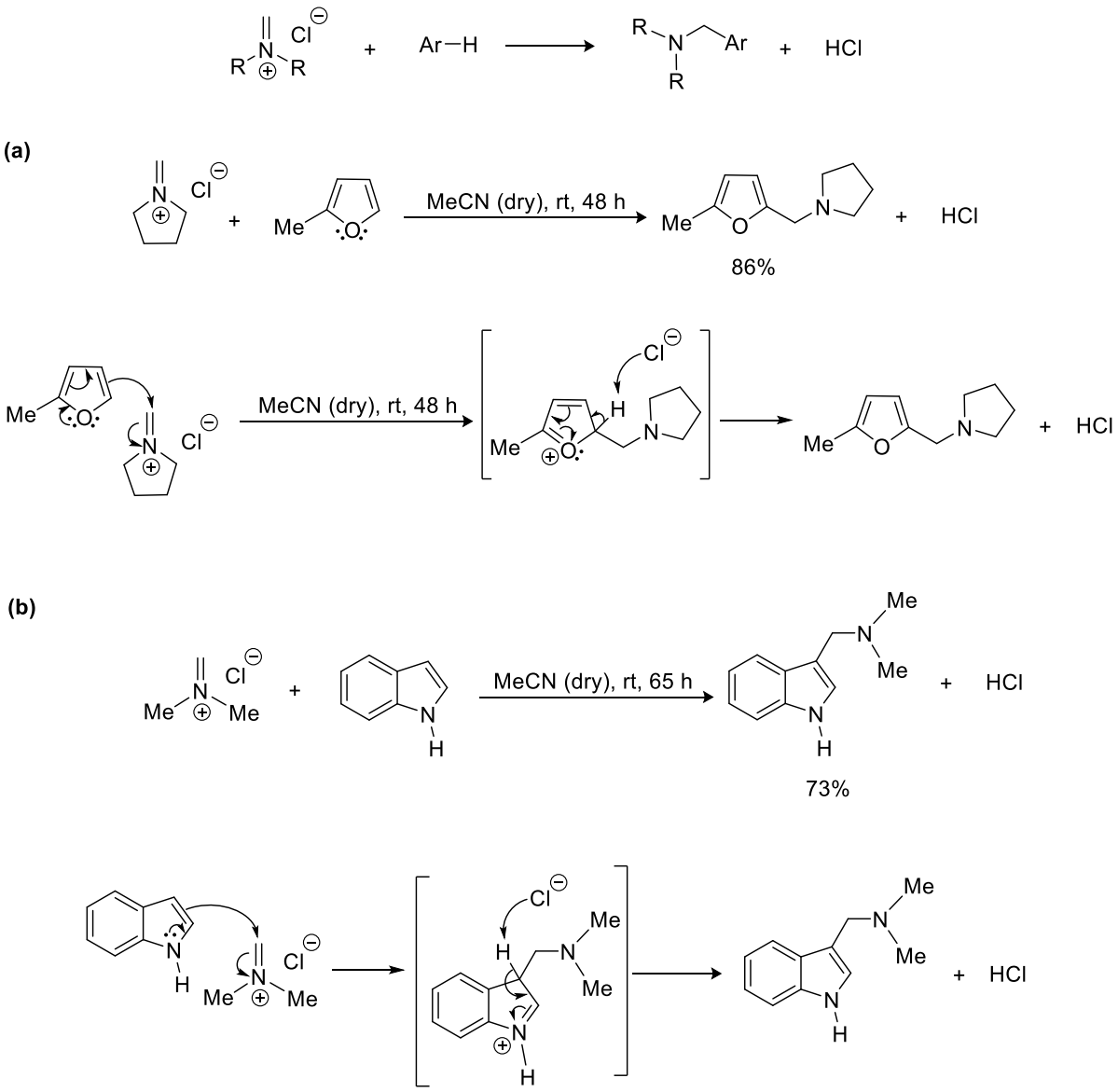

Scheme 1.10: Reactions with mechanism for methylene Schiff base chloride with heterocycle compounds such as **(a)** furan and **(b)** indole.

Schiff base salts of morpholine and piperidine were used to substitute onto cyclic enones (Scheme 1.11).[17]

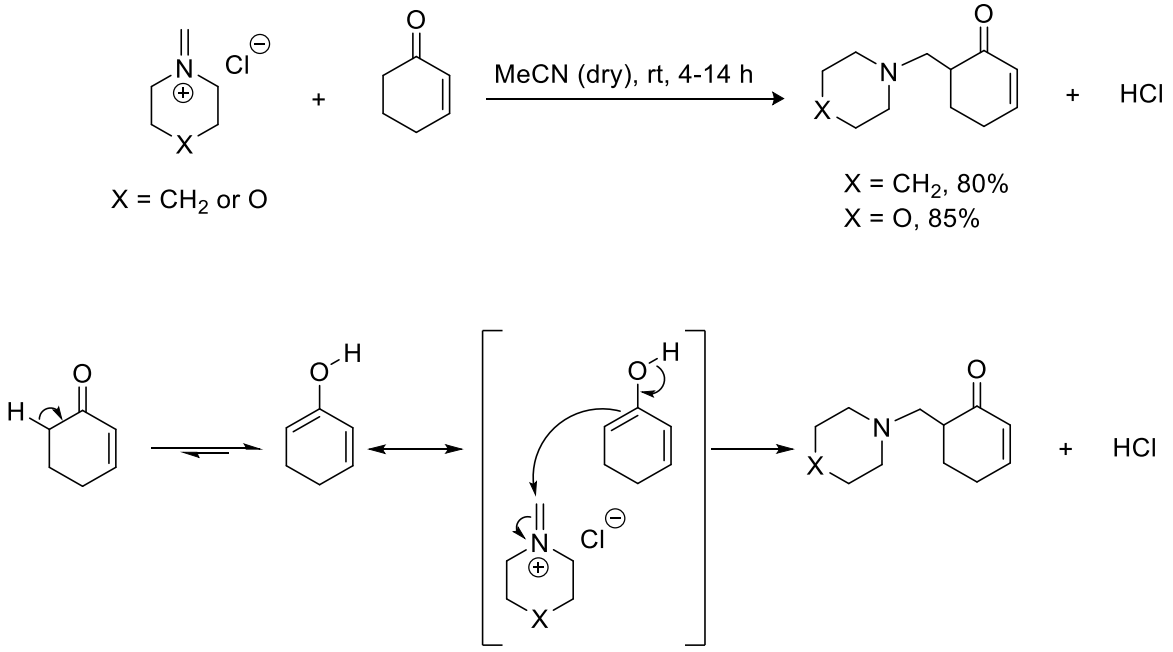

Scheme 1.11: Reaction with mechanism for methylene Schiff base chloride with cyclic enone.

Eschenmoser's salt reacted with organometallic reagents such as (Grignard reagent, RMgX), which included functionalization of ketones (Scheme 1.12).[32-33]

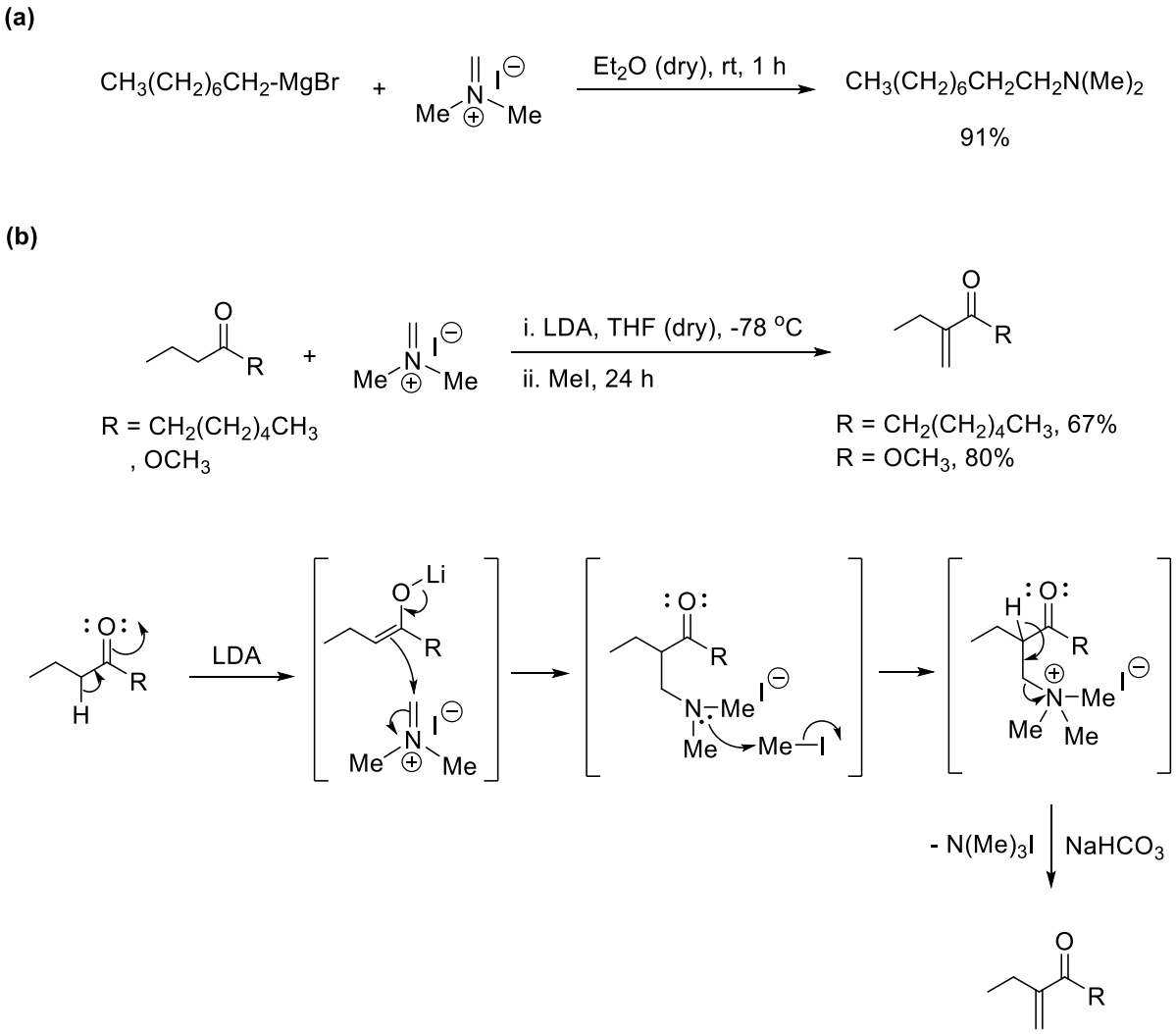

Scheme 1.12: Reactions of Eschenmoser's salt with **(a)** organometallic reagents, and **(b)** enolate.

Non-vinylic amides have been added to Schiff base salts, including *tert*-butylcarbamate and succinimide (Scheme 1.13).[31]

(a)

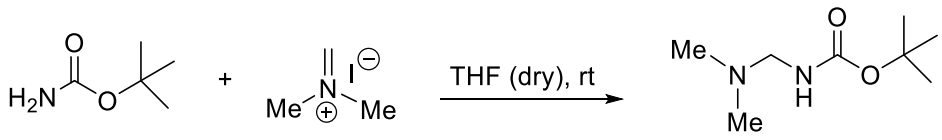

(b)

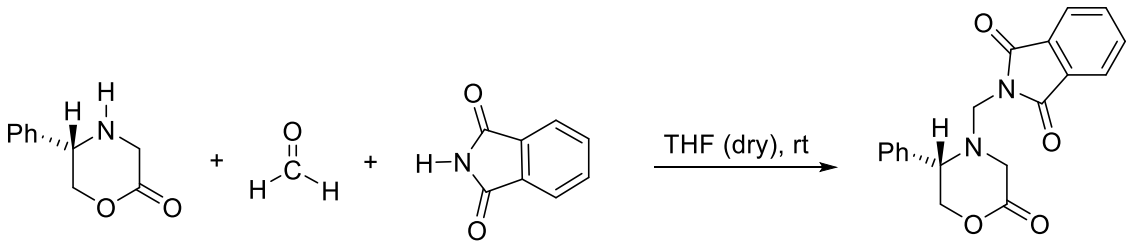

49%

Scheme 1.13: Reactions of Eschenmoser's salt with **(a)** *tert*-butyl carbamate and **(b)** succinimide compound.

Möhrle and Keller added hydrazones onto aminals possibly via *in situ* generated Schiff base in dry 1,4-dioxane at room temperature, although the authors proposed a concerted reaction (Scheme 1.14).[34]

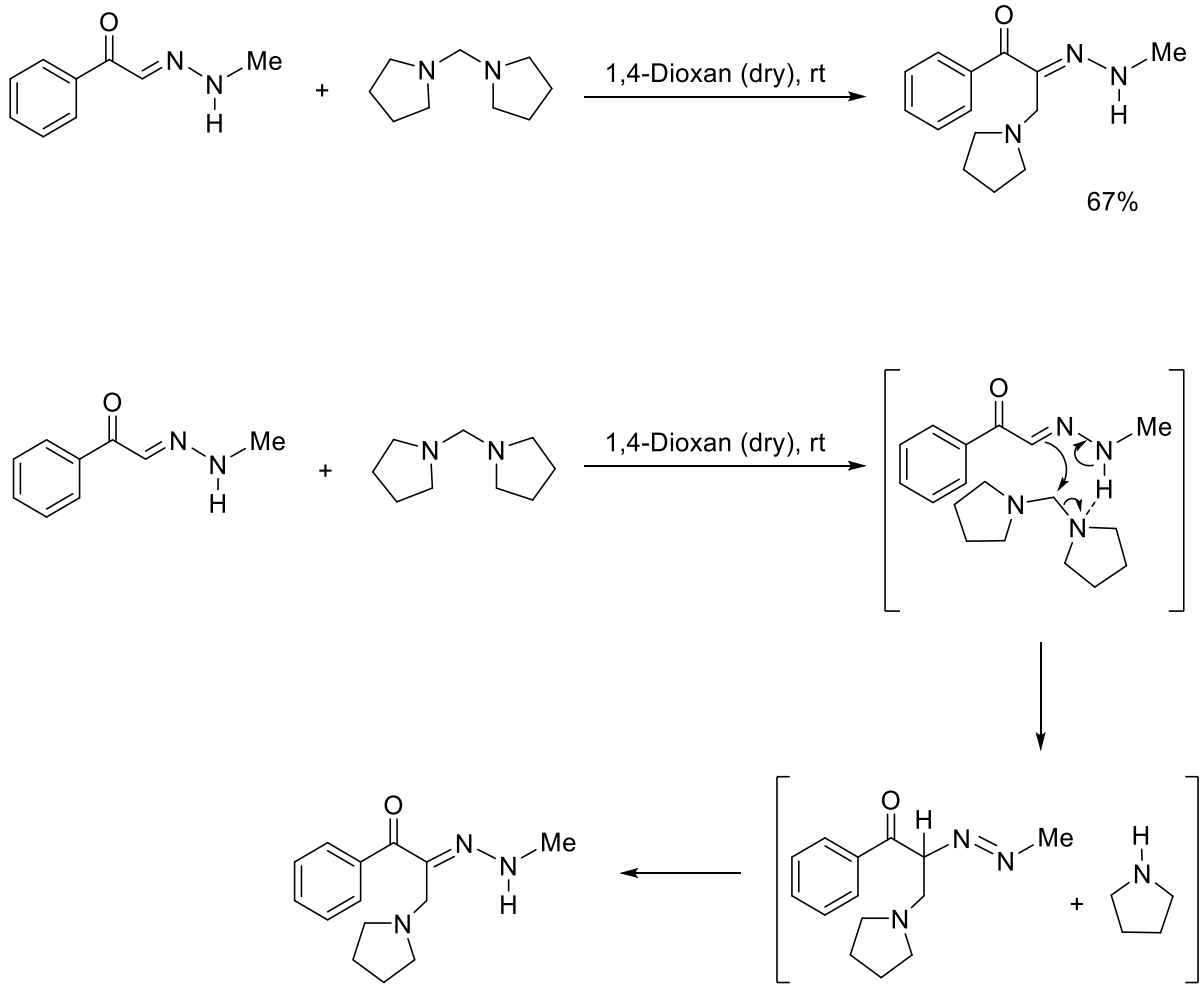

Scheme 1.14: Reaction of hydrazones with aminal.

Inspired by the simplicity and low temperatures, acrylamide and methacrylamide were added onto *in situ* generated methylene Schiff salts chloride to give the monomer hydrochloride salts of morpholine, pyrrolidine and piperidine.

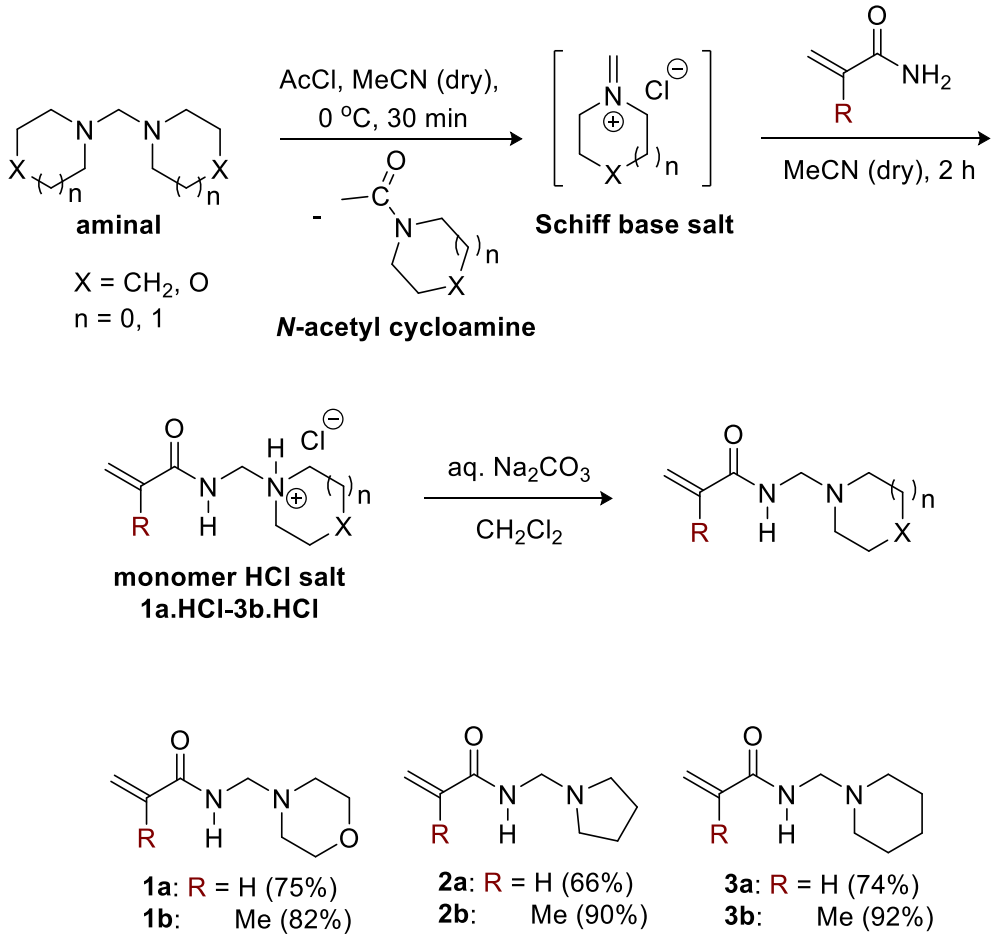

Scheme 1.15: Synthesis of *N*-[(cycloalkylamino)methyl)]acrylamides **1a–3a**, and *N*-[(cycloalkylamino)methyl)]methacrylamides **1b–3b** using the *in situ* Schiff base salt approach.

The monomer hydrochloride salts **1a.HCl–3b.HCl** were precipitated upon addition of diethyl ether to the reaction in acetonitrile, which allowed separation of the soluble *N*-acetyl cycloamines (Scheme 1.15). The isolable **1a.HCl–3b.HCl** are themselves useful as monomeric building blocks in aqueous solution polymerizations.[14] Basification of the latter, allowed the free *N*-[(cycloalkylamino)methyl)]acrylamides **1a**–**3a** to be isolated in 20–25 g scale in yields of 66–75%.[14, 35] The *N*-[(cycloalkylamino)methyl)]methacrylamides **1b**–**3b** were isolated in higher yields of 82–92% and in ≥30 g scale by the author this thesis.

Nucleophilic addition of acrylamide or methacrylamide onto the freshly prepared Schiff base salts of azepane and azocane **11a** and **11b** gave the hydrochloride monomer salts (**4a.HCl**, **4b.HCl**, **5a.HCl** and **5b.HCl**) after precipitation from diethyl ether (Scheme 1.16). The monomer HCl salts were suspended in dichloromethane and basified to give the monomers **4a**–**4b** and **5a**–**5b** in high yields of 84–91% (from **11a–11b**). Attempts to react acrylamide and methacrylamide with an analytically pure sample of *N*-(hydroxymethyl)azocan-1-ium chloride (**12b**) in dried acetonitrile resulted in isolation of unreacted **12b** and some degradation with release of formaldehyde. It follows that yields of monomer from addition onto methylene Schiff base salts were determined by the extent of hydration of the latter substrate.

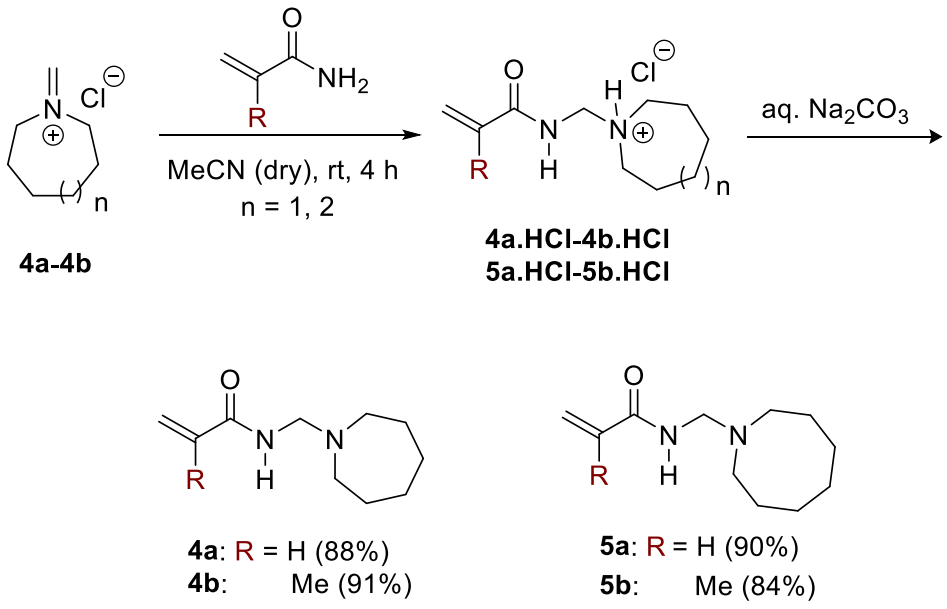

Scheme 1.16: Synthesis of seven and eight-membered *N*-[(cycloalkylamino)methyl)]-acrylamides **4a–5a** and *N*-[(cycloalkylamino)methyl)]methacrylamides **4b–5b** from the freshly prepared Schiff base salts.

Our *in situ* Schiff base salt approach was not applicable for larger cycloamines (azepane and azocane) and acyclic analogues. Isolation of the methylene Schiff base salts was deemed necessary for larger cycloamines due to the poor solubility of their aminals in acetonitrile. Seven and eight-membered heterocyclic base-containing monomers are useful for increased hydrophobicity in the ionizable block segment of amphiphilic copolymers promoting sharper pH-sensitivity of micelles.[11-12] Hong-Jun *et al*, developed ultra-pH-sensitive cluster nanobombs for improved delivery of Pt-drugs to solid tumors. The block containing azocane was sensitive to protonation at the elevated acidity of the solid tumor allowing the self-assembled particle to contract in size to nanoparticles (~10 nm in diameter) capable of effective tumor penetration (Figure 1.7 and Scheme 1.17).

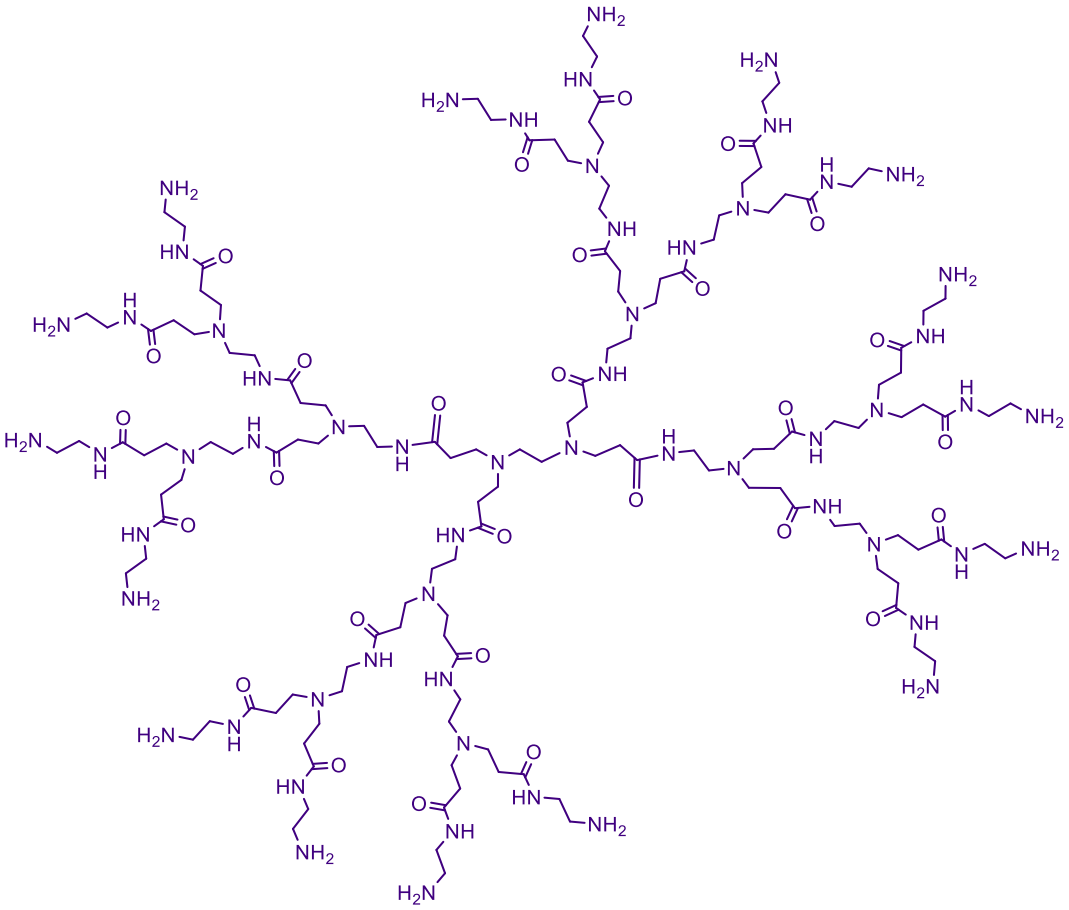

Figure 1.7: PAMAM dendrimer (polyamidoamines).

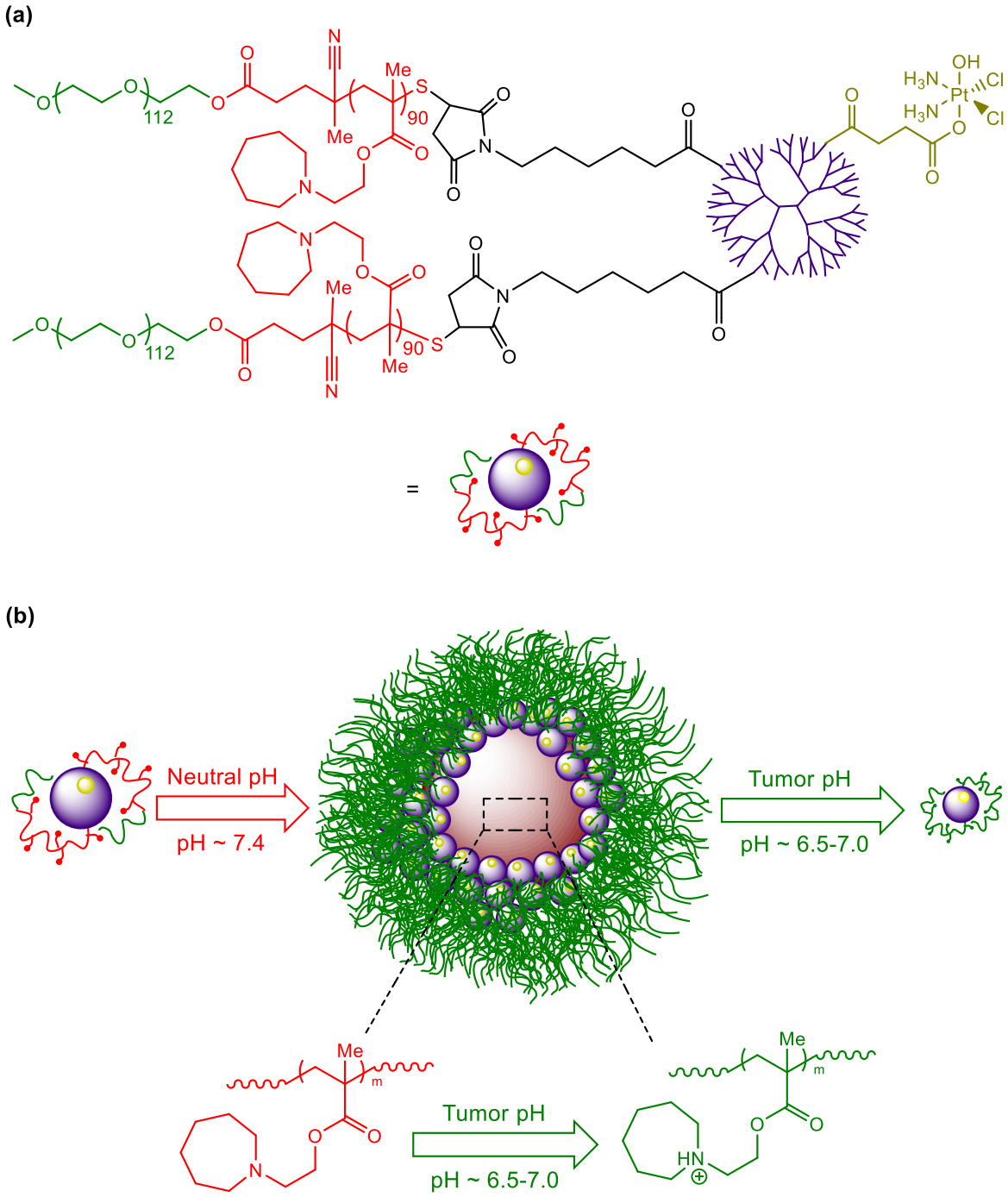

Scheme 1.17: (a) Structure of drug-loaded polymer and **(b)** the self-assembly into cluster nanobombs at neutral pH and tumor acidic pH.

On the contrary linear dialkyl amine-containing polyacrylamides generally have greater water solubility in comparison to heterocyclic amine-containing analogues affording higher LCSTs.[10] Polymers were made by reversible addition fragmentation chain transfer (RAFT) polymerization of appropriate 2-(dialkylamino)ethyl]acrylamide using 4-cyano-4-[(dodecyl-sulfanylthiocarbonyl)sulfanyl]pentanoic acid (CDTPA), as the chain transfer agent (Table 1.3).[10]

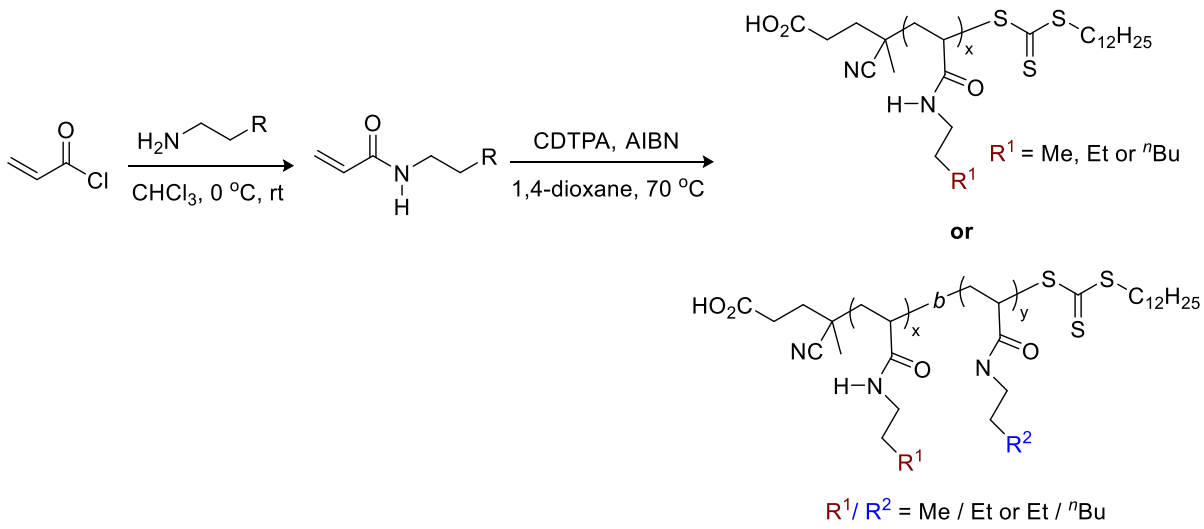

R	LCST (°C)
$N(Me)_2$	100
$N(Me)_2$ / $N(Et)_2$	37
$N(Et)_2$	33.5
	30
$N(Et)_2$ / $N(^nBu)_2$	18.3
$N(^nBu)_2$	0

Table 1.3: Synthesis of *N*-[2-(dialkylamino)ethyl]acrylamides and poly[*N*-[2-(dialkylamino)-ethyl]acrylamide]s with polymer LCST.

X-ray crystal structure of *N*-[(azocan-1-yl)methyl]prop-2-enamide hydrochloride (**5a.HCl**) was obtained with the very small fitting errors suggesting the ring is in the optimal conformation (Figure 1.8). The crystal structure showed N-H bonds forming H-bonding interactions with the chloride anions and the oxygen atoms resulting in intermolecular packing with some weaker C-H…Cl and C-H…O (Table 1.4, Figures 1.9).

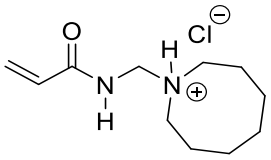

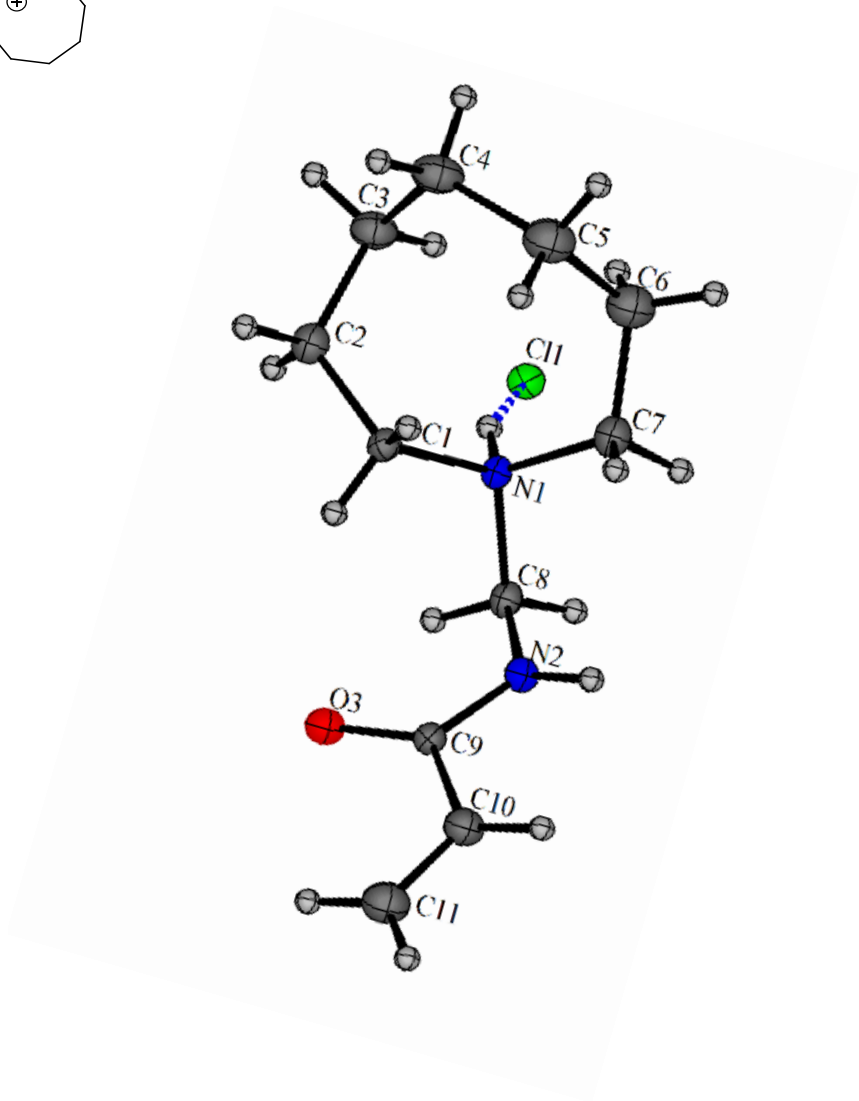

Figure 1.8: The X-ray crystal structure of *N*-[(azocan-1-yl)methyl]prop-2-enamide hydrochloride (**5a.HCl**) with one molecule from the asymmetric unit shown.

D-H...A	d(D-H)	d(H...A)	d(D...A)	<(DHA)
N(4)-H(4)...Cl(2)	0.86	2.34	3.188(3)	170.7
N(1)-H(1)...Cl(1)	0.98	2.18	3.103(3)	156.9
N(3)-H(3)...Cl(1)	0.98	2.16	3.097(3)	159.1
N(2)-H(2)...Cl(2)#1	0.86	2.35	3.199(3)	168.6
C(1)-H(1A)...O(3)	0.97	2.45	3.309(4)	147.6
C(1)-H(1B)...Cl(2)#2	0.97	2.93	3.783(4)	147.5
C(2)-H(2B)...O(3)#2	0.97	2.57	3.368(5)	139.7
C(8)-H(8A)...O(3)#2	0.97	2.45	3.311(4)	147.7
C(8)-H(8B)...O(4)#3	0.97	2.31	3.276(5)	171.9
C(10)-H(10)...Cl(2)#1	0.93	2.96	3.714(4)	138.7
C(17)-H(17A)...O(4)#3	0.97	2.63	3.385(5)	134.8
C(18)-H(18A)...Cl(2)#4	0.97	2.89	3.773(4)	151.4
C(18)-H(18B)...O(4)	0.97	2.51	3.348(5)	145.2
C(19)-H(19A)...O(4)#3	0.97	2.38	3.251(4)	148.8
C(19)-H(19B)...O(3)#2	0.97	2.34	3.307(5)	172.8

Table 1.4: Hydrogen bonds for *N*-[(azocan-1-yl)methyl]prop-2-enamide hydrochloride (**5a**.**HCl**) [Å (**d** = distance) and ° (< for angle)].

Symmetry transformations used to generate equivalent atoms:

#1 x,y-1,z #2 -x,-y+1,-z+1 #3 -x+1,-y+1,-z+1 #4 -x+1,-y+2,-z+1

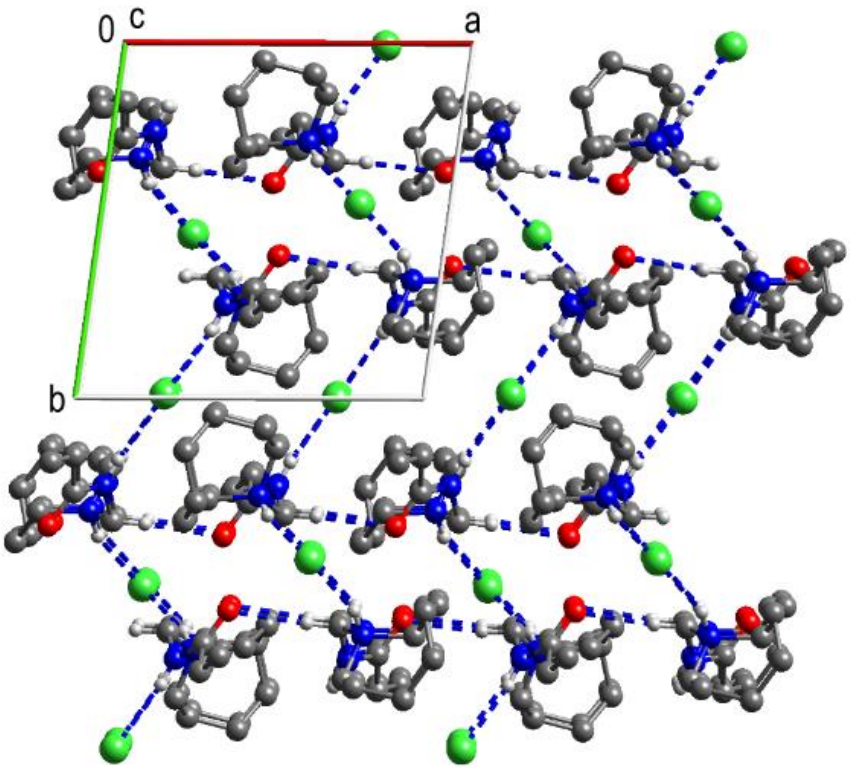

Figure 1.9a: Crystal structure of *N*-[(azocan-1-yl)methyl]prop-2-enamide hydrochloride (**5a**.**HCl**) viewed down the *c*-axis.

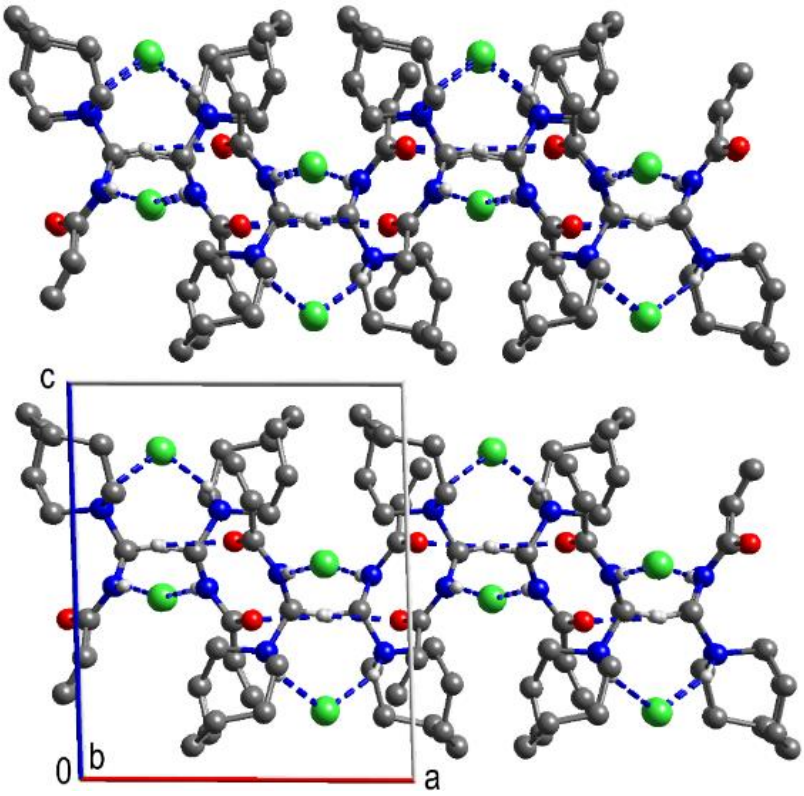

Figure 1.9b: Crystal structure of *N*-[(azocan-1-yl)methyl]prop-2-enamide hydrochloride (**5a**.**HCl**) viewed down the *b*-axis.

For the preparation of *N*-dialkyl substituted monomers, *N*-[(dialkylamino)methyl)]-acrylamides **6a–9a** and *N*-[(dialkylamino)methyl)]methacrylamides **6b–9b**, freshly prepared acyclic Schiff base salts **11c–11f** were reacted with acrylamide and methacrylamide in acetonitrile (Scheme 1.18). In this case however, the isolation of the *N*-dialkyl substituted monomer hydrochloride salts proved difficult due to its appreciable solubility in the reaction solvent and attempted precipitation solvents (including diethyl ether). Thus, basification of the reaction mixture was preferred, and the free monomer bases were isolated in multi-gram quantities (22 – 49 g) in yields of 69–90% without the isolation of the intermediate salts.

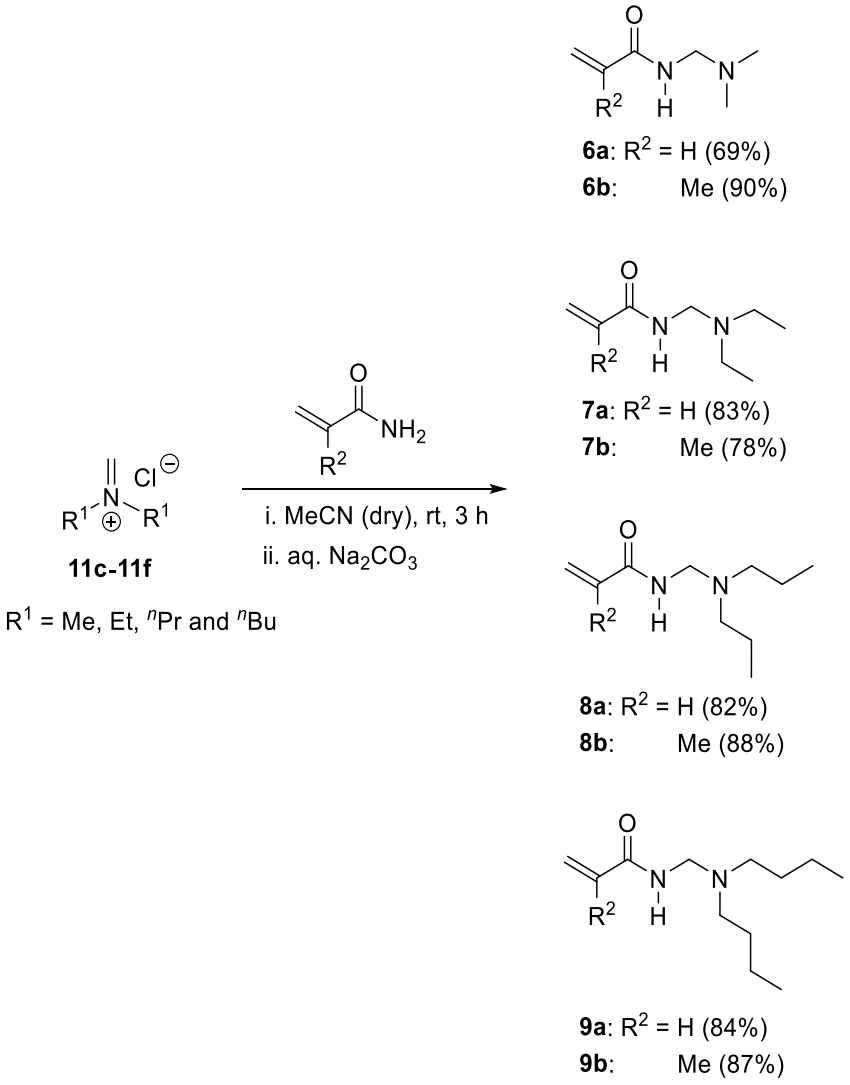

Scheme 1.18: Synthesis of *N*-[(dialkylamino)methyl)]acrylamides **6a–9a** and *N*-[(dialkyl-amino)methyl)]methacrylamides **6b–9b** from the freshly prepared Schiff base salts.

1.4 Conclusions

Readily accessible methylene Schiff base (iminium) salts have allowed the preparation of twenty two previously inaccessible acrylamides and methacrylamides containing β-amino methylated groups (both heterocyclic and acyclic). Heterocyclic substituted monomer syntheses have the added advantage of allowing the isolation of the monomer hydrochloride salt intermediate useful for polymerizations in water. For the preparation of monomers substituted with azepane, azocane, and acyclic derivatives, the iminium salts should be first isolated, prior to reactions with acrylamide and methacrylamide. Iminium salts are however hygroscopic and X-ray crystal structure of the hydrated eight-membered Schiff base salt, 1-(hydroxymethyl)azocan-1-ium chloride (**12b**), and related monomer, *N*-[(azocan-1-yl)methyl]prop-2-enamide hydrochloride (**5a.HCl**) are described.

1.5 Future Work

Future research will involve controlled radical polymerizations (CRP) of this new vinyl monomer class to give amphiphilic block copolymers for use as smart stimuli (temperature, pH, CO_2)-responsive materials. The Aldabbagh group has had a long interest in stimuli-responsive polyacrylamides, in particular well-defined thermoresponsive poly(NIPAM)s.[36-39] Recently Aldabbagh *et al*, carried out by RAFT polymerizations of *N*-(2-morpholin-4-ylethyl)acrylamide (MEA) giving amphiphilic block copolymers containing CO_2-responsive morpholine moieties.[13] It is now proposed to replace MEA with *N*-[(morpholino-4-yl)methyl]-prop-2-enamide (**1a**) for CO_2-responsive properties. ^{1}H NMR can be used to monitor the polymer reaction with CO_2,[13] with chemical shifts reversed upon removal of CO_2 by bubbling of nitrogen gas (Scheme 1.19). All cyclic and non-cyclic tertiary amine containing polymers derived from the monomers prepared in this Chapter will be expected to be CO_2-responsive. By reducing the spacer between the heterocycle and polyacrylamide by CH_2 from *N*-methyl to *N*-ethyl, greater sensitivity to pH and CO_2 is expected.

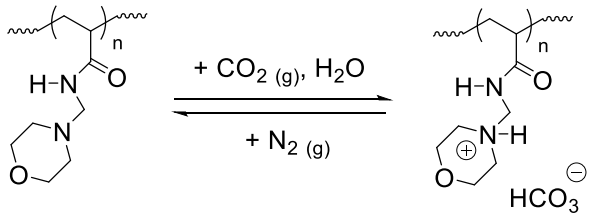

Scheme 1.19: CO_2-responsive moieties.

Self-assembly of amphiphilic block copolymers will be carried out using the method of Zhang and Eisenberg.[40] TEM micrographs of micelles before and after the addition of CO_2 in water will be obtained, as well as, the monitoring of micelle formation by NMR spectroscopy.[13, 41] Solubility of micelles is expected to increase with CO_2 leading to significantly less aggregation, and/or larger particles. A process reversible upon addition of nitrogen gas used to remove dissolved CO_2 (Scheme 1.20). The poly(*tert*-butyl acrylamide, TBAM) block as well as the large hydrophobic RAFT-end group behaves as the hydrophobic block in an AB block copolymer. Such stimuli-responsive polymers have found many applications in the fields of biology and medicine and can be used as sensors and biosensors,[50] drug delivery,[51] chemo-mechanical actuators,[52] environmental remediation,[53] and for many other applications.[54]

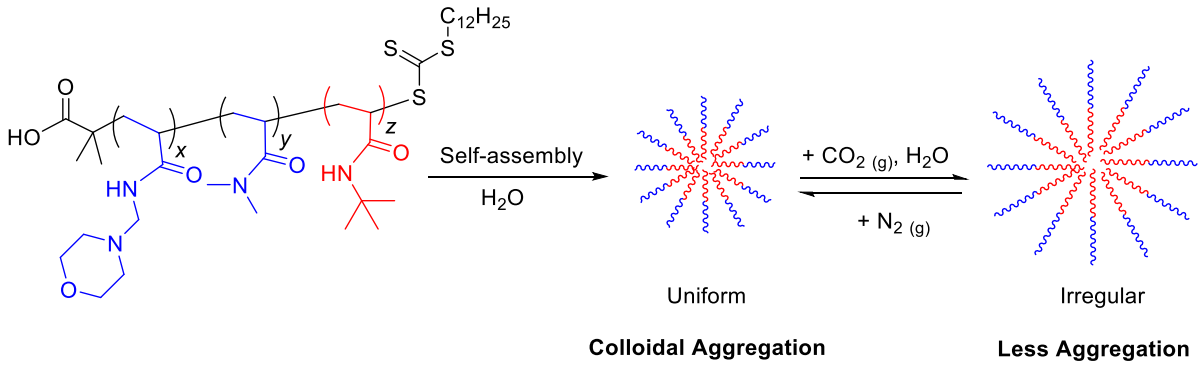

Scheme 1.20: Proposed CO_2-expandable micelles.

Scheme 1.21 shows proposed RAFT polymerizations with high blocking efficiencies using the RAFT agent, 2-(dodecylthiocarbonothioylthio)-2-methylpropionic acid (DDMAT). When beginning with RAFT of TBAM an ABA´ block copolymer can be generated.[13] Where the self-assembly will be more complicated, when the large hydrophobic RAFT dodecyl -$S(C=S)SC_{12}H_{25}$ moiety is attached to the hydrophilic poly(**1a**) block, leading to an ABA′ type-structure. Overall, we propose that a wide range of CO_2-tunable morphologies are accessible using well-defined polyacrylamide block copolymers containing cyclic or non-cyclic tertiary amine moieties.

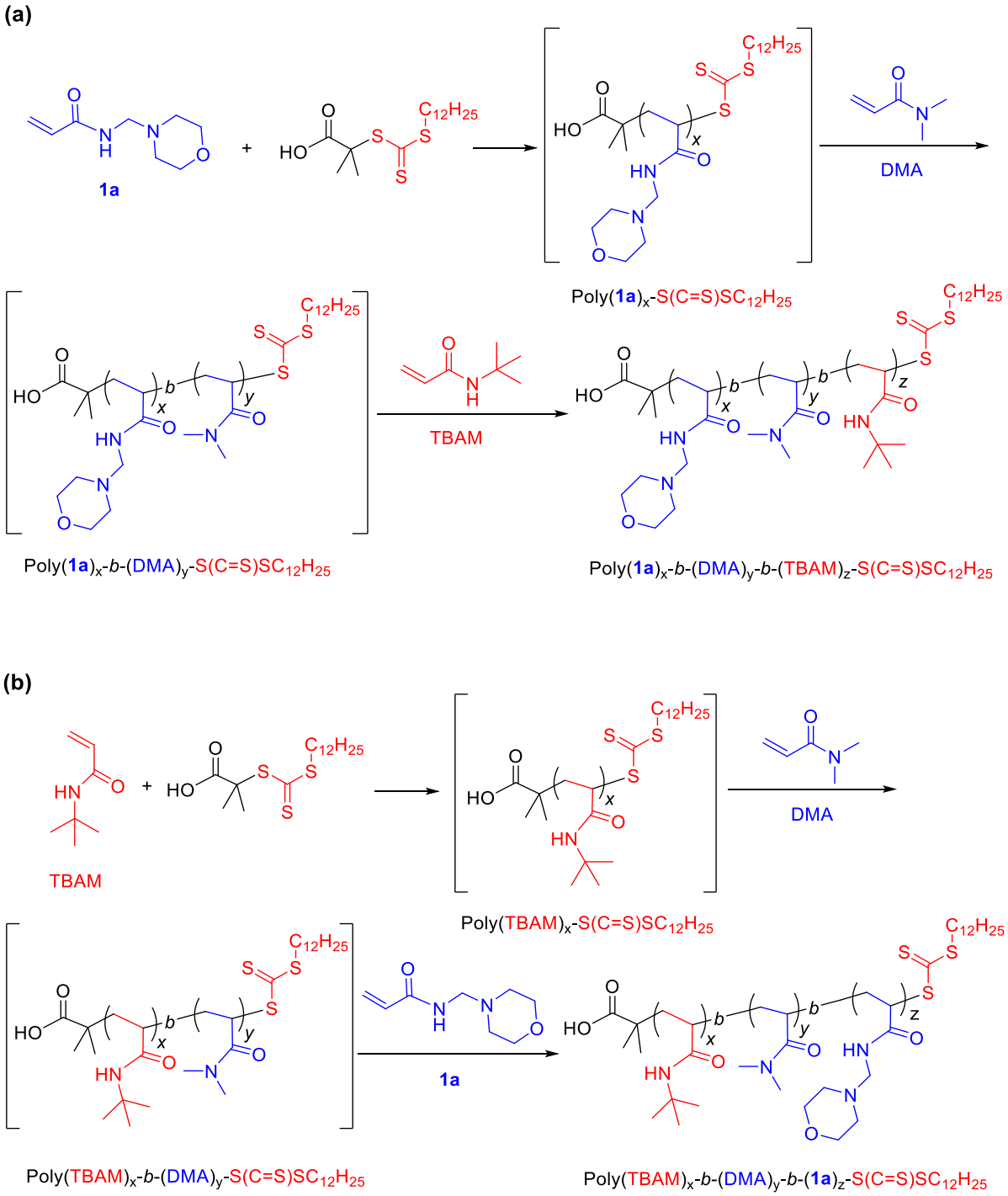

Scheme 1.21: Proposed preparation of poly(**1a**)$_x$-*b*-(DMA)$_y$-*b*-(TBAM)$_z$-S(C=S)SC$_{12}$H$_{25}$ shown in **(a)** and poly(TBAM)$_x$-*b*-(DMA)$_y$-*b*-(**1a**)$_z$-S(C=S)SC$_{12}$H$_{25}$ shown in **(b)** using RAFT polymerization.

1.6 Experimental

1.6.1 General information

Melting points were measured on a Stuart Scientific melting point apparatus SMP1. Infrared spectra were recorded using a Perkin-Elmer Spec 1 with ATR attached. ^{1}H NMR spectra were recorded at 400 or 500 MHz and ^{13}C NMR were recorded at 101 or 125 MHz using JEOL ECX 400 MHz and Varian 500 MHz instrument respectively. The chemical shifts were recorded in ppm relative to Me_4Si. NMR assignments were supported by DEPT. Deuterated solvents were used for homonuclear lock, and the signals were referenced to the deuterated solvent peaks. 1,4-Dioxane was used as a reference for ^{13}C NMR in D_2O. High resolution mass spectra (HRMS) were carried out using ESI time-of-flight mass spectrometer (TOFMS) in positive mode. The precision of all accurate mass measurements was better than 5 ppm. All reactions were performed under inert conditions.

1.6.2 Materials

All chemicals were obtained from commercial sources. Aminals, 4,4′-methylenebis(morpholine),[17] 1,1′-methylenedipyrrolidine,[16] 1,1′-methylenedipiperidine,[17] 1,1′-methylenebis(azepane),[42] *N*,*N*,*N*′,*N*′-tetramethylmethanediamine,[16] *N*,*N*,*N*′,*N*′-tetraethyl-methanediamine,[16] and *N*,*N*,*N*′,*N*′-tetrapropylmethanediamine[18] were readily prepared in high yields from the reaction of formaldehyde (Sigma-Aldrich, 37 wt. % in H_2O) with the appropriate secondary amine accordingly to literature procedures. Distilled aminals were stored under vacuum and dry atmospheres in desiccators at room temperature. Pyrrolidine (Across Organics, 99%), piperidine (Sigma-Aldrich, ≥99%), morpholine (Sigma-Aldrich, ≥99%), dimethylamine (Sigma-Aldrich, 40 wt. % in H_2O), diethylamine (TCI, >99.0%), dipropylamine (Sigma-Aldrich, ≥99%), dibutylamine (Sigma-Aldrich, ≥99.5%), hexamethyleneimine (azepane, TCI, >98.0%), heptamethyleneimine (azocane, TCI, >98.0%), acetyl chloride (AcCl, Sigma-Aldrich, 98%), acrylamide (Sigma-Aldrich, 97%), methacrylamide (Sigma-Aldrich, 98%), 1,4-dioxane (Sigma-Aldrich, ≥99.0%), acetonitrile (MeCN, Sigma-Aldrich, ≥99.9%), dichloromethane (CH_2Cl_2, Sigma-Aldrich, ≥99%), diethyl ether (Et_2O, Sigma-Aldrich, ≥99.5%), chloroform-d ($CDCl_3$, Sigma-Aldrich, 99.8 atom%), deuterium oxide (D_2O, Sigma-Aldrich, 99.9 atom%), dimethyl sulfoxide (DMSO-d_6, Sigma-Aldrich, ≥99.9%), potassium hydroxide pellets (KOH, Fisher Chemical, ≥85.0%), sodium carbonate (Na_2CO_3, Sigma-Aldrich, ≥99%), magnesium sulphate anhydrous ($MgSO_4$, Sigma-Aldrich, ≥99.99%), were used as received. The synthesis of *N*-[(morpholin-4-yl)methyl]prop-

2-enamide hydrochloride (**1a.HCl**), *N*-[(morpholin-4-yl)methyl]prop-2-enamide (**1a**), *N*-[(pyrrolidin-1-yl)methyl]prop-2-enamide hydrochloride (**2a.HCl**), *N*-[(pyrrolidin-1-yl)methyl]-prop-2-enamide (**2a**), *N*-[(piperidin-1-yl)methyl]prop-2-enamide hydrochloride (**3a.HCl**) and *N*-[(piperidin-1-yl)methyl]-prop-2-enamide (**3a**) are included in Gerard Hawkins Ph.D. thesis, and in our recent communication.[14, 35] For the Schiff base salts and the monomer synthesis all solvents were freshly distilled, and reactions were carried out using anhydrous solvents using an inert nitrogen atmosphere. MeCN was freshly distilled over 3 Å molecular sieves and then CaH_2 (Sigma-Aldrich, 95%), and Et_2O was freshly distilled over Na wire and benzophenone (Sigma-Aldrich, 95%).

1.6.3 Synthesis of *N*-[(cycloalkylamino)methyl)]acrylamides and *N*-[(cycloalkylamino)-methyl)]methacrylamides using the *in situ* Schiff base salt approach

AcCl (14.30 mL, 0.20 mol) was added over 30 min to a stirred solution of aminal (0.20 mol) in MeCN (40 mL) at *ca*. 0 °C. Methacrylamide (17.02 g, 0.20 mol) solution in MeCN (40 mL) was added, and stirred at 20 °C for 2 hours. Et_2O (200 mL) was added and the hydrochloride salt of the monomer precipitated, filtered, and dried under vacuum. The hydrochloride salts (**1a.HCl–3b.HCl**) were recrystallized, dried, and characterized. An aqueous solution of Na_2CO_3 (100 mL, 3M) was added to a suspension of the hydrochloride salt in CH_2Cl_2 (100 mL) and stirred for 30 min. The organic layer was separated, and the aqueous layer washed with CH_2Cl_2 (4 x 250 mL). The combined organic extracts were dried ($MgSO_4$), filtered, and evaporated to dryness to give the monomer, which was recrystallized.

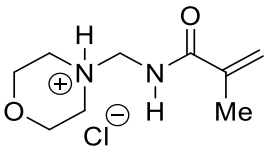

1b.HCl

2-Methyl-*N*-[(morpholin-4-yl)methyl]prop-2-enamide hydrochloride (1b.HCl). white solid, mp 123–125°C (recryst. from MeCN); ^{1}H NMR (400 MHz, DMSO-d_6) δ 1.91 (s, 3H), 2.96–3.33 (m, 4H), 3.69–4.01 (m, 4H), 4.50 (d, *J* 6.7 Hz, 2H), 5.59 (s, 1H), 5.95 (s, 1H), 9.16–9.25 (brs, 1H), 10.84–11.22 (m, 1H); ^{13}C NMR (101 MHz, DMSO-d_6) δ 18.4 (Me), 48.7, 59.2, 62.9, 122.0 (all CH_2), 138.4 (C), 169.8 (C=O).

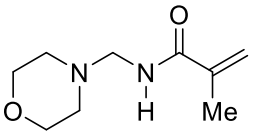

1b

2-Methyl-*N*-[(morpholin-4-yl)methyl]prop-2-enamide (1b). (30.2 g, 82%) white solid, mp 56–58°C (recryst. from MeCN), ν_{max} (neat, cm^{-1}) 3315, 2960, 2853, 1655 (C=O), 1616, 1523, 1453, 1295, 1216, 1139, 1049, 1014; ^{1}H NMR (400 MHz, $CDCl_3$) δ 1.97 (s, 3H), 2.57 (t, *J* 4.7 Hz, 4H), 3.70 (t, *J* 4.7 Hz, 4H), 4.15 (d, *J* 6.4 Hz, 2H), 5.36–5.37 (m, 1H), 5.70–5.74 (m, 1H), 6.15–6.25 (brs, 1H); ^{13}C NMR (101 MHz, $CDCl_3$) δ 18.8 (Me), 50.5, 61.6, 66.9, 119.9 (all CH_2), 140.0 (C), 169.0 (C=O); HRMS (ESI) *m/z* $[M+H]^+$, $C_9H_{17}N_2O_2$ calcd 185.1290, observed 185.1371.

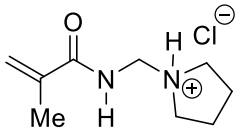

2b.HCl

2-Methyl-*N*-[(pyrrolidin-1-yl)methyl]prop-2-enamide hydrochloride (2b.HCl). white solid; mp 131–133 °C (recryst. from MeCN); ^{1}H NMR (400 MHz, DMSO-d_6) δ 1.87–1.94 (m, 7H), 3.05–3.41 (m, 4H), 4.49 (d, *J* 6.7 Hz, 2H), 5.55–5.57 (m, 1H), 5.92–5.94 (m, 1H), 9.33–9.36 (t, *J* 6.7 Hz 1H, NH), 10.61–10.94 (brs, 1H, NH); ^{13}C NMR (101 MHz, DMSO-d_6) δ 18.4 (Me), 22.9, 50.4, 56.4, 122.0 (all CH_2), 138.4 (C), 168.8 (C=O).

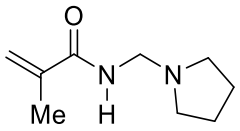

2b

2-Methyl-*N*-[(pyrrolidin-1-yl)methyl]prop-2-enamide (2b). (30.29 g, 90%), white solid; mp 56–58 °C (recryst. from MeCN); ν_{max} (neat, cm^{-1}) 3215, 2962, 2819, 1655, 1619, 1521 (C=O), 1450, 1362, 1356, 1299, 1208, 1134, 1046; ^{1}H NMR (400 MHz, $CDCl_3$) δ 1.75–1.79 (m, 4H), 1.96 (s, 3H), 2.62 (t, *J* 6.4 Hz, 4H), 4.24 (dd, *J* 0.7, 6.2 Hz, 2H), 5.33–5.34 (m, 1H), 5.69–5.70 (m, 1H), 6.17–6.31 (brs, 1H, NH); ^{13}C NMR (101 MHz, $CDCl_3$) δ 18.8 (Me), 23.7, 51.0, 58.6, 119.8 (all CH_2), 140.1 (C), 168.7 (C=O); HRMS (ESI) m/z $[M+H]^+$, $C_9H_{17}N_2O$ calcd. 169.1341 observed 169.1334.

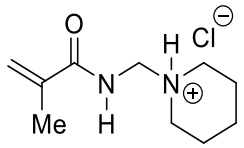

3b.HCl

2-Methyl-*N*-[(piperidin-1-yl)methyl]prop-2-enamide hydrochloride (3b.HCl). white solid; mp 143–145 °C (recryst. from MeCN); ^{1}H NMR (400 MHz, DMSO-d_6) δ 1.34–1.76 (m, 6H), 1.91 (s, 3H), 2.82–2.85 (m, 2H), 3.26–3.29 (m, 2H), 4.42 (d, *J* 6.6 Hz, 2H), 5.56 (s, 1H), 5.92 (s, 1H), 9.13 (t, *J* 6.6 Hz, 1H, NH), 10.12–10.32 (brs, 1H, NH); ^{13}C NMR (101 MHz, DMSO-d_6) δ 18.4 (Me), 21.2, 22.1, 49.7, 59.1, 121.9 (all CH_2), 138.4 (C), 168.7 (C=O).

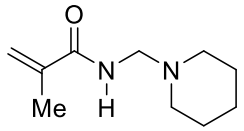

3b

2-Methyl-*N*-[(piperidin-1-yl)methyl]prop-2-enamide (3b). (33.54 g, 92%), white solid; mp 67–69 °C (recryst. from MeCN); ν_{max} (neat, cm^{-1}) 3353, 2934, 2852, 1671 (C=O), 1655, 1615, 1453, 1453, 1440, 1368, 1333, 1306, 1158, 1110, 1034; ^{1}H NMR (400 MHz, $CDCl_3$) δ 1.38–1.44 (m, 2H), 1.54–1.59 (m, 4H), 1.95 (s, 3H), 2.45–2.59 (m, 4H), 4.10 (d, *J* 6.4 Hz, 2H), 5.34 (s, 1H), 5.71 (s, 1H), 6.29–6.38 (brs, 1H, NH); ^{13}C NMR (101 MHz, $CDCl_3$) δ 18.8 (Me), 24.2, 25.9, 51.6, 62.4, 119.8 (all CH_2), 140.2 (C), 168.9 (C=O); HRMS (ESI) m/z $[M+H]^+$, $C_{10}H_{19}N_2O$ calcd. 183.1497 observed 183.1493.

1.6.4 Synthesis of 1,1'-methylenebis(azocane) (10e)

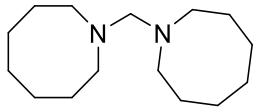

Heptamethyleneimine (17.70 mL, 0.13 mol) was added over 30 min to formaldehyde (37 wt. % in H_2O, 6.20 mL, 0.07 mol) with stirring at *ca*. 0 °C. The solution was stirred overnight at *ca*. 20 °C, after which KOH pellets were added to form a saturated solution, and stirring was continued for 30 min. H_2O (40 mL) was added and the mixture extracted with Et_2O (4 x 40 mL). The organic layers were combined and washed with H_2O (3 x 20 mL), dried ($MgSO_4$), and evaporated to dryness. Fractional distillation under reduced pressure gave *the title compound* as colorless liquid (14.69 g, 88%); bp 138–140 °C (0.25 mmHg); ν_{max} (neat, cm^{-1}) 2915, 2846, 2779, 1657, 1472, 1448, 1358, 1250, 1158, 1094, 1046, 1017; ^{1}H NMR (400 MHz, $CDCl_3$) δ 1.51–1.68 (m, 20H), 2.53–2.60 (m, 8H), 3.02 (s, 2H); ^{13}C NMR (101 MHz, $CDCl_3$) δ 26.1, 27.9, 28.2, 52.9, 83.8 (all CH_2); HRMS (ESI) m/z $[M+H]^+$, $C_{15}H_{31}N_2$, calcd. 239.2487, observed 239.2312.

1.6.5 Synthesis of *N,N,N',N'*-tetrabutylmethanediamine (10i)

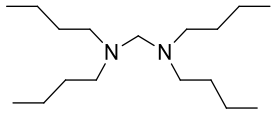

Dibutylamine (68.00 mL, 0.40 mol) was added over 30 min to formaldehyde (37 wt. % in H_2O, 15.00 mL, 0.20 mol) with stirring at *ca*. 0 °C. The solution was stirred overnight at *ca*. 20 °C, after which KOH pellets were added to form a saturated solution, and the drying agent was removed. Fractional distillation under reduced pressure gave *the title compound* as colorless liquid (45.98 g, 85%); bp 112–114 °C (0.25 mmHg); ν_{max} (neat, cm^{-1}) 2956, 2929, 2861, 2798, 1466, 1376, 1305, 1243, 1184, 1079, 1029, 1094, 1046, 1017; ^{1}H NMR (400 MHz, $CDCl_3$) δ 0.89 (t, *J* 7.3 Hz, 12H), 1.28 (sext, *J* 7.3 Hz, 8H), 1.33–1.41 (m, 8H), 2.42 (t, *J* 7.3 Hz, 8H), 2.98 (s, 2H); ^{13}C NMR (101 MHz, $CDCl_3$) δ 14.3 (Me), 20.9, 29.5, 52.0, 75.6 (all CH_2); HRMS (ESI) m/z $[M+H]^+$, $C_{17}H_{39}N_2$ calcd. 271.3113 observed 271.3143.

1.6.6 Synthesis of Schiff base salts

AcCl (21.33 mL, 0.30 mol) was added over 30 min to a stirred solution of aminal (0.30 mol) in Et_2O (150 mL) at *ca*. 0 °C, and the resulting white precipitate stirred for an additional of 30 min. Et_2O (200 mL) was added and the precipitate filtered, and dried under vacuum to give the methylene Schiff-base salt (**11a–11f**). Iminium salts **11a–11f** were immediately used in addition reactions with acrylamide and methacrylamide due to their hygroscopic nature.

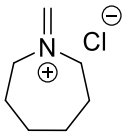

11a

1-Methylideneazepan-1-ium chloride (11a). (white solid, 43.85 g, 99%); was characterized as ***N*-(hydroxymethyl)azepan-1-ium chloride (12a).** ^{1}H NMR (400 MHz, D_2O) δ 1.63–1.66 (m, 4H), 1.78–1.85 (brs, 4H), 3.17–3.21 (m, 4H), 4.77 (d, *J* 0.8 Hz, 2H); ^{13}C NMR (101 MHz, D_2O, 1,4-dioxane added) δ 25.2, 26.6, 46.8, 82.4 (all CH_2).

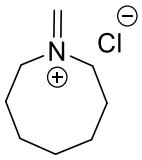

11b

1-Methylideneazocan-1-ium chloride (11b). (white solid, 47.04 g, 97%) was characterized as ***N*-(hydroxymethyl)azocan-1-ium chloride (12b).** ^{1}H NMR (500 MHz, D_2O) δ 1.57–1.67 (m, 6H), 1.81–1.86 (m, 4H), 3.21 (t, *J* 5.8 Hz, 4H), 4.74 (s, 2H); ^{13}C NMR (125 MHz, D_2O, 1,4-dioxane added) δ 23.9, 24.8, 25.2, 45.8, 82.4 (all CH_2).

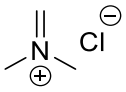

11c

***N,N*-Dimethylmethaniminium chloride (11c).**[44] (white solid, 23.85 g, 85%) was characterized as **hydroxy-*N,N*-dimethylmethaniminium chloride (12c).** ^{1}H NMR (400 MHz, D_2O) δ 2.79 (s, 6H), 4.56 (s, 2H); ^{13}C NMR (101 MHz, D_2O, 1,4-dioxane added) δ 35.2 (Me), 82.4 (CH_2).

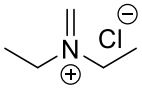

11d

***N,N*-Diethylmethaniminium chloride (11d).**[45] (white solid, 31.74 g, 87%) was characterized as ***N*-ethyl-*N*-(hydroxymethyl)ethaniminium chloride (12d).** ^{1}H NMR (400 MHz, D_2O) δ 1.23 (t, *J* 7.3 Hz, 6H), 3.00–3.07 (m, 4H), 4.78 (s, 2H); ^{13}C NMR (101 MHz, D_2O, 1,4-dioxane added) δ 11.2 (Me), 42.9, 82.4 (both CH_2).

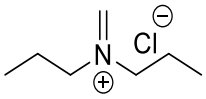

11e

***N,N*-Dipropylmethaniminium chloride (11e).**[22,45] (white solid, 40.85 g, 91%) was characterized as ***N*-(hydroxymethyl)-*N*-propylpropan-1-iminium chloride (12e).** ^{1}H NMR (400 MHz, D_2O) δ 0.92 (t, *J* 7.6 Hz, 6H), 1.65 (sext, *J* 7.6 Hz, 4H), 2.95 (t, *J* 7.6 Hz, 4H), 4.78 (s, 2H); ^{13}C NMR (101 MHz, D_2O, 1,4-dioxane added) δ 10.8 (Me), 19.7, 49.7, 82.4 (all CH_2).

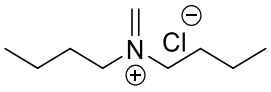

11f

***N,N*-Dibutylmethaniminium chloride (11f).**[45] (white solid, 44.78 g, 84%) was characterized as ***N*-butyl-*N*-(hydroxymethyl)butan-1-iminium chloride (12f).** ^{1}H NMR (400 MHz, D_2O) δ 0.93 (t, *J* 6.0 Hz, 6H), 1.39 (sext, *J* 6.0 Hz, 4H), 1.66 (quint, *J* 6.0 Hz, 4H), 3.04 (t, *J* 6.0 Hz, 4H), 4.83 (s, 2H); ^{13}C NMR (101 MHz, D_2O, 1,4-dioxane added) δ 13.4 (Me), 19.8, 28.2, 47.9, 82.4 (all CH_2).

1.6.7 Synthesis of seven and eight-membered *N*-[(cycloalkylamino)methyl)]acrylamides and *N*-[(cycloalkylamino)methyl)]methacrylamides

A solution of acrylamide or methacrylamide (0.03 mol) in MeCN (10 mL) was added to a solution of freshly prepared Schiff base salt **11a** or **11b** (0.04 mol) in MeCN (30 mL) and stirred at *ca*. 20 °C for 4 h. Et_2O (200 mL) was added and the hydrochloride salt of the monomer precipitated, filtered, and dried under vacuum. The hydrochloride salt (**4a.HCl–4b.HCl** and **5a.HCl–5b.HCl**) was recrystallized, dried, and characterized. An aqueous solution of Na_2CO_3 (15 mL, 3M) was added to a suspension of the hydrochloride salt in CH_2Cl_2 (20 mL) and left to stir for an additional 30 min and extracted with CH_2Cl_2 (4 x 50 mL). The organic layer was dried ($MgSO_4$), filtered and evaporated to dryness to give the corresponding monomers **4a–4b** and **5a–5b**.

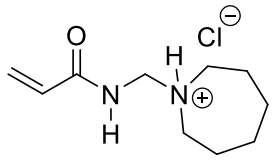

4a.HCl

***N*-[(Azepan-1-yl)methyl]prop-2-enamide hydrochloride (4a.HCl).** white solid; mp 136–138 °C (recryst. from MeCN); ^{1}H NMR (400 MHz, DMSO-d_6) δ 1.55–1.62 (m, 4H), 1.79–1.82 (m, 4H), 3.03–3.09 (m, 2H), 3.23–3.32 (m, 2H), 4.49 (d, *J* 6.8 Hz, 2H), 5.80 (dd, *J* 1.9, 10.2 Hz, 1H), 6.26 (dd, *J* 1.9, 17.2 Hz, 1H), 6.41 (dd, *J* 10.2, 17.2 Hz, 1H), 9.53 (t, *J* 6.8 Hz, 1H, NH), 10.46–10.63 (brs, 1H, NH); ^{13}C NMR (101 MHz, DMSO-d_6) δ 22.9, 26.1, 51.3, 59.2, 128.2 (all CH_2), 130.4 (CH), 166.2 (C=O).

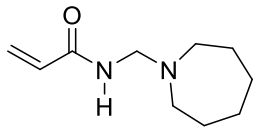

4a

***N*-[(Azepan-1-yl)methyl]prop-2-enamide (4a).** (4.81 g, 88%) colourless liquid; bp 134–136 °C (0.25 mmHg); ν_{max} (neat, cm^{-1}) 3278, 2922, 2852, 2852, 1656 (C=O), 1623, 1539, 1452, 1405, 1365, 1309, 1227, 1133, 1080; ^{1}H NMR (400 MHz, $CDCl_3$) δ 1.52–1.61 (m, 8H), 2.68 (t, *J* 5.6 Hz, 4H), 4.23 (d, *J* 6.2 Hz, 2H), 5.61 (dd, *J* 1.6, 10.2 Hz, 1H), 6.11 (dd, *J* 10.2, 17.0 Hz, 1H), 6.25 (dd, *J* 1.6, 17.0 Hz, 1H), 6.31–6.40 (brs, 1H, NH); ^{13}C NMR (101 MHz, $CDCl_3$) δ 26.9, 28.6, 53.1, 62.6, 126.7 (all CH_2), 131.1 (CH), 166.1 (C=O); HRMS (ESI) m/z $[M+H]^+$, $C_{10}H_{19}N_2O$ calcd. 183.1497 observed 183.1516.

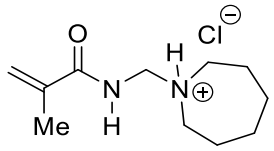

4b.HCl

***N*-[(Azepan-1-yl)methyl]-2-methylprop-2-enamide hydrochloride (4b.HCl).** white solid; mp 88–90 °C (recryst. from THF); ^{1}H NMR (400 MHz, DMSO-d_6) δ 1.53–1.64 (m, 4H), 1.79–1.81 (m, 4H), 1.91 (s, 3H), 3.02–3.15 (m, 2H), 3.23–3.30 (m, 2H), 4.46 (d, J 4.3 Hz, 2H), 5.57 (s, 1H), 5.92 (s, 1H), 9.19 (m, 1H, NH), 10.28–10.44 (brs, 1H, NH); ^{13}C NMR (101 MHz, DMSO-d_6) δ 18.4 (Me), 22.8, 26.2, 51.4, 59.7, 122.0 (all CH_2), 138.4 (C), 168.7 (C=O).

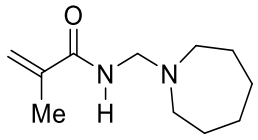

4b

***N*-[(Azepan-1-yl)methyl]-2-methylprop-2-enamide (4b).** (5.36 g, 91%) colourless liquid; bp 139–141 °C (0.25 mmHg); ν_{max} (neat, cm^{-1}) 3328, 2923, 2852, 1655, 1616 (C=O), 1526, 1373, 1313, 1201, 1133, 1088, 1020; ^{1}H NMR (400 MHz, $CDCl_3$) δ 1.56–1.68 (m, 8H), 1.96 (s, 3H), 2.72 (t, J 5.5 Hz, 4H), 4.24 (d, J 6.1 Hz, 2H), 5.33 (s, 1H), 5.69 (s, 1H), 6.12–6.22 (brs, 1H, NH); ^{13}C NMR (101 MHz, $CDCl_3$) δ 18.8 (Me), 27.0, 28.6, 53.2, 62.7, 119.6 (all CH_2), 140.3 (C), 168.8 (C=O); HRMS (ESI) m/z [M+H]$^+$, $C_{11}H_{21}N_2O$ calcd. 197.1654 observed 197.1708.

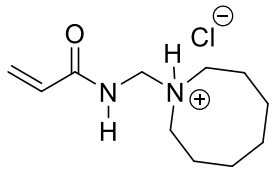

5a.HCl

***N*-[(Azocan-1-yl)methyl]prop-2-enamide hydrochloride (5a.HCl).** white solid; mp 87–89 °C (recryst. from EtOAc); ^{1}H NMR (400 MHz, DMSO-d_6) δ 1.43–1.70 (m, 6H), 1.76–1.96 (m, 4H), 3.10–3.16 (m, 2H), 3.22–3.32 (m, 2H), 4.48–4.68 (m, 2H), 5.69 (d, *J* 10.1 Hz, 1H), 6.25 (d, *J* 17.1 Hz, 1H), 6.43 (dd, *J* 10.1, 17.1 Hz, 1H), 9.58–9.67 (m, 1H, NH), 10.25–10.38 (brs, 1H, NH); ^{13}C NMR (101 MHz, DMSO-d_6) δ 22.1, 24.0, 25.1, 48.8, 59.2, 128.2 (all CH_2), 130.4 (CH), 166.2 (C=O).

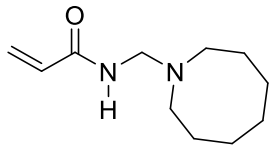

5a

***N*-[(Azocan-1-yl)methyl]prop-2-enamide (5a).** (5.30 g, 90%) colourless oil; ν_{max} (neat, cm^{-1}) 3328, 2917, 2850, 1657 (C=O), 1624, 1536, 1363, 1232, 1162, 1095, 1060; ^{1}H NMR (400 MHz, $CDCl_3$) δ 1.50–1.62 (m, 10H), 2.62–2.70 (m, 4H), 4.27 (d, *J* 6.0 Hz, 2H), 5.65 (d, *J* 10.2 Hz, 1H), 5.91–6.02 (brs, 1H), 6.10 (dd, *J* 10.2, 17.0 Hz, 1H), 6.28 (d, *J* 17.0 Hz, 1H); ^{13}C NMR (101 MHz, $CDCl_3$) δ 26.1, 27.7, 28.0, 51.6, 62.6, 126.7 (all CH_2), 131.2 (CH), 166.0 (C=O); HRMS (ESI) m/z $[M+H]^+$, $C_{11}H_{21}N_2O$, calcd. 197.1656, observed 197.1654.

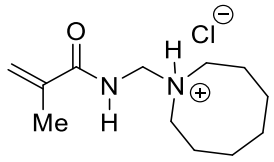

5b.HCl

***N*-[(Azocan-1-yl)methyl]-2-methylprop-2-enamide hydrochloride (5b.HCl).** white solid; mp 128–130 °C (recryst. from EtOAc); ^{1}H NMR (400 MHz, DMSO-d_6) δ 1.46–1.75 (m, 6H), 1.81–1.99 (m, 7H), 3.07–3.18 (m, 2H), 3.23–3.35 (m, 2H), 4.45–4.53 (m, 2H), 5.70 (s, 1H), 5.93 (s, 1H), 9.17–9.27 (brs, 1H, NH), 9.94–10.09 (brs, 1H, NH); ^{13}C NMR (101 MHz, DMSO-d_6) δ 18.4 (Me), 22.2, 24.0, 25.0, 48.9, 59.8, 122.0 (all CH_2), 138.4 (C), 168.6 (C=O).

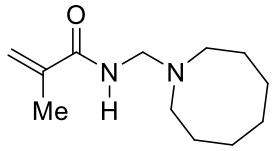

5b

***N*-[(Azocan-1-yl)methyl]-2-methylprop-2-enamide (5b).** (5.30 g, 84%) colourless oil; ν_{max} (neat, cm^{-1}) (neat, cm^{-1}) 3324, 2918, 2850, 1655, 1618 (C=O), 1523, 1452, 1363, 1201, 1162, 1095, 1060; ^{1}H NMR (400 MHz, $CDCl_3$) δ 1.49–1.59 (m, 10H), 1.93 (s, 3H), 2.61–2.66 (m, 4H), 4.21 (t, J 4.3 Hz, 2H), 5.28 (s, 1H), 5.64 (s, 1H), 6.12–6.26 (brs, 1H, NH); ^{13}C NMR (101 MHz, $CDCl_3$) δ 18.8 (Me), 26.0, 27.7, 28.0, 51.5, 62.7, 119.2 (all CH_2), 140.4 (C), 168.9 (C=O); HRMS (ESI) m/z $[M+H]^+$, $C_{12}H_{23}N_2O$, calcd. 211.1838, observed 211.1810.

1.6.8 Synthesis of *N*-[(dialkylamino)methyl)]acrylamides and *N*-[(dialkylamino)-methyl)]methacrylamides

A solution of acrylamide or methacrylamide (0.25 mol) in MeCN (50 mL) was added to a stirred solution of freshly prepared Schiff base salt **11c–11f** (0.25 mol) in MeCN (50 mL) and stirred at *ca*. 20 °C for 3 hours. An aqueous solution of Na_2CO_3 (150 mL, 3M) was added and the solution stirred for an additional of 30 min and extracted with CH_2Cl_2 (4 x 250 mL). The organic layer was dried ($MgSO_4$), filtered and evaporated to give the corresponding acrylamides **6a–9a** and methacrylamides **6b–9b**.

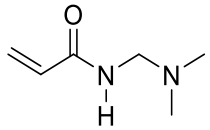

6a

***N*-[(Dimethylamino)methyl]prop-2-enamide (6a).** (22.11 g, 69%) colourless liquid; bp 64–66 °C (760 mmHg); ν_{max} (neat, cm^{-1}) 3281, 2942, 2827, 2780, 1659 (C=O), 1625, 1536, 1407, 1230, 1029; ^{1}H NMR (400 MHz, $CDCl_3$) δ 2.24 (s, 6H), 4.05 (d, *J* 6.4 Hz, 2H), 5.62 (dd, *J* 1.6, 10.2 Hz, 1H), 6.12 (dd, *J* 10.2, 17.0 Hz, 1H), 6.26 (dd, *J* 1.6, 17.0 Hz, 1H), 6.71–6.82 (brs, 1H); ^{13}C NMR (101 MHz, $CDCl_3$) δ 41.8 (Me), 61.5, 126.0 (both CH_2), 130.7 (CH), 166.2 (C=O); HRMS (ESI) *m/z* $[M+H]^+$, $C_6H_{13}N_2O$, calcd. 129.1028, observed 129.1026.

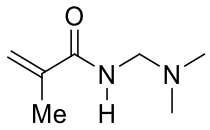

6b

***N*-[(Dimethylamino)methyl]-2-methylprop-2-enamide (6b).** (32.10 g, 90%) colourless liquid, bp 60–62 °C (0.25 mmHg); ν_{max} (neat, cm^{-1}) 3323, 2942, 2827, 1658 (C=O), 1619, 1523, 1453, 1311, 1196, 1049, 1033; ^{1}H NMR (400 MHz, $CDCl_3$) δ 1.92 (s, 3H), 2.23 (s, 6H), 4.03 (d, *J* 6.3 Hz, 2H), 5.30 (s, 1H), 5.66 (s, 1H), 6.31–6.45 (brs, 1H); ^{13}C NMR (101 MHz, $CDCl_3$) δ 18.7, 42.3 (both Me), 62.2, 119.5 (both CH_2), 140.1 (C), 169.0 (C=O); HRMS (ESI) *m/z* $[M+H]^+$, $C_7H_{15}N_2O$ calcd 143.1184, observed 143.1180.

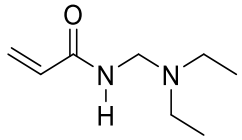

7a

***N*-[(Diethylamino)methyl]prop-2-enamide (7a).** (32.39 g, 83%) yellow oil; bp 65–67 °C (0.25 mmHg); ν_{max} (neat, cm^{-1}) 3289, 2969, 2828, 1657 (C=O), 1624, 1536, 1464, 1233, 1206, 1067; ^{1}H NMR (400 MHz, $CDCl_3$) δ 1.08 (t, *J* 7.2 Hz, 6H), 2.56 (q, *J* 7.2 Hz, 4H), 4.29 (d, *J* 6.1 Hz, 2H), 5.64 (dd, *J* 1.4, 10.2 Hz, 1H), 5.90–5.99 (brs, 1H), 6.09 (dd, *J* 10.2, 17.0 Hz, 1H), 6.28 (dd, *J* 1.4, 17.0 Hz, 1H); ^{13}C NMR (101 MHz, $CDCl_3$) δ 12.7 (Me), 45.4, 56.9, 126.6 (all CH_2), 131.0 (CH), 166.1 (C=O); HRMS (ESI) *m/z* $[M+H]^+$, $C_8H_{17}N_2O$, calcd. 157.1341, observed 157.1337.

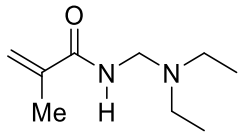

7b

***N*-[(Diethylamino)methyl]-2-methylprop-2-enamide (7b).** (33.21 g, 78%) colourless liquid, bp 72–74 °C (0.25 mmHg); ν_{max} (neat, cm^{-1}) 3344, 2970, 2827, 1656 (C=O), 1617, 1522, 1455, 1375, 1197, 1066, 1046; ^{1}H NMR (400 MHz, $CDCl_3$) δ 1.03 (t, *J* 7.2 Hz, 6H), 1.90 (s, 3H), 2.52 (q, *J* 7.2 Hz, 4H), 4.22 (d, *J* 6.0 Hz, 2H), 5.27 (s, 1H), 5.63 (s, 1H), 6.11–6.21 (brs, 1H); ^{13}C NMR (101 MHz, $CDCl_3$) δ 12.7, 18.8 (both Me), 45.4, 57.3, 119.5 (all CH_2), 140.2 (C), 168.9 (C=O); HRMS (ESI) *m/z* $[M+H]^+$, $C_9H_{19}N_2O$ calcd. 171.1497, observed 171.1789.

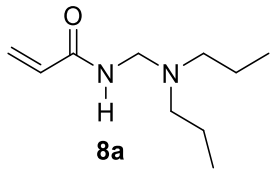

8a

***N*-[(Dipropylamino)methyl]prop-2-enamide (8a).** (37.80 g, 82%) colourless plates, mp 25–26 °C; ν_{max} (neat, cm^{-1}) 3269, 2959, 2930, 1657 (C=O), 1623, 1550, 1457, 1246, 1185, 1069; ^{1}H NMR (500 MHz, $CDCl_3$) δ 0.82 (t, *J* 7.4 Hz, 6H), 1.44 (sext, *J* 7.4 Hz, 4H), 2.39 (t, *J* 7.4 Hz, 4H), 4.23 (d, *J* 6.0 Hz, 2H), 5.58 (dd, *J* 1.6, 10.2 Hz, 1H), 6.11 (dd, *J* 10.2, 17.0 Hz, 1H), 6.22 (dd, *J* 1.6, 17.0 Hz, 1H), 6.28–6.39 (brs, 1H); ^{13}C NMR (125 MHz, $CDCl_3$) δ 11.9 (Me), 20.9, 54.0, 58.1, 126.5 (all CH_2), 131.1 (CH DEPT up issue), 166.1 (C=O); HRMS (ESI) *m/z* $[M+H]^+$, $C_{10}H_{21}N_2O$ calcd. 185.1654, observed 185.1663.

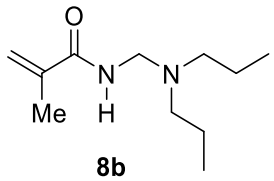

8b

***N*-[(Dipropylamino)methyl]-2-methylprop-2-enamide (8b).** (43.62 g, 88%) colourless liquid, bp 86–88 °C (0.25 mmHg); ν_{max} (neat, cm^{-1}) 3316, 2959, 2934, 2873, 1655 (C=O), 1619, 1524, 1456, 1374, 1183, 1075, 1052; ^{1}H NMR (400 MHz, $CDCl_3$) δ 0.85 (t, *J* 7.4 Hz, 6H), 1.46 (sext, *J* 7.4 Hz, 4H), 1.93 (s, 3H), 2.42 (t, *J* 7.4 Hz, 4H), 4.22 (d, *J* 6.0 Hz, 2H), 5.29 (s, 1H), 5.65 (s, 1H), 6.02–6.15 (brs, 1H); ^{13}C NMR (101 MHz, $CDCl_3$) δ 11.9, 18.8 (both Me), 20.9, 54.1, 58.5, 119.4 (all CH_2), 140.3 (C), 168.9 (C=O); HRMS (ESI) *m/z* $[M+H]^+$, $C_{11}H_{23}N_2O$ calcd. 199.1810, observed 199.1800.

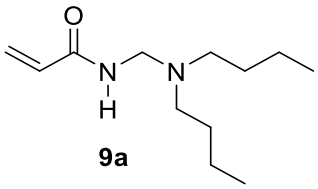

9a

***N*-[(Dibutylamino)methyl]prop-2-enamide (9a).** (44.56 g, 84%) colourless liquid, bp 124–126 °C (0.25 mmHg); ν_{max} (neat, cm^{-1}) 3281, 3069, 2957, 2863, 1658 (C=O), 1625, 1542, 1456, 1459, 1366, 1180, 1071; ^{1}H NMR (400 MHz, $CDCl_3$) δ 0.89 (t, *J* 7.3 Hz, 6H), 1.24–1.33 (m, 4H), 1.40–1.47 (m, 4H), 2.45 (t, *J* 7.5 Hz, 4H), 4.26 (d, *J* 6.0 Hz, 2H), 5.63 (dd, *J* 1.5, 10.2 Hz, 1H), 5.88–6.00 (brs, 1H), 6.10 (dd, *J* 10.2, 17.0 Hz, 1H), 6.27 (dd, *J* 1.5, 17.0 Hz, 1H); ^{13}C NMR (101 MHz, $CDCl_3$) δ 14.1 (Me), 20.7, 30.0, 51.9, 58.3, 126.7 (all CH_2), 131.0 (CH), 166.0 (C=O); HRMS (ESI) *m/z* $[M+H]^+$, $C_{12}H_{25}N_2O$ calcd 213.1967, observed 213.1952.

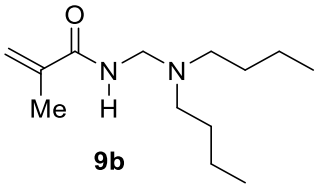

9b

***N*-[(Dibutylamino)methyl]-2-methylprop-2-enamide (9b).** (49.21 g, 87%) colourless liquid, bp 133–135 °C (0.25 mmHg); ν_{max} (neat, cm^{-1}) 3325, 2957, 2931, 2872, 1625 (C=O), 1525, 1456, 1374, 1296, 1179, 1083, 1034; ^{1}H NMR (400 MHz, $CDCl_3$) δ 0.89 (t, *J* 7.4 Hz, 6H), 1.25–1.34 (m, 4H), 1.40–1.47 (m, 4H), 1.95 (s, 3H), 2.46 (t, *J* 7.4 Hz, 4H), 4.24 (d, *J* 5.9 Hz, 2H), 5.32 (s, 1H), 5.66 (s, 1H), 5.98–6.06 (brs, 1H); ^{13}C NMR (101 MHz, $CDCl_3$) δ 14.1, 18.8 (both Me), 20.7, 30.0, 51.9, 58.6, 119.4 (all CH_2), 140.4 (C), 168.9 (C=O); HRMS (ESI) *m/z* $[M+H]^+$, $C_{13}H_{27}N_2O$ calcd. 227.2123, observed 227.2129.

1.7 X-Ray Crystallographic Studies

Single Crystal X-ray Diffraction. Single crystal data was collected using an Oxford Diffraction Xcalibur system operated using the CrysAlisPro software[46] and the data collection temperature was controlled at 150 K using a Cryojet system from Rigaku Oxford Diffraction. The crystals were hygroscopic and were first coated in cold paraffin oil before being transferred to the cold stream on the diffractometer. The crystal structures were solved using ShelxT version 2014/5,[47] and refined using ShelxL version 2017/1[48] both of which were operated within the Oscail software package.[49]

1.7.1 Crystal refinement data for 1-(hydroxymethyl)azocan-1-ium chloride (12b). Colourless crystals, $C_8H_{18}ClNO$, M = 179.68, Monoclinic, space group $P2_1/c$, a = 11.3190(18) , b = 10.9194(16) , c = 7.7658(10) Å, α = 90, β = 90.269(13), γ = 90°, V = 959.8(2) $Å^3$, Z = 4, T = 150.0(1) K, ρcalcd = 1.243 g cm^{-3}, Refinement of 147 parameters on 2345 independent reflections out of 7528 measured reflections (Rint = 0.0709) led to R1 = 0.0857 (I > 2σ(I)), wR2 = 0.2182 (all data), and S = 1.119 with the largest difference peak and hole of 0.396 and −0.398 e $Å^{-3}$.

1.7.2 Crystal refinement data for *N*-[(azocan-1-yl)methyl]prop-2-enamide hydrochloride (5a.HCl). Colourless needle crystals, $C_{11}H_{21}ClN_2O$, M = 232.75, Triclinic, space group P-1, a = 10.1121(7) , b = 10.4420(6) , c = 12.0205(14) Å, α = 95.695(8), β = 91.086(8), γ = 97.671(5)°, V = 1251.02(19) $Å^3$, Z = 4, T = 150.0(1) K, ρcalcd = 1.236 g cm^{-3}, Refinement of 271 parameters on 4487 independent reflections out of 7456 measured reflections (Rint = 0.0638) led to R1 = 0.0684 (I > 2σ(I)), wR2 = 0.2128 (all data), and S = 0.979 with the largest difference peak and hole of 0.852 and −0.705 e $Å^{-3}$.

References:

1. V. C. Mannich and W. Krösche, *Archiv. der Pharmazie*, **1912**, *250*, 647–667. https://doi.org/10.1002/ardp.19122500151
2. F. F. Blicke, (2011). "The Mannich Reaction". Organic Reactions. **1** (10): 303–341. https://doi.org/10.1002/0471264180.or001.10
3. V. E. Müller, K. Dinges and W. Graulich, *Die Makromol. Chem.*, **1962**, *57*, 27–51. https://doi.org/10.1002/macp.1962.020570103
4. V. E. Müller and H. Thomas, *Angew. Makromol. Chem.*, **1973**, *34*, 111–133. https://doi.org/10.1002/apmc.1973.050340108
5. R. C. Baltieri, L. H. Innocentini-Mei, W. M. S. C. Tamashiro, L. Peres and E. Bittencourt, *Eur. Polym. J.*, **2002**, *38*, 57–62. https://doi.org/10.1016/S0014-3057(01)00177-X
6. M. L. Eritsyan, Z. B. Barsegyan, R. A. Karamyan, S. M. Manukyan, T. D. Karapetyan and K. A. Martirosyan, *Russ. J. Appl. Chem.*, **2011**, *84*, 1257–1260. https://doi.org/10.1134/S1070427211070238
7. E. C. Cho, J. Lee and K. Cho, *Macromolecules*, **2003**, *36*, 9929–9934. https://doi.org/10.1021/ma034851d
8. D. Roy, W. L. A. Brooks and B. S. Sumerlin, *Chem. Soc. Rev.*, **2013**, *42*, 7214–7243. https://doi.org/10.1039/c3cs35499g
9. Z. Song, K. Wang, C. Gao, S. Wang and W. Zhang, *Macromolecules*, **2015**, *49*, 162–171. https://doi.org/10.1021/acs.macromol.5b02458
10. K. Wang, Z. Song, C. Liu and W. Zhang, *Polym. Chem.*, **2016**, *7*, 3423–3433. https://doi.org/10.1039/c6py00526h
11. K. Zhou, Y. Wang, X. Huang, K. Luby-Phelps, B. D. Sumer and J. Gao, *Angew. Chem. Int. Ed.*, **2011**, *50*, 6109–6114. https://doi.org/10.1002/anie.201100884
12. H. –J. Li, J. –Z. Du, J. Liu, X. –J. Du, S. Shen, Y. –H. Zhu, X. Wang, X. Ye, S. Nie and J. Wang, *ACS Nano*, **2016**, *10*, 6753–6761. https://doi.org/10.1021/acsnano.6b02326
13. B. A. Chalmers, C. Magee, D. L. Cheung, P. B. Zetterlund and F. Aldabbagh, *Eur. Polym. J.*, **2017**, *97*, 129–137. https://doi.org/10.1016/j.eurpolymj.2017.10.004
14. B. A. Chalmers, A. Alzahrani, G. Hawkins and F. Aldabbagh, *J. Polym. Sci.: Part A: Polym. Chem.*, **2017**, *55*, 2123–2128. https://doi.org/10.1002/pola.28607

15. X. Su, M. F. Cunningham and P. G. Jessop, *Polym. Chem.*, **2014**, *5*, 940–944. https://doi.org/10.1039/c3py01382k
16. H. Heaney, G. Papageorgiou and R. F. Wilkins, *Tetrahedron.*, **1997**, *53*, 2941–2958. https://doi.org/10.1016/S0040-4020(96)01174-X
17. A. Porzelle and C. M. Williams, *Synthesis*., **2006**, *18*, 3025–3030.
18. S. Melis, F. Monni, P. P. Piras, F. Sotgiu, *J. Heterocyclic Chem*, **1983**, *20*, 463. https://doi.org/10.1002/jhet.5570200239
19. H. Böhme and K. Hartke, *Chem. Ber.*, **1960**, *93*, 1305–1309. https://doi.org/10.1002/cber.19600930610
20. H. Böhme and P. Backhaus, *Liebigs Ann. Chem.*, **1975**, 1790–1796. https://doi.org/10.1002/jlac.197519751007
21. G. Kinast and L. –F. Tietze, *Angew Chem. Int. Ed.*, **1976**, *15*, 239–240. https://doi.org/10.1002/anie.197602391
22. C. Rochin, O. Babot, J. Dunoguès and F. Duboudin, *Synthesis*, **1986**, *1986*, 228–229. https://doi.org/10.1055/s-1986-627
23. J. Schreiber, H. Maag, N. Hashimoto and A. Eschenmoser, *Angew Chem. Int. Ed.*, **1971**, *10*, 330–331. https://doi.org/10.1002/anie.197103301
24. T. A. Bryson, G. H. Bonitz, C. J. Reichel and R. E. Dardis, *J. Org. Chem.*, **1980**, *45*, 524–525. https://doi.org/10.1021/jo01291a032
25. C. A. M. A. Huq, S. Fouzia and M. NizamMohideen, *Acta. Cryst. Section E: Structure Reports Online.*, **2013**, *69*, 1766. https://doi.org/10.1107/S1600536813030559
26. N. Abe, F. Fujisaki and K. Sumoto, *Chem. Pharm. Bull.*, **1998**, *46*, 142–144. https://doi.org/10.1248/cpb.46.142
27. N. Pemberton, V. Åberg, H. Almstedt, A. Westermark and F. Almqvist, *J. Org. Chem.*, **2004**, *69*, 7830–7835. https://doi.org/10.1021/jo048554y
28. Y. –Y. Ku, T. Grieme, Y. –M. Pu, A. V. Bhatia and S. A. King, *Tetrahedron Lett.*, **2005**, *46*, 1471–1474. https://doi.org/10.1016/j.tetlet.2005.01.027
29. B. R. Buckley, P. C. B. Page, H. Heaney, E. P. Sampler, S. Carley, C. Brocke and M. A. Brimble, *Tetrahedron.*, **2005**, *61*, 5876–5888. https://doi.org/10.1016/j.tet.2005.03.130
30. V. Werner, M. Ellwart, A. J. Wagner and P. Knochel, *Org. Lett.*, **2015**, *17*, 2026–2029. https://doi.org/10.1021/acs.orglett.5b00801
31. D. Alker, L. M. Harwood and C. E. Williams, *Tetrahedron*, **1997**, *53*, 12671–12678. https://doi.org/10.1016/S0040-4020(97)00788-6

32. J. L. Roberts, P. S. Borromeo and C. D. Poulter, *Tetrahedron Lett.* **1977**, *15*, 1299–1302. https://doi.org/10.1016/S0040-4039(01)93001-1
33. J. L. Roberts, P. S. Borromeo and C. D. Poulter, *Tetrahedron Lett.* **1977**, *19*, 1621–1624. https://doi.org/10.1016/S0040-4039(01)93231-9
34. H. Möhrle and G. Keller, *Z. Naturforsch. B. Chem. Sci.*, **2003**, *58*, 885–902. https://doi.org/10.1515/znb-2003-0911
35. G. Hawkins Ph.D. Thesis, August 2017-National University of Ireland Galway, Ireland.
36. O. Gibbons, W. M. Carroll, F. Aldabbagh and B. Yamada, *J. Polym. Sci.: Part A: Polym. Chem.*, **2006**, *44*, 6410–6418. https://doi.org/10.1002/pola.21751
37. P. O'Connor, R. Yang, W. M. Carroll, Y. Rochev and F. Aldabbagh, *Eur. Polym. J.*, **2012**, *48*, 1279–1288. https://doi.org/10.1016/j.eurpolymj.2012.04.011
38. Y. Sugihara, P. O'Connor, P. B. Zetterlund and F. Aldabbagh, *J. Polym. Sci.: Part A: Polym. Chem.*, **2011**, *49*, 1856–1864. https://doi.org/10.1002/pola.24612
39. C. Magee, Y. Sugihara, P. B. Zetterlund and F. Aldabbagh, *Polym. Chem.*, **2014**, *5*, 2259–2265. https://doi.org/10.1039/C3PY01441J
40. L. Zhang and A. Eisenberg, *Science.*, **1995**, *268*, 1728–1731. https://doi.org/10.1126/science.268.5218.1728
41. S. B. Lee, A. J. Russell and K. Matyjaszewski, *Biomacromolecules*, **2003**, *4*, 1386–1393. https://doi.org/10.1021/bm034126a
42. A. R. Bhat, A. I. Bhat, F. Athar and A. Azam, *Helv. Chim. Acta.*, **2009**, *92*, 1644–1656. https://doi.org/10.1002/hlca.200800461
43. C. Karakus, L. H. Fischer, S. Schmeding, J. Hummel, N. Risch, M. Schäferling and E. Holder, *Dalton Trans.*, **2012**, *41*, 9623–9632. https://doi.org/10.1039/C2DT30835E
44. K. A. Jensen and L. Henriksen, *Acta. Chemica. Scandinavica. B*, **1975**, *29*, 877–883. https://doi.org/10.3891/acta.chem.scand.29b-0877
45. H. Böhme and E. Raude, *Chem. Ber.*, **1981**, *114*, 3421–3429. https://doi.org/10.1002/cber.19811141023
46. *CrysAlisPro*, 1.171.37.38; Rigaku Corporation: Oxford, UK, **2015**. http://journals.iucr.org/e/services/stdswrefs.html
47. G. M. Sheldrick, *Acta. Cryst. Section A*: Foundations of Crystallography, **2015**, *71*, 3–8. https://doi.org/10.1107/S2053273314026370

48. G. Sheldrick, *Acta. Cryst. Section C*: Crystal Structure Communications, **2015**, *71*, 3–8. https://doi.org/10.1107/S2053229614024218
49. P. McArdle, *J. Appl. Crystallogr*., **2017**, *50*, 320–326. https://doi.org/10.1107/S1600576716018446
50. J. Hu and S. Liu, *Macromolecules*, **2010**, *43*, 8315–8330. https://doi.org/10.1021/ma1005815
51. A. Bajpai, S. K. Shukla, S. Bhanu and S. Kankane, *Prog*. *Polym*. *Sci*., **2008**, *33*, 1088–1118. https://doi.org/10.1016/j.progpolymsci.2008.07.005
52. M. Ma, L. Guo, D. G. Anderson and R. Langer, *Science*, **2013**, *339*, 186–189. https://doi.org/10.1126/science.1230262
53. D. Parasuraman and M. J. Serpe, *ACS Appl. Mater*. *Interfaces*, **2011**, *3*, 2732–2737. https://doi.org/10.1021/am2005288
54. H. Koerner, G. Price, N. A. Pearce, M. Alexander and R. A. Vaia, *Nat*. *Mater*., **2004**, *3*, 115–120. https://doi.org/10.1038/nmat1059
55. C. Pietsch, R. Hoogenboom and U. S. Schubertab, *Polym*. *Chem*., **2010**, *1*, 1005–1008. https://doi.org/10.1039/c0py00162g

Chapter 2

Reversible Addition Fragmentation Chain Transfer(RAFT) of *N*-[(cycloalkylamino)methyl]acrylamides

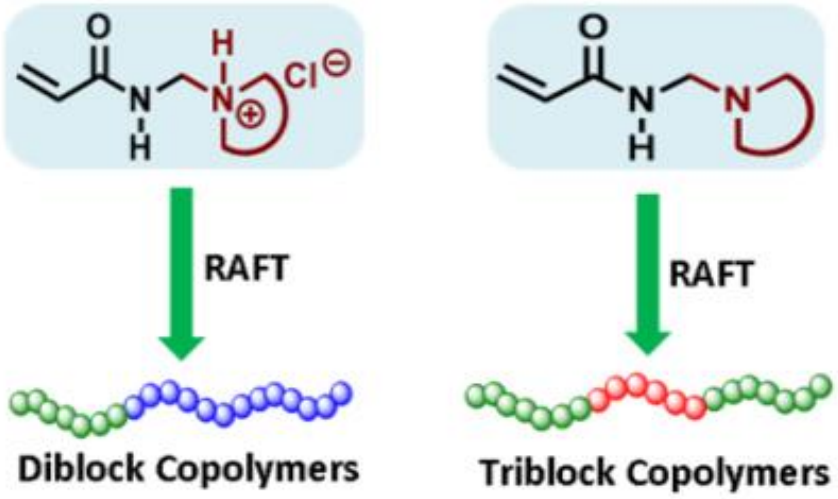

Parts of this chapter have been taken from the publication listed below (this publication is also appended to the end of this thesis). B. A. Chalmers, A. Alzahrani, G. Hawkins and F. Aldabbagh, *J. Polym. Sci.: Part A: Polym. Chem.*, **2017**, *55*, 2123–2128.

2.1 Introduction

2.1.1 Reversible Addition-Fragmentation Chain Transfer (RAFT)

RAFT polymerization was first reported and named in 1998 by Moad, Rizzardo and Thang *et al*. of the Commonwealth Scientific and Industrial Research Organization (CSIRO) in Australia.[1-2] At the same time, a similar process called macromolecular design via interchange of xanthate (MADIX) was reported in France by Zard *et al*, which follows the same mechanism as RAFT, but MADIX is limited to the use of xanthates as chain transfer agents.[3] RAFT is the most popular method for controlling radical polymerization, which are defined by IUPAC as reversible deactivation radical polymerization.[4] The term reversible deactivation radical polymerization replaced controlled/living polymerization. In terms of this thesis, RAFT was utilized for the efficient preparation of block copolymers via sequential monomer addition.[5] RAFT works on the principle of reversible deactivation of propagating radicals and the mechanism of RAFT polymerization differs from other common reversible deactivation radical polymerizations (such as atom transfer radical polymerization, ATRP [6-7] and nitroxide-mediated radical polymerization, NMP)[8] in that it relies upon degenerative chain transfer. Control/living character is achieved by equilibria between polymer chains led by a reversible transfer reaction using a thiocarbonylthio compound (the RAFT agent). The degenerative transfer gives all polymer chains equal opportunities to grow and thus achieves a controlled/living polymerization. A general mechanism of RAFT polymerization is shown in (Scheme 2.1).

Initiation:

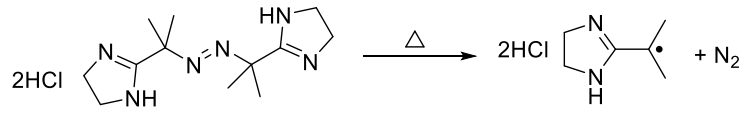

VA-044

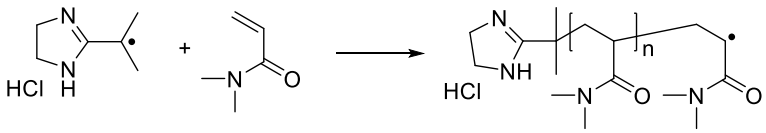

= $P_n^{\bullet}$

Reversible chain transfer:

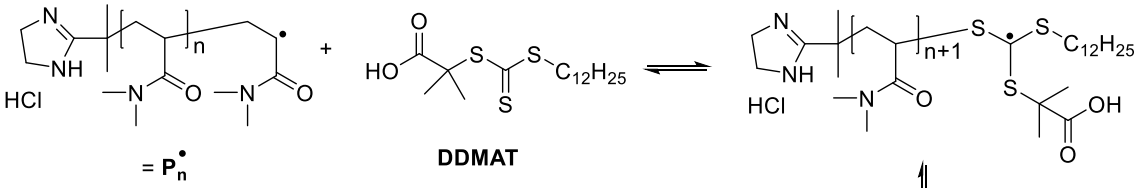

= $P_n^{\bullet}$ **DDMAT**

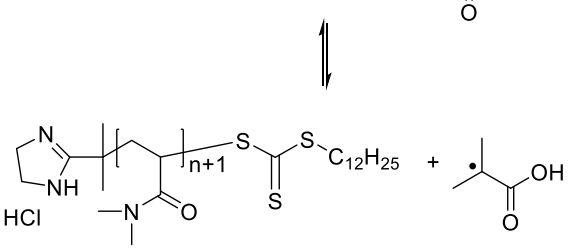

Re-initiation:

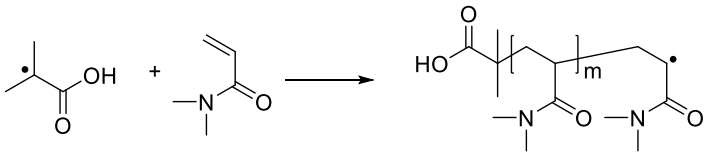

= $P_m^{\bullet}$

Chain equilibrium:

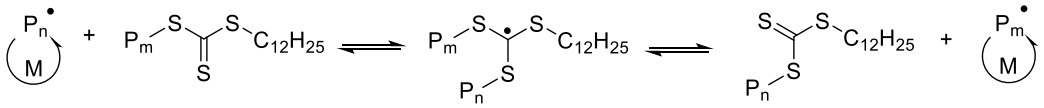

Termination:

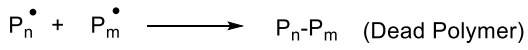

Scheme 2.1: Mechanism for RAFT polymerization using the RAFT agent, 2-(dodecylthiocarbonothioylthio)-2-methylpropionic acid (DDMAT), *N*,*N*-dimethylacrylamide as monomer, and 2,2′-azobis[2-(2-imidazolin-2-yl)propane]dihydrochloride (VA-044) as the azo-initiator.

In a degenerative chain transfer process, the number of chains that undergo termination is dictated solely by the initiator decomposition, assuming that all living chains are derived from the RAFT agent. Therefore the requirement for initiator in RAFT polymerizations will inevitably lead to some bimolecular termination. It follows that the choice of initiation in terms type of initiator, concentration and temperature will influence the rate of the RAFT polymerization, as well as, the number fraction of living chains. Perrier and Zetterlund have used equation (2.1) to relate initiation to livingness.[9-11]

$$L = \frac{[RAFT]_0}{[RAFT]_0 + 2f[I]_0(1 - e^{-k_d t})\left(1 - \frac{f_c}{2}\right)} \qquad (2.1)$$

Equation. 2.1 estimates the theoretical fraction of living chains (L). The factor "2" accounts for one molecule of azo-initiator yielding two primary radicals with the efficiency f (assumed to be equal to 0.5). The decomposition rate constant is k_d. The quantity $1 - \frac{f_c}{2}$ represents the number of chains produced in a radical−radical termination event with the coupling factor f_c assumed to be zero. Dead chains include those without thiocarbonyl-thio moiety at the ω-end group, as well as, initiator derived chains with an initiator fragment at the α-end (regardless of the ω-end).

Gody *et al*,[9] synthesized sequence-controlled multiblock copolymers in a one-pot multistep process via RAFT polymerization using different acrylamide monomers and two different initiators (Figure 2.1); 2,2′-azobis(2-methylpropionitrile (AIBN, half-life time of 10 hours at 70 °C) and VA-044 (half-life time of 2 hours at 44 °C). To insure each block is of high purity, each polymerization was taken to almost complete conversion (~98–99%), and AIBN allowed each ten-acrylamide containing blocks to be produced in 24 hours. Under these conditions 81% of AIBN is decomposed in 24 hours at 65 °C in dioxane. Using equation 2.1, it follows that the dodecablock copolymer was prepared with L = 90.4%. The advantage of VA-044 is it allowed each block to be prepared faster, in 2 hours ours at 70 °C due to its higher rate of decomposition compared to AIBN. For the icosablock the fraction of living chains was estimated using equation 2.1 as L = 93.8%.

(a)

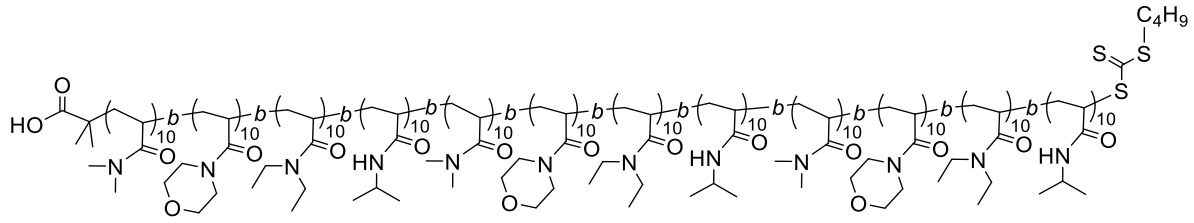

Dodecablock copolymer

(b)

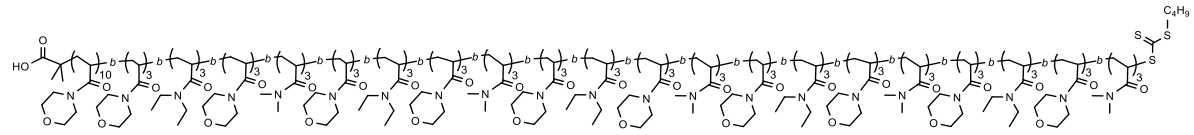

Icosablock copolymer

Figure 2.1: Structure of the multiblock copolymers **(a)** prepared using AIBN as initiator at 65 ^{o}C in dioxane in 24 hours per block and **(b)** prepared using VA-044 as initiator in 2 hours per block at 70 ^{o}C in water.

It follows in order to minimize termination reactions then, the number of initiator derived radicals in a RAFT polymerization should be minimized. This is illustrated in Scheme 2.2 where the fraction (%) of living chains increases as the number of RAFT agent molecules relative to initiator radicals [I$^{\bullet}$] increases.[12] The livingness of a system with 2 initiator radicals and 4 RAFT agents *L* (%) is 4/(2 + 4) × 100 = 67% (Scheme 2.2a) or if we assume all chains containing an initiator fragment are also dead then, *L* (%) as shown = 50%. In contrast a system with a higher proportion of RAFT agent relative to initiator will give a higher *L*. For example, Scheme 2.2b has 2 initiator radicals and 8 RAFT agent molecules will give ten chains comprising two dead chains and eight living chains. The livingness of the system *L* (%) is therefore 8/(8 + 2) × 100 = 80% or if we assume all chains shown containing an initiator fragment are also dead, *L* (%) = 70%.

The degree of polymerization (*DP*) for a RAFT process is shown to be dictated by the number of living chains (containing the RAFT end-group, Z−C(=S)S), which is approximated from the $[Monomer]_0$ to $[RAFT\ agent]_0$ ratio, such as the degree of polymerization (*DP*) of Scheme 2.2a is 16/4 = 4, but the degree of polymerization (*DP*) of Scheme 2.2b is 16/8 = 2. It follows in RAFT, at a given initiator concentration, livingness decreases with increasing degree of

polymerization (*DP*) or targeted molecular weight ($M_{n,th}$). Since the number of dead chains and monomer is the same in the two systems shown in Scheme 2.2, but the fraction of living chains is greater in the system with more RAFT agent (which gives shorter polymer chains).

Theoretical number average molecular weight ($M_{n,th}$) in RAFT is calculated according to equation 2.2:

$$M_{n,th} = \left(\frac{[Monomer]_0}{[RAFT]_0} \times MW_{Monomer} \times Conversion\right) + MW_{RAFT} \qquad (2.2)$$

Where, RAFT represents DDMAT or polymeric macro-RAFT, $MW_{monomer}$ and MW_{RAFT} are the molecular weights of the monomer and macro-RAFT agent respectively.

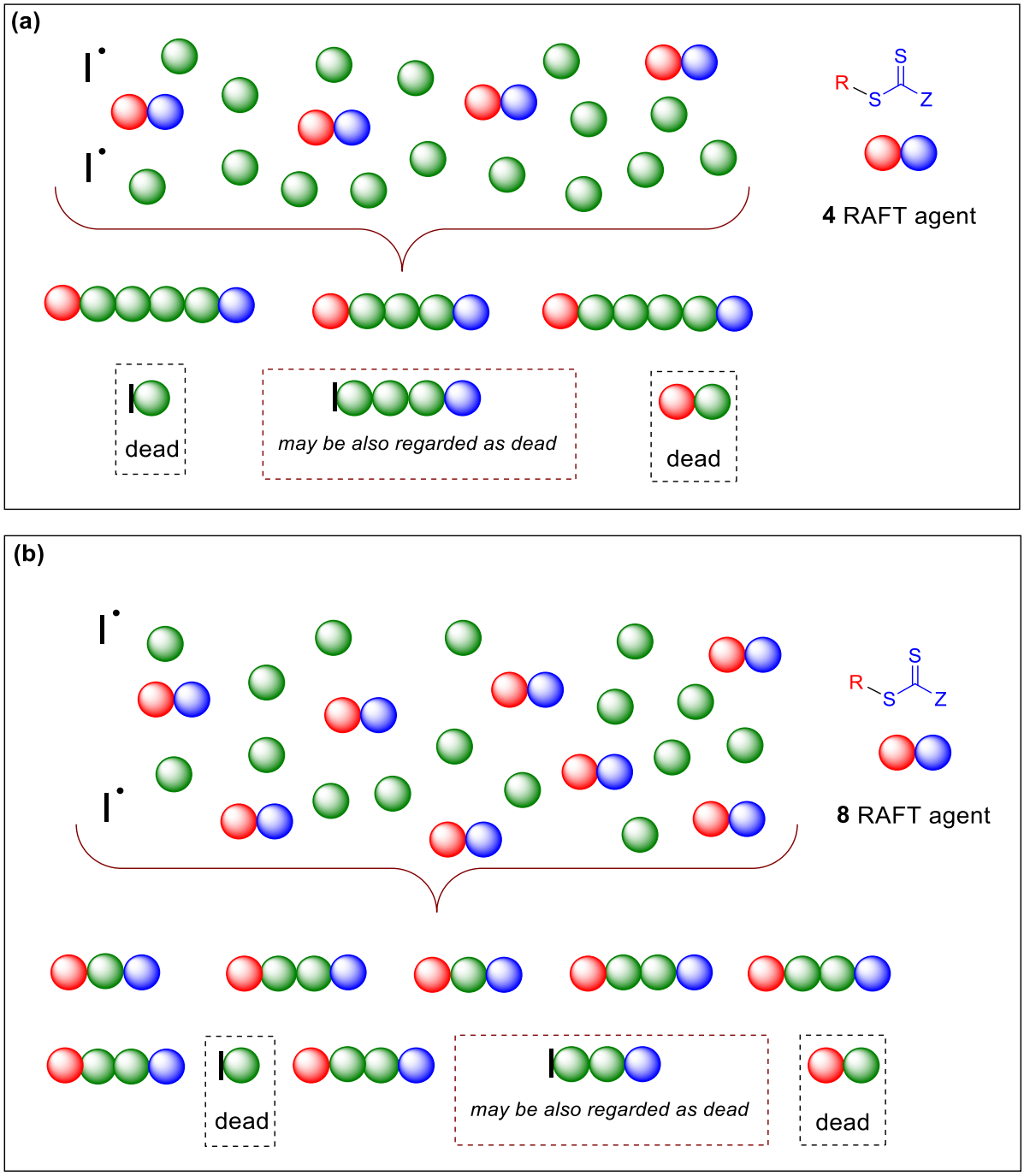

Scheme 2.2: Schematic representation of the RAFT process. **(a)** Two radicals (I) are introduced in a system containing sixteen monomers (green) and four RAFT agents (red R-group and blue Z−C(=S)S) and **(b)** Two radicals (I) are introduced in a system containing sixteen monomers (green) and eight RAFT agents (red R-group and blue Z−C(=S)S).

It follows in order to improve control/living character the concentration of initiator should be reduced, so to improve control (give narrow molecular weight distribution (MWD)), and optimize livingness (the number fraction of chains that retain the desired ω-end group functionality (RAFT end group) at a given monomer conversion. However, reducing initiator concentration may reduce the rate of polymerization, which in a RAFT process should be the same as that for a conventional radical polymerization. The rate of propagation, R_p, can be expressed by equation 2.3:

$$R_p = \frac{-\,d\,[M]}{dt} = k_p\,[P^\bullet]\,[M] \qquad (2.3)$$

Where k_p is the rate coefficient for propagation, $[P^\bullet]$ is the propagating radical concentration and $[M]$ is the monomer concentration. The propagating radical concentration can be determined by equation 2.4:

$$[P^\bullet] = \sqrt{\frac{f \times k_d \times [I]_0 \times e^{-k_d t}}{k_t}} \qquad (2.4)$$

Therefore the overall rate of polymerization is determined by the rate of propagation (R_p). Inserting propagating radical concentration $[P^\bullet]$ from equation 2.4 into the rate of propagation (equation 2.3) gives the rate of conventional radical polymerization under steady state kinetics (radical concentration remains essentially constant) equation 2.5:

$$R_P = k_p \times [M] \times \sqrt{\frac{f \times k_d \times [I]_0 \times e^{-k_d t}}{k_t}} \qquad (2.5)$$

Where, the propagation rate coefficients (k_p) of monomers classes, $[M]$ the monomer concentration, f the initiator efficiency, k_d the decomposition rate coefficient of the initiator, $[I]_0$ the initial initiator concentration, and k_t the termination rate coefficient. $[P^\bullet]$ is thus a function of the rates of initiation and termination, and these are equal under steady state kinetics, when propagating radical concentration does not change.

Recently the Aldabbagh group carried out RAFT polymerizations using VA-044 initiator and DDMAT, as RAFT agent to give amphiphilic polyacrylamide block copolymers containing *N*-(2-morpholin-4-ylethyl)acrylamide (MEA) (Schemes 2.3a and 2.4a). The morpholine part was ionized to give CO_2-response by simply bubbling CO_2 gas into a solution of the polymer in water, and removing CO_2 by bubbling N_2 gas. The AB block copolymer type-structure (Scheme 2.3a) was prepared by first carrying out the RAFT polymerization of MEA and extending with hydrophilic *N*,*N*-dimethylacrylamide (DMA). The hydrophobic block was added last using RAFT of *tert*-butylacrylamide (TBAM). In order to insure high blocking efficiency almost complete conversions were achieved in this one-pot triblock copolymer synthesis. The resulting self-assembly of the poly(MEA)$_{51}$-*b*-(DMA)$_{50}$-*b*-(TBAM)$_{40}$-S(C=S)S$C_{12}H_{25}$, triblock copolymer (AB type-structure) gave spherical vesicles in Scheme 2.3b.

The structurally analogous (almost identical in chemical composition) block copolymer was then made efficiently in one-pot starting with poly(TBAM) macro-RAFT. For both amphiphilic triblock copolymers, the use of VA-044 facilitated the preparation of each block in almost 100% conversion in 2 hours. In this case (poly(TBAM)$_{40}$-*b*-(DMA)$_{50}$-*b*-(MEA)$_{49}$-S(C=S)S$C_{12}H_{25}$), the large hydrophobic dodecyl group of the trithiocarbonate derived from DDMAT greatly influenced self-assembly, which led to ABA′ type-structure in Scheme 2.4b. Self-assembly was more complex leading to compound micelles suggesting specific interactions between the large hydrophobic end-group.[13]

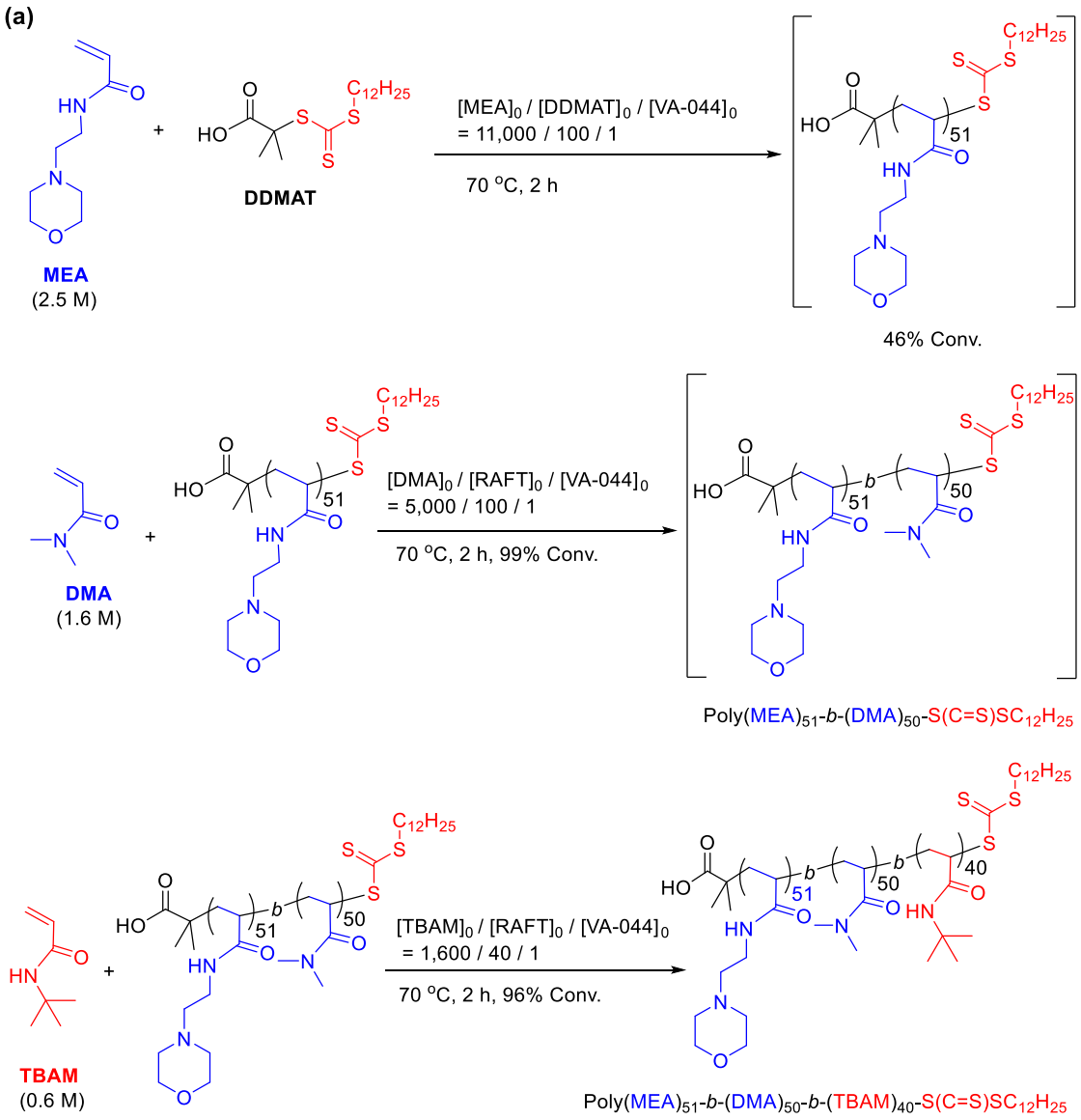

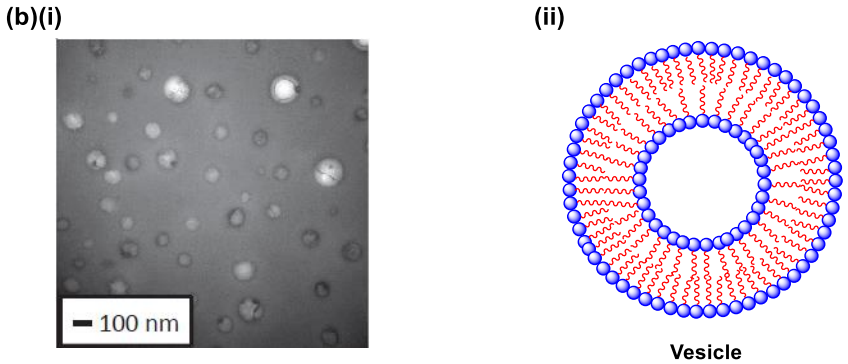

Scheme 2.3: (a) Preparation of triblock copolymer {poly(MEA)$_{51}$-*b*-(DMA)$_{50}$-*b*-(TBAM)$_{40}$-S(C=S)SC$_{12}$H$_{25}$} and **(b)(i)** TEM image and **(ii)** Self-assembly of triblock copolymer (AB type-structure) into vesicles.

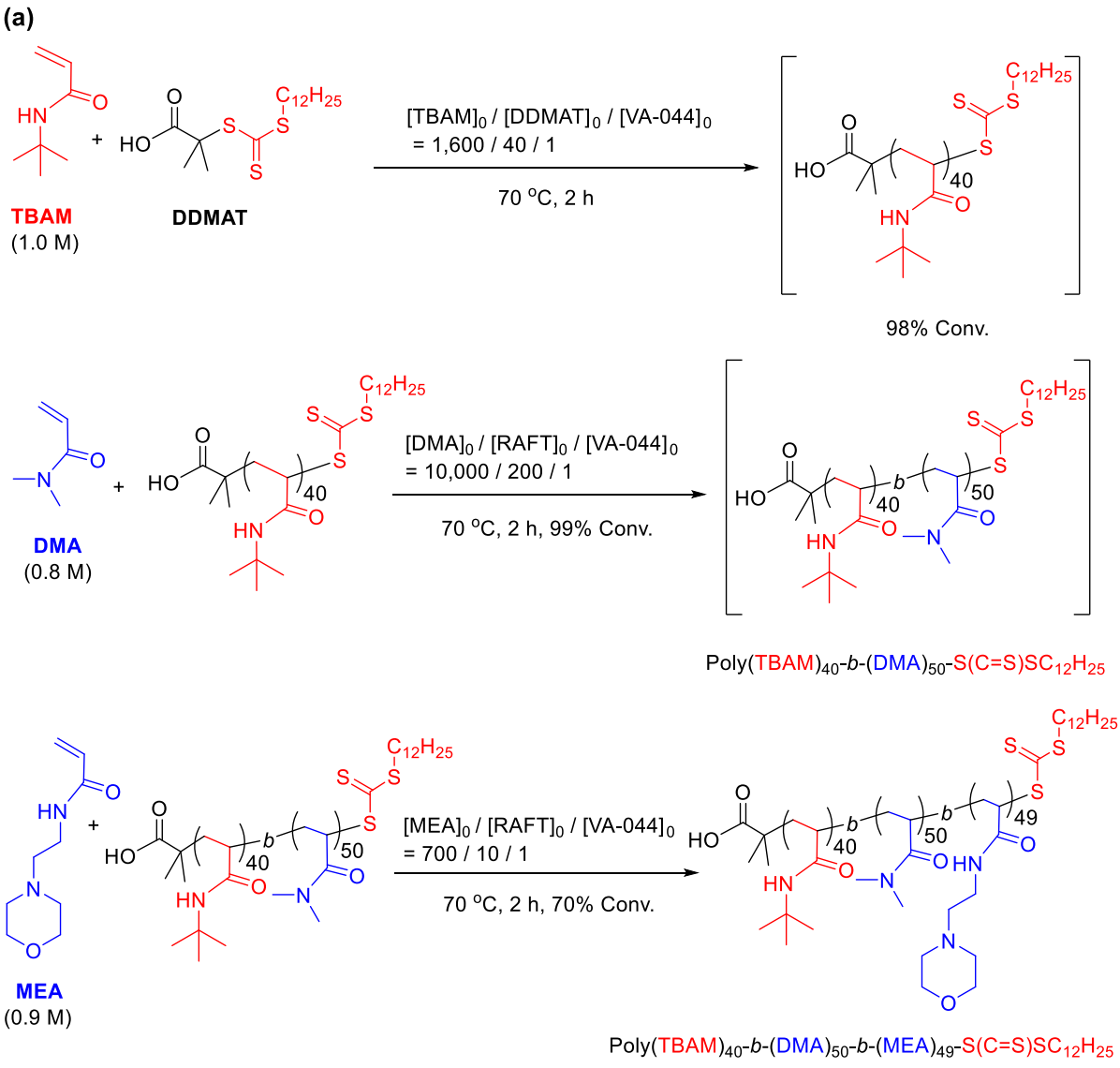

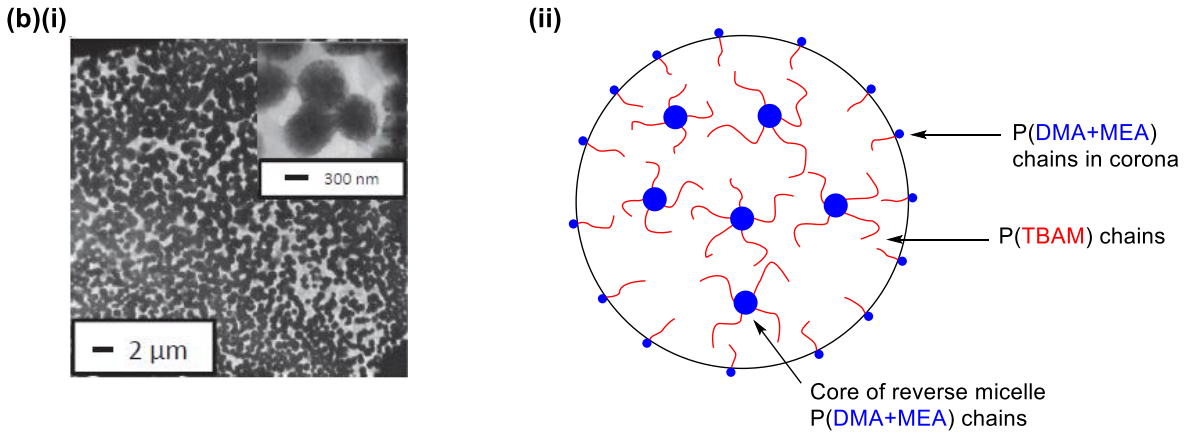

Scheme 2.4: (a) Preparation of triblock copolymer {poly(TBAM)$_{40}$-*b*-(DMA)$_{50}$-*b*-(MEA)$_{49}$-S(C=S)SC$_{12}$H$_{25}$} and **(b)(i)** TEM image and **(ii)** Self-assembly of triblock copolymer (ABA′ type-structure) into CO_2-senstive compound micelles.

To remove the large hydrophobic dodecyl moiety derived group from the DDMAT on poly(TBAM)$_{40}$-*b*-(DMA)$_{50}$-*b*-(MEA)$_{49}$-S(C=S)SC$_{12}$H$_{25}$, this moiety was removed by reaction with excess (AIBN) initiator (20 equiv.) in 1,4-dioxane. The cleavage of the trithiocarbonate (-S(C=S)SC$_{12}$H$_{25}$) group was evidenced by a reduction in UV-absorbance from 0.3 to 0.15 low absorbance (a.u.) at wavelength (230-340 nm) of the polymer. As a result, the large compound micelle structure due to ABA′ type-structure reverted to smaller spherical entities, most likely vesicles due to simpler AB self-assembly in Scheme 2.5.[13]

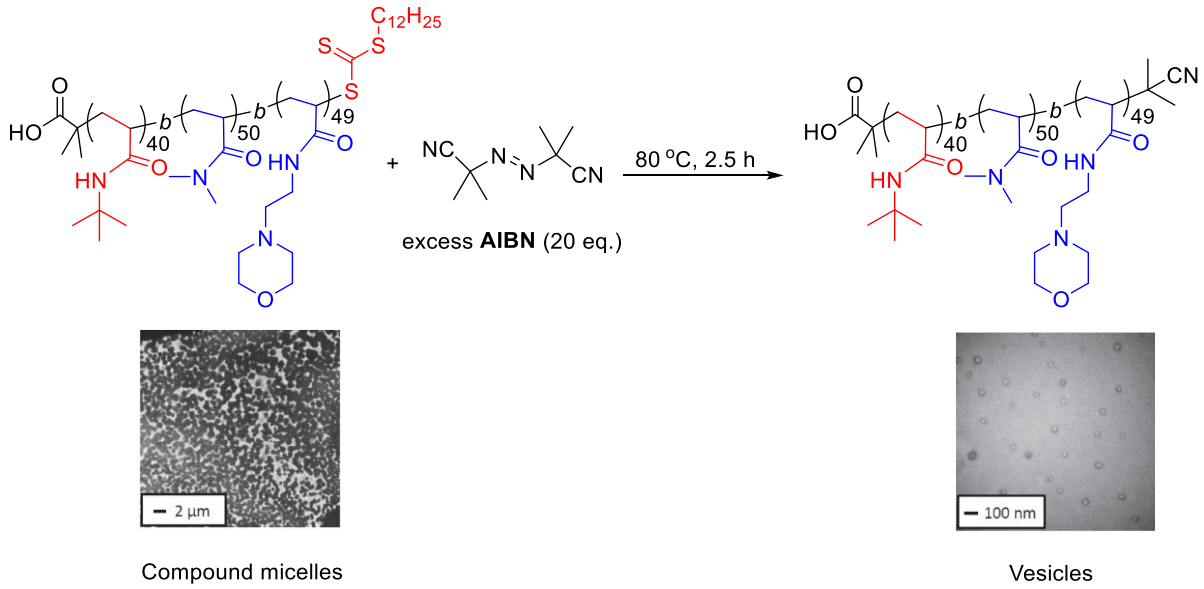

Scheme 2.5: End-group removal from poly(TBAM)$_{40}$-*b*-(DMA)$_{50}$-*b*-(MEA)$_{49}$-(C=S)SC$_{12}$H$_{25}$ triblock copolymer (ABA′ type-structure) with TEM images.

2.2 Aims and Objectives

The previous Chapter described the first viable synthesis of acrylamides and methacrylamides containing bridged methylene *N*-amino substituents, including those possessing morpholine, pyrrolidine and piperidine heterocycles.[14] The objective herein is to carry out the first controlled/living polymerizations of this new acrylamide monomer class, with the versatile reversible deactivation radical polymerization, RAFT adopted. Therefore, the aim is to prepare the first block copolymers of *N*-[(morpholin-4-yl)methyl]prop-2-enamide (**1a**), *N*-[(pyrrolidin-1-yl)methyl]prop-2-enamide (**2a**) and *N*-[(piperidin-1-yl)methyl]prop-2-enamide (**3a**) in (Figure 2.2), and where possible the respective HCl synthetic intermediate monomer salts will also be polymerized.

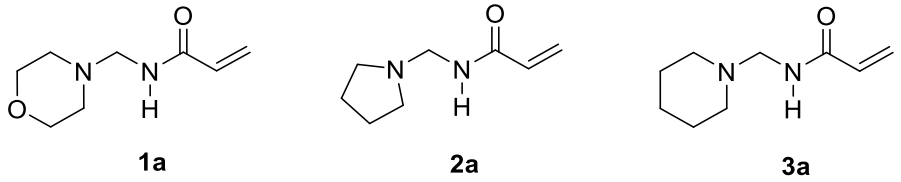

Figure 2.2: Structures of acrylamide monomers.

Our polymerization strategy was based upon that of Zetterlund and Perrier *et al*. who demonstrated the use of the RAFT process in yielding well-defined multi-component polyacrylamide block copolymers in one pot without intermittent purification by use of the water soluble azo-initiator, VA-044, where each block was prepared in ~99% conversion in 2 hours at 70 °C.[10-12] Initial attempts in our group at one-pot block copolymer synthesis (without intermediate polymer isolation) were however hampered by the inability to achieve full conversion for the RAFT of *N*-[(morpholino-4-yl)methyl]prop-2-enamide (**1a**) using 2 hours polymerizations with VA-044 and longer polymerization times with AIBN in Scheme 2.6.[5, 15]

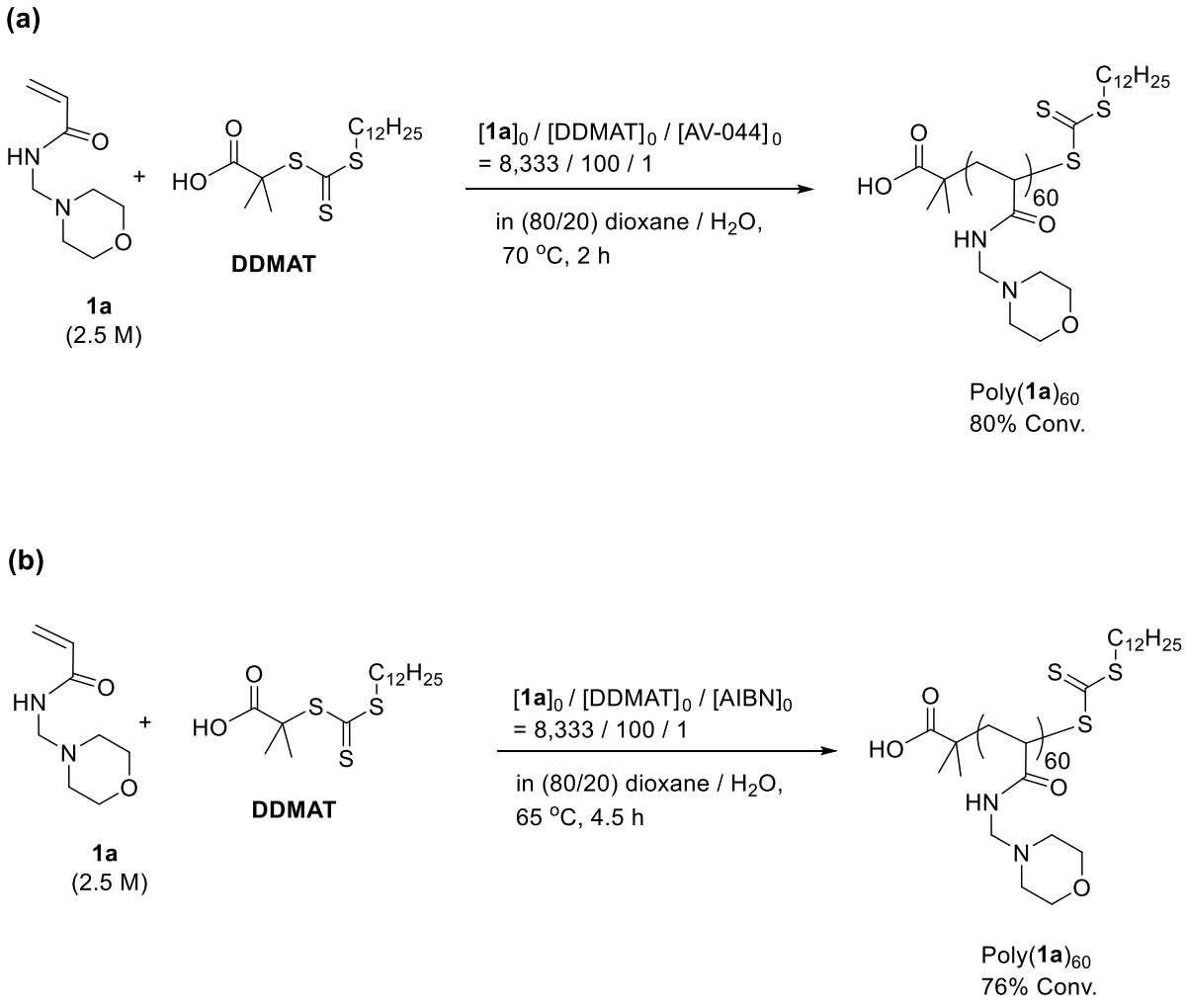

Scheme 2.6: Preparations of macro-RAFT agent poly(**1a**)$_{60}$ using **(a)** VA-044 to give poly(**1a**) M_n = 10,600 g.mol^{-1}, M_w/M_n = 1.21, and **(b)** AIBN to give poly(**1a**), M_n = 10,550 g.mol^{-1}, M_w/M_n = 1.21.[5, 15]

2.3 Results and Discussion

2.3.1 Preparation of macro-RAFT agent poly(DMA)$_{41}$

Block copolymer synthesis the employed water-soluble poly(*N*,*N*-dimethylacrylamide, DMA)$_{41}$ as the macro-RAFT agent. This could be prepared in high conversion and theoretical livingness (both 99%) so providing the ideal start for two sequential 2 hours one-pot chain extensions at 70 ^{o}C.[10-11] DDMAT and DMA were added to VA-044 from a stock solution dioxane / water (80/20) and heated at 70 °C for 2 hours. The polymer was precipitated from Et_2O to give poly(DMA)$_{41}$ macro-RAFT, M_n = 4,450 g.mol^{-1}, M_w/M_n = 1.11, 99% conv., isolated = 2.28 g (Scheme 2.7 and Figure 2.3).

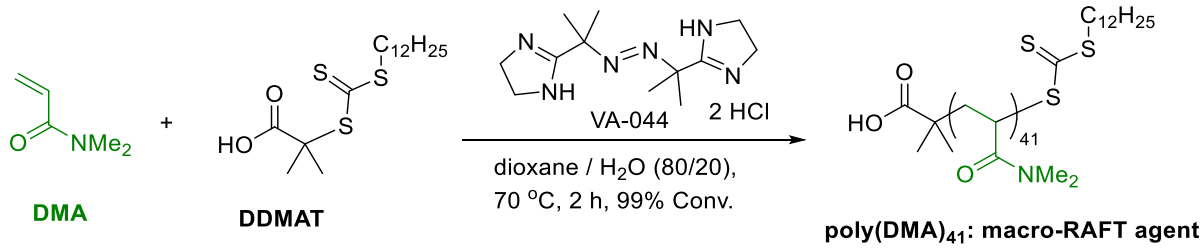

Scheme 2.7: Preparation of poly(*N*,*N*-dimethylacrylamide).

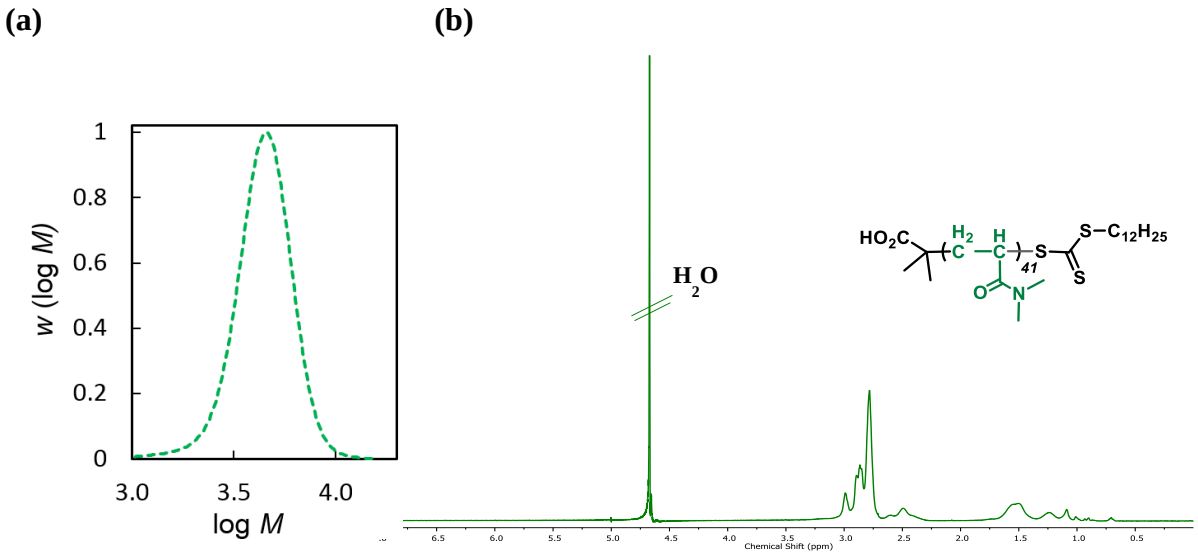

Figure 2.3: (a) MWD for poly(DMA)$_{41}$ and **(b)** ^{1}H NMR spectra (D_2O, 400 MHz) of poly(DMA)$_{41}$ macro-RAFT agent.

2.3.2 One-pot RAFT polymerizations to give polyacrylamide block copolymers

Under these conditions at 70 °C for 2 hours, VA-044 undergoes near-complete homolytic decomposition (~95%) into radicals, and an almost quantitative fraction of living chains is maintained by use of high $[RAFT]_0/[VA\text{-}044]_0$ ratios (e.g. $[RAFT]_0/[VA\text{-}044]_0$ = 10–100 provides 91–99% livingness, according to equation 2.1).

Two one-pot chain extensions were carried out to near full conversion (~99%), as monitored by ^{1}H NMR (Scheme 2.8). The solubility of the macro-RAFT agent and initiator allowed chain extensions of poly(DMA)$_{41}$ to give poly(DMA)$_{41}$-*b*-(*N*-[(morpholin-4-yl)methyl]prop-2-enamide, **1a**)$_{69}$-*b*-(DMA)$_{192}$ to be carried out in water. In order to negate purification prior to chain extension with DMA polymerizations to give the intermediate diblock using morpholine **1a** and piperidine **3a** required a relatively high VA-044 concentration ($[RAFT]_0/[VA\text{-}044]_0$ = 10) for near-complete conversion. For the synthesis of water soluble poly(DMA)$_{41}$-*b*-(**1a**)$_{69}$-*b*-(DMA)$_{192}$, MWDs (molecular weight distributions) remained relatively narrow (M_w/M_n = 1.35-1.50) shifting to higher MW with M_n values close to theoretical ($M_{n,th}$) despite inherent GPC error due to calibration to linear poly(MMA) standards (Figures 2.4, Table 2.1). Incorporation of blocks and near-complete conversions obtained confirmed by ^{1}H NMR spectroscopy (Figure 2.5).

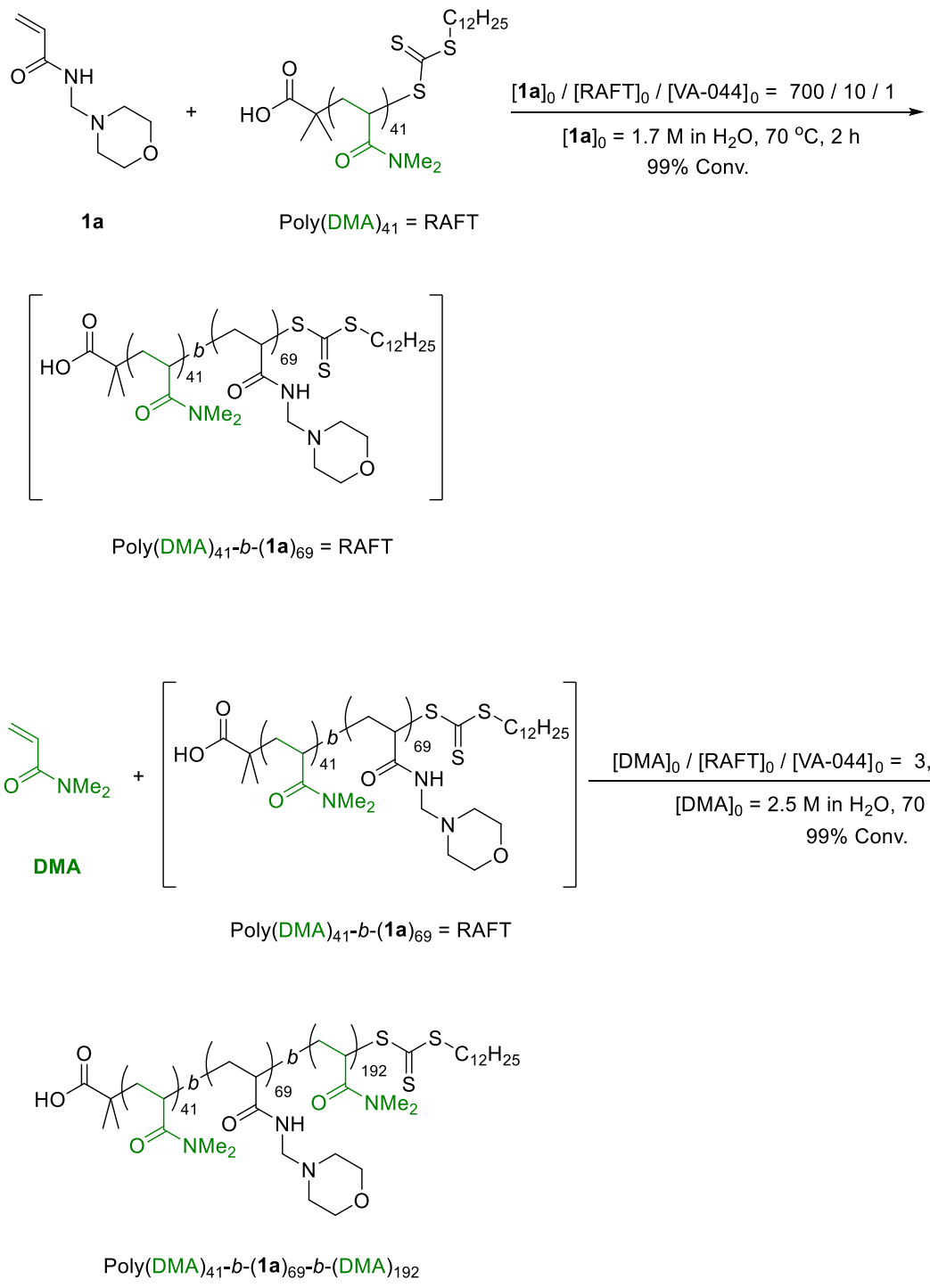

Scheme 2.8: One-pot RAFT polymerization (without intermediate purifications) to give triblock copolymers poly(DMA)$_{41}$-*b*-(**1a**)$_{69}$-*b*-(DMA)$_{192}$.

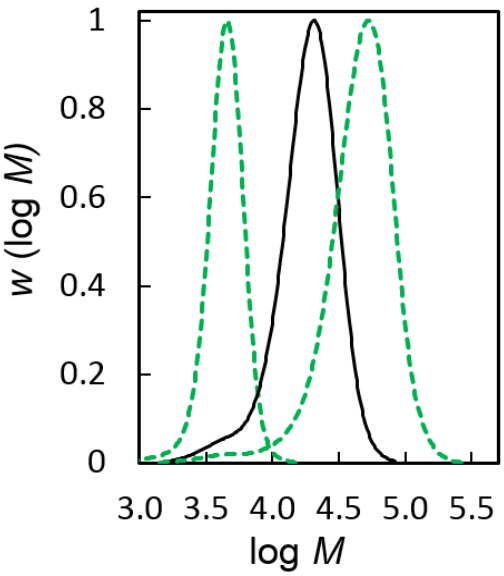

Figure 2.4: MWDs for one-pot 2 hours sequential RAFT polymerizations at 70 °C taken to 99% conversion of poly(DMA) macro-RAFT (green dashed line) with *N*-[(morpholino-4-yl)methyl]prop-2-enamide (**1a**) (continuous line) and DMA to give triblock copolymer poly(DMA)$_{41}$-*b*-(**1a**)$_{69}$-*b*-(DMA)$_{192}$ (green dashed line).

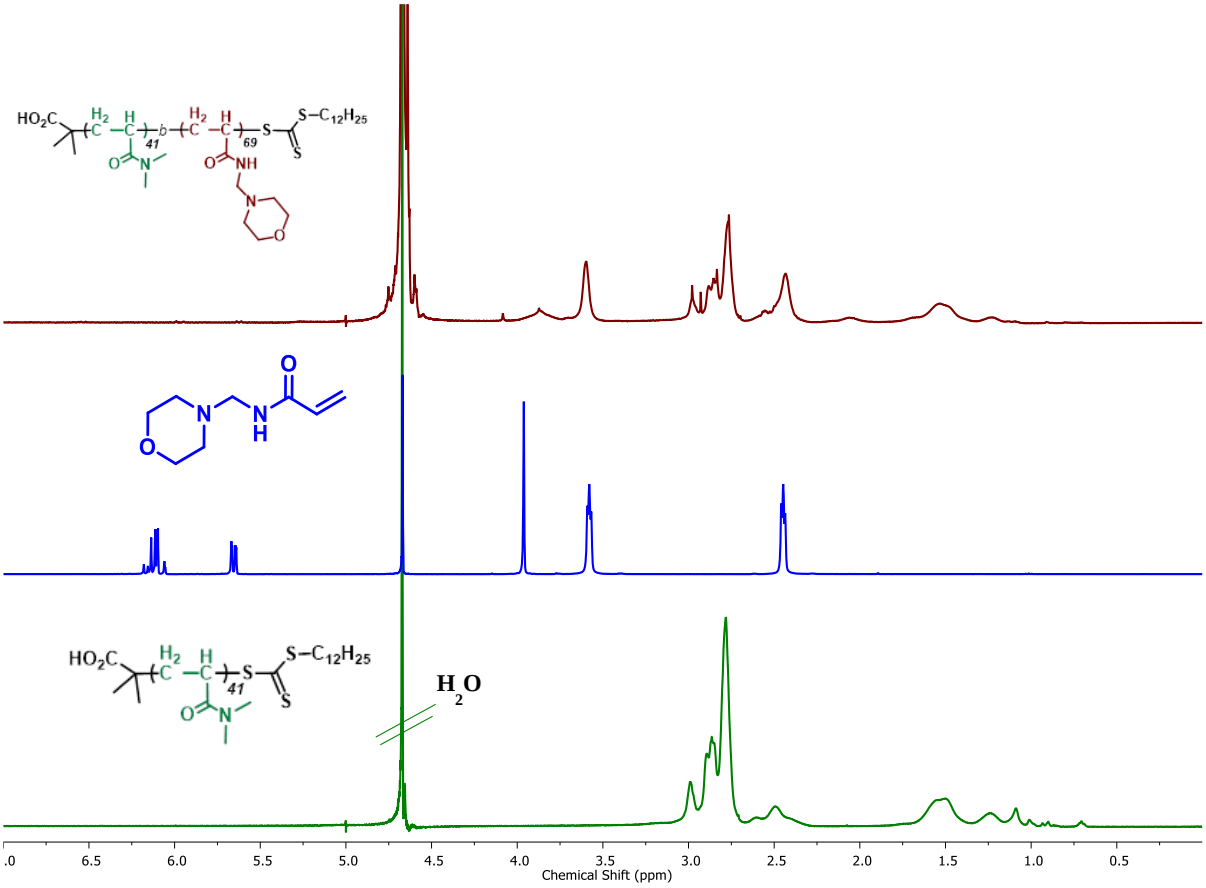

Figure 2.5: ^{1}H NMR spectra (D_2O, 400 MHz) monitoring of one-pot 2 hours sequential RAFT polymerizations of *N*-[(morpholino-4-yl)methyl]prop-2-enamide (**1a**, blue) and diblock copolymer poly(DMA)$_{41}$-*b*-(**1a**)$_{69}$ (dark red), The conversion for each new block is 99%. NMR spectra of polymers obtained without purification.

In contrast, the polymerization of piperidine **3a** required dioxane due to the formation of a more hydrophobic diblock, however mixtures using varied dioxane/water gave broad MWDs for chain extension of poly(DMA)$_{41}$ with **3a** in Figure 2.6.

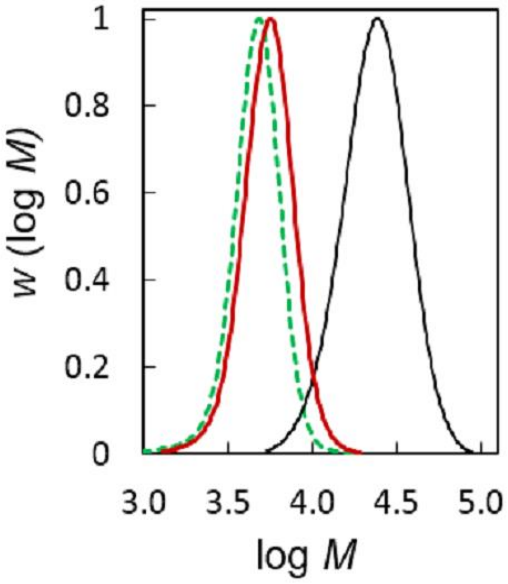

Figure 2.6: Attempts to chain extend poly(DMA) macro-RAFT (green dashed line) with *N*-[(piperidin-1-yl)methyl]prop-2-enamide (**3a**) at 70 ^{o}C for 2 hours using (40/60) dioxane / H_2O without HCl (red continuous line) and by replacing water with HCl (black continuous line) to give diblock copolymer poly(DMA)$_{41}$-*b*-(**3a**)$_{97}$.

Abel and McCormick carried out RAFT polymerization of methacrylamides showing that livingness through preservation of the trithiocarbonate end-group can be achieved by utilizing acidic solutions, which protonate nucleophilic sites (including the *N* atom of the amide)[16-17] in Scheme 2.9.

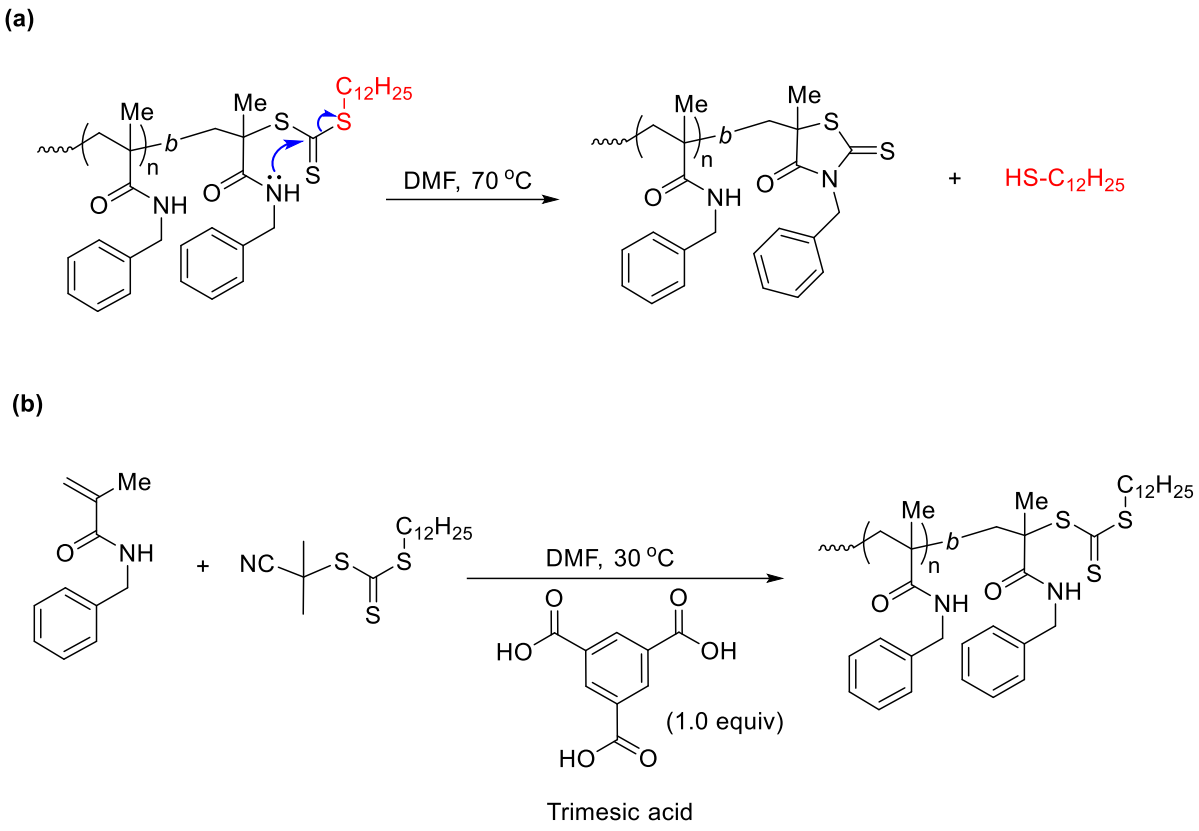

Scheme 2.9: (a) Proposed trithiocarbonate degradation by nucleophilic attack at the terminal end of the methacrylamide monomer and **(b)** retention of the RAFT-end group in acidic condition.

This led us to the addition of 1.15 equivalents of HCl to the chain extension of poly(DMA)$_{41}$, which gave poly(DMA)$_{41}$-*b*-(**3a**)$_{97}$ in 97% conversion with excellent control/living character, as demonstrated by narrow MWD (M_w/M_n = 1.22) with M_n close to $M_{n,th}$ (Scheme 2.10, Figure 2.7 and Table 2.1). It seems that protonation of the piperidine ring of the poly(**3a**) block prevented aminolysis side-reactions that cleave the trithiocarbonate end-group, and that this phenomenon is decreased or is absent for morpholine **1a** due to the electronegative oxygen atom of the heterocycle. Subsequent one-pot chain extension with DMA gave poly(DMA)$_{41}$-*b*-(**3a**)$_{97}$-*b*-(DMA)$_{116}$ with no noticeable loss of control/livingness. Incorporation of blocks and near-complete conversions verified by ^{1}H NMR spectroscopy (Figure 2.8).

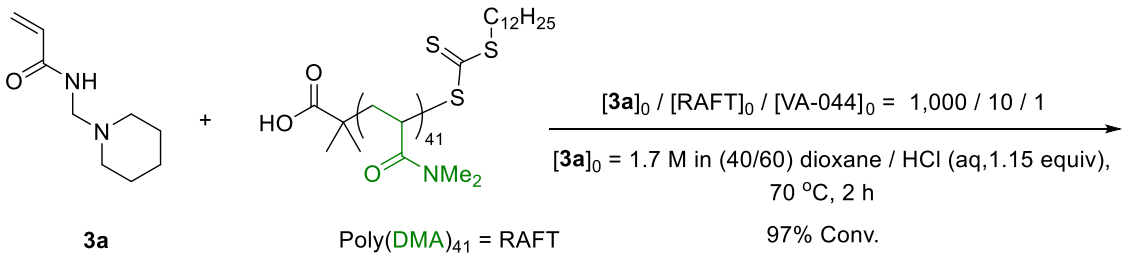

3a Poly(DMA)$_{41}$ = RAFT

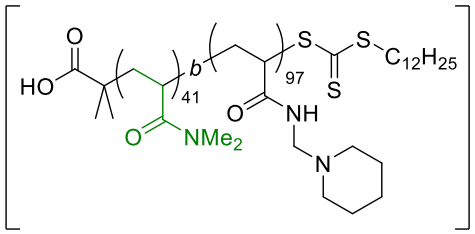

Poly(DMA)$_{41}$-*b*-(**3a**)$_{97}$ = RAFT

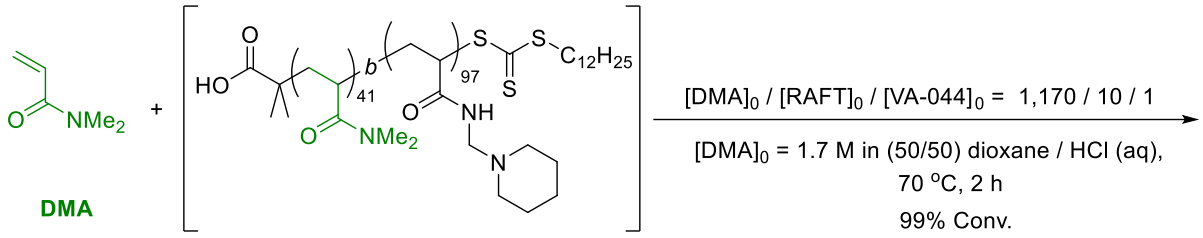

DMA

Poly(DMA)$_{41}$-*b*-(**3a**)$_{97}$ = RAFT

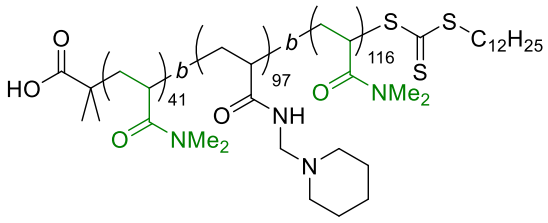

Poly(DMA)$_{41}$-*b*-(**3a**)$_{97}$-*b*-(DMA)$_{116}$

Scheme 2.10: One-pot RAFT polymerization (without intermediate purifications) to give triblock copolymers poly(DMA)$_{41}$-*b*-(3**a**)$_{97}$-*b*-(DMA)$_{116}$.

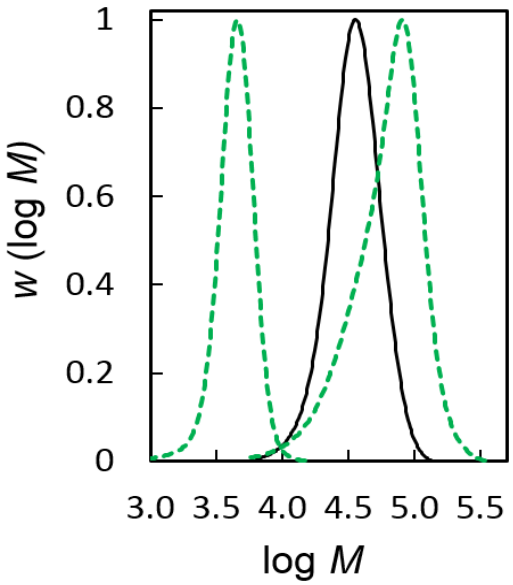

Figure 2.7: MWDs for one-pot 2 hours sequential RAFT polymerizations at 70 °C taken to 97% conversion of poly(DMA) macro-RAFT (green dashed line) with *N*-[(piperidin-1-yl)methyl]prop-2-enamide (**3a**) (continuous line). Polymerizations in dioxane / 1.15 equiv. HCl (aq) of **(3a)** and DMA to give triblock copolymer poly(DMA)$_{41}$-*b*-(**3a**)$_{97}$-*b*-(DMA)$_{116}$ (green dashed line).

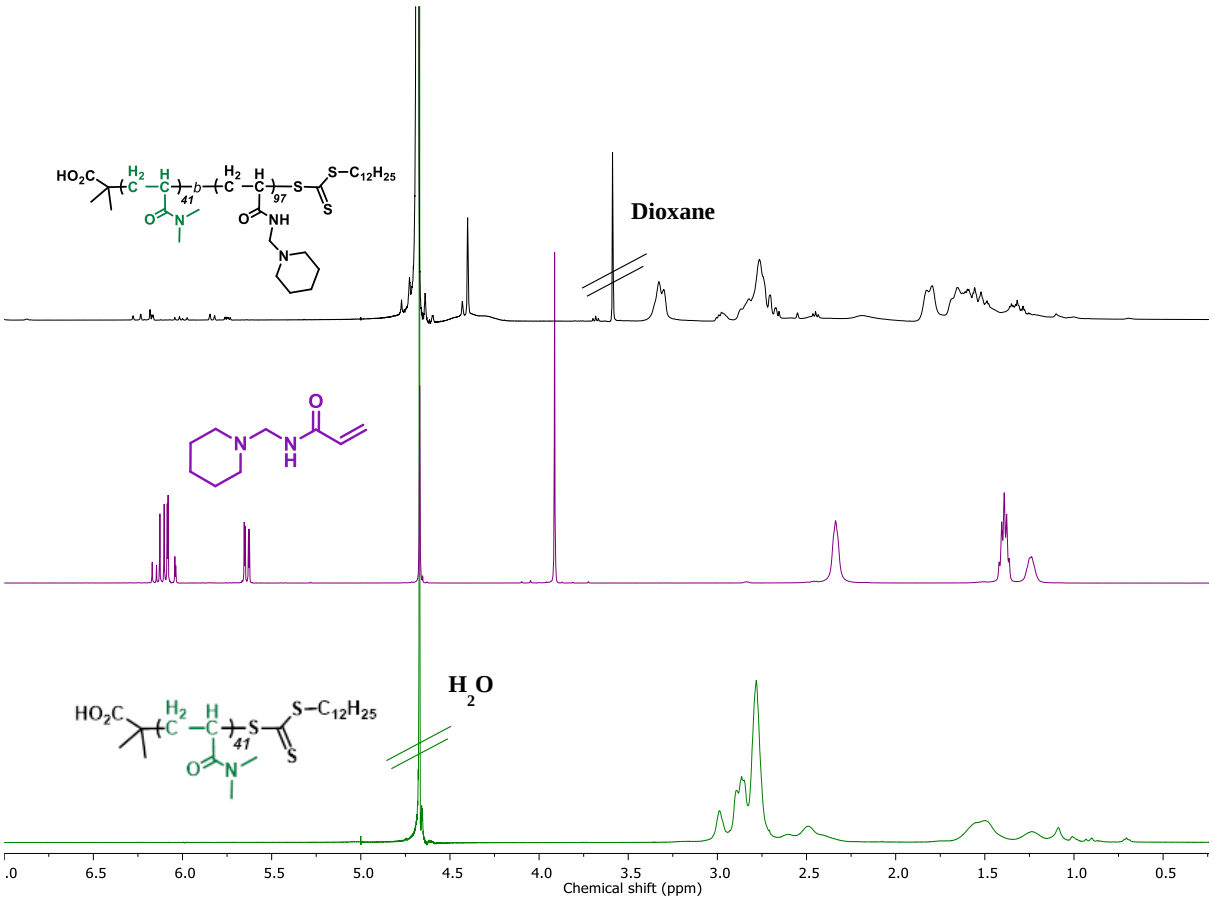

Figure 2.8: ^{1}H NMR spectra (D_2O, 400 MHz) monitoring of one-pot 2 hours sequential RAFT polymerizations of *N*-[(piperidin-1-yl)methyl]prop-2-enamide (**3a**, purple) and diblock copolymer poly(DMA)$_{41}$-*b*-(**3a**)$_{97}$ (black), The conversion for each new block are 99 and 97% respectively. NMR spectra of polymers obtained without purification.

The polymerization of the hydrochloride salts were carried out in (60/40) DMF / water reaction solutions, rather than pure water, since the mixed solvent system maintained a homogeneous reaction mixture (Schemes 2.11 and 2.12). VA-044 and the HCl monomers being water soluble, while the RAFT agent is hydrophobic. Two sequential chain extensions of poly(DMA)$_{41}$ with the monomer salts were indicative of good control/living character (Figures 2.9 and 2.10). Lower initiator concentrations were required for the first chain extension compared to the second for polymerizations with piperidine hydrochloride **3a.HCl** and pyrrolidine hydrochloride **2a.HCl** with high conversion and theoretical livingness (both ~99%) achieved. The successful RAFT polymerization of the ionized monomer salts **3a.HCl** and **2a.HCl**, overcame the lack of chain extension of poly(DMA)$_{41}$ with the free heterocyclic base monomers (*N*-[(piperidin-1-yl)methyl]prop-2-enamide (**3a**) and *N*-[(pyrrolidin-1-yl)methyl]prop-2-enamide (**2a**)) (Figures 2.6 and 2.13). Although MWDs shifted to higher MW with M_n close to $M_{n,th}$ (Table 2.1), the MWDs for **2a.HCl** (M_w/M_n = 1.66–1.80) were noticeably broader than **3a.HCl** (M_w/M_n = 1.31–1.40).

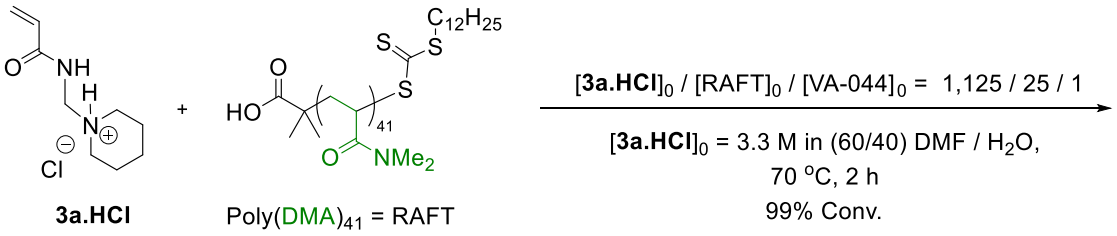

3a.HCl Poly(DMA)$_{41}$ = RAFT

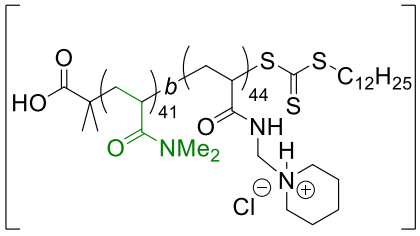

Poly(DMA)$_{41}$-*b*-(**3a.HCl**)$_{44}$ = RAFT

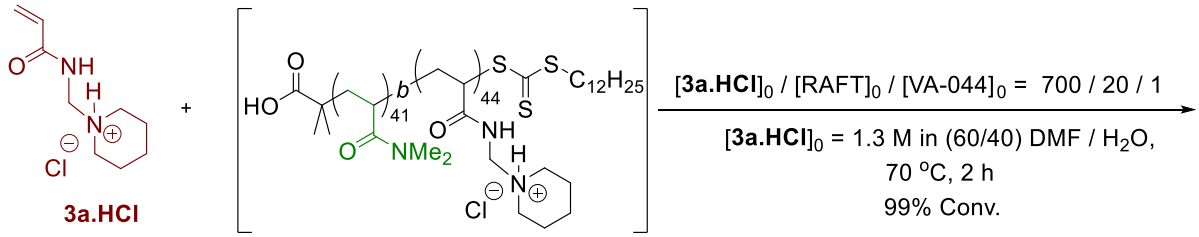

3a.HCl

Poly(DMA)$_{41}$-*b*-(**3a.HCl**)$_{44}$ = RAFT

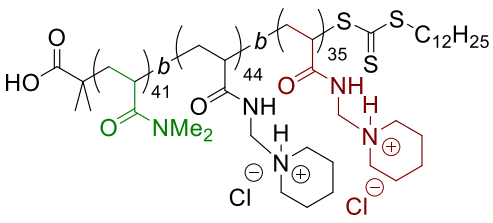

Poly(DMA)$_{41}$-*b*-(**3a.HCl**)$_{44}$-*b*-(**3a.HCl**)$_{35}$

Scheme 2.11: One-pot RAFT polymerization (without intermediate purifications) of *N*-[(piperidin-1-yl)methyl]prop-2-enamide hydrochloride (**3a.HCl)** to give block copolymer poly(DMA)$_{41}$-*b*-(**3a.HCl**)$_{44}$-*b*-(**3a.HCl**)$_{35}$.

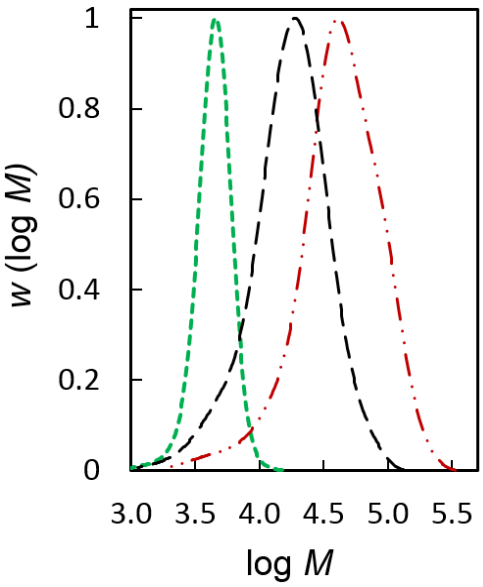

Figure 2.9: MWDs for one-pot 2 hours sequential RAFT polymerizations at 70 °C taken to 99% conversion of poly(DMA) macro-RAFT (green dashed line) with *N*-[(piperidin-1-yl)methyl]prop-2-enamide hydrochloride (**3a**.**HCl**) (black long dashed line) and (**3a**.**HCl**). Polymerizations in DMF / water (60/40) of (**3a.HCl**) to give block copolymer poly(DMA)$_{41}$-*b*-(**3a.HCl**)$_{44}$-*b*-(**3a.HCl**)$_{35}$ (red long dashed dot dot line).

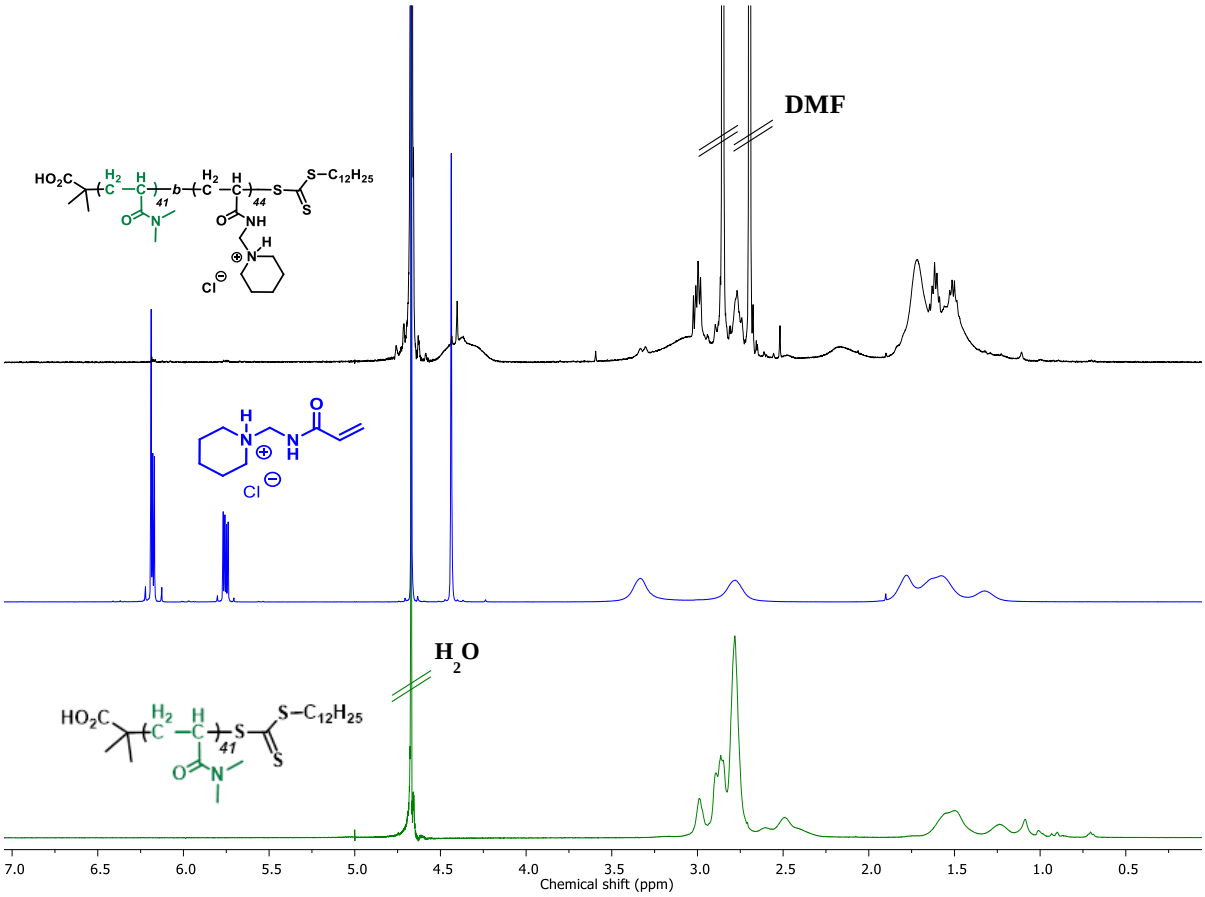

Figure 2.10: ^{1}H NMR spectra (D_2O, 400 MHz) monitoring of one-pot 2 hours sequential RAFT polymerizations of *N*-[(piperidin-1-yl)methyl]prop-2-enamide hydrochloride (**3a.HCl**, blue) and diblock copolymer poly(DMA)$_{41}$-*b*-(**3a.HCl**)$_{44}$ (black), The conversion for each new block is 99%. NMR spectra of polymers obtained without purification.

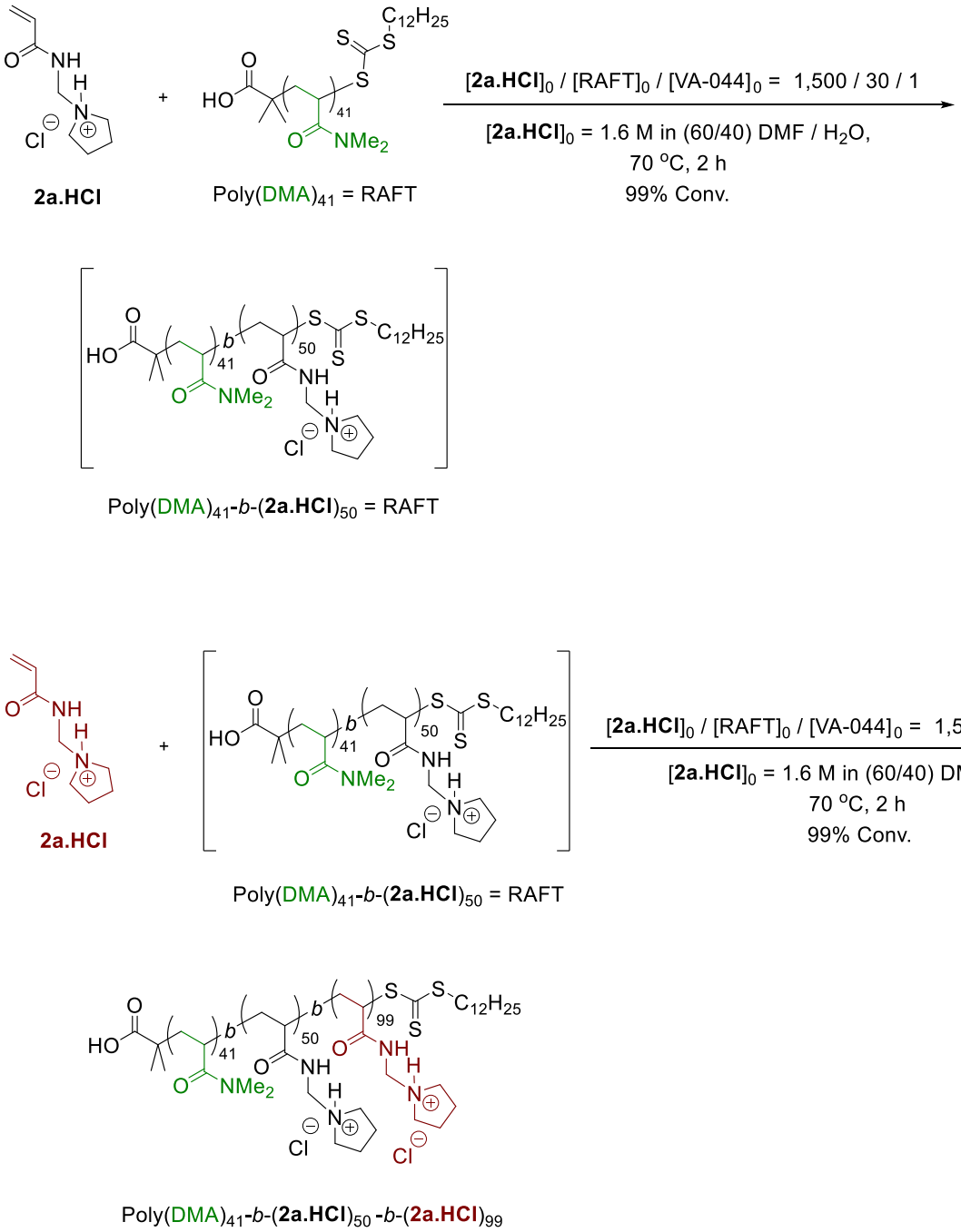

Scheme 2.12: One-pot RAFT polymerization (without intermediate purifications) of *N*-[(pyrrolidin-1-yl)methyl]prop-2-enamide hydrochloride (**2a.HCl**) to give block copolymer poly(DMA)$_{41}$-*b*-(**2a.HCl**)$_{50}$-*b*-(**2a.HCl**)$_{99}$.

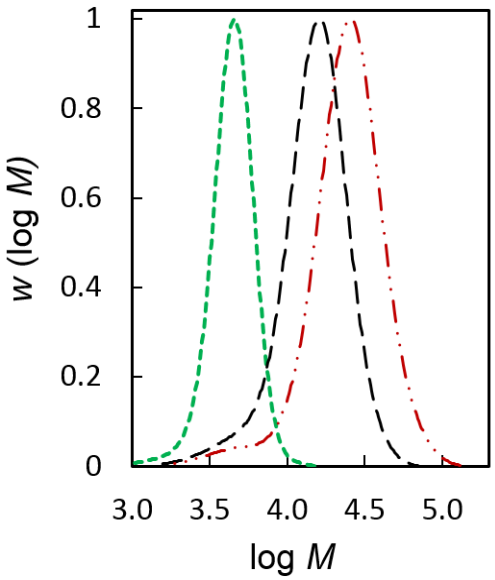

Figure 2.11: MWDs for one-pot 2 hours sequential RAFT polymerizations at 70 °C taken to 99% conversion of poly(DMA) macro-RAFT (green dashed line) with *N*-[(pyrrolidin-1-yl)methyl]prop-2-enamide hydrochloride (**2a.HCl**) (black long dashed line) and (**2a**.**HCl**). Polymerizations in DMF / water (60/40) of (**2a.HCl**) to give block copolymer poly(DMA)$_{41}$-*b*-(**2a.HCl**)$_{50}$-*b*-(**2a.HCl**)$_{99}$ (red long dashed dot dot line).

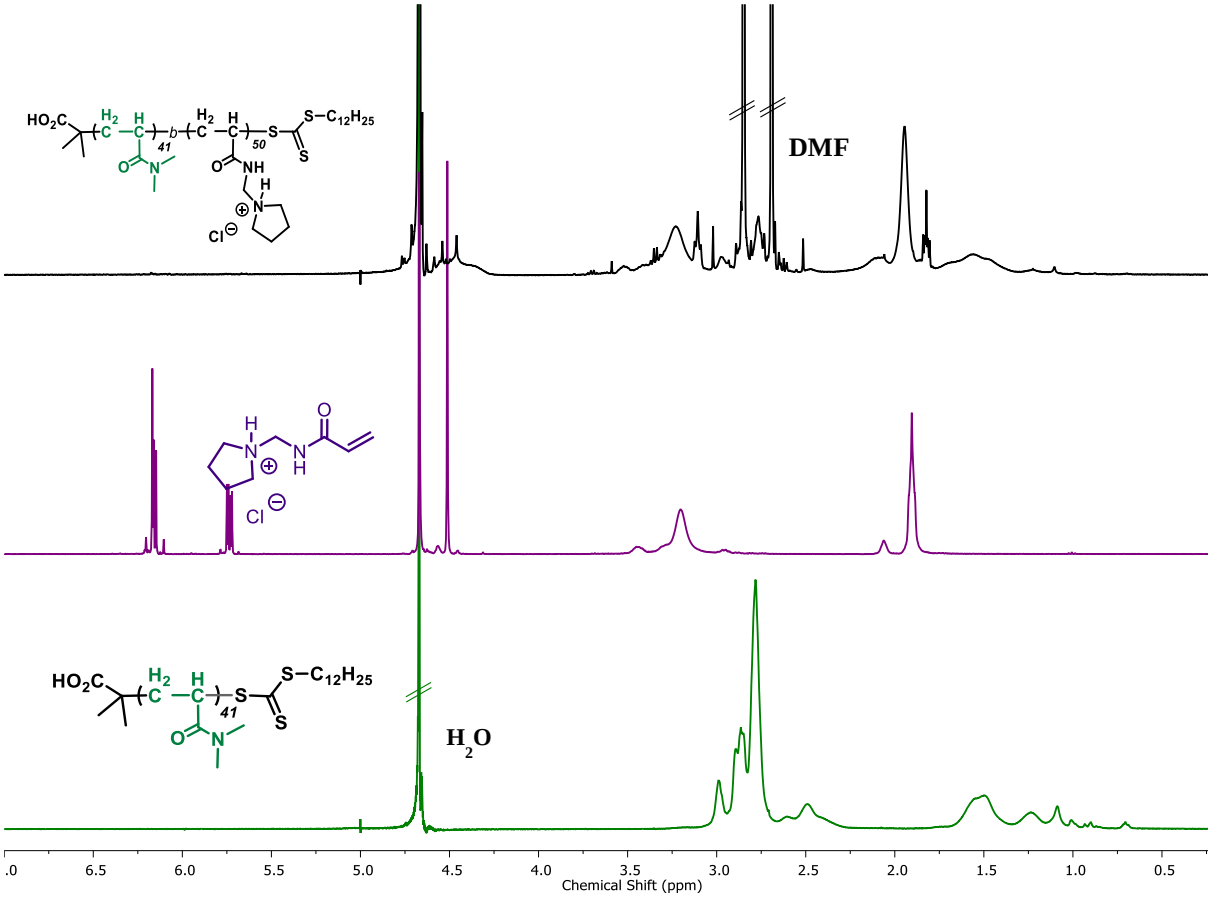

Figure 2.12: ^{1}H NMR spectra (D_2O, 400 MHz) monitoring of one-pot 2 hours sequential RAFT polymerizations of *N*-[(pyrrolidin-1-yl)methyl]prop-2-enamide hydrochloride (**2a.HCl**, purple) and diblock copolymer poly(DMA)$_{41}$-*b*-(**2a.HCl**)$_{50}$ (black), The conversion for each new block is 99%. NMR spectra of polymers obtained without purification.

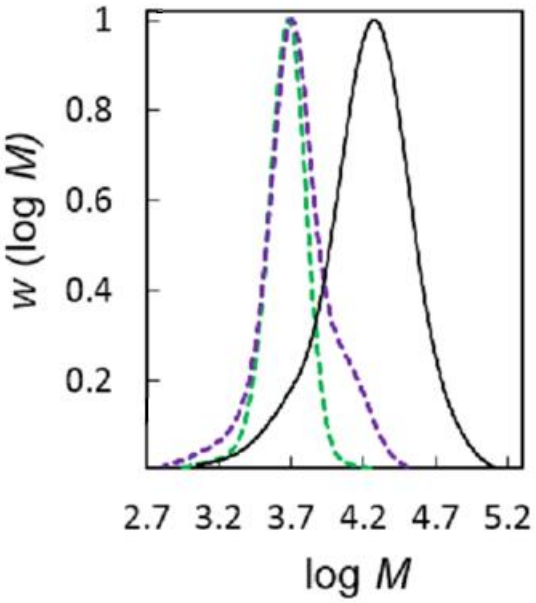

Figure 2.13: Attempts to chain extend poly(DMA) macro-RAFT (green dashed line) at 70 ^{o}C for 2 hours with *N*-[(pyrrolidin-1-yl)methyl]prop-2-enamide (**2a**) using (60/40) DMF / H_2O (purple dashed line) and with *N*-[(pyrrolidin-1-yl)methyl]prop-2-enamide hydrochloride (**2a.HCl**) (black continuous line) to give diblock copolymer poly(DMA)$_{41}$-*b*-(**2a.HCl**)$_{50}$.

Figure	Polymer [a]	$M_{n,th}$ [b]	M_n [d]	M_w/M_n [d]
2.3a	Poly(DMA)$_{41}$	5300	4450	1.10
2.4	Poly(DMA)$_{41}$-*b*-(**1a**)$_{69}$	16250	15280	1.35
	Poly(DMA)$_{41}$-*b*-(**1a**)$_{69}$-*b*-(DMA)$_{192}$	34300	34850	1.50
2.7	Poly(DMA)$_{41}$-*b*-(**3a**)$_{97}$	20750 [c]	20800	1.22
	Poly(DMA)$_{41}$-*b*-(**3a**)$_{97}$-*b*-(DMA)$_{116}$	32300 [c]	29200	1.25
2.10	Poly(DMA)$_{41}$-*b*-(**3a.HCl**)$_{44}$	13550	12750	1.31
	Poly(DMA)$_{41}$-*b*-(**3a.HCl**)$_{44}$-*b*-(**3a.HCl**)$_{35}$	19850	19750	1.40
2.12	Poly(DMA)$_{41}$-*b*-(**2a.HCl**)$_{50}$	13900	12850	1.66
	Poly(DMA)$_{41}$-*b*-(**2a.HCl**)$_{50}$-*b*-(**2a.HCl**)$_{99}$	31750	29800	1.80

Table 2.1: Characterization of polyacrylamides made using one-pot RAFT polymerizations. [a] The degree of polymerization for poly(DMA)$_{41}$ is calculated using M_n from GPC (deducting the MW of the RAFT end groups), and for all other polymers degree of polymerization is calculated from conversion by ^{1}H NMR (= 99%, except for chain extension with **3a**, which was 97%). In each case the degree of polymerization is obtained by deducting the M_n(GPC) of the extended macro-RAFT. [b] $M_{n,th}$ is calculated according to equation 2.2. [c] $M_{n,th}$ does not take into account the addition of HCl to these polymerizations. [d] Determined by GPC/RI in DMF (0.01 M LiBr) using commercial linear poly(methyl methacrylate, MMA) as molecular weight standards.

2.4 Conclusions

RAFT polymerization has allowed the first preparation of well-defined block copolymers of *N*-[(cycloalkylamino)methylene]acrylamides. The close proximity of the trithiocarbonate end group to the tertiary amino substituent made control/living character for the piperidine and pyrrolidine monomers superior when the heterocyclic pendant was ionized. Therefore, *N*-[(piperidin-1-yl)methyl]prop-2-enamide (**3a**) and *N*-[(pyrrolidin-1-yl)methyl]prop-2-enamide **(2a)** could only be polymerized in a controlled/living manner in the presence of HCl.

2.5 Future Work

Future research will involve controlled radical polymerizations (CRP) of the new methacrylamide monomer class.[14] This may give multi-stimuli response block copolymers (temperature, pH, CO_2), where the thermal response is expected to be in line with other well-known temperature responsive polyacrylamide and polymethacrylamide {e.g. poly(*N*-isopropylacrylamide) (PNIPAM),[18] poly(*N*-ethylmethacrylamide) (PNEMAM)}.[19] Water solubility may be manipulated by protonation of the heterocycle using weakly acidic solutions, including CO_2 in water. Alternatively, water-soluble block copolymer may be extended with hydrophobic monomer {e.g. *tert*-butyl acrylamide, TBAM} to make amphiphilic block copolymer self-assembly leading to CO_2 responsive polymersomes. Scheme 2.13 shows proposed RAFT polymerizations with high blocking efficiencies using the RAFT agent, 2-cyano-2-propyldodecyltrithiocarbonate (CPDTTC). The latter reagent is well-used in the formation of poly(MMA) macro-RAFT[20] or alternatively cyanoisopropyl dithiobenzoate (CPDB) can be used to make poly(MMA) macro-RAFT, which is extended with monomers that form bulky tertiary radicals.[21] We propose RAFT of MMA to give macro-RAFT and the chain extension with a new cyclic methacrylamide monomers such as 2-methyl-*N*-[(morpholin-4-yl)methyl]prop-2-enamide (**1b**) to give diblock copolymers and extending again with non-cyclic monomers such as *N*-[(dimethylamino)methyl]prop-2-enamide (**6a**) in to give triblock copolymers. Overall, we propose that a wide range of CO_2-tunable morphologies are accessible using well-defined polymethacrylamide block copolymers containing cyclic and non-cyclic tertiary amine moieties.

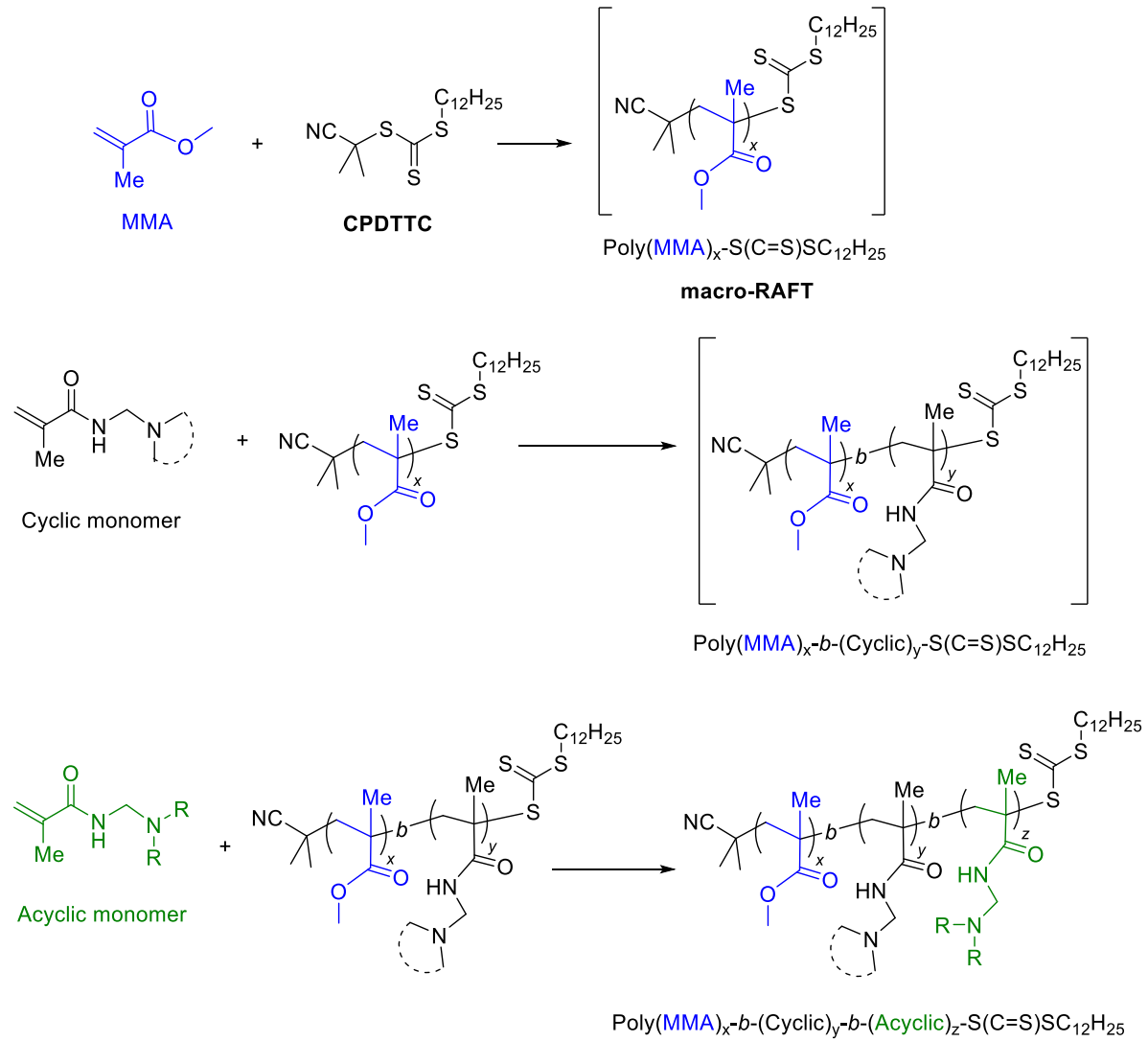

Scheme 2.13: Proposed preparation of poly(MMA)$_x$-*b*-(*N*-[(cycloalkylamino)methyl)]-methacrylamides)$_y$-*b*-(*N*-[(dialkylamino)methyl]methacrylamides)$_z$-S(C=S)SC$_{12}$H$_{25}$ triblock copolymers using RAFT polymerization.

Wang *et al*,[22] synthesized diblock copolymer via RAFT polymerization using different monomers classes (both acrylamide and methacrylate monomers) to give poly(NIPAM)$_x$-*b*-(2-nitrobenzyl methacrylate, NBM)$_y$ in Scheme 2.14. It should therefore be possible to prepare diblock copolymers containing *N*-[(dialkylamino)methyl)]acrylamides and *N*-[(dialkylamino)-methyl)]methacrylamides monomers to give poly(*N*-[(dialkylamino)methyl)]acrylamide)$_x$-*b*-(*N*-[(dialkylamino)methyl)]methacrylamide)$_y$-S(C=S)SC$_{12}$H$_{25}$, as shown in Scheme 2.15.

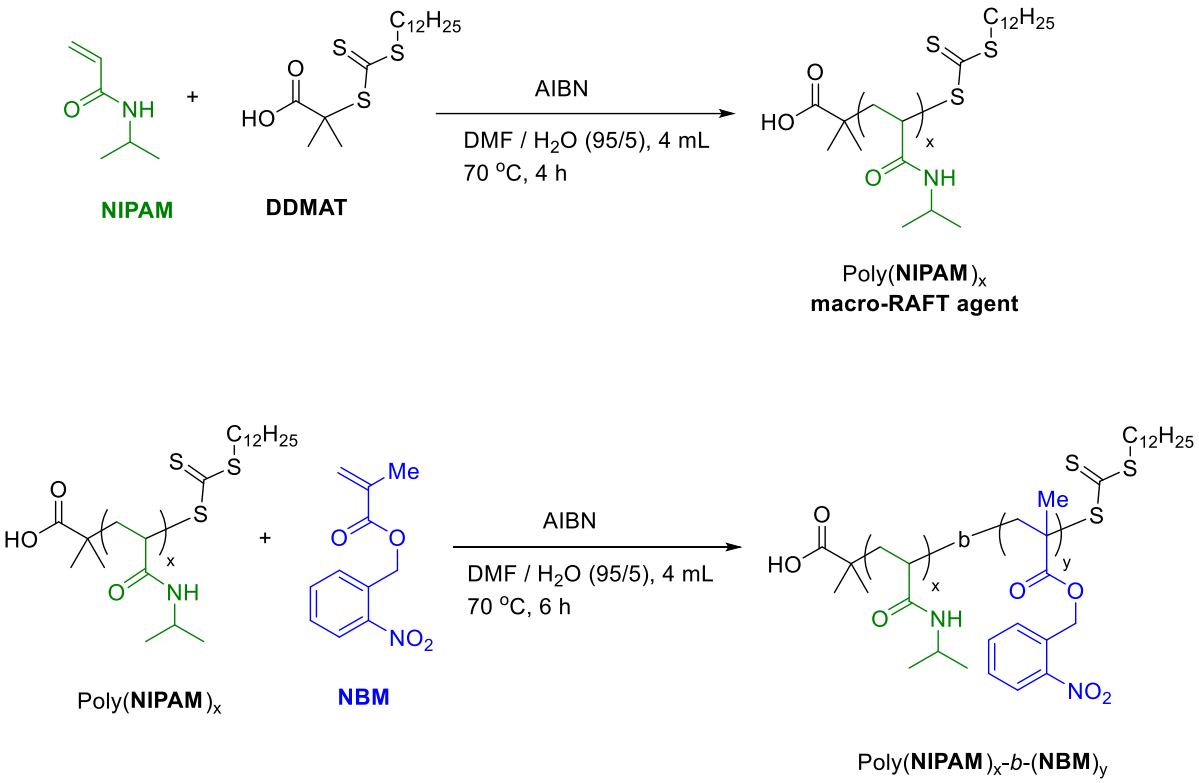

Scheme 2.14: Synthesis of diblock copolymer poly(NIPAM)$_x$-*b*-(NBM)$_y$ via RAFT polymerization.

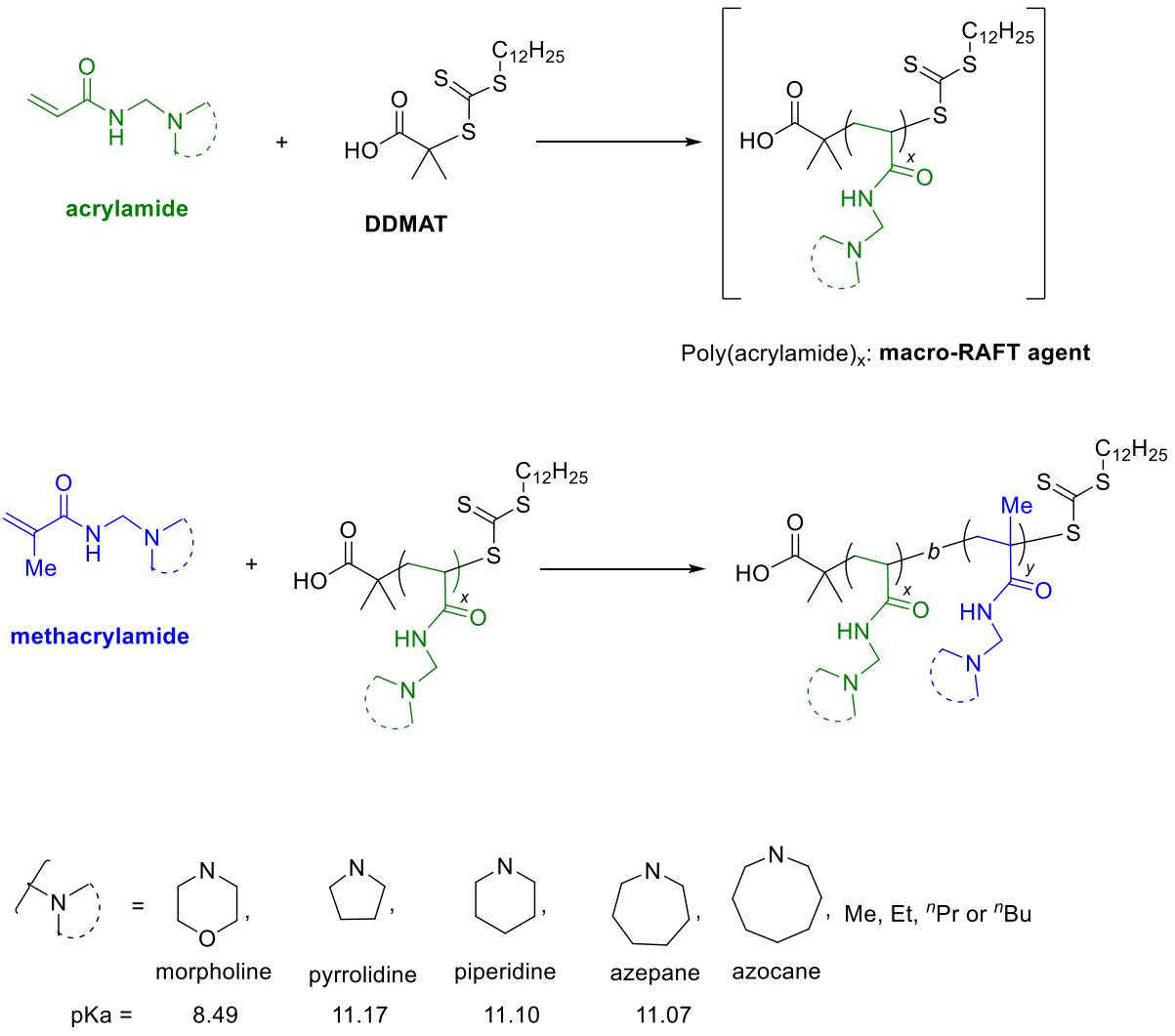

Scheme 2.15: Proposed preparation of poly(*N*-[(dialkylamino)methyl)]acrylamide)$_x$-*b*-(*N*-[(dialkylamino)methyl)]methacrylamide)$_y$-S(C=S)SC$_{12}$H$_{25}$ diblock copolymers using RAFT polymerization.

2.6 Experimental

2.6.1 Materials

2,2′-Azobis[2-(2-imidazolin-2-yl)propane]dihydrochloride (VA-044, Wako) and 2-(dodecylthiocarbonothioylthio)-2-methylpropionic acid (DDMAT, Sigma-Aldrich, 98%) were used as received. 1,4-Dioxane (Sigma-Aldrich, ≥99.0%) and Milli-Q water were used directly as solvents for polymerization. *N*,*N*-dimethylacrylamide (DMA, TCI, 98%) was distilled *in vacuo* to remove radical inhibitor. *N*,*N*-Dimethylformamide (DMF, Sigma-Aldrich, HPLC-grade, ≥99.9%), diethyl ether (Et_2O, Sigma-Aldrich, ≥99.5%), hydrochloric acid (HCl, Sigma-Aldrich, 36.5-38%), deuterium oxide (D_2O, Sigma-Aldrich, 99.9 atom%), and lithium bromide (LiBr, Sigma-Aldrich, 99%) were used as received. The preparations of *N*-[(morpholin-4-yl)-methyl]prop-2-enamide **(1a),** *N*-[(piperidin-1-yl)methyl]prop-2-enamide **(3a)**, *N*-[(piperidin-1-yl)methyl]prop-2-enamide hydr-ochloride (**3a.HCl**) and *N*-[(pyrrolidin-1-yl)methyl]prop-2-enamide hydrochloride **(2a.HCl**) are included in Gerard Hawkins Ph.D. thesis.[15]

2.6.2 Equipment and measurements

Polymerizations. All were carried out in borosilicate glass tubes sealed with septa and flushed with N_2 for 30 min.

Nuclear Magnetic Resonance (NMR) Spectroscopy. ^{1}H NMR spectra were recorded using a JEOL GXFT 400 MHz instrument equipped with a DEC AXP 300 computer workstation. For water soluble polymers D_2O was used as the NMR solvent. Conversion was estimated by sampling directly from the reaction mixture (without purification) and estimated using the integral for a polymer peak (where appropriate deducting the monomeric contribution of peaks containing both polymer and monomer contributions) relative to a monomer vinyl peak.

Theoretical number average molecular weight ($M_{n,th}$) was calculated according to equation 2.2:

$$M_{\mathrm{n,th}} = \left(\frac{[Monomer]_0}{[RAFT]_0} \times MW_{Monomer} \times Conversion\right) + MW_{RAFT} \qquad (2.2)$$

Where, RAFT represents DDMAT or polymeric macro-RAFT, MW_{monomer} and MW_{RAFT} are the molecular weights of the monomer and macro-RAFT agent respectively. Conversion was measured by ^{1}H NMR (as above).

Gel Permeation Chromatography (GPC). Molar mass distributions were measured using Agilent Technologies 1260 Infinity liquid chromatography system using a Polar Gel-M guard column (50 × 7.5 mm) and two Polar Gel-M columns (300 × 7.5 mm). DMF containing LiBr (0.01 M) was used as eluent at 1.0 $mL \cdot min^{-1}$ at 60 °C. Twelve narrow polydispersity poly(methyl methacrylate, MMA) standards (EasiVial PM 2 mL, Agilent) were used to calibrate the GPC system. Samples were dissolved in the eluent and filtered through a PTFE membrane with 0.2 μm pore size before injection (100 μL). Experimental molar mass (M_n) and polydispersity (M_w/M_n) values were determined by conventional calibration using Agilent GPC/SEC Software for Windows (version 1.2; Build 3182.29519). (M_n = 550–2,136,000 $g.mol^{-1}$). Number average molecular weight (M_n) values are not absolute, but relative to linear poly(MMA) standards (as above).

2.6.3 Preparation of macro-RAFT agent poly(DMA)$_{41}$

DDMAT (0.163 g, 0.45 mmol) and DMA (2.21 g, 0.022 mol) were added to VA-044 (4.5×10^{-3} mmol from a stock solution) in 5.0 mL dioxane/water (80/20) and heated at 70 °C for 2 hours. The polymer was precipitated from Et_2O, filtered, and dried at room temperature under vacuum for 24 hours to give poly(DMA)$_{41}$ macro-RAFT, M_n = 4,450 $g.mol^{-1}$, M_w/M_n = 1.11, 99% conv., isolated = 2.28 g.

2.6.4 General one-pot sequential polymerization procedure

Solutions were heated at 70 °C in an aluminum heating block for 2 hours. Polymerizations were stopped by placing test tubes in an ice-water bath. Conversion, M_n, and M_w/M_n were measured as described above. Unless otherwise stated sequential chain, extension reactions were performed directly on the macro-RAFT reaction solution with the amount of initiator remaining after each cycle taken into account.[10-11]

2.6.4.1 Preparation of poly(DMA)$_{41}$-*b*-(1a)$_{69}$-*b*-(DMA)$_{192}$ copolymer

Poly(DMA)$_{41}$ (1.43 x 10^{-2} mmol) and **1a** (0.170 g, 1.00 mmol) were added to VA-044 (1.43 x 10^{-3} mmol from a stock solution) in 0.60 mL water and heated as described above. DMA (0.275 g, 2.78 mmol) and VA-044 (6.5 x 10^{-4} mmol from a stock solution) in 0.50 mL water were added to the latter poly(DMA)$_{41}$-*b*-(**1a**)$_{69}$ solution and heated as described above.

2.6.4.2 Preparation of poly(DMA)$_{41}$-*b*-(3a)$_{97}$-*b*-(DMA)$_{116}$ copolymer

Poly(DMA)$_{41}$ (8.54 x 10^{-3} mmol) and **3a** (0.144 g, 0.854 mmol) were added to VA-044 (8.54 x 10^{-4} mmol from a stock solution) in 0.30 mL HCl (3.28 M, 1.15 eq. HCl : Monomer) solution and 0.20 mL dioxane, and heated as described above. DMA (0.100 g, 1.01 mmol) and VA-044 (8.6 x 10^{-4} mmol from a stock solution) in 0.10 mL water were added to the latter poly(DMA)$_{41}$-*b*-(**3a**)$_{97}$ solution and heated as described above.

2.6.4.3 Preparation of poly(DMA)$_{41}$-*b*-(3a.HCl)$_{44}$-*b*-(3a.HCl)$_{35}$ copolymer

Poly(DMA)$_{41}$ (37.1 x 10^{-3} mmol) and **3a.HCl** (0.342 g, 1.67 mmol) were added to VA-044 (1.48 x 10^{-3} mmol from a stock solution) in 0.50 mL DMF / water (60/40) solution, and heated as described above. Monomer **3a.HCl** (0.264 g, 1.29 mmol) and VA-044 (1.84 x 10^{-3} mmol from a stock solution) in 0.50 mL DMF / water (60/40) were added to the latter poly(DMA)$_{41}$-*b*-(**3a.HCl**)$_{44}$ solution and heated as described above.

2.6.4.4 Preparation of poly(DMA)$_{41}$-*b*-(2a.HCl)$_{50}$-*b*-(2a.HCl)$_{99}$ copolymer

Poly(DMA)$_{41}$ (16.4 x 10^{-3} mmol) and **2a.HCl** (0.156 g, 0.82 mmol) were added to VA-044 (5.46 x 10^{-4} mmol from a stock solution) in 0.50 mL DMF / water (60/40) solution, and heated as described above. Monomer **2a.HCl** (0.313 g, 1.64 mmol) and VA-044 (1.09 x 10^{-3} mmol from a stock solution) in 0.50 mL DMF / water (60/40) were added to the latter poly(DMA)$_{41}$-*b*-(**2a.HCl**)$_{50}$ solution and heated as described above.

References:

1. J. Chiefair, R. T. Mayadunne, G. Moad, E. Rizzardo and S. H. Thang, WO99031144A1, 1998.
2. J. Chiefari, Y. K. Chong, F. Ercole, J. Krstina, J. Jeffery, T. P. T. Le, R. T. A. Mayadunne, G. F. Meijs, C. L. Moad, G. Moad, E. Rizzardo and S. H. Thang, *Macromolecules*, **1998**, *31*, 5559–5562. https://doi.org/10.1021/ma9804951
3. P. Corpart, D. Charmot, T. Biadatti, S. Zard and D. Michelet, WO98058974A1, 1998.
4. A. D. Jenkins, R. G. Jones and G. Moad, *Pure Appl. Chem.* **2010**, *82*, 483–491. https://doi.org/10.1351/PAC-REP-08-04-03
5. B. A. Chalmers, A. Alzahrani, G. Hawkins and F. Aldabbagh, *J. Polym. Sci.: Part A: Polym. Chem.*, **2017**, *55*, 2123–2128. https://doi.org/10.1002/pola.28607
6. K. Matyjaszewski and Y. Xia, *Chem. Rev.* **2001**, *101*, 2921–2990. https://doi.org/10.1021/cr940534g
7. K. Matyjaszewski, *Adv. Mater.* **2018**, *30*, 1706441. https://doi.org/10.1002/adma.201706441
8. J. Qiu, B. Charleux, K. Matyjaszewski, *Prog. Polym. Sci.* **2001**, *26*, 2083–2134. https://doi.org/10.1016/S0079-6700(01)00033-8
9. G. Gody, T. Maschmeyer, P. B. Zetterlund, S. Perrier, *Nat. Commun*, **2013**, *4*, 2505–2514. https://doi.org/10.1038/ncomms3505
10. G. Gody, T. Maschmeyer, P. B. Zetterlund and S. Perrier, *Macromolecules*, **2014**, *47*, 639–649. https://doi.org/10.1021/ma402286e
11. G. Gody, T. Maschmeyer, P. B. Zetterlund and S. Perrier, *Macromolecules*, **2014**, *47*, 3451–3460. https://doi.org/10.1021/ma402435n
12. S. Perrier, *Macromolecules*, **2017**, *50*, 7433–7447. https://doi.org/10.1021/acs.macromol.7b00767
13. B. A. Chalmers, C. Magee, D. L. Cheung, P. B. Zetterlund and F. Aldabbagh, *Eur. Polym. J.*, **2017**, *97*, 129–137. https://doi.org/10.1016/j.eurpolymj.2017.10.004
14. A. Alzahrani, S. I. Mirallai, B. A. Chalmers, P. McArdle and F. Aldabbagh. *Org. Biomol. Chem.*, **2018**, *16*, 4108–4116. https://doi.org/10.1039/C8OB00811F
15. G. Hawkins Ph.D. Thesis, August 2017-National University of Ireland Galway, Ireland.
16. B. A. Abel and C. L. McCormick, *Macromolecules*, **2016**, *49*, 465–474. https://doi.org/10.1021/acs.macromol.5b02463

17. B. A. Abel and C. L. McCormick, *Macromolecules*, **2016**, *49*, 6193–6202. https://doi.org/10.1021/acs.macromol.6b01512
18. P. O' Connor, R. Yang, W. M. Carroll, Y. Rochev and F. Aldabbagh. *Eur. Poly. J.* **2012**, *48*, 1279–1288. https://doi.org/10.1016/j.eurpolymj.2012.04.011
19. P. Hazot, T. Delair, C. Pichot, J. -P. Chapel, A. Elaissari, *C. R. Chimie*, **2003**, *6*, 1417–1424. https://doi:10.1016/j.crci.2003.09.003
20. R. Hlushko, H. Hlushko and S. A. Sukhishvili, *Polym. Chem.*, **2018**, *9*, 506–516. https://doi.org/10.1039/C7PY01973D
21. C. Duffy, M. Phelan, P. B. Zetterlund, F. Aldabbagh, *J. Polym. Sci.: Part A: Polym. Chem.*, **2017**, 55, 1397–1408. https://doi.org/10.1002/pola.28509
22. F. Yang, Z. Cao and G. Wang, *Polym. Chem.*, **2015**, *6*, 7995–8002. https://doi.org/10.1039/C5PY01435B

Chapter 3

Preparation of vesicles using Polymerization-Induced Self-Assembly (PISA) based on ATRP in Supercritical Carbon Dioxide

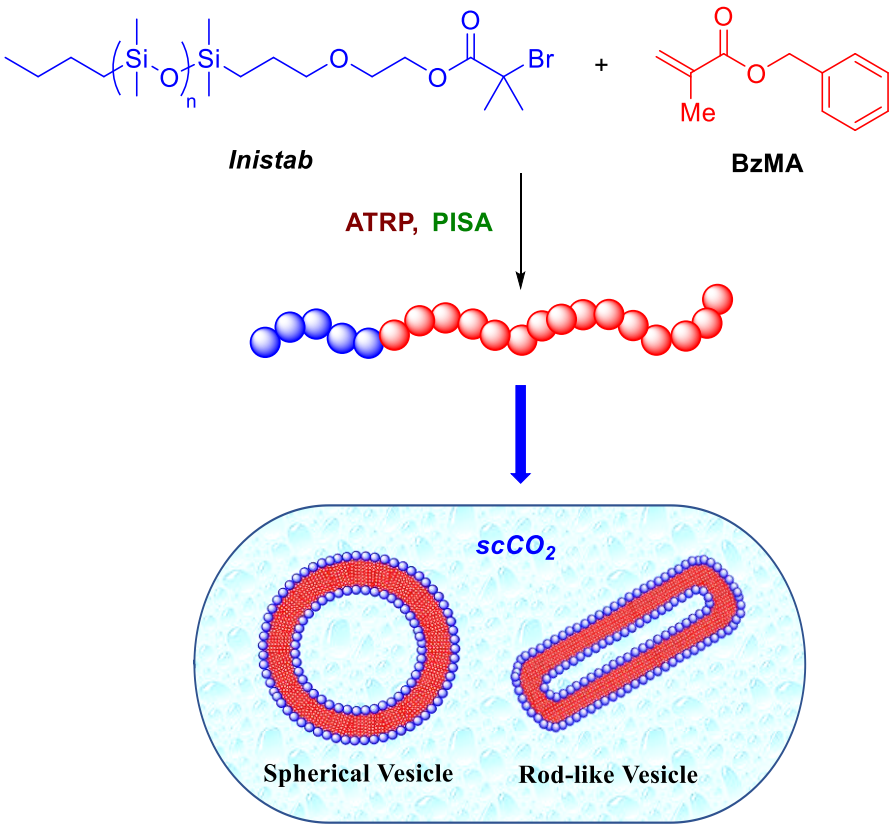

3.1 Introduction

3.1.1 Atom Transfer Radical Polymerization (ATRP)

Atom transfer radical polymerization (ATRP) is type a reversible deactivation radical polymerization (RDRP),[1] first reported by Matyjaszewski[2] and Sawamoto[3] in 1995. Sawamoto reported ruthenium-mediated ($[RuCl_2(PPh_3)_3]$) ATRP and Matyjaszewski reported a similar process with the more popular copper-catalysis (CuBr). ATRP involves a reversible dissociation-combination mechanism (Scheme 3.1). ATRP is a multi-component system incorporating, monomer, initiator (which is an alkyl halide, R-X) and a catalyst (a transition metal complex species with a suitable ligand). The R-X undergoes fast homolytic fission upon reduction by the metal complex species (e.g. $Cu^{(I)}$) capable of increasing its oxidation number, and complexing with ligand (L). The formed metal complex ($X\text{-}Cu^{(II)}\text{-}L$) is then reversibly deactivated upon reduction with $R^{\bullet}$. The initiating radical, $R^{\bullet}$ is in the active state, and can add to monomer to form a propagating radical ($P_n^{\bullet}$). $P_n^{\bullet}$ will propagate further until it is reversibly deactivated to form a dormant halide capped polymer chain (P_n-X) and the original metal complex ($Cu^{(I)}$/L). For a successful ATRP, initiation needs to be fast and quantitative, so that all propagating species can begin propagating at the same time yielding polymers with narrow molecular weight distributions. ATRP is a robust technique applicable to a range of monomers and is tolerant of many functional groups such as styrenes, acrylates, methacrylate, acrylamides, methacrylamides, acrylonitrile and l,3-dienes.[4-5]

The theoretical molecular weight, $M_{n,th}$, is determined by the alkyl halide initiator concentration relative to the monomer as shown in equation 3.1.

$$M_{n,th} = \frac{\alpha[M]_0 \, MW_{mono}}{[\text{Alkyl halide}]_0} + MW_{\text{Alkyl halide}} \qquad (3.1)$$

Where, α is monomer conversion, $[M]_0$ is the initial monomer concentration, MW_{mono} is the molecular weight of the monomer and $[\text{Alkyl halide}]_0$ is the initial concentration of the alkyl halide initiator. The theoretical molecular weight ($M_{n,th}$) value in this chapter was derived using equation 3.2.

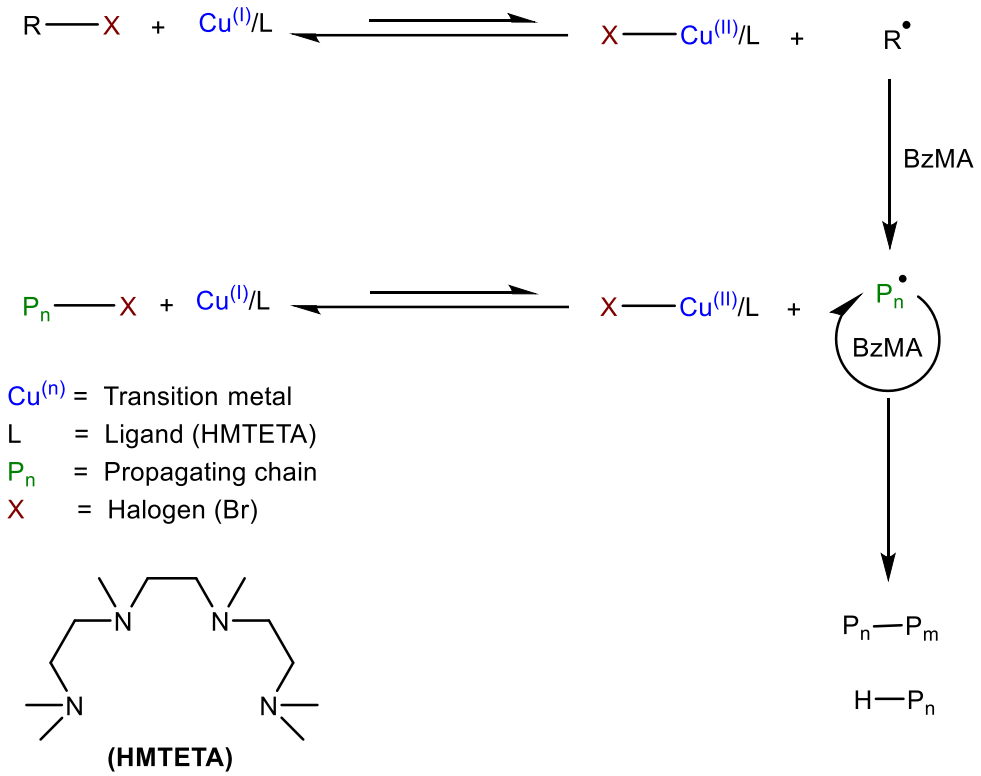

Scheme 3.1: General mechanism for traditional ATRP using benzyl methacrylate (BzMA) as the monomer, $Cu^{(I)}$ as the catalyst and 1,1,4,7,10,10-hexamethyltriethylenetetramine (HMTETA) as the ligand.

$$M_{n,th} = \frac{\alpha[BzMA]_0 \, MW_{BzMA}}{[PDMS\text{-}Br]_0} + MW_{PDMS\text{-}Br} \qquad (3.2)$$

Where, α is monomer (BzMA) conversion, $[BzMA]_0$ is the initial monomer concentration, MW_{BzMA} is the molecular weight of the monomer, $[PDMS\text{-}Br]_0$ is the initial concentration of bromo-terminated poly(dimethylsiloxane, DMS) macroinitiator and $MW_{PDMS\text{-}Br}$ is the molecular weight of the PDMS-Br determined by GPC.

ATRP has been reported with several different transition metals, including copper,[2] iron,[6] cobalt,[7] ruthenium,[2] and nickel,[8] but the most often used are the transition metals based on copper (the two oxidation states are $Cu^{(I)}$ and $Cu^{(II)}$, such as CuCl/dNdpy (4,4'-dinonyl-2,2'-dipyridyl).[9]

In a normal ATRP, a transition metal complex with low oxidation state is used as a catalyst. This metal can be easily oxidized, which makes normal ATRP very sensitive to air. In "reverse" ATRP,[10] a transition metal with higher oxidation state is used as a catalyst, and a conventional free radical initiator is used instead of the halogenated initiator. The mechanism is shown in (Scheme 3.2). The thermal decomposition of the conventional free radical initiator such as 2,2′-azobis(2-methylpropionitrile) AIBN, generates radicals ($I^{\bullet}$), which react with catalyst complex in the higher oxidation state ($X\text{-}Cu^{(II)}/L$) complex to form alkyl halide initiators (dormant species) (I-X) *in situ*, and a catalyst ($Cu^{(I)}/L$) complex in lower oxidation state. Alternatively, $I^{\bullet}$ reacts with monomer such as styrene (St), methyl acrylate (MA) or methyl methacrylate (MMA) to form a propagating radical, $I\text{-}P_n^{\bullet}$. Deactivation is by reaction of propagating radicals with the added $X\text{-}Cu^{(II)}/L$.[11]

Another major limitation for ATRP is the stoichiometric amounts of metal catalyst required to control polymerizations. This has been overcome using activators regenerated by electron transfer (ARGET) in which small amounts of catalyst as low as 50 ppm is continuously regenerated by addition of a reducing agent {e.g. $tin^{(II)}$ 2-ethylhexanoate ($Sn(EH)_2$)}. The PMDETA as ligand has high value for deactivation (k_{deact}) rate constants in addition to higher (k_{ATRP}) led to fast polymerization in (Scheme 3.3)[12] than HMTETA in (Scheme 3.1).

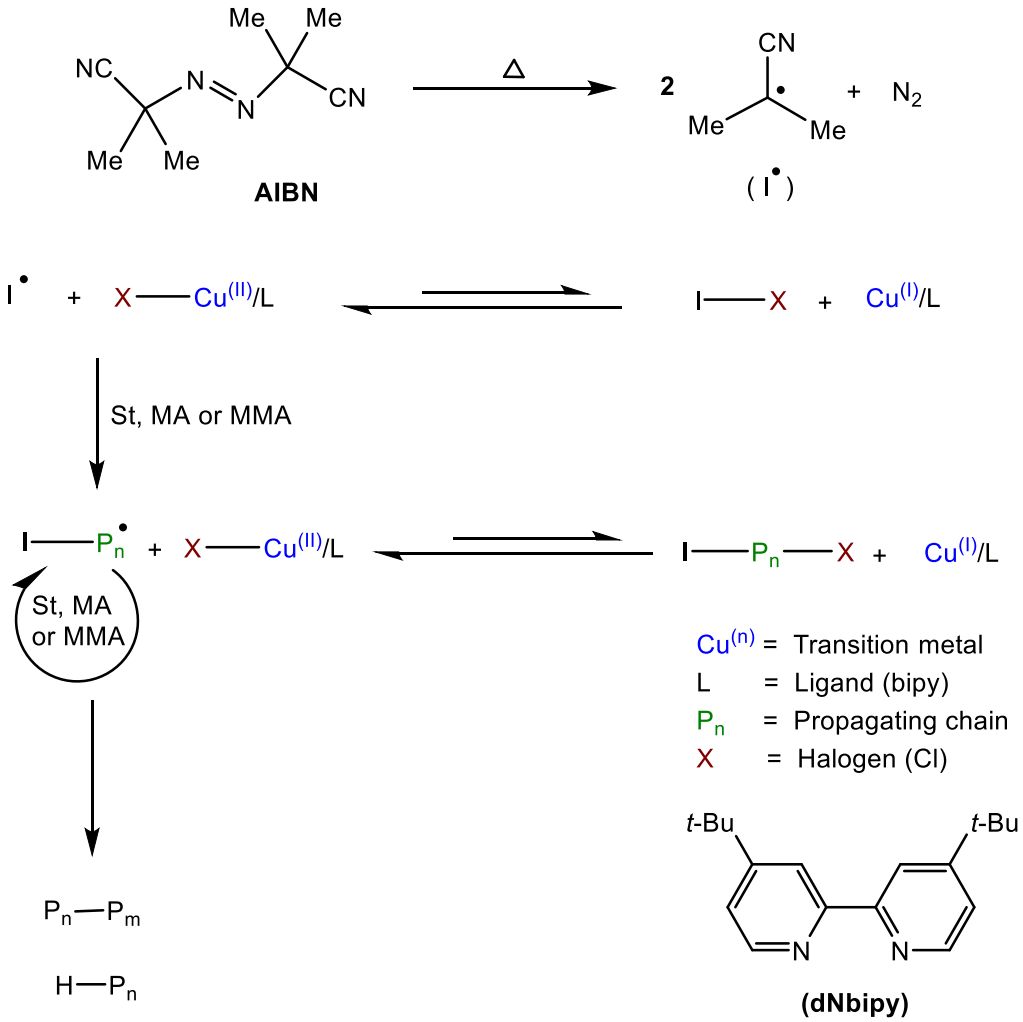

Scheme 3.2: Mechanism for "reverse" ATRP using St, MA or MMA as the monomers, $Cu^{(II)}$ as the catalyst and 4,4′-di-*tert*-butyl-2,2′-dipyridyl (dNbipy) as ligand at 110 ^{o}C.

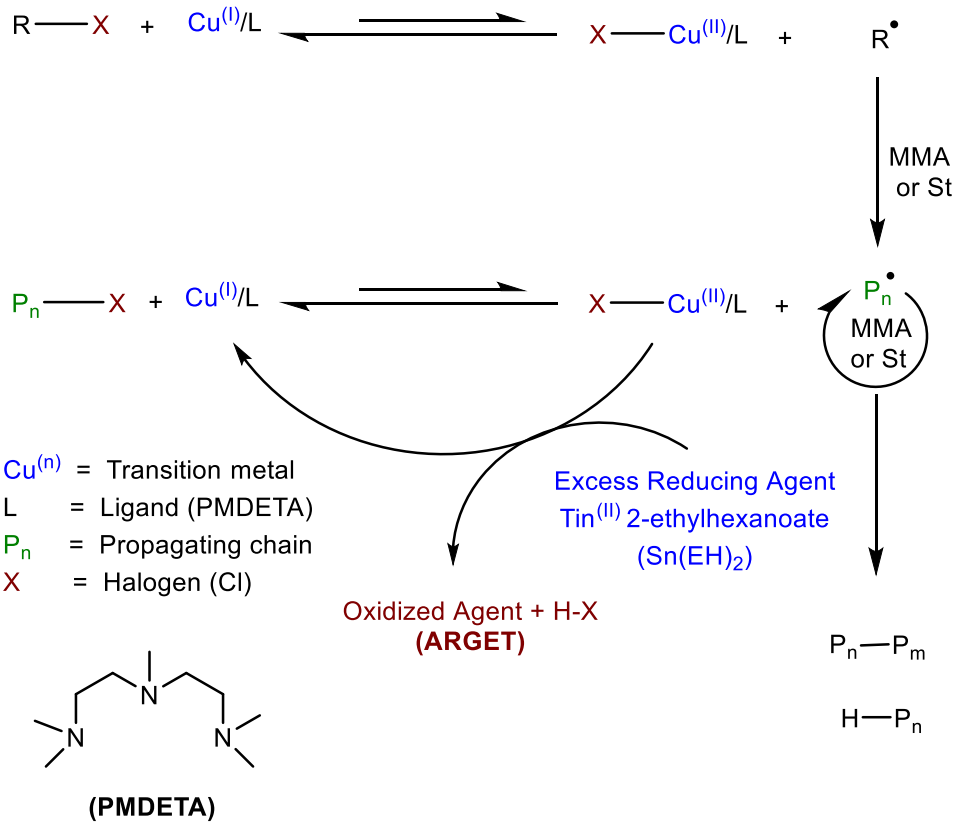

Scheme 3.3: Mechanism for activator regenerated by electron transfer (ARGET) ATRP using MMA or St as the monomers, $Cu^{(I)}$ as the catalyst and *N*,*N*,*N'*,*N''*,*N''*-pentamethyl-diethylenetriamine (PMDETA) as ligand at 90–110 ^{o}C.

3.1.2 Polymerization Induced Self-Assembly (PISA)

Over the past decade there has been intense interest in the preparation of non-spherical polymer particles by polymerization-induced self-assembly (PISA) (Scheme 3.4).[13-29]

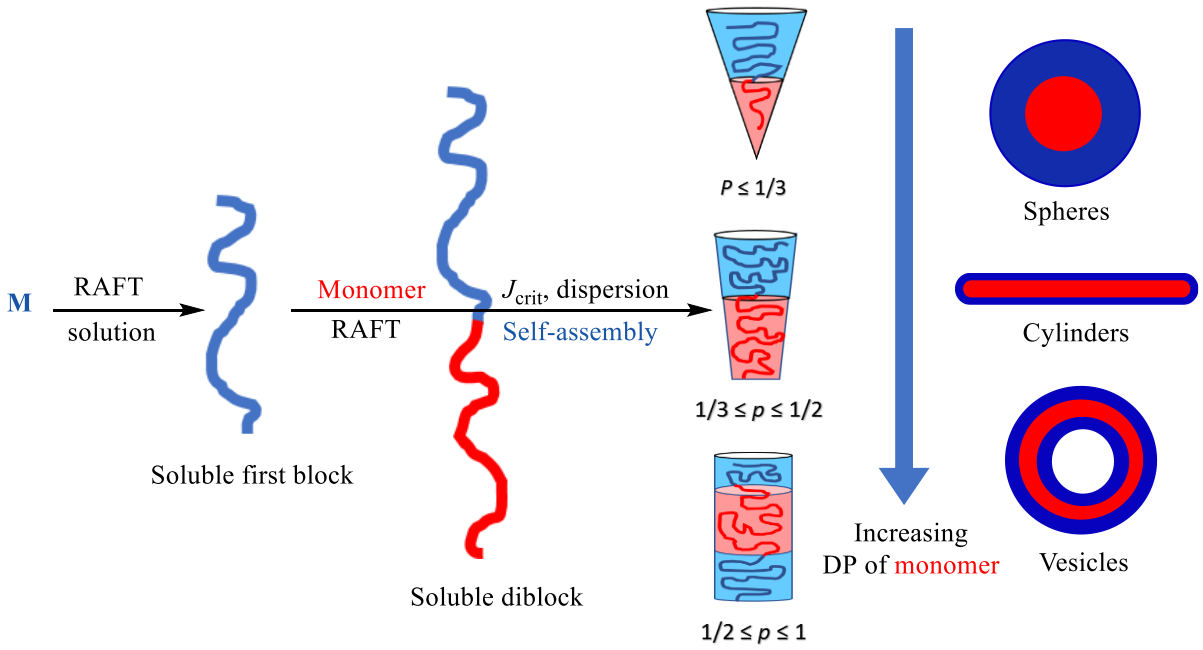

Scheme 3.4: Schematic of the synthesis of diblock copolymer nano-objects via polymerization-induced self-assembly (PISA).

The shape of the nanoparticle is due to how amphiphilic block copolymers undergo self-assembly to minimize interactions between the hydrophobic block and water. The preferred shape of the nanoparticle is determined by packing parameter of the amphiphilic molecules. The packing of the copolymer chains affect the molecular curvature of the nanoparticle and can be predicted with the following equation (3.3).

$$p = \frac{v}{a_o\, l_c} \tag{3.3}$$

Where p is the packing parameter, v is the volume of the hydrophobic block, a_o is the optimal area of the head group and l_c is the length of the hydrophobic tail. In general spherical particles are favoured when $p \leq 1/3$, cylindrical particles or rods when $1/3 \leq p \leq 1/2$, and vesicles when $1/2 \leq p \leq 1$.[30]

Vesicles are known as polymersomes, where the hollow solution filled core can typically encapsulate drugs allowing controlled release.[31-32] PISA typically uses RDRP implemented as a dispersion polymerization, mostly commonly reversible addition-fragmentation chain transfer (RAFT) polymerization, to extend a solvophilic macro-RAFT agent (also acting as steric stabilizer) with a dissolved monomer forming the solvophobic polymer core (Scheme 3.4).[18-22,26-28, 33-34]

One of the main advantages of PISA is its ability to prepare higher order morphologies (e.g., worms, vesicles) at high block copolymer concentrations in one polymerization step from monomer, without recourse to any post polymerization processing. Traditionally, diblock copolymer self-assembly in solution requires post-polymerization processing, where the copolymer chains were initially dissolved in a good solvent for both blocks and then a selective solvent for one of the blocks is added in order to induce self-assembly. The traditional approach usually requires additional purification steps to remove the non-selective solvent, e.g. by dialysis with the disadvantage: it is almost invariably conducted in dilute solution (<1%).[35]

BzMA is a common monomer used for PISA. This is because unlike St and MMA, it has a relatively low glass transition temperature (T_g) in the resultant polymer, which is associated with increased chain mobility in the core facilitating morphology transition from spheres to worm-like and vesicular morphologies.[18-20, 23, 29]

3.1.2.1 PISA using RAFT polymerization

Most reported PISA in conventional media were carried out using RAFT dispersion polymerizations. Armes *et al*, carried out PISA as an emulsion RAFT polymerization of BzMA in water (Scheme 3.5a). Emulsion because a water immiscible monomer, BzMA was polymerized by extending a water soluble poly(glycerol monomethacrylate) poly(GMA)$_{51}$ macro-RAFT giving reasonably well-defined spherical particles.[36] The same group carried out a RAFT alcoholic dispersion polymerization of BzMA using poly(2-hydroxypropyl methacrylate) poly(HPMA)$_{48}$ macro-RAFT in Scheme 3.5b.[37] The produced poly(HPMA)$_{48}$-*b*-(BzMA)$_{150}$ diblock copolymer morphologies obtained were of higher order; worms and vesicles.

Most commonly, spherical nanoparticles have been used for drug delivery, whilst in contrast, other morphologies have received little attention, despite evidence that not only size, but also morphology can make a considerable difference to the efficacy.[38] RAFT dispersion polymerization formulation for non-polar solvents such as *n*-heptane or *n*-dodecane solvents used long poly(lauryl methacrylate), poly(LMA)$_{17}$ macro-RAFT. This allowed the formation of vesicles nanoparticles with BzMA, well-defined vesicles were obtained for poly(LMA)$_{17}$-*b*-(BzMA)$_{100\text{-}250}$ and thicker vesicle membranes are produced when targeting higher *DP* values for the membrane-forming poly(BzMA)$_n$ block, such as the degree of polymerization (*DP*) was 250, with high conversions (98%) and low polydispersity (M_w/M_n = 1.26) at 90 ^oC at 20 wt% solid giving poly(LMA)$_{17}$-*b*-(BzMA)$_{250}$ in Scheme 3.5c.[19]

(a) RAFT aqueous emulsion polymerization

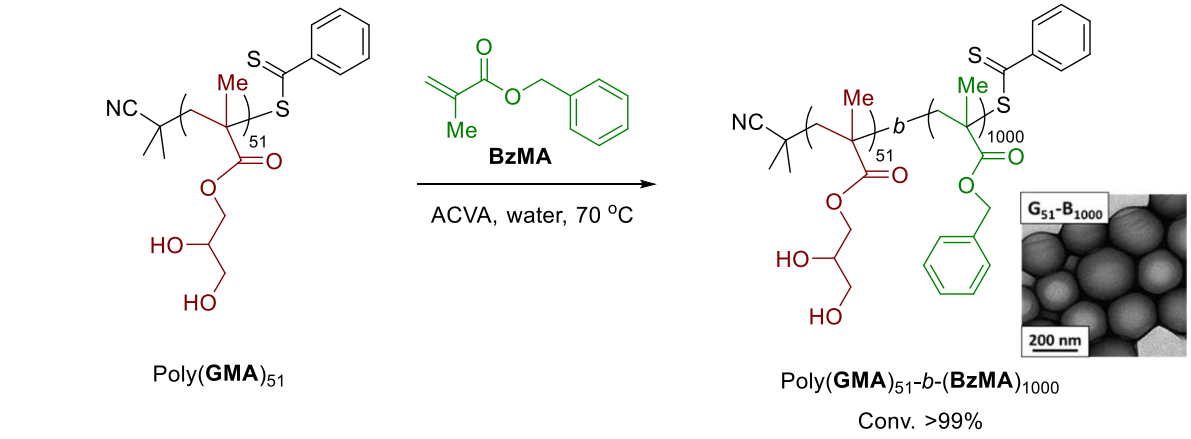

Poly(**GMA**)$_{51}$

Poly(**GMA**)$_{51}$-*b*-(**BzMA**)$_{1000}$

Conv. >99%

(b) RAFT acoholic dispersion polymerization

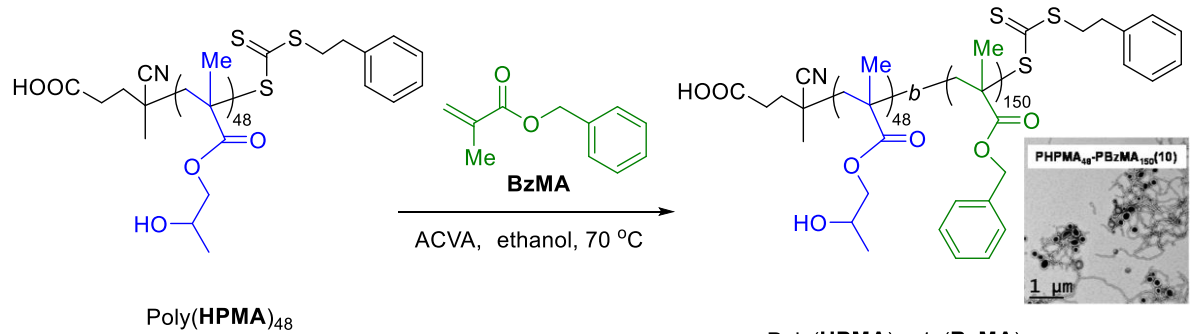

Poly(**HPMA**)$_{48}$

Poly(**HPMA**)$_{48}$-*b*-(**BzMA**)$_{150}$

Conv. >99%

(c) RAFT dispersion polymerization in *n*-alkanes

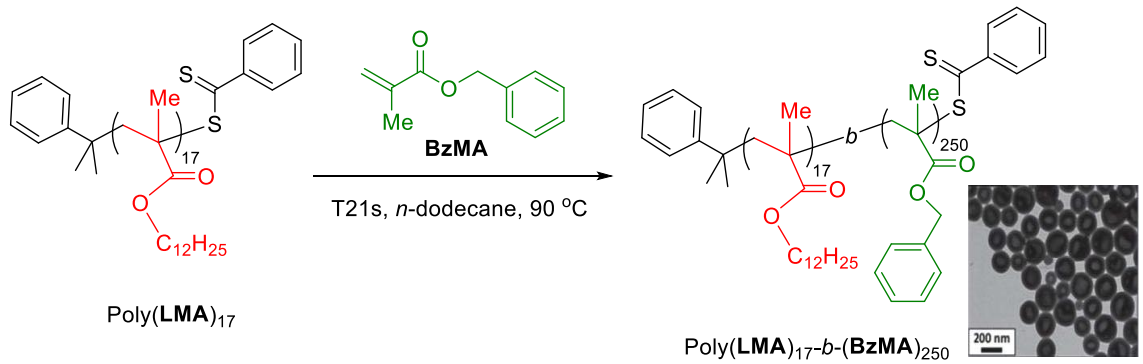

Poly(**LMA**)$_{17}$

Poly(**LMA**)$_{17}$-*b*-(**BzMA**)$_{250}$

Conv. >97%

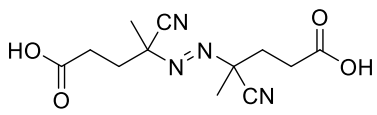

4,4'-Azo-bis(4-cyanopentanoic acid)

ACVA

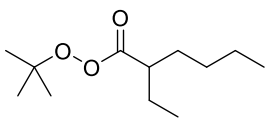

Tert-Butyl peroxy-2-ethylhexanoate

T21s

Scheme 3.5: Examples of PISA formulations carried out by Armes *et al*, mediated by **(a)** RAFT aqueous emulsion polymerization, **(b)** RAFT alcoholic dispersion polymerization and **(c)** RAFT dispersion polymerization in *n*-alkanes. Embedded TEMs give indications of polymer morphologies.

RAFT dispersion PISA has also been carried out in an ionic liquid [bmim][PF_6] (1-butyl-3-methylimidazolium hexafluorophosphate), a recyclable green solvent, giving nanoaggregates of multiple morphologies in Scheme 3.6.[21]

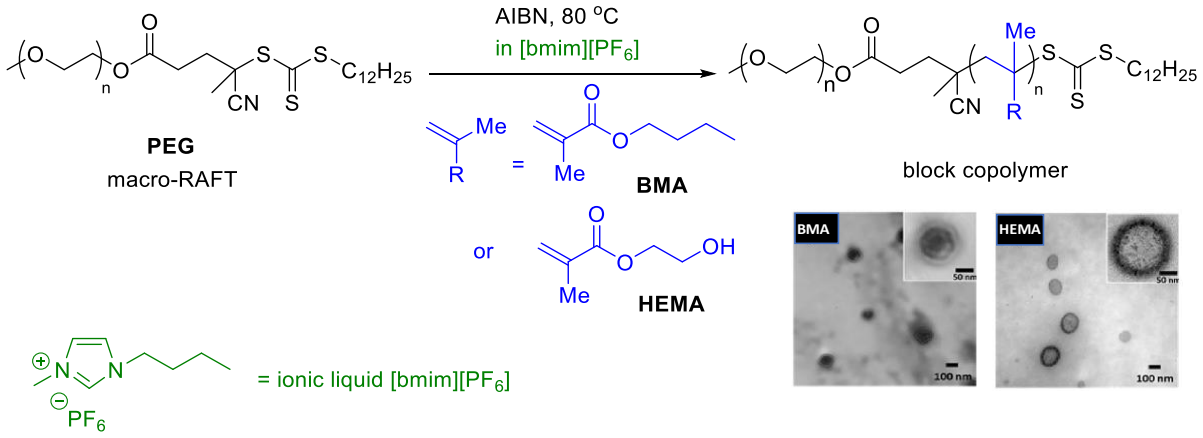

Scheme 3.6: RAFT dispersion polymerization for the preparation of vesicles using polymerization-induced self-assembly (PISA) in ionic liquid (1-butyl-3-methylimidazolium hexafluorophosphate, [bmim][PF_6]). Embedded TEMs give indications of polymer morphologies.

3.1.2.2 PISA using Reversible Deactivation Radical Polymerization (RDRP) techniques

PISA can also be implemented as other living processes, such as atom transfer radical polymerization (ATRP). Matyjaszewski *et al*, carried out PISA by conducting an initiator for continuous activator regeneration atom transfer radical polymerization (ICAR). ICAR could simplistically be considered as a "reverse" ARGET ATRP.[4] ICAR ATRP was carried out at low ppm of $Cu^{(II)}$ catalyst concentration as a dispersion polymerization of BzMA in ethanol. The latter gave short wormlike at *DP* = 450 and spherical particles solid at *DP* = 300 of poly(OEOMA)$_{50}$-*b*-(BzMA)$_n$. The macroinitiator poly(oligo-(ethylene oxide) methyl ether-methacrylate)$_{50}$, poly(OEOMA)$_{50}$ block was made in an aqueous solution polymerization using ICAR, using the water-soluble initiator VA-044 at 44 °C in Scheme 3.7.[23]

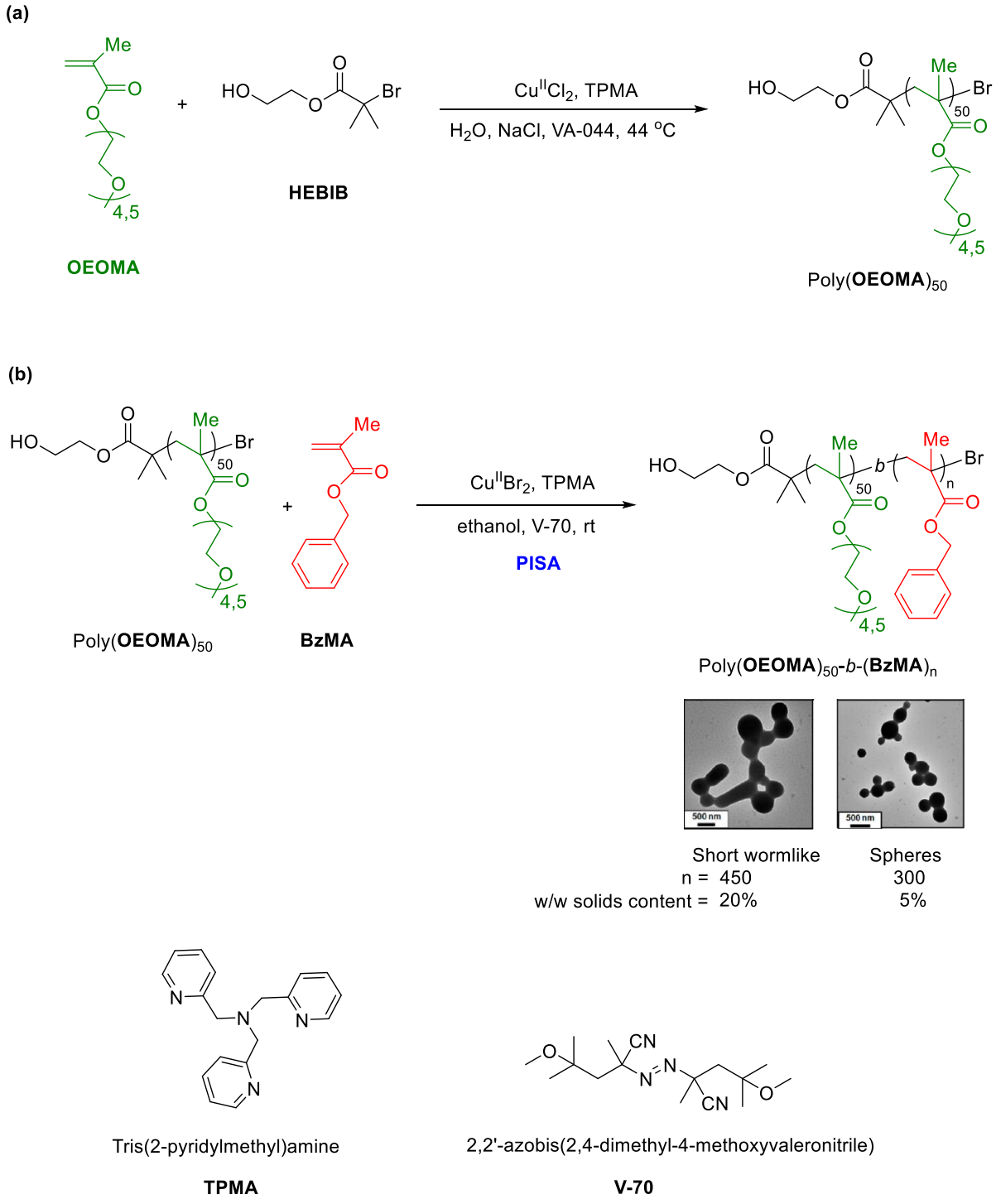

Scheme 3.7: (a) Synthesis of macroinitiator using a aqueous solution ATRP and **(b)** PISA of BzMA using dispersion ATRP to give poly(oligo(ethylene oxide) methyl ethermethacrylate, OEOMA)$_{50}$-*b*-(BzMA)$_n$ observed by TEMs.

Charleux *et al*, carried out PISA by nitroxide-mediated polymerization (NMP) using poly(poly(ethylene)oxide methacrylate, PEOMA-*co*-St)-SG1 macroalkoxyamine initiator. The macroalkoxyamine was employed to initiate the emulsion polymerization of *n*-butyl methacrylate (BMA) with a small amount of St at 85 °C in 1,4 dioxane, to give poly(PEOMA)$_{20}$-*co*-(St)$_2$-*b*-poly(BMA-*co*-St)$_{211}$-SG1 amphiphilic diblock copolymer. The morphologies obtained were well-defined spherical particles (Scheme 3.8).[39] Methacrylate monomers can be controlled by NMP (including by *N*-*tert*-butyl-*N*-(1-diethylphosphono-2,2-dimethylpropyl) nitroxide, SG1) by addition of a small amount of as St (below 10 mol%), as a co-monomer.[40] St has a lower activation-deactivation equilibrium constant, *K*, which reduces the overall *K* of the system leading to a higher degree of living polymer. It is known that methacrylate polymerizations are difficult to control by NMP due to hydrogen-abstraction by the nitroxide leading to macromonomer formation at the elevated temperatures used with NMP.[41]

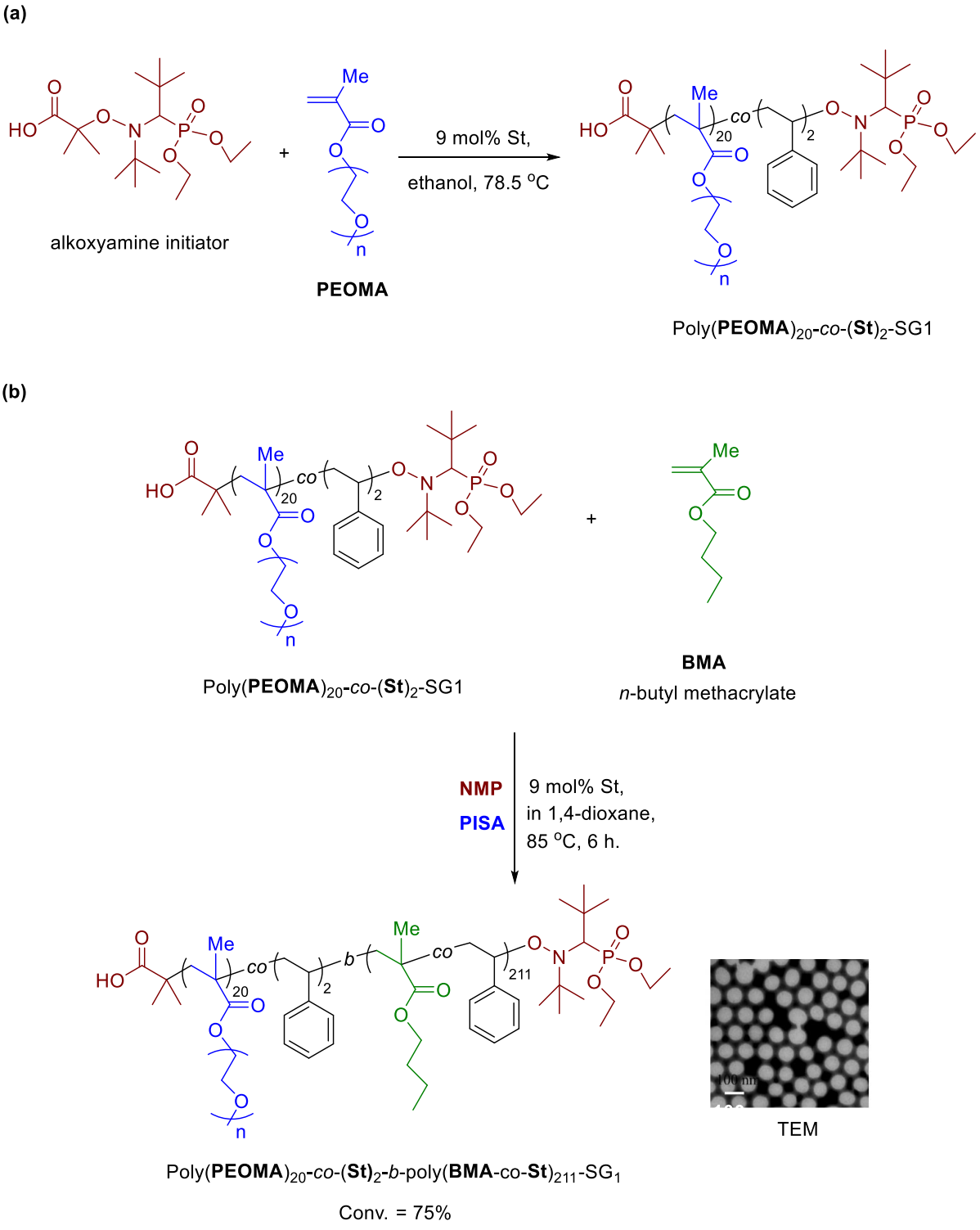

Scheme 3.8: (a) Synthesis of macroalkoxyamine initiator using a solution NMP in the presence of 9% St and **(b)** PISA of *n*-butyl methacrylate (BMA) using emulsion NMP in the presence of 9% St to give poly(PEOMA)$_{20}$-*co*-(St)$_2$-*b*-poly(BMA-*co*-St)$_{211}$-SG1 observed by TEM.

3.1.3 Supercritical Carbon Dioxide ($ScCO_2$)

Carbon dioxide is a gas under standard temperature and pressure. It can be converted to the liquid and supercritical phase by increasing temperature and pressure. A supercritical fluid (SCF) is defined as a substance above its critical temperature and pressure, known as the critical point (Figure 3.1), where distinct liquid and gas phases do not exist. Above its critical point CO_2 demonstrates gas like diffusivity, with liquid-like density and can dissolve materials like a liquid. Carbon dioxide has a critical point of 31.10 ^oC and 7.38 MPa,[42] which are relatively mild when compared to other supercritical fluids such as water (374.20 ^oC and 22.05 MPa).[43] A widely utilized industrial application of $scCO_2$ is in the dry cleaning industry[44] and for the decaffeination of coffee.[45] Supercritical carbon dioxide ($scCO_2$) is a well-known benign effective replacement for environmentally damaging volatile organic compounds (VOCs).[46-47]

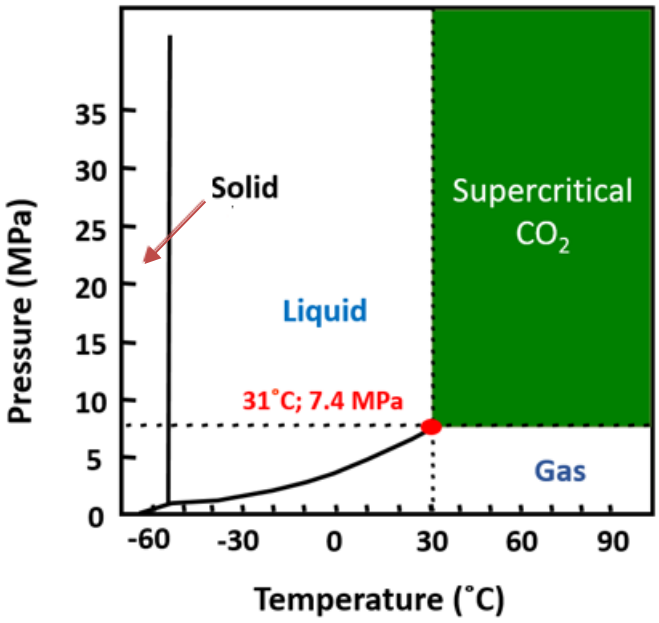

Figure 3.1: Phase diagram for carbon dioxide.

CO_2 is cheap and non-flammable with its utility making positive use of a green-house gas. $ScCO_2$ holds considerable merit as a medium for heterogeneous RDRP, in particular precipitation and dispersion polymerizations,[48] given that most vinyl monomers are soluble in $scCO_2$, but the resultant polymer becomes insoluble at a critical degree of polymerization (J_{crit}).

The Aldabbagh group has measure J_{crit} as a function of monomer loading and pressure using NMP precipitation of St and *n*-butyl acrylate (*t*-BA) in $scCO_2$.[49] The critical degree of polymerization (J_{crit}) is the point at which particle nucleation or precipitation occurs. Figure 3.2a shows J_{crit} increases with St monomer loading, that is poly(St) becomes more soluble in the continuous phase, and precipitates at a higher M_n. These mathematical principles apply to any RDRP dispersed system ($scCO_2$, water etc), establishing when particle (polymer) colloid formation begins in the presence of an appropriate stabilizer. J_{crit} was measured by observing the in-built sapphire viewing window in our stainless steel reactor, when it changed from transparent (solution) to opaque (precipitation). J_{crit} is not measurable for conventional radical polymerizations, where high MW polymer is formed instantaneously, but is slow and measurable in RDRP. Figure 3.2b shows J_{crit} increasing with pressure for the NMP of St at 110 °C and *t*-BA in $scCO_2$ at 118 °C. The Figure demonstrates how the solvent properties of $scCO_2$ can readily be altered by adjusting the pressure. The higher J_{crit} indicates that poly(St) is more soluble than poly(*t*-BA) in $scCO_2$.

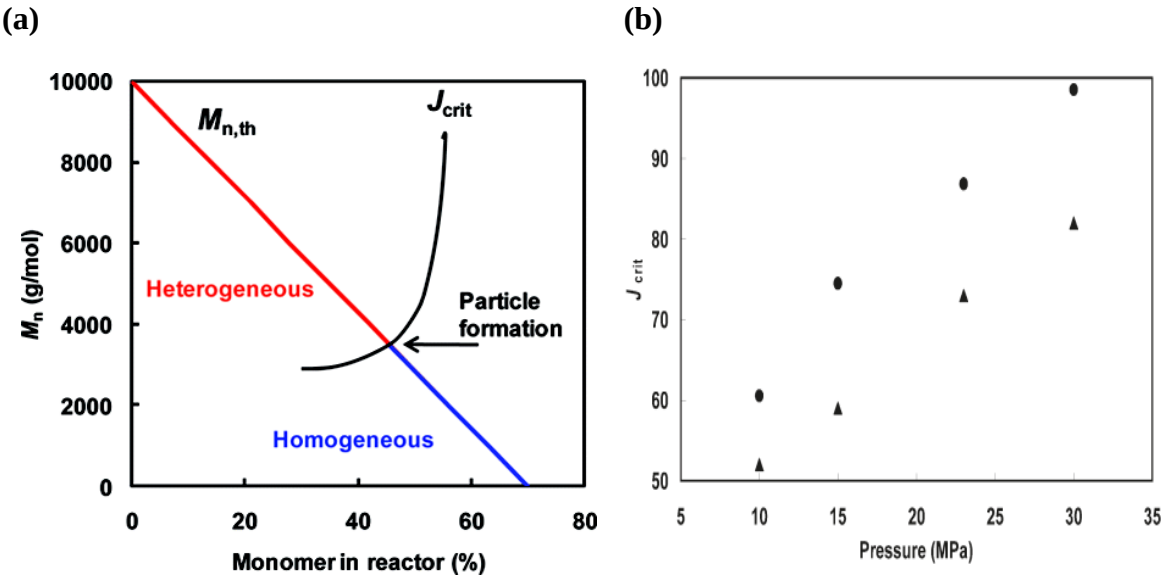

Figure 3.2: (a) M_n versus monomer loading in $scCO_2$: variance of J_{crit} with monomer loading and **(b)** Plot of J_{crit} variance with pressure for the SG1-mediated precipitation polymerization in $scCO_2$ of 70% w/v St (▲) at 110 °C and 60% w/v *t*-BA (●) at 118 °C.

It follows advantages of radical polymerization in $scCO_2$ include the easy adjustment of polymer solubility by altering of pressure and monomer loading, and at high conversions the vented gas leaves a dry polymer powder, which circumvents the requirement for VOC.

There are a plethora of reports on dispersion RDRP in $scCO_2$, which are based on two approaches: (i) the use of a separate CO_2-soluble steric stabilizer,[51-55] and (ii) the use of $scCO_2$-soluble first block that is subsequently chain extended via RDRP in an approach that is analogous to PISA in conventional media.[56-65] Amphorous fluoropolymers and polysiloxanes are the only polymers with appreciable solubility in $scCO_2$, and are usually used as macroinitiators for dispersion polymerizations in $scCO_2$.

3.1.3.1 ATRP dispersion polymerizations in $scCO_2$ analogous to PISA

In 1999, Matyjaszewski and DeSimone carried out the first dispersion RDRP in $scCO_2$ by extending bromine-terminated poly(1,1-dihydroperfluorooctyl methacrylate-Br) with MMA and 2-(dimethylamino)ethyl methacrylate using ATRP.[56] Okubo and co-workers carried out dispersion ATRP of MMA in $scCO_2$ at 5 wt% monomer, using bromo-terminated poly(dimethylsiloxane) (PDMS-Br), and referred to the CO_2-soluble block as *inistab* (initiator + stabilizer). The morphologies of the poly(DMS)$_{79}$-*b*-(MMA)$_{667}$ diblock copolymer were not spherical indicating imperfect stabilization at 71% conversion (Scheme 3.9).[57]

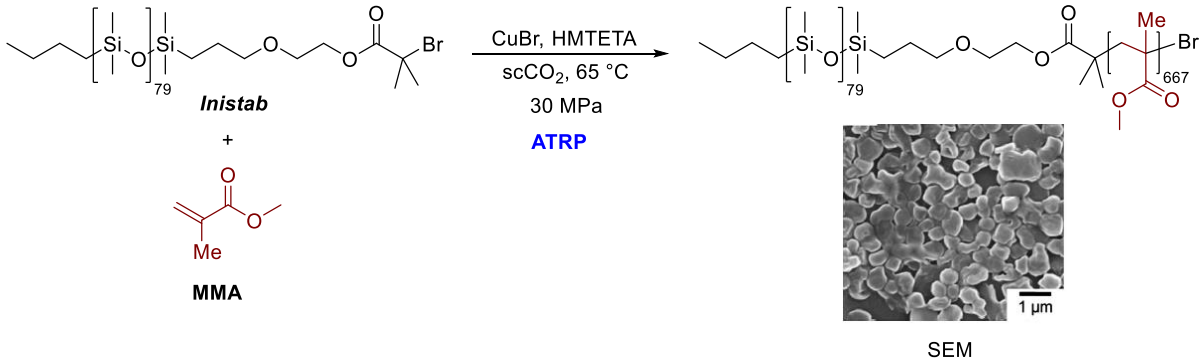

Scheme 3.9: ATRP dispersion of MMA in $scCO_2$ at 30 MPa, with a bromine terminated PDMS-Br *inistab*, and SEM photograph of poly(DMS)$_{79}$-*b*-(MMA)$_{667}$ particles at 5 wt% monomer loading.

In this Chapter, we report the synthesis of higher order morphologies, namely vesicles, via PISA in $scCO_2$ implemented using ATRP. We have taken the *inistab* approach (in Scheme 3.9), however, the MMA monomer has been replace by BzMA monomer (which produces lower T_g polymer). We have used higher monomer loadings and the temperature is increased from 65 ^oC to 80 ^oC, at same pressure of 30 MPa.

3.1.3.2 NMP dispersion polymerizations in $scCO_2$ analogous to PISA

Aldabbagh with Okubo performed the first dispersion NMP in $scCO_2$ by generating the *inistab in situ* by heating the poly(dimethylsiloxane) (PDMS)-based azo-initiator (VPS-0501) and St as monomer, AIBN as initiator with SG1, at 110 °C (Scheme 3.10).[58] Control for the St polymerizations was limited due to the bifunctional nature of the initiator and the very large equilibrium constant for the reversible cleavage of the alkoxyamine between the initiating radicals and SG1.[41] SEM of the poly(St) powder generated showed that stabilization was imperfect with significant coagulation presumably due to chains growing from both ends, so that the middle part extends into the $scCO_2$ medium reducing the colloidal protective layer.

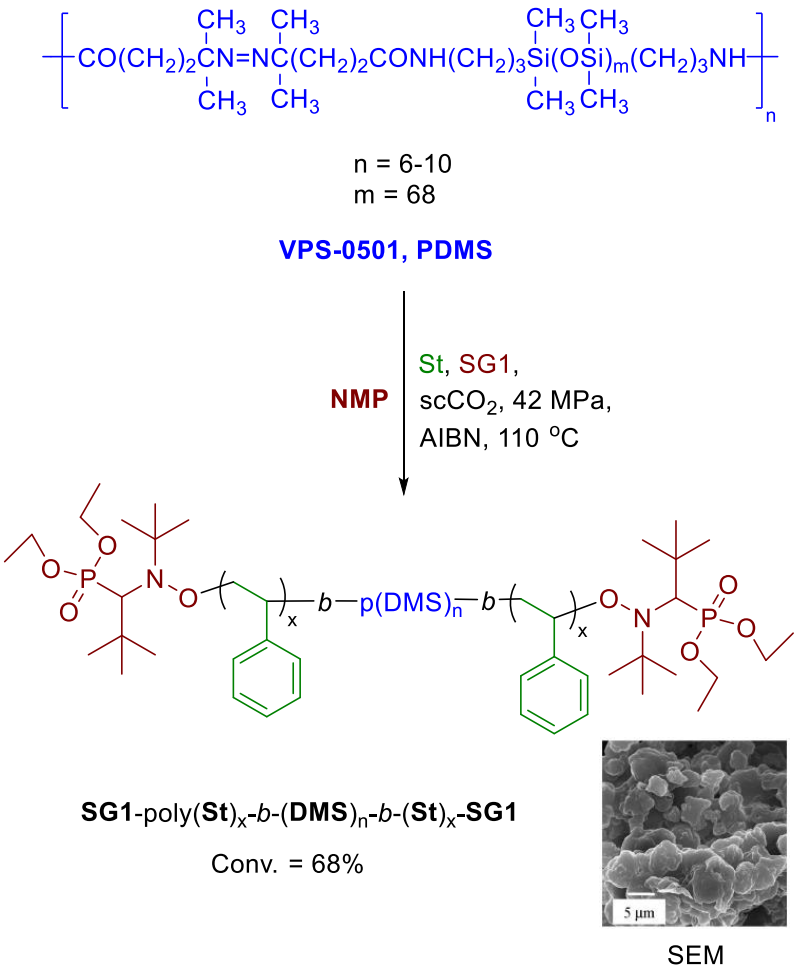

Scheme 3.10: Dispersion NMP in $scCO_2$ with SEM image using a PDMS azo-macroinitiator that decomposes into initiating radicals that couple with the SG1 radical.

A more efficient SG1-*inistab* alkoxyamine was subsequently prepared from PDMS-Br and extended with St using ATRP with SG1 exchange of the bromine ω-end group (Scheme 3.11).[59] A more efficient dispersion NMP of St was achieved in terms of control/livingness giving uniform spherical poly(St) particles, as indicated in the TEM image, the number-average diameter of particles ~132 nm. This *inistab* had anchor solubility balance of 4500/6500 poly(St):poly(DMS), which is within the range 1/3 or 3/1 of P(St)/P(DMS) reported suitable for colloidal stabilization.[66]

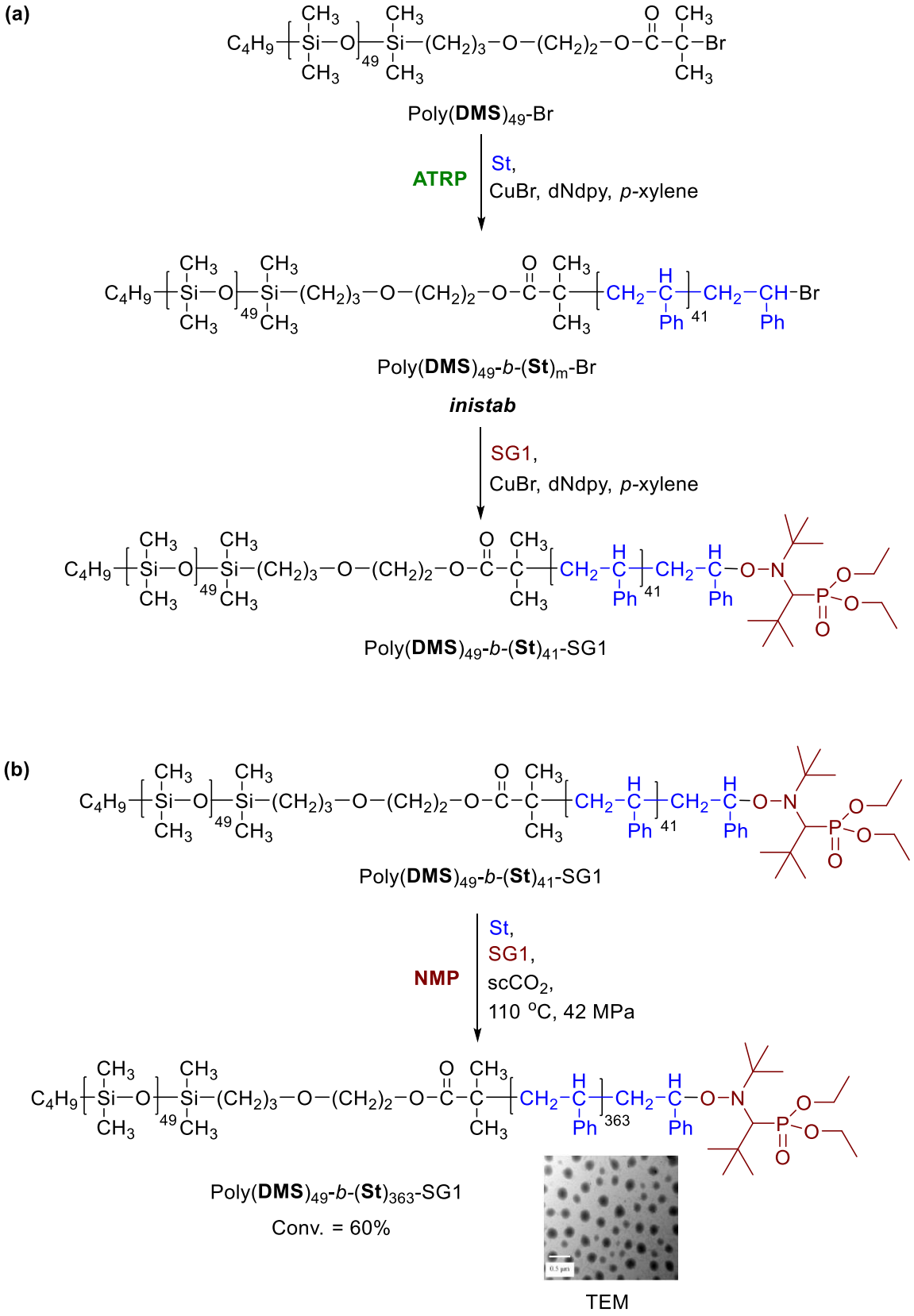

Scheme 3.11: (a) Synthesis of *inistab* using PDMS-Br using solution ATRP, where; dNdpy is 4,4'-dinonyl-2,2'-dipyridyl and **(b)** Dispersion NMP of St in $scCO_2$ with TEM image.

3.1.3.3 RAFT dispersion polymerizations in $scCO_2$ analogous to PISA

Howdle and co-workers performed a dispersion RAFT polymerization on MMA by using the CO_2-philic macro-RAFT agent made from the fluorinated monomer 1*H*,1*H*,2*H*,2*H*-perfluorooctyl methacrylate (M_n = 15000 g mol^{-1}) (Scheme 3.12). High conversion (99%) was achieved after 20 hours with the M_n of 76,000 g mol^{-1} in close agreement of the theoretical value of 74,970 g mol^{-1}, with an 80:20 ratio of CO_2-phobic to CO_2-philic chains of the block copolymer, and a narrow polydispersity (M_w/M_n of 1.22), and well-defined spherical particles of a broad size distribution observed.[63]

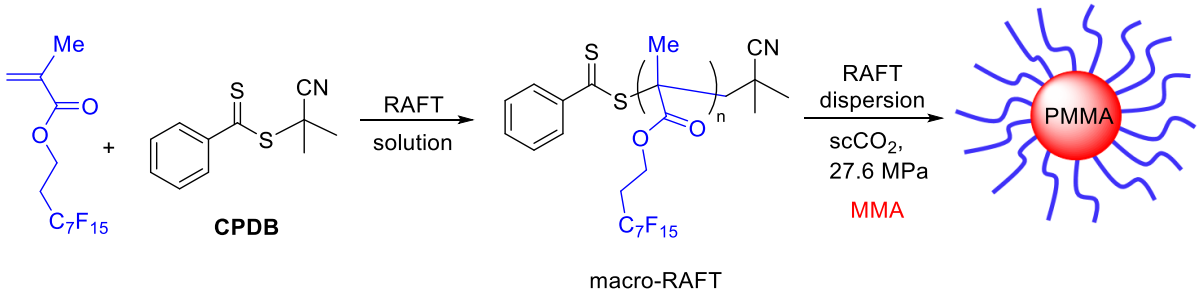

Scheme 3.12: Synthesis of diblock copolymers of poly(PFOMA)$_n$-*b*-(MMA)$_m$ using RAFT dispersion polymerization in $scCO_2$.

Howdle *et al*, carried out dispersion RAFT polymerization on vinyl butyrate (VB) monomer by using the poly(VAc) macro-RAFT agent. The macro-RAFT was made using vinyl acetate (VAc) monomer and (*S*-(1-ethoxycarbonylethyl) *O*-ethyl xanthate) as RAFT agent. The dispersion polymerization yielded poly(VAc)$_{110}$-*b*-(VB)$_{123}$ diblock copolymer with high monomer conversion >99% (50:50, M_n = 24000 g mol^{-1}) and a narrow polydispersity (M_w/M_n of 1.29), and well-defined solid spherical particles morphology observed by SEM (Scheme 3.13).[64]

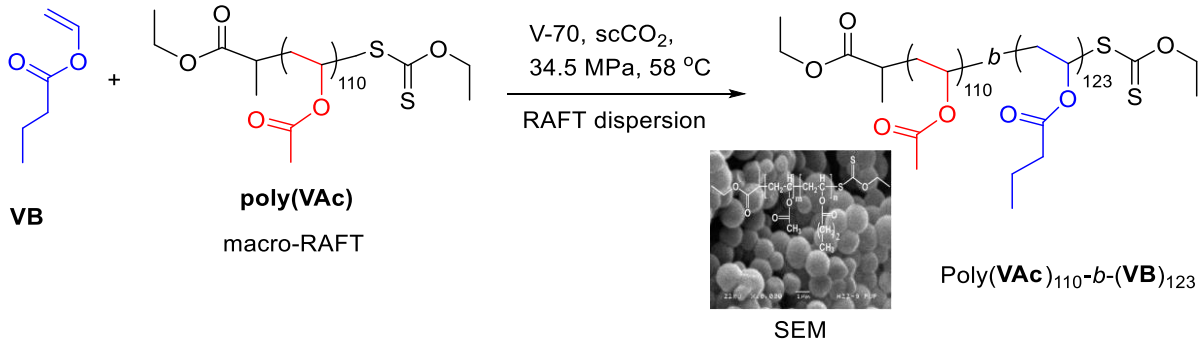

Scheme 3.13: Synthesis of poly(VAc)$_{110}$-*b*-(VB)$_{123}$ diblock copolymers via RAFT dispersion polymerization in scCO$_2$ with SEM image.

3.2 Aims and Objectives

The aim of this chapter is to prepare the ***first*** *higher order morphologies, namely vesicles via PISA in* $scCO_2$. There are to date no reports on the dispersion polymerization of BzMA in $scCO_2$, despite its frequent use for PISA in conventional media. [18-20, 23, 29] Dispersion ATRP of BzMA will be carried out using the *inistab* macroinitiator (PDMS-Br) at 80 °C and 30 MPa using the CuBr / HMTETA system established by Matyjaszewski *et al*.[2] Self-assembly should occur at J_{crit}.[49] As the BzMA CO_2-*phobic* block length increases in size, higher order morphologies (vesicles, rods etc) are expected to form (Scheme 3.14). These may be high aspect ratio objects. The high aspect ratio, $a = L/d$ is taken as the ratio of the particle length (L is length of cylinder) to the thickness (d is the diameter of cylinder), where the L value is much bigger than d value in Figure 3.3.[67]

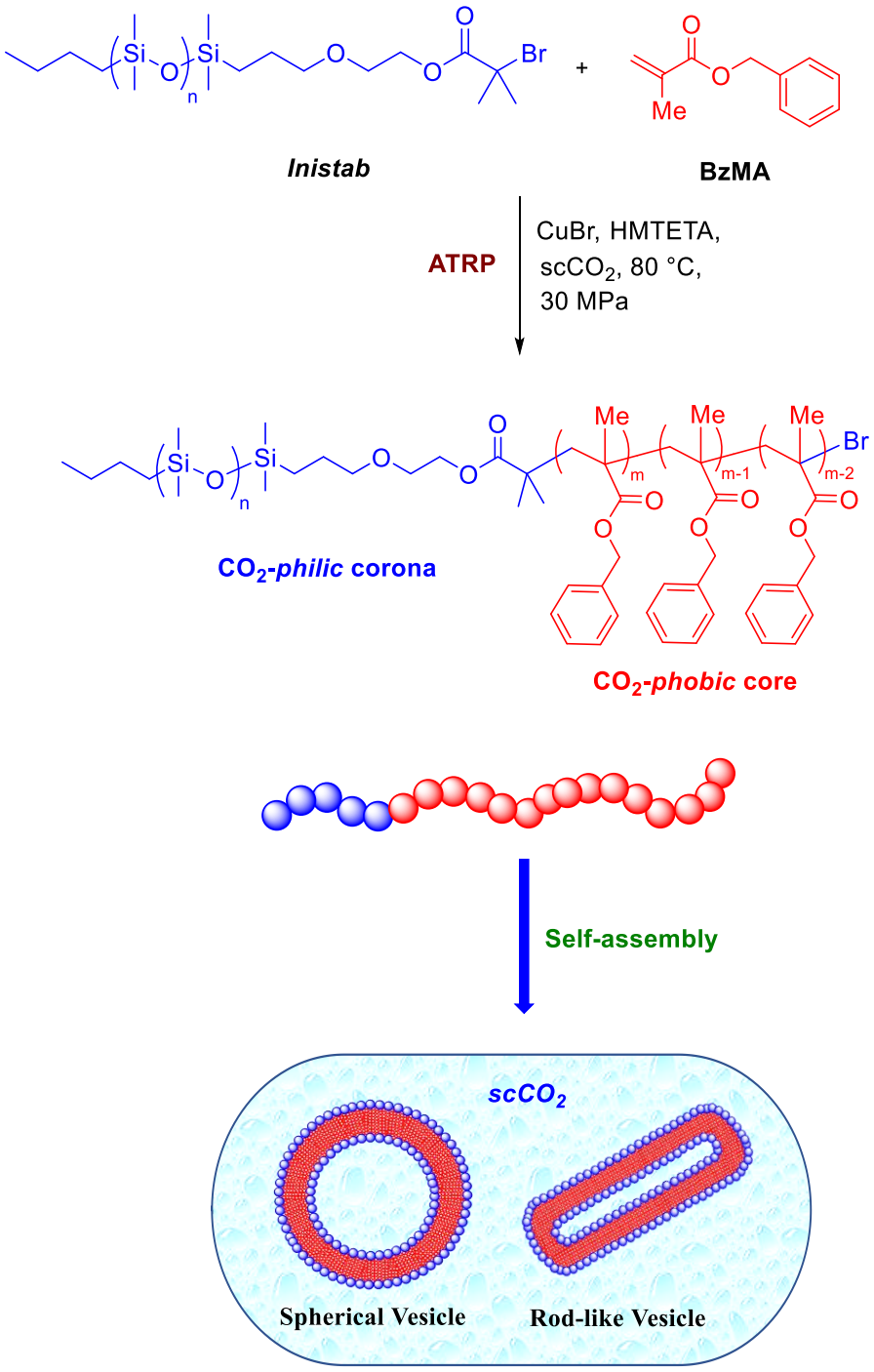

Scheme 3.14: Proposed PISA ATRP in $scCO_2$.

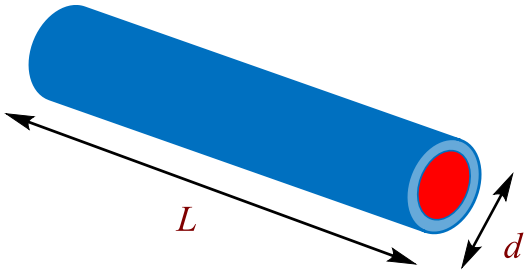

Figure 3.3: High aspect ratio object structure, $a = L/d$, where the L (length) > d (diameter) values.

3.3 Results and Discussion

3.3.1 Preparation of PDMS-Br (*inistab*)

The condensation of PDMS-OH (M_n = 5150 g mol^{-1} and M_w/M_n = 1.12) with 2-bromoisobutyryl bromide gave PDMS-Br macroinitiator (*inistab*) in 92% yield and low polydispersity (M_w/M_n = 1.12), M_n = 5350 g mol^{-1} (which is close to the $M_{n,th}$ = 5335 g mol^{-1}) (Figure 3.4 Table 3.1). The use of poly(St) standards for GPC inevitably leads to error. The by-product is Et_3NHBr salt was removed by filtering the THF at the end of the reaction (Scheme 3.15). PDMS-OH was completely converted to PDMS-Br as indicated by the ^{1}H NMR spectrum in Figure 3.5, with the less than quantitative yield presumably due to losses upon work up. NMR assignments were in agreement with Okubo *et al*, and Haddleton *et al*.[57, 68]

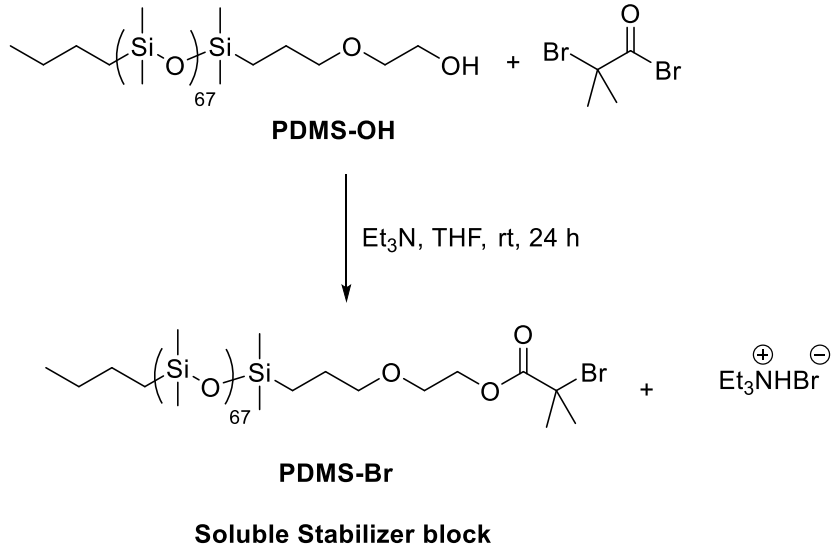

Scheme 3.15: Synthesis of PDMS-Br (*inistab*).

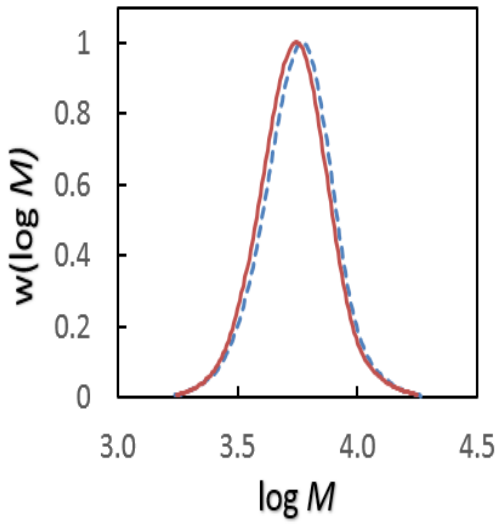

Figure 3.4: MWDs for PDMS-OH (red continuous line) (M_n = 5150 g mol^{-1} and M_w/M_n = 1.12) and PDMS-Br (*inistab*) (blue dashed line) (M_n = 5350 g mol^{-1} and M_w/M_n = 1.12).

PDMS	M_n Commercial [a]	$M_{n,GPC}$ (g mol^{-1})[b]	M_w/M_n[b]	$M_{n,th}$ (g mol^{-1})[c]
PDMS-OH	4670	5150	1.12	-
PDMS-Br	-	5350	1.12	5335

Table 3.1: $M_{n,GPC}$ and $M_{n,th}$ of PDMS-X.

[a]M_n Commercial as indicated by the manufacture, [b]Determined by GPC/RI in THF using commercial linear poly(St) as molecular weight standards and [c]$M_{n,th}$ is the molecular weight of (PDMS-OH) by GPC + molecular weight of $CO_2C(CH_3)_2Br$.

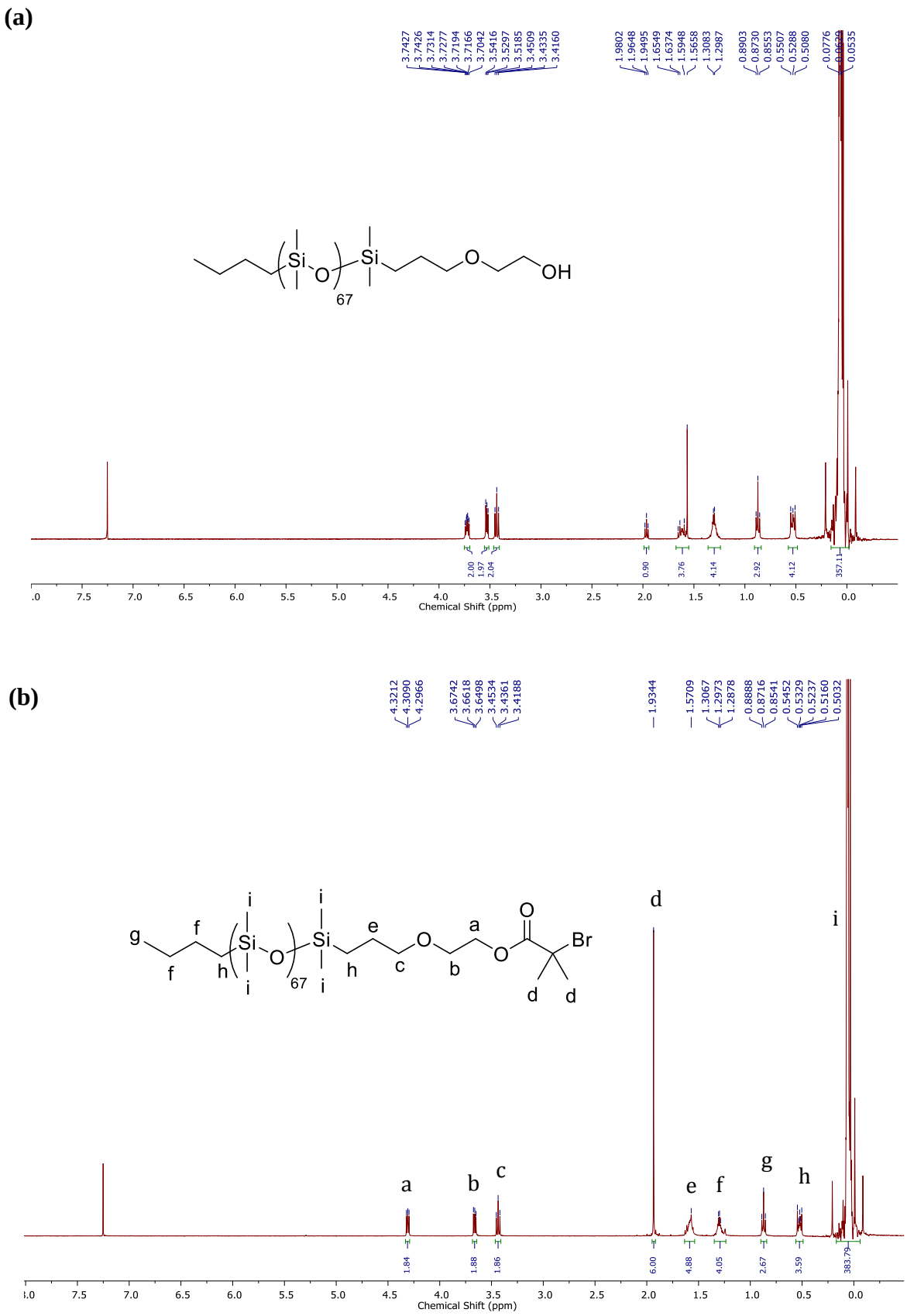

Figure 3.5: ^{1}H NMR spectra ($CDCl_3$, 400 MHz) of **(a)** PDMS-OH and **(b)** PDMS-Br.

3.3.2 Dispersion ATRP of BzMA in $scCO_2$

3.3.2.1 Solubility of the monomer (BzMA) in $scCO_2$

The appreciable solubility of the monomer (BzMA) in $scCO_2$ (a requirement for a dispersion polymerization) was confirmed using a 100 mL stainless steel reactor with 180° inline sapphire windows, where at 80 °C and 30 MPa a transparent solution was observed using 35, 50 and 65 v/v(%) BzMA loadings.

3.3.2.2 Establishing controlled / living character for the dispersion polymerizations in $scCO_2$

Copper$^{(I)}$ bromide (CuBr) was purified according to the method by Keller and Wycoffand,[69] The CuBr contained various amounts of impurities, presumably $CuBr_2$ and oxides. These impurities were quite soluble in methanol and therefore could readily be washed out and the pure CuBr stored in an airtight container. ATRP dispersion polymerizations were then performed in a windowless 25 mL stainless steel reactor.

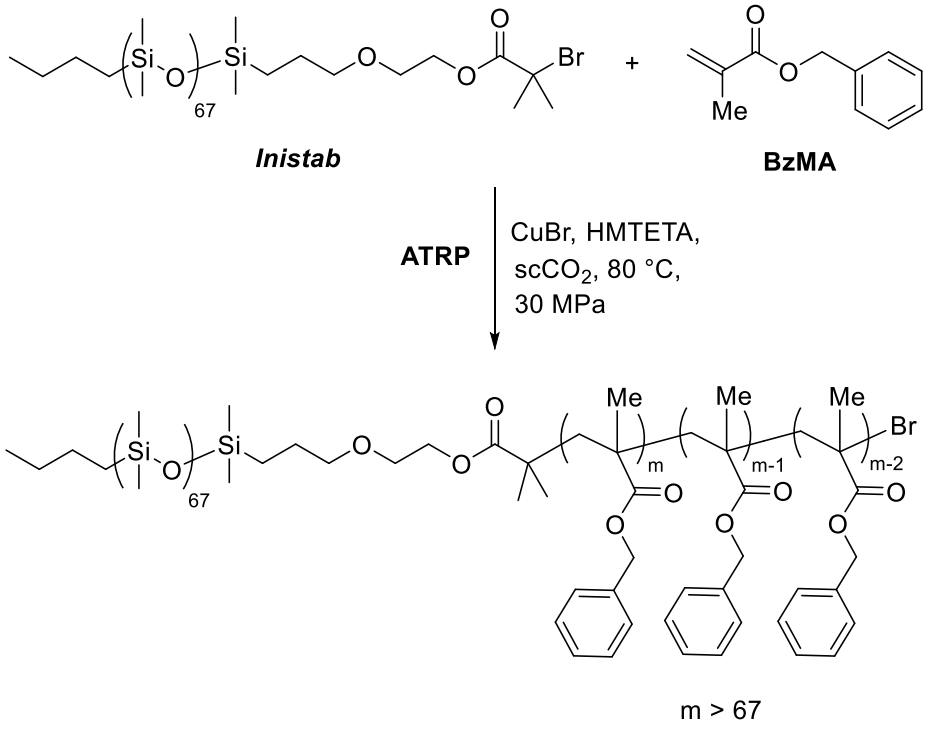

Scheme 3.16: Dispersion ATRP of BzMA in $scCO_2$.

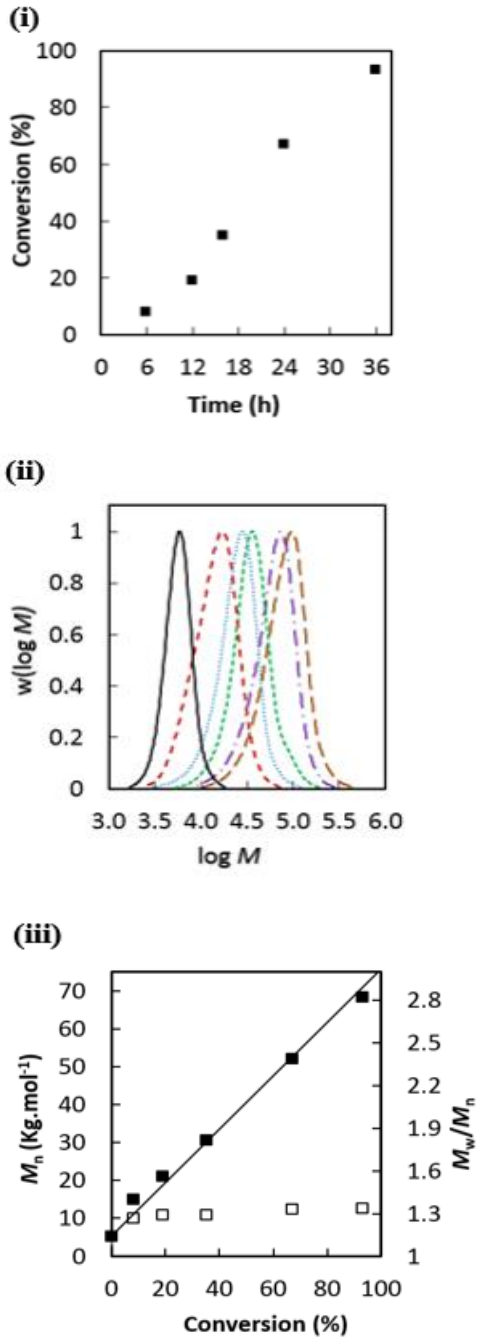

Figure 3.6: ATRP dispersion in $scCO_2$ at 80 °C and 30 MPa of 35 v/v(%) BzMA using [BzMA]/[PDMS-Br]/[CuBr]/[HMTETA] = 400:1:1.5:1.5: **(i)** Conversion versus time plot, **(ii)** GPC MWDs (normalized to peak height) corresponding to PDMS-Br (black solid line), and polymerizations at 11% (red dashed line, 6 hours), 25% (blue round dotted line, 12 hours), 40% (green short dotted line, 16 hours), 67% (purple long dash dotted line, 24 hours) and 93% (brown long dashed line, 36 hours) conversion, and **(iii)** M_n (■) and M_w/M_n (□) versus conversion plot. $M_{n,th}$ is the continuous line calculated according to equation 3.2.

Polymerizations of 35 v/v(%) BzMA in $scCO_2$ at 80 °C and 30 MPa using [BzMA]/[PDMS-Br]/[CuBr]/[HMTETA] = 400:1:1.5:1.5 were stopped after 6, 12, 16, 24 and 36 hours with conversions measured by weight of polymer, as 11%, 25%, 40%, 67% and 93% conversion respectively (Figure 3.6). Conversions were not obtained until the PDMS-*b*-PBzMA samples were determined to be free of BzMA monomer using ^{1}H NMR spectra of the polymer (Figure 3.7). Unreacted monomer was removed by pipetting for low conversion samples, while for the high conversions (67% and 93%) most of the residual monomer disappeared upon simple venting of the reactor. All polymer samples were, then washed with $scCO_2$ at 50 °C and 30 MPa. Polymer was isolated as dry sky blue powders (free of monomer) upon venting without the use of VOCs at any stage (Figure 3.8).

Control/living character was indicated by M_n values being in close agreement with $M_{n,th}$ determined by the ratio of amount of monomer to macroinitiator (PDMS-Br), outlined in equation 3.2. Figure 3.6 (ii) shows narrow molecular weight distributions (MWD) were obtained throughout that shifted to higher MW with conversion.

Re-dispersing the polymer powder in pentane and observing with transmission electron microscopy (TEM) indicated mainly spherical particles for the 67% conversion sample from a few 100 nm in diameter to 4.10 μm in diameter with the occasional rods also apparent (Figure 3.9). The rod-like structures are the first examples of high aspect ratio objects prepared in $scCO_2$.

After 36 hours, the degree of polymerization had increased from 266 to 359 BzMA monomeric units (Table 3.2), and giant rods were apparent of up to 27 μm in length (Figure 3.10). Giant vesicles of up to 10 μm in diameter were also formed as indicated in the TEM. The vesicle structure is apparent in the TEMs images of Figure 3.10 with large hollow light interior encircled by external darker ring corona. Vesicles are closed bilayers, namely hollow spheres with a bilayer wall sandwiched with internal core poly(BzMA) and PDMS corona. These vesicles are much larger than the typical nano-objects created by PISA in conventional media.

(a)

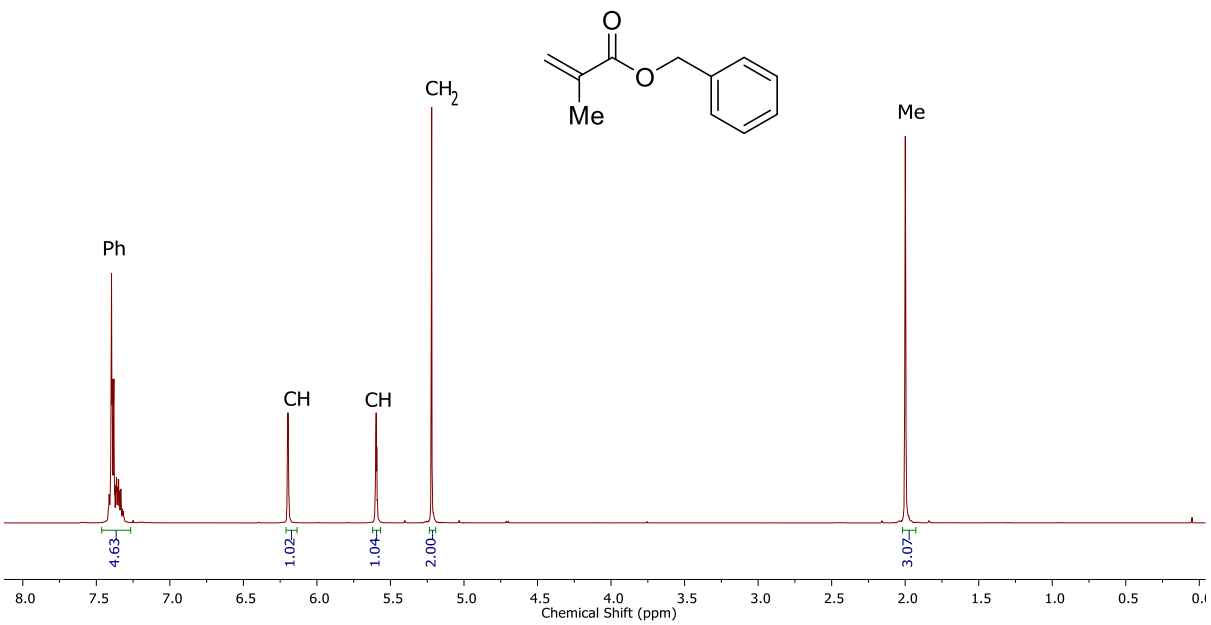

(b)

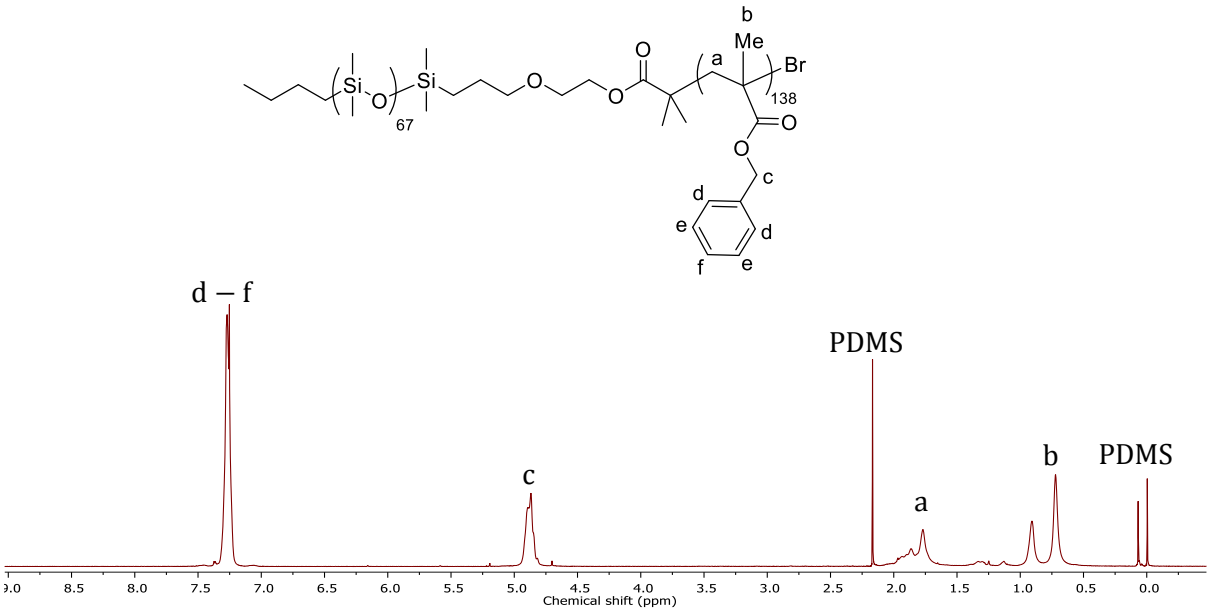

Figure 3.7: ^{1}H NMR spectra ($CDCl_3$, 400 MHz) of **(a)** BzMA monomer and **(b)** PDMS-*b*-$(BzMA)_{138}$.

Figure 3.8: Optical image (Samsung Galaxy A5 2016) of the dry PDMS-*b*-$(BzMA)_{138}$ powder after purification using $scCO_2$.

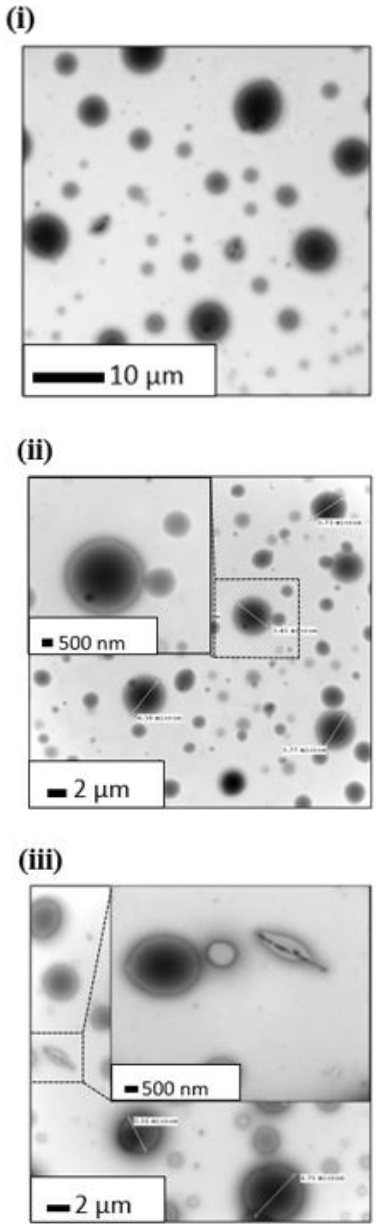

Figure 3.9: TEM images of PDMS-*b*-$(BzMA)_{266}$ particles at 67% conversion (Run 1) prepared by the ATRP dispersion polymerization of 35 v/v(%) BzMA in $scCO_2$ at 80 °C and 30 MPa using [BzMA]/[PDMS-Br]/[CuBr]/[HMTETA] = 400:1:1.5:1.5, after purification by washing with $scCO_2$ and re-dispersed in pentane in $scCO_2$.

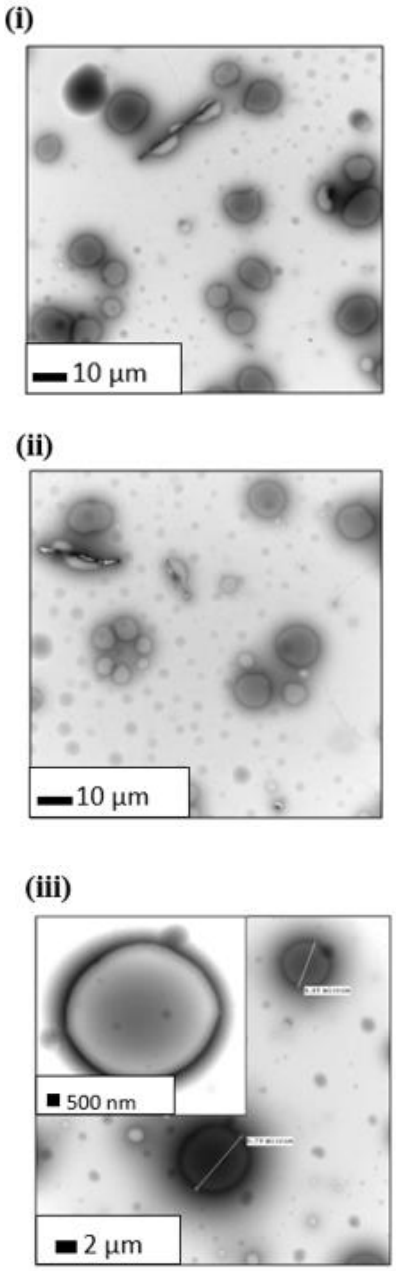

Figure 3.10: TEM images of PDMS-*b*-$(BzMA)_{359}$ particles at 93% conversion (Run 2) prepared by the ATRP dispersion polymerization of 35 v/v(%) BzMA in $scCO_2$ at 80 °C and 30 MPa after 36 hours, using [BzMA]/[PDMS-Br]/[CuBr]/[HMTETA] = 400:1:1.5:1.5, after purification by washing with $scCO_2$ and re-dispersed in pentane in $scCO_2$.

There is to the best of our knowledge only one report of PISA yielding giant vesicles; Albertsen *et al.*[17] synthesized spherical vesicles with diameter ~20 μm using an aqueous RAFT dispersion system. This was carried out using poly(ethylene glycol) PEG-functional RAFT agent, 2-hydroxypropyl methacrylate (HPMA) as the monomer in H_2O with $Ru(bpy)_3^{2+}$ (Ruthenium tris 2,2′-bipyridyl chloride) as free radical initiator (photoredox catalyst).[70] The polymerization was at 30 °C and proceeded with light-emitting diode (LED) lights. Small polymerized mixtures were transferred to a frame sealed, microscope slide and observed using fluorescence microscopy after staining with the fluorescent dye Rhodamine 6 G for better image quality in Scheme 3.17. As the dispersion polymerization progresses the HPMA polymer becomes increasingly hydrophobic, but this PEG chain nevertheless ensures that the polymerized product will be amphiphilic to form giant vesicles in the aqueous solution.

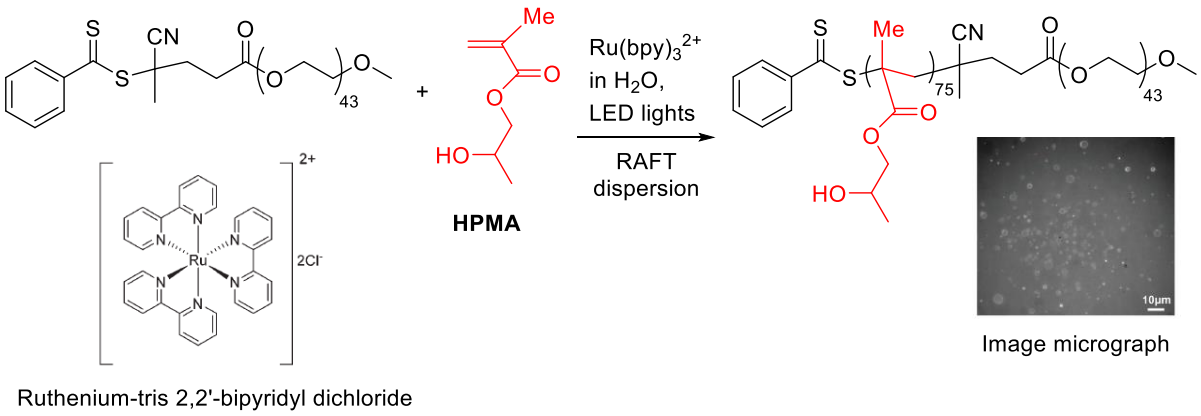

Scheme 3.17: RAFT using photoredox catalyst at 30 °C for aqueous dispersion polymerization of 2-hydroxypropyl methacrylate (HPMA) controlled by a poly(ethylene glycol) PEG-functional RAFT agent and optical micrograph of giant vesicles formed.

3.3.2.3 Influence of degree of polymerization (*DP*) on PISA in $scCO_2$

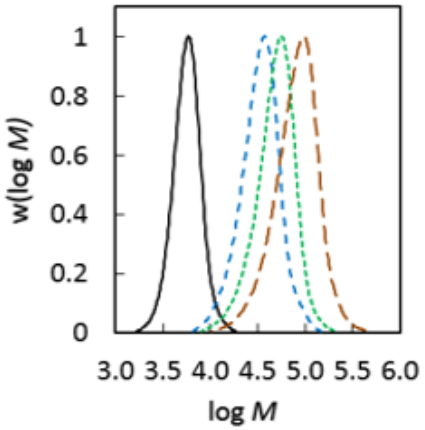

Figure 3.11: GPC MWDs (normalized to peak height) assessing the influence of the degree of polymerization (*DP*) on particle morphology for the ATRP dispersion of 35 v/v(%) BzMA in $scCO_2$ at 80 °C and 30 MPa using 1.5 equiv of CuBr and 1.5 equiv HMTETA. Corresponding to PDMS-Br (black solid line), and polymerizations using [BzMA] : [PDMS-Br] = 168 : 1 after 24 hours at 88% conversion (Run 3, blue dashed line), [BzMA] : [PDMS-Br] = 280 : 1 after 24 hours at 83% conversion (Run 4, green square dotted line), and [BzMA] : [PDMS-Br] = 400 : 1 after 36 hours at 93% conversion (Run 2, brown long dash line).

Conversions of 88% and 83% and narrow molecular weight distributions of M_n = 29650 and M_n = 42650 were obtained when lowering the *DP* to 138 and 212 by respectively reducing the [BzMa] / [PDMS-Br] ratio to 168:1 (Run 3) and 280:1 (Run 4) (Figure 3.11 and Table 3.2). At the lowest *DP*, the smallest particles were formed from spherical to irregular of less than 1 micron in size (Figure 3.12). At the higher *DP* of 212 obtained from the [BzMA] / [PDMS-Br] ratio of 280, larger vesicular spherical particles of diameter 5 µm were obtained, as well as, vesicular rods of 7 µm in length (Figure 3.13). It is clear from image 3.13(i) that this polymerization produced a relatively high amount of high aspect ratio objects.

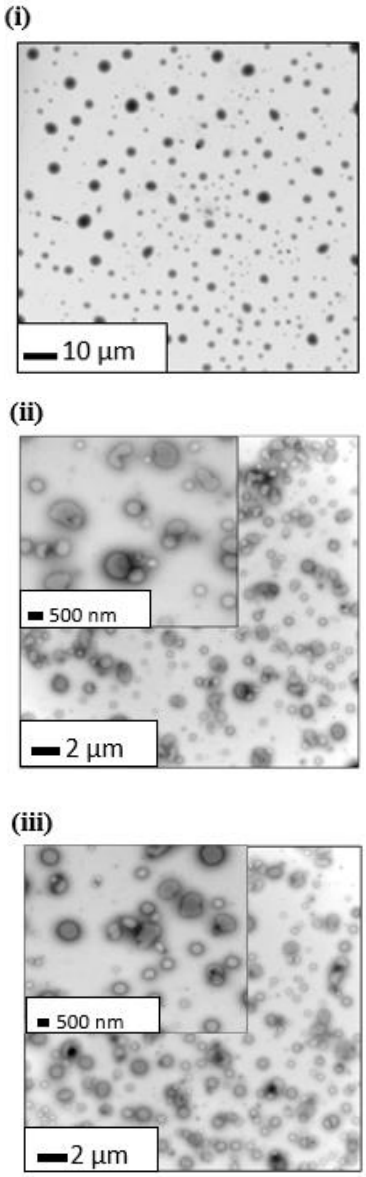

Figure 3.12: TEM images of PDMS-*b*-$(BzMA)_{138}$ particles at 88% conversion (Run 3) prepared by the ATRP dispersion polymerization of 35 v/v(%) BzMA in $scCO_2$ at 80 °C and 30 MPa using [BzMA]/[PDMS-Br]/[CuBr]/[HMTETA] = 168:1:1.5:1.5, after purification by washing with $scCO_2$ and re-dispersed in pentane in $scCO_2$.

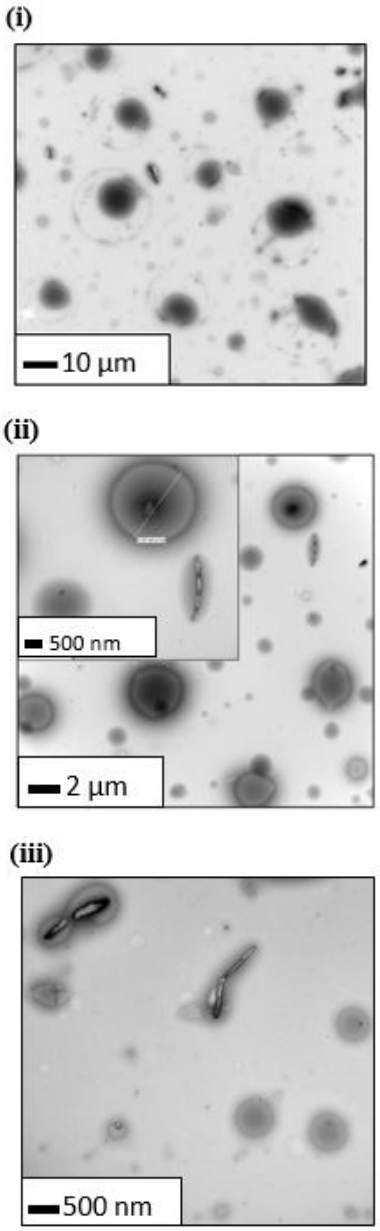

Figure 3.13: TEM images of PDMS-*b*-$(BzMA)_{212}$ particles at 83% conversion (Run 4) prepared by the ATRP dispersion polymerization of 35 v/v(%) BzMA in $scCO_2$ at 80 °C and 30 MPa using [BzMA]/[PDMS-Br]/[CuBr]/[HMTETA] = 280:1:1.5:1.5, after purification by washing with $scCO_2$ and re-dispersed in pentane in $scCO_2$.

3.3.2.4 Influence of monomer loading on the ATRP dispersion polymerization of BzMA in $scCO_2$

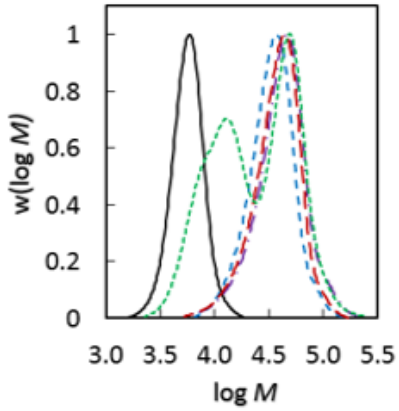

Figure 3.14: GPC MWDs (normalized to peak height) assessing the influence of monomer (BzMA) loading on the ATRP dispersion in $scCO_2$ at 80 °C and 30 MPa after 24 hours using [BzMA] : [PDMS-Br] : [CuBr] : [HMTETA] = 168 : 1 : 1.5 : 1.5. Corresponding to PDMS-Br (black solid line), and polymerizations at 20 v/v(%) BzMA loadings at 13% conversion (green square dotted line), 35 v/v(%) BzMA loadings at 88% conversion (Run 3, blue dashed line), 50 v/v(%) BzMA loadings at 94% conversion (Run 5, purple long dash dotted line), and 65 v/v(%) BzMA loadings at 89% conversion (Run 6, red long dashed line).

At the lowest monomer loading, a bimodal MWD was obtained with low conversion after 24 hours reaction time (Figure 3.14). This is most probably due to the high heterogeneity of the system with partitioning of the catalyst and ligand away from the locality of polymerization. Aldabbagh *et al*,[71-72] have attributed poor controlled/living character for precipitation NMPs in $scCO_2$ to the high heterogeneity of the system. The monomer loading affects the level of control via the value of J_{crit}, i.e. the conversion at the onset of heterogeneity. The value of J_{crit} is lower at lower monomer loadings because the polymer chain solubility in the CO_2/monomer mixture decreases with decreasing monomer content, as was observed in the NMP of St mediated by the nitroxides, (2,2,5-trimethyl-4-phenyl-3-azahexane-3-aminoxyl) TIPNO and SG1. Increasing the monomer loading in our ATRP dispersion polymerizations to 35 v/v(%), and up to 65 v/v(%), while keeping all other factors constant led to high conversion (89%) and controlled/living character as signified by narrow MWDs (Figure 3.14).

The polymerization with the highest solids content of 65 v/v(%) monomer loading gave the largest proportion of non-spherical vesicles (Run 6, Figure 3.16), which appeared as high aspect ratio objects of 1 – 4 μm in cross-section and 4 – 39 μm in length. These giant vesicles are significantly larger than at the lower solid content of 50 v/v(%) monomer loading (Run 5, Figure 3.15), which appeared largely, as spherical vesicles with occasional rods of 3 – 4 μm in length. It is important to highlight that these rod-like structures are very different from the rods (also referred to as worm-like micelles) normally observed in PISA – the latter are of much lower diameter, typically corresponding to that of the spherical micelles from which they originate (normally less than 100 nm). The present rod-like structures have far greater diameters and presumably comprise a bilayer vesicular structure, *i.e.* they are hollow structures.

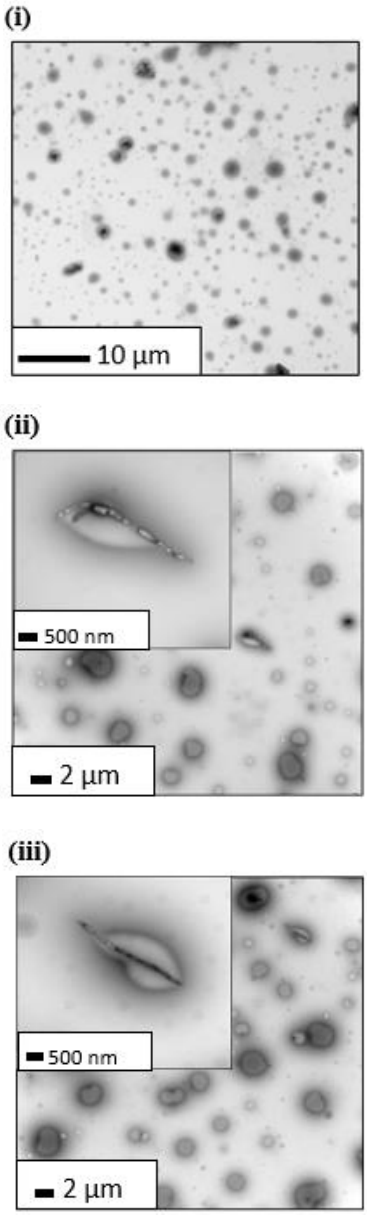

Figure 3.15: TEM images of PDMS-*b*-$(BzMA)_{167}$ particles at 94% conversion (Run 5) prepared by the ATRP dispersion polymerization of 50 v/v(%) BzMA in $scCO_2$ at 80 °C and 30 MPa using [BzMA]/[PDMS-Br]/[CuBr]/[HMTETA] = 168:1:1.5:1.5, after purification by washing with $scCO_2$ and re-dispersed in pentane in $scCO_2$.

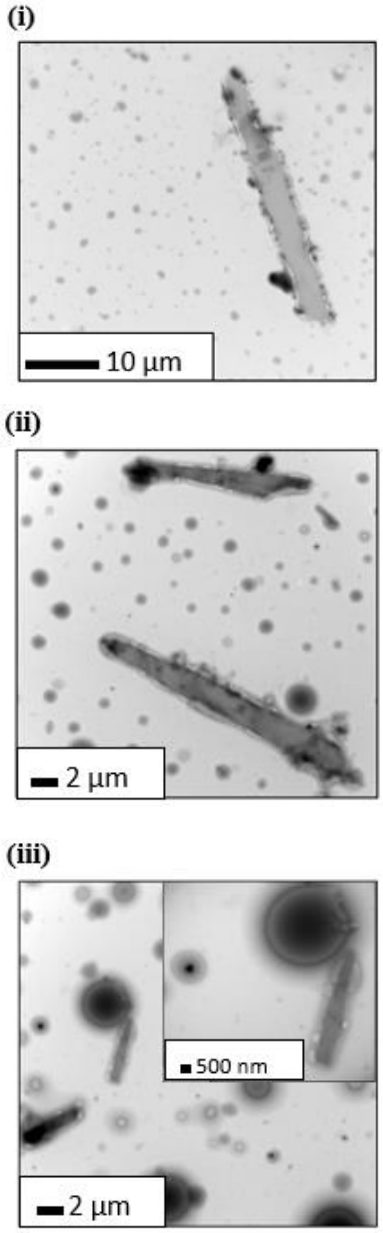

Figure 3.16: TEM images of PDMS-*b*-$(BzMA)_{153}$ particles at 89% conversion (Run 6) prepared by the ATRP dispersion polymerization of 65 v/v(%) BzMA in $scCO_2$ at 80 °C and 30 MPa using [BzMA]/[PDMS-Br]/[CuBr]/[HMTETA] = 168:1:1.5:1.5, after purification by washing with $scCO_2$ and re-dispersed in pentane in $scCO_2$.

Run[a]	[BzMA] / [PDMS-Br]	BzMA loading v/v(%)	TEM Figure	Polymer[b]	$M_{n,th}$ [c]	Conv. (%)[d]	M_n [e]	M_w/M_n [e]
1	400	35	**3.9**	PDMS-*b*-$(BzMA)_{266}$	52550	67	52200	1.33
2	400	35	**3.10**	PDMS-*b*-$(BzMA)_{359}$	70900	93	68450	1.34
3	168	35	**3.12**	PDMS-*b*-$(BzMA)_{138}$	31400	88	29650	1.25
4	280	35	**3.13**	PDMS-*b*-$(BzMA)_{212}$	45900	83	42650	1.25
5	168	50	**3.15**	PDMS-*b*-$(BzMA)_{167}$	33200	94	34800	1.33
6	168	65	**3.16**	PDMS-*b*-$(BzMA)_{153}$	31700	89	32300	1.30

Table 3.2: Summary of molecular weight data of the specific samples subjected to TEM analysis (ATRP dispersion polymerization of BzMA at 80 °C and 30 MPa).

[a] All polymerization contained [PDMS-Br]/[CuBr]/[HMTETA] = 1:1.5:1.5 and were for 24 hours, except run **2** was 36 hours. [b] The degree of polymerization of the BzMA block was obtained by deducting the M_n(GPC) of PDMS-Br (M_n = 5350 g mol^{-1} measured by GPC [e]) and Br-end group is not shown in block copolymers. [c] Calculated according to equation 3.2. [d] Measured by gravimetry. [e] Determined by GPC/RI in THF using commercial linear poly(St) as molecular weight standards.

3.4 Conclusions

We have successfully accomplished the first controlled/living dispersion polymerization in $scCO_2$ to give higher order objects, including vesicles and high aspect ratio objects. Multiple morphologies were observed, which varied with reactor composition, in particular giant vesicles (> 10 μm) formed at high *DP*s and solids content. This one-step approach to dry-polymeric vesicles that circumvents the use of VOCs and aqueous media holds considerable industrial promise.

3.5 Future Work

Polymer powders (PDMS-*b*-PBzMA) have been sent to the UNSW (Prof P. B. Zetterlund) for the optical imaging of the giant vesicles, as well as, Dynamic Light Scattering (DLS) analysis. For sub-200 nm narrow size particles, DLS is a very good and fast method of measuring the actual particle size distribution of polymer particles (e.g. in Figure 3.12).

Future research we propose initiator for continuous activator regeneration atom transfer radical polymerization (ICAR) ATRP, at low ppm of $Cu^{(II)}$ catalyst concentration making ATRP a completely "green" environmentally friendly process. In order to tailor-make vesicles in $scCO_2$, we will need to also vary the CO_2-philic PDMS part. PDMS is prepared by hydrolysis of dimethyldichlorosilane gives a mixture of cyclic and linear polysiloxane. The silane end-group of the linear polysiloxane can be readily functionalized to give PDMS-OH derivatives. The size of the polysiloxane repeat unit is determined by the initial hydrolysis reaction of Me_2SiCl_2 (Scheme 3.18).[73]

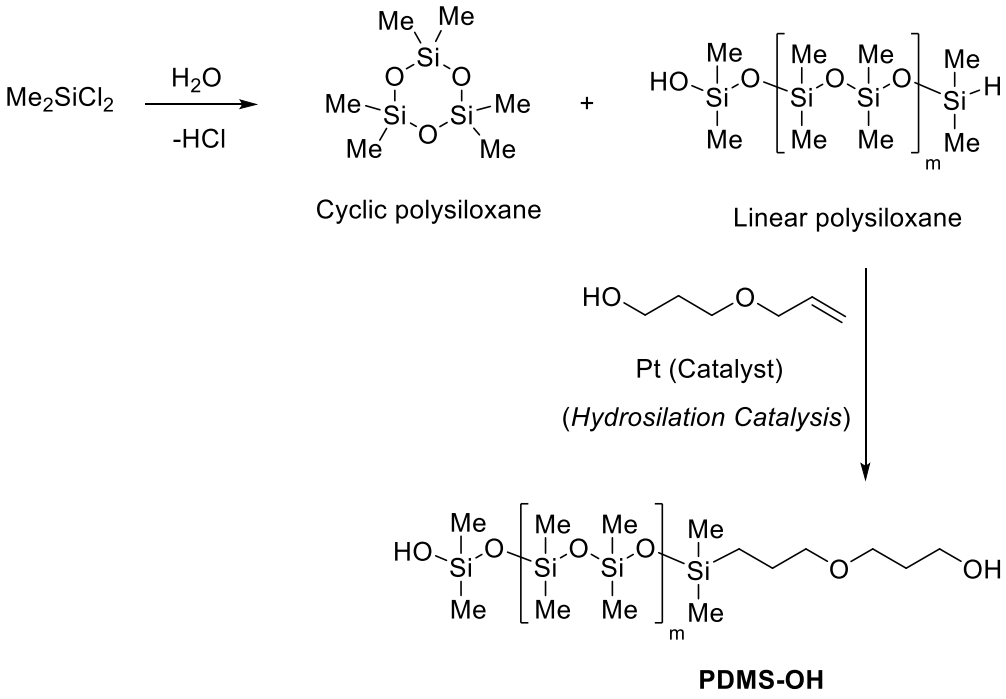

Scheme 3.18: Synthesis of PDMS-OH derivatives.

3.6 Experimental

3.6.1 Materials

Benzyl Methacrylate (BzMA, Sigma-Aldrich, 96%) was distilled *in vacuo* to remove radical inhibitor. Hydroxyl terminated poly(dimethylsiloxane) (PDMS-OH, Sigma-Aldrich, av. M_n ~4670 g mol^{-1}, M_n = 5150 g mol^{-1} and M_w/M_n = 1.12 determined by GPC, as described below), 1,1,4,7,10,10-hexamethyltriethylenetetramine (HMTETA, Sigma-Aldrich, 97%), triethylamine (Sigma-Aldrich, ≥99%), and 2-bromoisobutyl bromide (Sigma-Aldrich, 98%) were used as received. Tetrahydrofuran (THF, Sigma-Aldrich, ≥99%) and diethyl ether (Et_2O, Sigma-Aldrich) were distilled over Na wire and benzophenone (Sigma-Aldrich, 95%). Na_2CO_3 (Sigma-Aldrich, ≥99%) and $MgSO_4$ (Sigma-Aldrich, ≥99.99%) were used as received. CH_2Cl_2 (Sigma-Aldrich, ≥99%), $CDCl_3$ (Sigma-Aldrich, 99.8 atom%), glacial acetic acid (Sigma-Aldrich, ≥99.5%), absolute ethanol (Sigma-Aldrich, ≥99.5%), and CO_2 (BOC, 99.8%) were used as received. CuBr (Acros Organics, 98%) was purified by washing slowly with glacial acetic acid (4 x 25 mL) followed by absolute ethanol (3 x 30 mL) and anhydrous Et_2O (6 x 15 mL).[74] CuBr was placed in a vacuum oven at ~75 °C for 25 mins and stored in an airtight container.

3.6.2 Equipment

Polymerizations in scCO_2 were conducted in a 25 mL stainless steel Parr reactor with maximum operating pressure and temperature of 40 MPa and 130 °C respectively (Figure 3.17). The pressure was produced by a Thar P-50 series high pressure pump to within ±0.2 MPa and the temperature was monitored by a Thar CN6 controller to within ±0.1 °C. Temperature was achieved with an oil bath and stirring was achieved using a magnetic stirring bar.

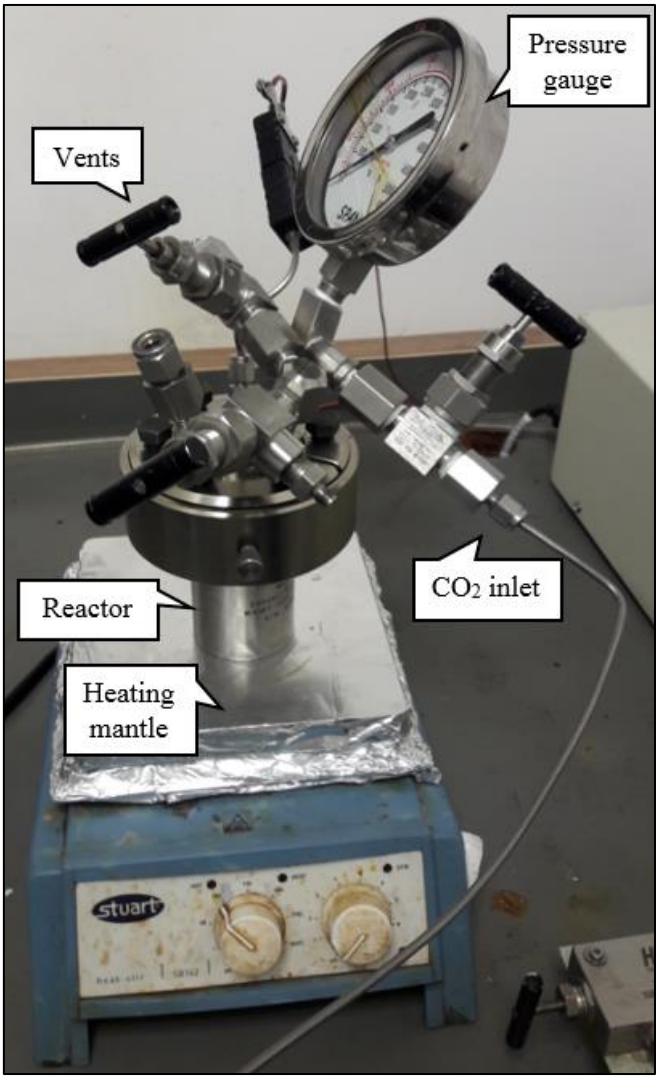

Figure 3.17: 25 mL Stainless steel supercritical CO_2 reactor.

3.6.3 Characterization

Gel Permeation Chromatography (GPC). M_n and polydispersity (M_w/M_n) values were measured using Agilent Technologies 1260 Infinity liquid chromatography system using a Polar Gel-M guard column (50 × 7.5 mm) and two Polar Gel-M columns (300 × 7.5 mm). Measurements were carried out at 50 °C at a flow rate of 1.0 mL min^{-1} using THF as the eluent. The columns were calibrated using twelve polystyrene poly(St) standards (EasiVial PS-H 2 mL, Agilent) (M_n = 580–6,035,000 g mol^{-1}). M_n is given in g mol^{-1} throughout. All GPC corresponds to polymer before purification, unless otherwise stated. The use of poly(St) standards inevitably leads to error, however control/living character was assessed based on the shapes of molecular weight distributions (MWDs) and trends in M_n and M_w/M_n versus conversion.

Nuclear Magnetic Resonance (NMR) Spectroscopy. ^{1}H NMR spectra were recorded using a Joel GXFT 400 MHz instrument equipped with a DEC AXP 300 computer workstation.

Transmission Electron Microscopy (TEM). TEM images were obtained using a Hitachi H7500 and Hitachi H7000 for TEMs at 10 micrometer, using formvar/carbon 200 mesh Cu grids. A small amount of PDMS-*b*-$BzMA_x$ sample (~5 mg/mL) was suspended in pentane and sonicated for 10 min. One drop (~ 0.1 ml) of the colloidal solution was placed on the copper grid and allowed to settle. After 2 min excess solution was carefully wicked with filter paper and allowed to dry prior to TEM analysis. Note: No staining used.

3.6.4 Typical polymerization procedure (e.g. Runs 1 and 2)

Dispersion ATRP of BzMA (~35 v/v(%)) in $scCO_2$ was conducted in a 25 mL stainless steel reactor. BzMA (9.10 g, 0.052 mol), PDMS-Br (0.69 g, 0.129 mmol), CuBr (28.0 mg, 0.195 mmol) and HMTETA (44.9 mg, 0.195 mmol) were added to the reactor. The reaction mixture was purged for 20 min by passing gaseous CO_2 through the mixture to remove oxygen. Liquid CO_2 (~5 MPa) was added and the reactor immersed in an oil bath. The temperature was raised to the reaction temperature of 80 °C followed by the pressure to the reaction pressure of 30 MPa by addition of CO_2. Separate reactions were quenched after 6, 12, 16, 24 and 36 hours by submersion of the reactor into an ice-water bath. When at approximately room temperature, the CO_2 was vented slowly from the reactor into a conical flask to prevent loss of the polymer. For high conversion polymerizations (after 24 and 36 hours), the light blue crystalline solid was washed three times using $scCO_2$ at 50 °C and 30 MPa in order to remove residual monomer (Figure 3.8). For all other polymerizations (taken to lower conversions), visible unreacted BzMA was removed by pipette, and the residue washed five times using $scCO_2$ at 50 °C and 30 MPa. ^1H NMR was used to confirm that the light blue polymer powders were free of BzMA monomer (Figure 3.7). Conversions in all cases were measured by gravimetry.

References:

1. D. Jenkins, R. G. Jones and G. Moad, *Pure Appl. Chem*, **2010**, *82*, 483–491. https://doi.org/10.1351/PAC-REP-08-04-03
2. J.-S. Wang and K. Matyjaszewki, *J. Am. Chem. Soc.*, **1995**, *117*, 5614–5615. https://doi.org/10.1021/ja00125a035
3. M. Kato, M. Kamigaito, M. Sawamoto and T. Higashimura, *Macromolecules*, **1995**, *28*, 1721–1723. https://doi.org/10.1021/ma00109a056
4. K. Matyjaszewski, *Adv. Mater.*, **2018**, *30*, 1706441. https://doi.org/10.1002/adma.201706441
5. W. A. Braunecker and K. Matyjaszewski, *Prog. Polym. Sci.*, **2007**, *32*, 93–146. https://doi.org/10.1016/j.progpolymsci.2007.10.001
6. R. K. O'Reilly, V. C. Gibson, A. J. P. White and D. J. Williams, *J. Am. Chem. Soc*, **2003**, *125*, 8450–8451. https://doi.org/10.1021/ja035458q
7. Z. Lu, M. Fryd and B. B. Wayland, *Macromolecules*, **2004**, *37*, 2686–2687. https://doi.org/10.1021/ma035924w
8. C. Granel, Ph. Dubois, R. Jérôme, and Ph. Teyssié, *Macromolecules*, **1996**, *29*, 8576–8582. https://doi.org/10.1021/ma9608380
9. M. Ouchi, T. Terashima and M. Sawamoto, *Chem. Rev.*, **2009**, *109*, 4963–5050. https://doi.org/10.1021/cr900234b
10. J. -S. Wang and K. Matyjaszewski, *Macromolecules*, **1995**, *28*, 7572–7573. https://doi.org/10.1021/ma00126a041
11. J. Xia and K. Matyjaszewski, *Macromolecules*, **1997**, *30*, 7692–7696. https://doi.org/10.1021/ma9710085
12. W. Jakubowski and K. Matyjaszewski, *Macromolecules*, **2005**, *38*, 4139–4146. https://doi.org/10.1021/ma047389l
13. J. Jennings, G. He, S. M. Howdle and P. B. Zetterlund, *Chem. Soc. Rev.*, **2016**, *45*, 5055–5084. https://doi.org/10.1039/C6CS00253F
14. B. Charleux, G. Delaittre, J. Rieger and F. D'Agosto, *Macromolecules*, **2012**, *45*, 6753–6765. https://doi.org/10.1021/ma300713f
15. S. L. Canning, G .N. Smith and S. P. Armes, *Macromolecules*, **2016**, *49*, 1985–2001. https://doi.org/10.1021/acs.macromol.5b02602

16. J. –T. Sun, C. –Y. Hong and C. –Y. Pan, *Soft Matter*, **2012**, *8*, 7753–7767. https://doi.org/10.1039/C2SM25537E
17. A. N. Albertsen, J. K. Szymański and J. Pérez-Mercader, *Sci. Rep.*, **2017**, *7*, article number 41534. https://doi.org/10.1038/srep41534
18. M. J. Derry, L. A. Fielding and S. P. Armes, *Prog. Polym. Sci.*, **2016**, *52*, 1–18. https://doi.org/10.1016/j.progpolymsci.2015.10.002
19. L. A. Fielding, M. J. Derry, V. Ladmiral, J. Rosselgong, A. M. Rodrigues, L. P. D. Ratcliffe, S. Sugihara and S. P. Armes, *Chem. Sci.*, **2013**, *4*, 2081–2087. https://doi.org/10.1039/C3SC50305D
20. M. J. Derry, L. A. Fielding and S. P. Armes, *Polym. Chem.*, **2015**, *6*, 3054–3062. https://doi.org/10.1039/C5PY00157A
21. Q. Zhang and S. Zhu, *ACS Macro Lett.* **2015**, *4*, 755–758. https://doi.org/10.1021/acsmacrolett.5b00360
22. D. Zhou, S. Dong, R. P. Kuchel, S. Perrier and P. B. Zetterlund, *Polym. Chem*. **2017**, *8*, 3082–3089. https://doi.org/10.1039/C7PY00552K
23. G. Wang, M. Schmitt, Z. Wang, B. Lee, X. Pan, L. Fu, J. Yan, S. Li, G. Xie, M. R. Bockstaller and K. Matyjaszewski, *Macromolecules* **2016**, *49*, 8605–8615. https://doi.org/10.1021/acs.macromol.6b01966
24. X. G. Qiao, O. Lambert, J. –C. Taveau, P. –Y. Dugas, B. Charleux, M. Lansalot and E. Bourgeat-Lami, *Macromolecules*, **2017**, *50*, 3796–3806. https://doi.org/10.1021/acs.macromol.7b00033
25. Y. Kitayama, K. Kishida, H. Minami and M. Okubo, *J. Polym. Sci.: Part A: Polym. Chem*. **2012**, *50*, 1991–1996. https://doi.org/10.1002/pola.25973
26. V. Kapishon, R. A. Whitney, P. Champagne, M. F. Cunningham and R. J. Neufeld, *Biomacromolecules*, **2015**, *16*, 2040–2048. https://doi.org/10.1021/acs.biomac.5b00470
27. C. Boyer and J. Yeow, *Adv. Sci*., **2017**, *4*, 1700137. https://doi.org/10.1002/advs.201700137
28. J. Tan, X. Li, R. Zeng, D. Liu, Q. Xu, J. He, Y. Zheng, X. Dai, L. Yu, Z. Zeng and L. Zhang, *ACS Macro Lett*. **2018**, *7*, 255–262. https://doi.org/10.1021/acsmacrolett.8b00035
29. D. Zhou, R. Kuchel and P. B. Zetterlund, *Polym. Chem.*, **2017**, *8*, 4177–4181. https://doi.org/ 10.1039/C7PY00998D

30. J. N. Israelachvili, D. J. Mitchell and B. W. Ninham, *Biochimica et Biophysica Acta*, **1977**, *470* 185–201. https://doi.org/10.1016/0005-2736(77)90099-2
31. Y. Mai and A. Eisenberg, *Chem. Soc. Rev.*, **2012**, *41*, 5969–5985. https://doi.org/10.1039/C2CS35115C
32. J. S. Lee and J. Feijen, *J. Control. Rel.*, **2012**, *161*, 473–483. https://doi.org/10.1016/j.jconrel.2011.10.005
33. Y. Pei, O. R. Sugita, L. Thurairajah and A. B. Lowe, *RSC Adv.*, **2015**, *5*, 17636–17646. https://doi.org/10.1039/C5RA00274E
34. Y. Pei, L. Thurairajah, O. R. Sugita and A. B. Lowe, *Macromolecules*, **2014**, *48*, 236–244. https://doi.org/10.1021/ma502230h
35. L. Zhang and A. Eisenberg, *Science*, **1995**, *268*, 1728–1731. https://doi.org/10.1126/science.268.5218.1728
36. V. J. Cunningham, A. M. Alswieleh, K. L. Thompson, M. Williams, G. J. Leggett, S. P. Armes, O. M. Musa, *Macromolecules*, **2014**, *47*, 5613–5623. https://doi.org/10.1021/ma501140h
37. D. Zehm, L. P. D. Ratcliffe, and S. P. Armes, *Macromolecules*, **2013**, *46*, 128–139. https://doi.org/10.1021/ma301459y
38. B. Karagoz, L. Esser, H. T. Duong, J. S. Basuki, C. Boyer and T. P. Davis, *Polym. Chem*, **2014**, *5*, 350–355. https://doi.org/10.1039/c3py01306e
39. X. G. Qiao, M. Lansalot, E. Bourgeat-Lami and B. Charleux, *Macromolecules*, **2013**, *46*, 4285–4295. https://doi.org/10.1021/ma4003159
40. J. Nicolas, C. Dire, L. Mueller, J. Belleney, B. Charleux, S. R. A. Marque, D. Bertin, S. Magnet and L. Couvreur, *Macromolecules*, **2006**, *39*, 8274–8282. https://doi.org/10.1021/ma061380x
41. R. McHale, F. Aldabbagh, P. B. Zetterlund, *J. Polym. Sci.: Part A: Polym. Chem.*, **2007**, *45*, 2194–2203. https://doi.org/10.1002/pola.21986
42. R. Span, and W. Wagner, *J. Phys. Chem. Ref. Data*, **1996**, *25*, 1509–1596. https://doi.org/10.1063/1.555991
43. N. Ajzenberg, F. Trabelsi and P. Recasens, *Chem. Eng. Technol.*, **2000**, *23*, 829–839. https://doi.org/10.1002/1521-4125(200010)23:10<829::AID-CEAT829>3.0.CO;2-R
44. M. McCoy, *Chem. Eng. News*, **2006**, *84*, 6–7.
45. M. A. McHugh and V. J. Krukonis, *Supercritical Fluid Extraction: Principles and Practice*. Butterworth-Heinemann: Boston, 1994.

46. S. L. Wells and J. DeSimone, *Angew. Chem. Int. Ed.*, **2001**, *40*, 518–527. https://doi.org/10.1002/1521-3773(20010202)40:3<518::AID-ANIE518>3.0.CO;2-4
47. J. Peach and J. Eastoe, *Bel. J. Org. Chem.*, **2014**, *10*, 1878–1895. https://doi.org/10.3762/bjoc.10.196
48. P. B. Zetterlund, F. Aldabbagh and M. Okubo, *J. Polym. Sci.: Part A: Polym. Chem.* **2009**, *47*, 3711–3728. https://doi.org/10.1002/pola.23432
49. P. O'Connor, P. B. Zetterlund and F. Aldabbagh, *Macromolecules*, **2010**, *43*, 914–919. https://doi.org/10.1021/ma9022179
50. F. Rindfleisch, T. P. DiNoia, M. A. McHugh, *J. Phys. Chem.*, **1996**, 100, 15581–15587. https://doi.org/10.1021/jp9615823
51. R. McHale, F. Aldabbagh, P. B. Zetterlund, H. Minami and M. Okubo, *Macromolecules*, **2006**, *39*, 6853–6860. https://doi.org/10.1021/ma061154n
52. A. M. Gregory, K. J. Thurecht and S. M. Howdle, *Macromolecules*, **2008**, *41*, 1215–1222. https://doi.org/10.1021/ma702017r
53. J. Jennings, M. Beija, A. P. Richez, S. D. Cooper, P. E. Mignot, K. J. Thurecht, K. S. Jack and S. M. Howdle, *J. Am. Chem. Soc*, **2012**, *134*, 4772–4781. https://doi.org/10.1021/ja210577h
54. B. Grignard, C. Jérôme, C. Calberg, R. Jérôme, W. Wang, S. M. Howdle and C. Detrembleur, *Chem. Commun.*, **2008**, 314–316. https://doi.org/10.1039/B716208A
55. B. Grignard, C. Jérôme, C. Calberg, R. Jérôme and C. Detrembleur, *Eur. Polym. J.*, **2008**, *44*, 861–871. https://doi.org/10.1016/j.eurpolymj.2007.11.020
56. J. Xia, T. Johnson, S. G. Gaynor, K. Matyjaszewski and J. DeSimone, *Macromolecules*, **1999**, *32*, 4802–4805. https://doi.org/10.1021/ma9900380
57. H. Minami, Y. Kagawa, S. Kuwahara, J. Shigematsu, S. Fujii and M. Okubo, *Des. Monomers Polym*, **2004**, *7*, 553–562. https://doi.org/10.1163/1568555042474103
58. J. Ryan, F. Aldabbagh, P. B. Zetterlund and M. Okubo, *Polymer*, **2005**, *46*, 9769–9777. https://doi.org/10.1016/j.polymer.2005.08.039
59. R. McHale, F. Aldabbagh, P. B. Zetterlund and M. Okubo, *Macromol. Rapid Commun.*, **2006**, *27*, 1465–1471. https://doi.org/10.1002/marc.200600383
60. B. Grignard, T. Phan, D. Bertin, D. Gigmes, C. Jérôme and C. Detrembleur, *Polym. Chem.*, **2010**, *1*, 837–840. https://doi.org/10.1039/C0PY00066C
61. T. Kuroda, A. Tanaka, T. Taniyama, H. Minami, A. Goto, T. Fukuda and M. Okubo, *Polymer*, **2012**, *53*, 1212–1218. https://doi.org/10.1016/j.polymer.2012.01.038

62. T. Hasell, K. J. Thurecht, R. D. W. Jones, P. D. Brown and S. M. Howdle, *Chem. Commun.*, **2007**, 3933–3935. https://doi.org/10.1039/B710503G
63. M. Zong, K. J. Thurecht and S. M. Howdle, *Chem. Commun.*, **2008**, 5942–5944. https://doi.org/10.1039/B812827H
64. H. Lee, E. Terry, M. Zong, N. Arrowsmith, S. Perrier, K. J. Thurecht and S. M. Howdle, *J. Am. Chem. Soc.*, **2008**, *130*, 12242–12243. https://doi.org/10.1021/ja8046156
65. N. A. Birkin, O. Wildig and S. M. Howdle, *Polym. Chem*, **2013**, *4*, 3791–3799. https://doi.org/10.1039/C3PY00275F
66. K. E. J. Barrett, *Dispersion Polymerization in Organic Media*. Wiley: London: 1975.
67. F. Chavarria and D. R. Paul, *Polymer*, **2004**, *45*, 8501–8515. https://doi.org/10.1016/j.polymer.2004.09.074
68. H. Huan, L. Bes, D. M. Haddleton and E. Khoshdel, *J. Polym. Sci.: Part A: Polym. Chem*. **2001**, *39*, 1833–1842. https://doi.org/10.1002/pola.1161
69. R. N. Keller, H. D. Wrcoff, L. E. Marchi, Copper$^{(I)}$ Chloride. *In Inorganic Syntheses*, John Wiley & Sons, Inc., **2007**, *2*, 1–4.
70. M. Gurry and F. Aldabbagh, *Org. Biomol. Chem*., **2016**, *14*, 3849–3862. https://doi.org/10.1039/c6ob00370b
71. F. Aldabbagh, P. B. Zetterlund and M. Okubo, *Eur. Polym. J.*, **2008**, *44*, 4037–4046. https://doi.org/10.1016/j.eurpolymj.2008.09.020
72. F. Aldabbagh, P. B. Zetterlund and M. Okubo, *Macromolecules*, **2008**, *41*, 2732–2734. https://doi.org/10.1021/ma702645b
73. A. Mitra and D. A. Atwood, *Encyclopedia of Inorganic Chemistry*, John Wiley & Sons, Ltd. **2006**, https://doi.org/10.1002/0470862106.ia201
74. R. N. Keller, H. D. Wrcoff and L. E. Marchi, Copper$^{(I)}$ Chloride. *In Inorganic Syntheses*, John Wiley & Sons, Inc., **2007**, *2*, 1–4. https://doi.org/10.1002/9780470132333.ch1

Publications

Efficient Synthesis and RAFT Polymerization of the Previously Elusive *N*-[(Cycloalkylamino)methyl]Acrylamide Monomer Class.

Benjamin A. Chalmers, Abdullah Alzahrani, Gerard Hawkins, Fawaz Aldabbagh,

Journal of Polymer Science, Part A: Polymer Chemistry, **2017**, *55*, 2123–2128. https://doi.org/10.1002/pola.28607

Synthesis of *N*-[(dialkylamino)methyl]acrylamides and *N*-[(dialkylamino)methyl]-methacrylamides from Schiff base salts: useful building blocks for smart polymers.

Abdullah Alzahrani, Styliana I. Mirallai, Benjamin A. Chalmers, Patrick McArdle and Fawaz Aldabbagh,
Organic and Biomolecular Chemistry, **2018**, *16*, 4108–4116. https://doi.org/10.1002/pola.28607

Conference Proceedings

Isolation of Methylene Schiff Base Salts and Use in Monomer Synthesis
XVIIth International Conference on Heterocycles in Bioorganic Chemistry, Galway, Ireland, May 28–31, 2017. P.O 6
Abdullah Alzahrani, Styliana I. Mirallai and Fawaz Aldabbagh.

Isolation of Methylene Schiff Base Salts and Use in Monomer Synthesis

Abdullah Alzahrani, Styliana I. Mirallai and Fawaz Aldabbagh*

School of Chemistry, National University of Ireland Galway, Ireland

NUI Galway
OÉ Gaillimh

Introduction

Acrylamide and methacrylamide monomers containing ionisable tertiary amino substituents allow access to smart materials with thermal and/or pH-responsiveness.[1]

Methylene Amino - Substituted Acrylamides and Methacrylamides

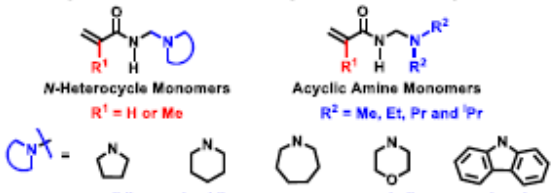

Literature Synthesis: Mannich Reaction

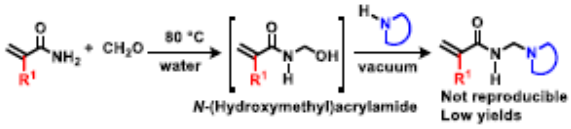

The Mannich approaches are low yielding due to inadvertent thermal polymerization or degradation of the monomer or intermediates at the elevated reaction temperatures (80 °C) with monomer isolation requiring difficult distillations from the aqueous reaction mix.[2]

New Facile Synthesis of Elusive Monomers [3]

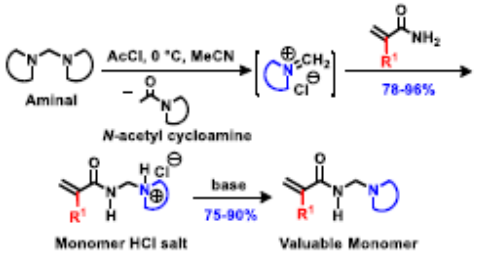

Nucleophilic addition of acrylamide and methacrylamide onto the Schiff base salts gave the hydrochloride monomer salts. The HCl salts were suspended in dichloromethane, and basified to give the saturated nitrogen heterocycle containing acrylamide and methacrylamide monomers, giving at any one time 20-25 g of each of the monomers.

First Block Copolymers [3]

The above first multi-gram preparation of this previously elusive monomer class and reversible addition fragmentation chain transfer radical polymerization (RAFT) gave well-defined diblock and triblock copolymers.[3]

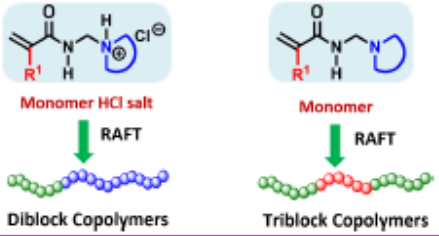

Isolation of Methylene Schiff Base Salts

Isolation of the Schiff base salt is necessary for the preparation of acyclic secondary amine substituted monomers.

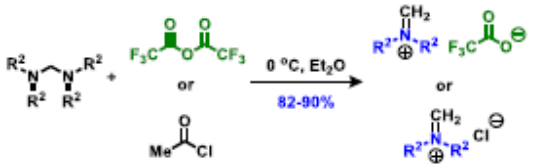

13C NMR of Schiff base salt

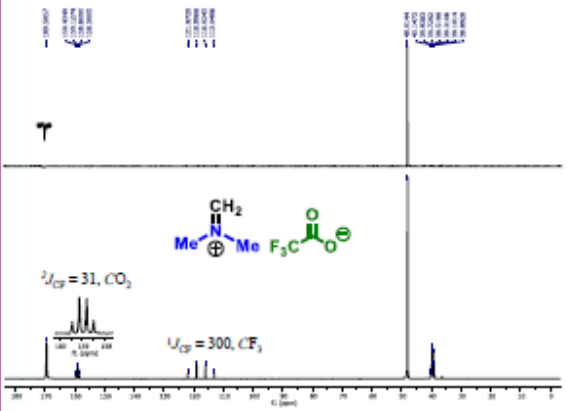

Methylene Schiff base salts as chlorides are hygroscopic, but useful in the synthesis of acyclic monomers.

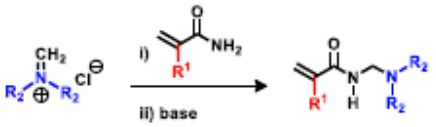

Conclusions and Future Work

- First efficient synthesis of previously elusive acrylamide and methacrylamide monomers containing methylene bridged saturated nitrogen heterocycles and acyclic dialkyl amines.
- Methylene Schiff base salts are best isolated as triflates.
- These new monomers have potential applications, including in the preparation of amphiphilic block copolymers and stimuli-responsive polymersomes for targeted delivery of therapeutics.

References

[1] P. Schattling, F. D. Jochum and P. Theato, Polym. Chem. 5 (2014) 25-36.
[2] H. Böhme and K. Hartke, Chem. Ber. 93 (1960) 1305-1309.
[3] B. A. Chalmers, A. Alzahrani, G. Hawkins and F. Aldabbagh, J. Polym. Sci. Part A: Polym. Chem. 55 (2017) 2123-2128.

Acknowledgements

ROYAL EMBASSY OF SAUDI ARABIA

We thank the Ministry of Education of the Kingdom of Saudi Arabia & the Irish Research Council for a Government of Ireland Postdoctoral Fellowship

IRISH RESEARCH COUNCIL
An Chomhairle um Thaighde in Éirinn

a.alzahrani1@nuigalway.ie; styliana.mirallai@nuigalway.ie; *fawaz.aldabbagh@nuigalway.ie

Efficient Synthesis and RAFT Polymerization of the Previously Elusive *N*-[(Cycloalkylamino)methyl]acrylamide Monomer Class

Benjamin A. Chalmers, Abdullah Alzahrani, Gerard Hawkins, Fawaz Aldabbagh

School of Chemistry, National University of Ireland Galway, University Road, Galway, Ireland
Correspondence to: F. Aldabbagh (E-mail: Fawaz.Aldabbagh@nuigalway.ie)

Received 7 March 2017; accepted 25 March 2017; published online 25 April 2017
DOI: 10.1002/pola.28607

KEYWORDS: block copolymers; heterocycles; living polymerization; reversible deactivation radical polymerization; Schiff base

INTRODUCTION Saturated nitrogen heterocycles (SNHs) have recently been utilized as ionisable tertiary amino groups in amphiphilic block copolymers allowing rapid switching between a hydrophobic and hydrophilic state. Gao et al. reported copolymers consisting of poly(ethylene oxide) (PEO) and methacrylate blocks containing SNH substituents, which self-assembled into micelles before lowered pH caused dissociation and increased fluorescence emission.[1] Efficient penetration of dendrimers incorporating platinum prodrugs was facilitated by analogous amphiphilic block copolymers with pH-sensitive azepane substituents enabling nanoparticle collapse in the acidic environments of tumour cells.[2] The pH-responsive SNH was incorporated using reversible deactivation radical polymerizations[3] of 2-(cycloalkylamino)ethyl (meth)acrylates or 2-(cycloalkylamino)ethyl (meth)acrylamides [Scheme 1a(i)] with nitroxide-mediated radical polymerization (NMP),[4] atom transfer radical polymerization (ATRP),[1,5] and reversible addition-fragmentation chain transfer radical polymerization (RAFT)[2,6,7] of these monomers reported. There are, however, scarce reports of polymerizations (including no controlled/living polymerizations) of *N*-[(cycloalkylamino)methyl] (meth)acrylamides containing a methylene amine (e.g. cycloalkylamino = SNH) rather than an ethyl amine pendent, presumably due to difficulties in their synthesis [Scheme 1a(ii)].[9–11]

The literature NMR data of *N*-[(morpholino-4-yl)methyl]-prop-2-enamide **1a**, which is erroneous (due to insufficient signals and incorrect chemical shifts) is evidence of the synthetic challenge posed by these molecules.[10] Müller et al described monomer preparations as far back as the early 1960s involving one-pot Mannich reactions of formaldehyde with acrylamide to give *N*-(hydroxymethyl)acrylamide followed by addition of the secondary amine [Scheme 1b(i)].[8,9] The Mannich approaches are however low yielding due to inadvertent thermal polymerization or degradation of the monomer or intermediates at the elevated reaction temperatures (~80 °C) with monomer isolation requiring difficult distillations from the aqueous reaction mix. A new monomer synthesis is now introduced based on the concept of Böhme,[12,13] involving *in situ* generation of the methylene Schiff base salt by convenient quaternization of the readily accessible aminal [Scheme 1b(ii)]. Herein, our new facile room temperature protocol has allowed the efficient multigram preparation of acrylamides **1a-1c** with methylene SNH substituents via basification of the respective heterocyclic monomer hydrochloride salts **1a.HCl–1c.HCl**. The expedient synthesis motivated us to carry out the first controlled/living polymerizations of this previously elusive monomer class, as well as, its hydrochloride salts using the RAFT process. Living polymerization infers the retention of the ω-end (RAFT) group, which we now demonstrate through efficient preparation of block copolymers by rapid sequential monomer addition so, providing a straightforward means of incorporating new acrylamides containing bridged pH-responsive SNHs into intricate well-defined polymer architectures.

Inexpensive aminals were first prepared in high yields (80–99%) by condensing formaldehyde (37% formalin) with secondary cyclic amines using well-established literature procedures.[14,15] Aminals were quaternized using acetyl chloride in dry acetonitrile, which formed *in situ* the methylene Schiff base salts, along with the *N*-acetyl cycloamine. Nucleophilic addition of acrylamide onto the Schiff base salts gave the hydrochloride monomer salts (**1a.HCl**, **1b.HCl**, **1c.HCl**) after precipitation from diethyl ether, which also served to separate the *N*-acetyl cycloamine since the latter remained in solution. The HCl salts were suspended in dichloromethane and basified to give the SNH containing acrylamide monomers **1a–1c**. The entire synthesis was conducted at 0 °C to room temperature, thus circumventing potential thermal

Additional Supporting Information may be found in the online version of this article.

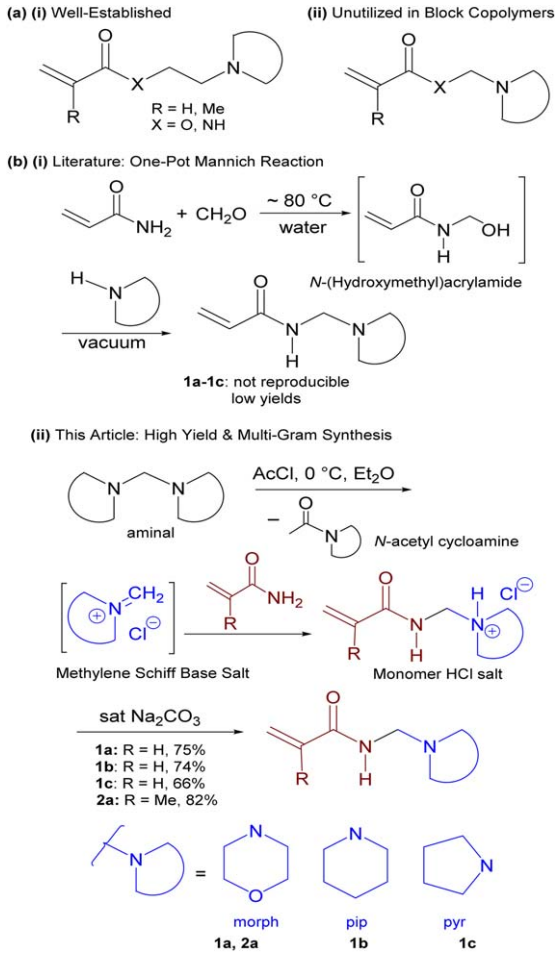

SCHEME 1 *N*-[(Cycloalkylamino)methyl]Acrylamides: (a) preponderance, (b) synthesis. [Color figure can be viewed at wileyonlinelibrary.com]

side-reactions and giving at any one time 20–25 g of each of the three monomers **1a–1c**. Overall monomer yields were ~75% for the morpholine **1a** and piperidine **1b** with a lower yield of 66% obtained for the pyrrolidine monomer **1c** due to its inherent hygroscopic nature and low melting point. The scope of the monomer synthesis is demonstrated by the easy preparation of methacrylamide analogues with over 30 g of morpholine analogue **2a** prepared in 82% yield.

Our polymerization strategy is based upon that of Zetterlund and Perrier et al., who demonstrated the use of the RAFT process in yielding well-defined multicomponent polyacrylamide block copolymers in one pot without intermittent purification by use of the water soluble azo-initiator, VA-044, where each block was prepared in ~99% conversion in 2 h at 70 °C.[16] Although evidence for living/controlled homopolymerization of **1a** was obtained through efficient chain extension of poly(**1a**)$_{60}$ to give poly(**1a**)$_{130}$ (Supporting Information Fig. S1), one-pot block copolymer synthesis (without intermediate polymer isolation) was hampered by the inability to achieve full conversion for the RAFT of **1a** using both 2 h polymerizations with VA-044 and longer polymerization times with AIBN. Consequently, polymerizations employed water-soluble poly(*N*,*N*-dimethylacrylamide, DMA)$_{41}$ as the macroRAFT agent, since this could be prepared in high conversion and theoretical livingness (both 99%, see Supporting Information) so providing the ideal start for two sequential 2 h one-pot chain extensions at 70 °C (Scheme 2).[16,17] Under these conditions VA-044 undergoes near-complete homolytic decomposition (~95%) into radicals, and an almost quantitative fraction of living chains is maintained by use of high [RAFT]$_0$/[VA-044]$_0$ ratios (e.g., [RAFT]$_0$/[VA-044]$_0$ = 10–100 provides 91–99% livingness, according to eq 1).

$$L = \frac{[RAFT]_0}{[RAFT]_0 + 2f[I]_0(1-e^{-k_d t})\left(1-\frac{f_c}{2}\right)} \quad (1)$$

Equation 1 estimates the theoretical fraction of living chains (L). The factor "2" accounts for one molecule of azo-initiator yielding two primary radicals with the efficiency f (assumed to be equal to 0.5). The decomposition rate constant is k_d is taken as 4.30×10^{-4} s^{-1} for VA-044 at 70 °C in water/dioxane (80:20).[17] The quantity $\left(1-\frac{f_c}{2}\right)$ represents the number of chains produced in a radical−radical termination event with the coupling factor f_c assumed to be zero.[16,17]

Two one-pot chain extensions were carried out to near full conversion (~99%), as monitored by ^{1}H NMR (Supporting Information Figs. S2 and S3). The solubility of the macroRAFT agent and initiator allowed chain extensions of poly(DMA)$_{41}$ to give poly(DMA)$_{41}$-*b*-(**1a**)$_{69}$-*b*-(DMA)$_{192}$ to be carried out in water [Scheme 2(a)]. In order to negate purification prior to chain extension with DMA polymerizations to give the intermediate diblock using morpholine **1a** and piperidine **1b** required a relatively high VA-044 concentration ([RAFT]$_0$/[VA-044]$_0$ = 10) for near-complete conversion. For the synthesis of water soluble poly(DMA)$_{41}$-*b*-(**1a**)$_{69}$-*b*-(DMA)$_{192}$, molecular weight distributions (MWDs) remained relatively narrow (M_w/M_n = 1.35–1.50) shifting to higher MW with M_n values close to theoretical ($M_{n,th}$) despite inherent GPC error due to calibration to linear poly(MMA) standards (Table 1). In contrast, the polymerization of piperidine **1b** required dioxane due to the formation of a more hydrophobic diblock, however, mixtures using varied dioxane/water gave broad MWDs for chain extension of poly(DMA)$_{41}$ with **1b**.

Recent work by Abel and McCormick on the RAFT polymerization of methacrylamides has shown that livingness through preservation of the trithiocarbonate end-group can be achieved by utilizing acidic solutions, which protonate nucleophilic sites (including the *N* atom of the amide).[18,19] This led to the addition of 1.15 equivalents of HCl to the chain extension of poly(DMA)$_{41}$, which gave poly(DMA)$_{41}$-*b*-(**1b**)$_{97}$ in 97% conversion with excellent control/living character as demonstrated by narrow MWD (M_w/M_n = 1.22) with M_n close to $M_{n,th}$ [Fig. 1(a(ii)) and Table 1]. It seems that protonation of the piperidine ring of the poly(**1b**) block prevented aminolysis side-reactions that cleave the trithiocarbonate

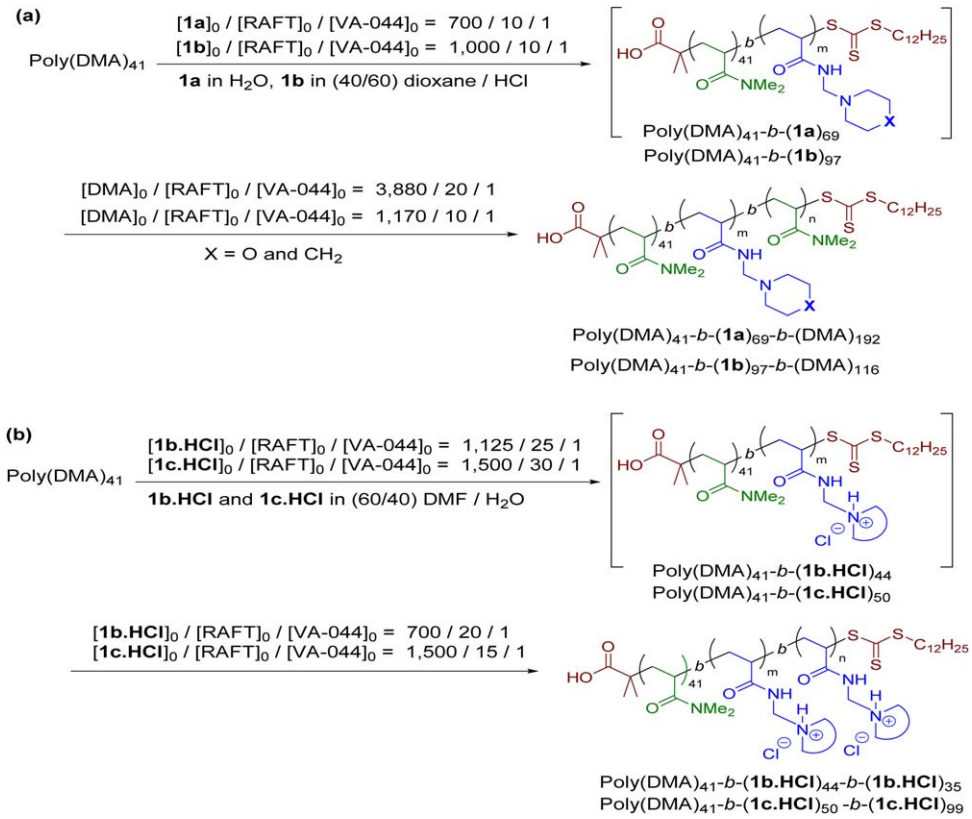

SCHEME 2 One-pot 2-hour sequential RAFT polymerizations at 70 °C without intermediate purifications of (a) acrylamide monomers and DMA (b) monomer hydrochloride salts. All conversions were 99% except for the chain extension with **1b**, which was 97%. [Color figure can be viewed at wileyonlinelibrary.com]

end-group, and that this phenomenon is decreased or is absent for morpholine **1a** due to the electronegative oxygen atom of the heterocycle. Subsequent one-pot chain extension with DMA gave poly(DMA)$_{41}$-*b*-(**1b**)$_{97}$-*b*-(DMA)$_{116}$ with no noticeable loss of control/livingness.

The polymerization of the hydrochloride salts were carried out in 60/40 DMF/water reaction solutions rather than pure water, since the mixed solvent system maintained a homogeneous reaction mixture [Scheme 2(b)]. Two sequential chain extensions of poly(DMA)$_{41}$ with the monomer salts were indicative of good control/living character [Fig. 1(b(i)(ii))]. Lower initiator concentrations were required for the first chain extension compared to the second for polymerizations with piperidine hydrochloride **1b.HCl** and pyrrolidine hydrochloride **1c.HCl** with high conversion and theoretical livingness (both ~99%) achieved. The successful RAFT polymerization of the ionized monomer salts **1b.HCl** and **1c.HCl**, overcame the lack of chain extension of poly(DMA)$_{41}$ with the free heterocyclic base monomers (Supporting Information Fig. S4). Although MWDs shifted to higher MW with M_n close to $M_{n,th}$ (Table 1), the MWDs for **1c.HCl** (M_w/M_n = 1.66–1.80) were noticeably broader than **1b.HCl** (M_w/M_n = 1.31–1.40).

In conclusion, *in situ* generated Schiff base salts have allowed the multigram preparation of previously difficult to

TABLE 1 Characterization of Polyacrylamides

Polymer[a]	$M_{n,th}$[b]	M_n[d]	M_w/M_n[d]
Poly(DMA)$_{41}$	5,300	4,450	1.10
Poly(DMA)$_{41}$-*b*-(**1a**)$_{69}$	16,250	15,280	1.35
Poly(DMA)$_{41}$-*b*-(**1a**)$_{69}$-*b*-(DMA)$_{192}$	34,300	34,850	1.50
Poly(DMA)$_{41}$-*b*-(**1b**)$_{97}$	20,750[c]	20,800	1.22
Poly(DMA)$_{41}$-*b*-(**1b**)$_{97}$-*b*-(DMA)$_{116}$	32,300[c]	29,200	1.25
Poly(DMA)$_{41}$-*b*-(**1b.HCl**)$_{44}$	13,550	12,750	1.31
Poly(DMA)$_{41}$-*b*-(**1b.HCl**)$_{44}$-*b*-(**1b.HCl**)$_{35}$	19,850	19,750	1.40
Poly(DMA)$_{41}$-*b*-(**1c.HCl**)$_{50}$	13,900	12,850	1.66
Poly(DMA)$_{41}$-*b*-(**1c.HCl**)$_{50}$-*b*-(**1c.HCl**)$_{99}$	31,750	29,800	1.80

[a] The degree of polymerization for poly(DMA)$_{41}$ is calculated using M_n from GPC (deducting the MW of the RAFT end groups) and for all other polymers degree of polymerization is calculated from conversion by ^{1}H NMR (= 99%, except for chain extension with **1b**, which was 97%). In each case, the degree of polymerization is obtained by deducting the M_n(GPC) of the extended macroRAFT.
[b] $M_{n,th}$ is calculated according to eq 2 (see Supporting Information).
[c] $M_{n,th}$ does not take into account the addition of HCl to these polymerizations.
[d] Determined by GPC/RI in DMF (0.01 M LiBr) using commercial linear poly(MMA) as molecular weight standards.

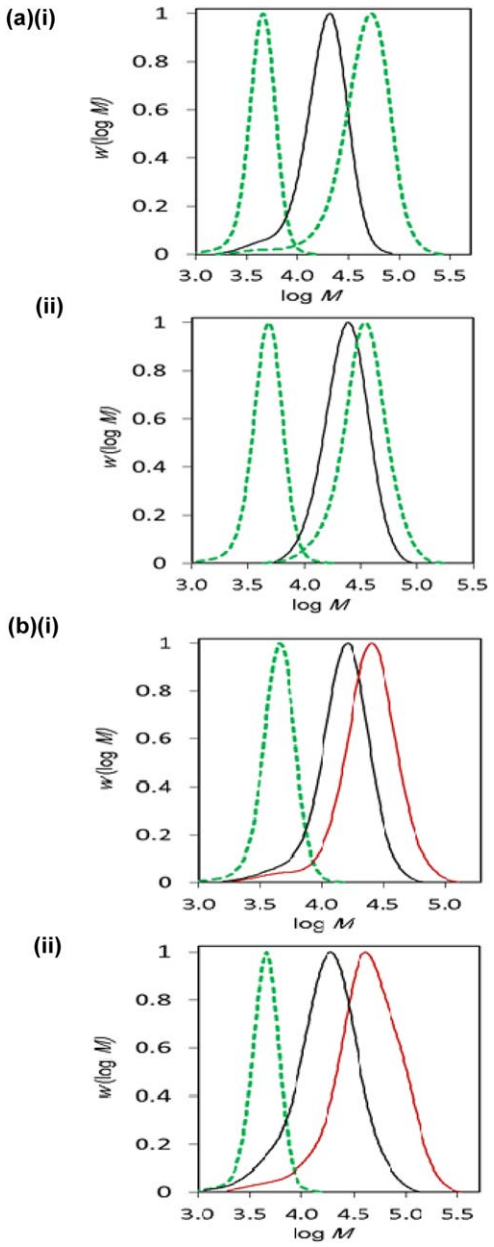

FIGURE 1 MWDs for one-pot RAFT polymerizations of *N*-[(cycloalkylamino)methylene]acrylamides (continuous lines) using poly(DMA) macroRAFT (where DMA polymerizations are dashed lines) to give (a) (i) poly(**DMA**)$_{41}$-*b*-(**1a**)$_{69}$-*b*-(**DMA**)$_{192}$; (ii) poly(**DMA**)$_{41}$-*b*-(**1b**)$_{97}$-*b*-(**DMA**)$_{116}$; (b) (i) poly(**DMA**)$_{41}$-*b*-(**1b.HCl**)$_{44}$-*b*-(**1b.HCl**)$_{35}$; (ii) poly(**DMA**)$_{41}$-*b*-(**1c.HCl**)$_{50}$-*b*-(**1c.HCl**)$_{99}$. [Color figure can be viewed at wileyonlinelibrary.com]

acquire methylene amino-substituted monomers, opening the way to the facile preparation of related acrylamides and methacrylamides with conceivable acyclic as well as cyclic amine substituents. RAFT polymerization has allowed the preparation of the first well-defined block copolymers, although the close proximity of the trithiocarbonate end-group to the tertiary amino substituent made control/living character for the piperidine and pyrrolidine monomers superior when the heterocyclic pendant was ionized. These new monomers undoubtedly have further synthetic potential and applications, including in the preparation of amphiphilic block copolymers and stimuli-responsive polymersomes for targeted delivery of therapeutics.

EXPERIMENTAL

Monomer Synthesis: *N*-[(Cycloamino)methyl]-acrylamides and methacrylamide (1a–1c and 2a)

AcCl (14.3 mL, 0.2 mol) was added over 30 min to the aminal (0.2 mol) in MeCN (40 mL) at 0 °C. Acrylamide (14.2 g, 0.2 mol) or methacrylamide (17.0 g, 0.2 mol) in MeCN (40 mL) was added and stirred at room temperature for 2 h. Et_2O (50 mL) was added and the hydrochloride salt of the monomer precipitated, filtered, and dried under vacuum. The hydrochloride salt **(1a.HCl–1c.HCl and 2a.HCl)** was recrystallized, dried, and characterized. Saturated Na_2CO_3 solution (50 mL) was added to a suspension of hydrochloride salt in CH_2Cl_2 (50 mL) and stirred for 20 min. The organic layer was separated and the aqueous layer was washed with CH_2Cl_2 (4 × 30 mL). The combined organic extracts were dried ($MgSO_4$), filtered, and evaporated to dryness to give the monomer, which was recrystallized.

***N*-[(Morpholin-4-yl)methyl]prop-2-enamide hydrochloride (1a.HCl)**: white solid; mp 146–148 °C (recryst. from MeCN); ^{1}H NMR (400 MHz, DMSO-d_6, δ, ppm): 2.84–3.36 (m, 4H), 3.66–4.05 (m, 4H), 4.54 (d, J = 6.8 Hz, 2H, 1-CH_2), 5.79 (dd, J = 10.2, 1.9 Hz, 1H, *cis*-H), 6.26 (dd, J = 17.2, 1.9 Hz, 1H, *trans*-H), 6.43 (dd, J = 17.2, 10.2 Hz, 1H), 9.60 (t, J = 6.8 Hz, 1H, NH), 11.22–11.42 (brs, 1H, NH); ^{13}C NMR (100 MHz, DMSO-d_6, δ, ppm): 48.6 (CH_2), 58.6 (1-CH_2), 63.0, 128.3 (both CH_2), 130.3 (CH), 166.2 (C = O).

***N*-[(morpholin-4-yl)methyl]prop-2-enamide (1a)**: 25.5 g, Yield: 75%, white solid; mp 93–95 °C (recryst. from MeCN); ν_{max} (neat, cm^{-1}) 3254, 2860, 2825, 1669, 1648 (C = O), 1608, 1535, 1228, 1155, 1109; ^{1}H NMR (400 MHz, $CDCl_3$, δ, ppm): 2.57 (t, J = 4.7 Hz, 4H), 3.69 (t, J = 4.7 Hz, 4H), 4.17 (d, J = 6.5 Hz, 2H, 1-CH_2), 5.70 (dd, J = 10.3, 1.4 Hz, 1H, *cis*-H), 5.91–6.05 (brs, 1H, NH), 6.10 (dd, J = 17.0, 10.3 Hz, 1H), 6.32 (dd, J = 17.0, 1.4 Hz, 1H, *trans*-H); ^{13}C NMR (100 MHz, $CDCl_3$, δ, ppm): 50.5 (CH_2), 61.6 (1-CH_2), 66.4, 127.5 (both CH_2), 130.6 (CH), 166.2 (C = O); HRMS (ESI) m/z $[M + H]^+$, $C_8H_{15}N_2O_2$, calcd 171.1134, observed 171.1136.

***N*-[(piperidin-1-yl)methyl]prop-2-enamide hydrochloride (1b.HCl)**: white solid, mp 143–145 °C (recryst. from MeCN); ^{1}H NMR (400 MHz, DMSO-d_6, δ, ppm): 1.27–1.42 (m, 1H), 1.60–1.84 (m, 5H), 2.82 (d, J = 11.2 Hz, 2H), 3.30 (d, J = 11.2 Hz, 2H), 4.47 (d, J = 6.5 Hz, 2H, 1-CH_2), 5.81 (dd, J = 10.0, 1.9 Hz, 1H, *cis*-H), 6.27 (dd J = 17.1, 1.9 Hz, 1H, *trans*-H), 6.38 (dd, J = 17.1, 10.0 Hz, 1H), 9.32–9.43 (brs, 1H, NH), 9.91–10.12 (brs, 1H, NH); ^{13}C NMR (100 MHz, DMSO-d_6, δ, ppm): 21.4, 22.3, 49.8 (all CH_2), 58.7 (1-CH_2), 128.3 (CH_2), 130.6 (CH), 166.4 (C = O).

***N*-[(piperidin-1-yl)methyl]prop-2-enamide (1b)**: 24.9 g, Yield: 74%, white solid, mp 55–57 °C (recryst. from Et_2O);

ν_{max} (neat, cm^{-1}) 3276, 2936, 2807, 1669, 1650 (C = O), 1611, 1528, 1372, 1227, 1216, 1175, 1027; ^{1}H NMR (400 MHz, $CDCl_3$, δ, ppm): 1.35–1.44 (m, 2H), 1.55 (p, J = 5.5 Hz, 4H), 2.49 (t, J = 5.5 Hz, 4H), 4.13 (d, J = 6.4 Hz, 2H, 1-CH_2), 5.65 (dd, J = 10.2, 1.4 Hz, 1H, *cis*-H), 6.10 (dd, J = 17.0, 10.2 Hz, 2H, CH, NH), 6.29 (dd, J = 17.0, 1.4 Hz, 1H, *trans*-H); ^{13}C NMR (100 MHz, $CDCl_3$, δ, ppm): 24.2, 26.0, 51.5 (all CH_2), 62.2 (1-CH_2) 126.8 (CH_2), 131.2 (CH), 166.6 (C = O); HRMS (ESI) *m/z* $[M + H]^+$, $C_9H_{17}N_2O$, calcd. 169.1341, observed 169.1335.

***N*-[(pyrrolidin-1-yl)methyl]prop-2-enamide hydrochloride (1c.HCl)**: white solid, mp 64–66 °C, (recryst. from EtOAc); ^{1}H NMR (400 MHz, DMSO-d_6, δ, ppm): 1.78–1.97 (m, 4H), 2.91–3.54 (m, 4H), 4.53 (d, J = 6.8 Hz, 2H, 1-CH_2), 5.78 (dd, J = 10.2, 1.9 Hz, 1H, *cis*-H), 6.24 (dd, J = 17.2, 1.9 Hz, 1H, *trans*-H), 6.41 (dd, J = 17.2, 10.2 Hz, 1H), 9.72 (t, J = 6.8 Hz, 1H, NH), 10.96–11.10 (brs, 1H, NH); ^{13}C NMR (100 MHz, DMSO-d_6, δ, ppm): 23.1, 50.6 (both CH_2), 56.0 (1-CH_2), 128.3 (CH_2), 130.6 (CH), 166.4 (C = O). **1c.HCl** should be stored under vacuum in a desiccator at room temperature.

***N*-[(pyrrolidin-1-yl)methyl]prop-2-enamide (1c)**: 20.3 g, Yield: 66%, white solid, mp 29–30 °C, (recryst. from EtOAc), ν_{max} (neat, cm^{-1}) 3268, 2964, 1656 (C = O), 1627, 1537, 1232, 1135, 1031; ^{1}H NMR (400 MHz, $CDCl_3$, δ, ppm): 1.69–1.81 (m, 4H), 2.57–2.65 (m, 4H), 4.25 (d, J = 6.3 Hz, 1H, 2H, 1-CH_2), 5.65 (dd, J = 10.2, 1.4 Hz, 1H, *cis*-H), 6.10 (dd, J = 17.0, 10.2 Hz, 1H), 6.28 (dd, J = 17.0, 1.4 Hz, 1H, *trans*-H), 6.31–6.37 (brs, 1H, NH); ^{13}C NMR (100 MHz, $CDCl_3$, δ, ppm): 23.7, 50.9 (both CH_2), 58.3 (1-CH_2), 127.0 (CH_2), 130.9 (CH), 165.9 (C = O); HRMS (ESI) *m/z* $[M + H]^+$, $C_8H_{15}N_2O$, calcd 155.1184, observed 155.1176. Monomer **1c** should be stored under vacuum in a desiccator at room temperature.

2-Methyl-*N*-[(morpholin-4-yl)methyl]prop-2-enamide hydrochloride (2a.HCl): white solid, mp 123–125 °C (recryst. from MeCN); ^{1}H NMR (400 MHz, DMSO-d_6, δ, ppm): 1.09 (s, 3H); 2.90–3.30 (m, 4H), 3.70–4.03 (m, 4H), 4.50 (d, J = 6.7 Hz, 2H), 5.58 (s, 1H), 5.95 (s, 1H), 9.20–9.22 (brs, 1H), 10.84–11.21 (m, 1H); ^{13}C NMR (100 MHz, DMSO-d_6, δ, ppm): 18.9 (CH_3). 49.2 (CH_2), 59.7 (1-CH_2), 63.5, 122.5 (both CH_2), 138.9 (C), 169.3 (C = O).

2-Methyl-*N*-[(morpholin-4-yl)methyl]prop-2-enamide (2a): 30.2 g, Yield: 82%, white solid, mp 56–58 °C (recryst. from MeCN), ν_{max} (neat, cm^{-1}) 3315, 2960, 2853, 1655 (C = O), 1616, 1523, 1453, 1295, 1216, 1139, 1049, 1014; ^{1}H NMR (400 MHz, $CDCl_3$, δ, ppm): 1.97 (s, 3H), 2.57 (t, J = 4.7 Hz, 4H), 3.70 (t, J = 4.7 Hz, 4H), 4.15 (d, J = 6.4 Hz, 2H), 5.36–5.37 (m, 1H), 5.70–5.71 (m, 1H), 6.15–6.25 (brs, 1H); ^{13}C NMR (100 MHz, $CDCl_3$, δ, ppm): 18.8 (Me); 50.5 (CH_2), 61.6 (1-CH_2), 66.9, 119.9 (both CH_2), 140.0 (C), 169.0 (C = O); HRMS (ESI) *m/z* $[M + H]^+$, $C_9H_{17}N_2O_2$ calcd 185.1290, observed 185.1371.

General One-Pot Sequential Polymerization Procedure

Solutions were heated at 70 °C in an aluminum-heating block for 2 h. Polymerizations were stopped by placing test tubes in an ice-water bath. Conversion, M_n, and M_w/M_n were measured as described in the Supporting Information. Unless otherwise stated sequential chain extension reactions were performed directly on the macroRAFT reaction solution with the amount of initiator remaining after each cycle taken into account.[16,17]

Preparation of Poly(DMA)$_{41}$-*b*-(1a)$_{69}$-*b*-(DMA)$_{192}$ Copolymer

Poly(DMA)$_{41}$ (1.43×10^{-2} mmol) and **1a** (0.170 g, 1.00 mmol) were added to VA-044 (1.43×10^{-3} mmol from a stock solution) in 0.6 mL water and heated as described above. DMA (0.275 g, 2.78 mmol) and VA-044 (6.5×10^{-4} mmol from a stock solution) in 0.5 mL water were added to the latter poly(DMA)$_{41}$-*b*-(**1a**)$_{69}$ solution and heated as described above.

Preparation of Poly(DMA)$_{41}$-*b*-(1b)$_{97}$-*b*-(DMA)$_{116}$ Copolymer

Poly(DMA)$_{41}$ (8.54×10^{-3} mmol) and **1b** (0.144 g, 0.854 mmol) were added to VA-044 (8.54×10^{-4} mmol from a stock solution) in 0.3 mL HCl (3.28 M, 1.15 eq. HCl:Monomer) solution and 0.2 mL dioxane and heated as described above. DMA (0.100 g, 1.01 mmol) and VA-044 (8.6×10^{-4} mmol from a stock solution) in 0.1 mL water were added to the latter poly(DMA)$_{41}$-*b*-(**1b**)$_{97}$ solution and heated as described above.

Preparation of Poly(DMA)$_{41}$-*b*-(1b.HCl)$_{44}$-*b*-(1b.HCl)$_{35}$ Copolymer

Poly(DMA)$_{41}$ (37.1×10^{-3} mmol) and **1b.HCl** (0.342 g, 1.67 mmol) were added to VA-044 (1.48×10^{-3} mmol from a stock solution) in 0.5 mL DMF/water (60/40) solution and heated as described above. Monomer **1b.HCl** (0.264 g, 1.29 mmol) and VA-044 (1.84×10^{-3} mmol from a stock solution) in 0.5 mL DMF/water (60/40) were added to the latter poly(DMA)$_{41}$-*b*-(**1b.HCl**)$_{44}$ solution and heated as described above.

Preparation of Poly(DMA)$_{41}$-*b*-(1c.HCl)$_{50}$-*b*-(1c.HCl)$_{99}$ Copolymer

Poly(DMA)$_{41}$ (16.4×10^{-3} mmol) and **1c.HCl** (0.156 g, 0.82 mmol) were added to VA-044 (5.46×10^{-4} mmol from a stock solution) in 0.5 mL DMF/water (60/40) solution and heated as described above. Monomer **1c.HCl** (0.313 g, 1.64 mmol) and VA-044 (1.09×10^{-3} mmol from a stock solution) in 0.5 mL DMF/water (60/40) were added to the latter poly(DMA)$_{41}$-*b*-(**1c.HCl**)$_{50}$ solution and heated as described above.

ACKNOWLEDGEMENTS

The authors thank the Irish Research Council (IRC) for a Government of Ireland Postdoctoral Fellowship for Benjamin A. Chalmers, and the Ministry of Education of the Kingdom of Saudi Arabia for supporting the PhD of Abdullah Alzahrani.

REFERENCES AND NOTES

1 K. Zhou, Y. Wang, X. Huang, K. Luby-Phelps, B. D. Sumer, J. Gao, *Angew. Chem. Int. Ed.* **2011**, *50*, 6109–6114.

2 H.-J. Li, J.-Z. Du, J. Liu, X.-J. Du, S. Shen, Y.-H. Zhu, X. Wang, X. Ye, S. Nie, J. Wang, *ACS Nano* **2016**, *10*, 6753–6761.

3 A. D. Jenkins, R. G. Jones, G. Moad, *Pure Appl. Chem.* **2010**, *82*, 483–491.

4 C. Magee, Y. Sugihara, P. B. Zetterlund, F. Aldabbagh, *Polym. Chem.* **2014**, *5*, 2259–2265.

5 Y. Li, Z. Wang, Q. Wei, M. Luo, G. Huang, B. D. Sumer, J. Gao, *Polym. Chem.* **2016**, *7*, 5949–5956.

6 L. Zhu, S. Powell, S. G. Boyes, *J. Polym. Sci. Part A: Polym. Chem.* **2015**, *53*, 1010–1022.

7 K. Wang, Z. Song, C. Liu, W. Zhang, *Polym. Chem.* **2016**, *7*, 3423–3433.

8 V. E. Müller, K. Dinges, W. Graulich, *Die Makromol. Chem.* **1962**, *57*, 27–51.

9 V. E. Müller, H. Thomas, *Angew. Makromol. Chem.* **1973**, *34*, 111–133.

10 M. L. Eritsyan, Z. B. Barsegyan, R. A. Karamyan, S. M. Manukyan, T. D. Karapetyan, K. A. Martirosyan, *Russ. J. Appl. Chem.* **2011**, *84*, 1257–1260.

11 R. C. Baltieri, L. H. Innocentini-Mei, W. M. S. C. Tamashiro, L. Peres, E. Bittencourt, *Eur. Polym. J.* **2002**, *38*, 57–62.

12 H. Böhme, K. Hartke, *Chem. Ber.* **1960**, *93*, 1305–1309.

13 H. Böhme, P. Backhaus, *Liebigs Ann. Chem.* **1975**, 1790–1796.

14 A. Porzelle, C. M. Williams, *Synthesis* **2006**, 3025–3030.

15 H. Heaney, G. Papageorgiou, R. F. Wilkins, *Tetrahedron* **1997**, *53*, 2941–2958.

16 G. Gody, T. Maschmeyer, P. B. Zetterlund, S. Perrier, *Macromolecules* **2014**, *47*, 3451–3460.

17 G. Gody, T. Maschmeyer, P. B. Zetterlund, S. Perrier, *Macromolecules* **2014**, *47*, 639–649.

18 B. A. Abel, C. L. McCormick, *Macromolecules* **2016**, *49*, 465–474.

19 B. A. Abel, C. L. McCormick, *Macromolecules* **2016**, *49*, 6193–6202.

Organic & Biomolecular Chemistry

PAPER

View Article Online
View Journal | View Issue

Check for updates

Cite this: *Org. Biomol. Chem.*, 2018, **16**, 4108

Synthesis of *N*-[(dialkylamino)methyl]acrylamides and *N*-[(dialkylamino)methyl]methacrylamides from Schiff base salts: useful building blocks for smart polymers†

Abdullah Alzahrani, Styliana I. Mirallai, * Benjamin A. Chalmers, Patrick McArdle and Fawaz Aldabbagh *‡

Received 5th April 2018,
Accepted 9th May 2018

DOI: 10.1039/c8ob00811f

rsc.li/obc

The traditional thermal Mannich reaction is unsuitable for preparing polymerizable *N*-methylene amino substituted acrylamides and methacrylamides. Herein we provide a facile multi-gram high yield synthesis of these monomeric precursors to stimuli-responsive polymers by the addition of acrylamides and methacrylamides onto *in situ* generated or freshly isolated methylene Schiff base (iminium) salts. The X-ray crystal structure of the hydrated iminium salt, 1-(hydroxymethyl)azocan-1-ium chloride and monomer·HCl salt (*N*-[(azocan-1-yl)methyl]prop-2-enamide hydrochloride) is described.

Introduction

The three-component Mannich reaction is fundamental, allowing access to β-amino methylated carbonyl compounds.[1,2] *N*-[(Dialkylamino)methyl]acrylamide and methacrylamide analogues are valuable monomeric precursors to smart polymers, with dual functionalities of temperature and pH-responsiveness (Fig. 1), however potential applications have not been realised due to problems with their synthesis.

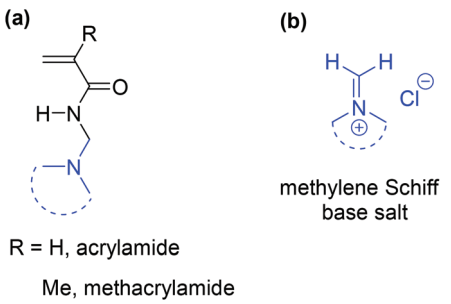

Fig. 1 (a) Synthetic targets and (b) precursors.

Literature routes have used one-pot Mannich condensation of (meth)acrylamide with formaldehyde to generate the Schiff base followed by secondary amine addition (Scheme 1).[3–6] The reaction operates thermally (at ~80 °C), and is inefficient in forming the Schiff base *in situ*, with the elevated temperature resulting in premature polymerization of the monomer and intermediates. The reaction has the added difficulty of monomer isolation, which requires vacuum distillation from the aqueous reaction mixture.

The most widely studied temperature-responsive polymers are those with lower critical solution temperature (LCST) close to physiological temperature, such as poly(*N*-isopropylacrylamide) and poly(*N*,*N*-diethylacrylamide) with LCST of 32–34 °C in water.[7–9] The *N*-dialkyl amino (including saturated nitrogen heterocycle) of substituted acrylamides and methacrylamides can be reversibly ionized allowing for a pH-response that alters polymer hydrophobicity.[9–15] Amphiphilic block copolymers comprising such monomers can self-assemble into a variety of nano-objects for use as stimuli-responsive

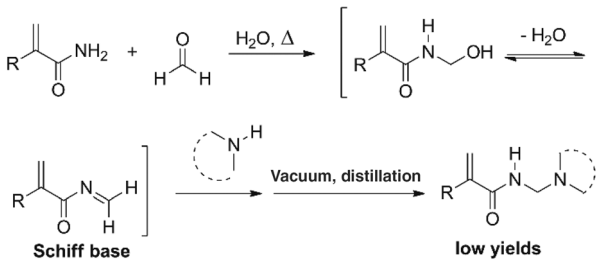

Scheme 1 One-pot thermal Mannich reaction route.

School of Chemistry, National University of Ireland Galway, University Road, Galway, Ireland. E-mail: Styliana.Mirallai@nuigalway.ie

†Electronic supplementary information (ESI) available. CCDC 1819144 and 1819145. For ESI and crystallographic data in CIF or other electronic format see DOI: 10.1039/c8ob00811f

‡Present address: Department of Pharmacy, School of Life Sciences, Pharmacy and Chemistry, Kingston University, Penrhyn Road, Kingston upon Thames, KT1 2EE, UK. E-mail: F.Aldabbagh@kingston.ac.uk.

polymersomes for targeted delivery of therapeutics.[11–13] In a recent communication, the synthesis of the selected acrylamides containing *N*-methylene saturated nitrogen heterocycles, and their incorporation into well-defined water-soluble block copolymer polyacrylamides was realised.[14] In this full paper, we expand on the monomer synthesis by providing efficient multi-gram routes to acrylamides and methacrylamides, including those with dialkyl acyclic and large saturated nitrogen heterocyclic rings. The synthesis involves efficient generation of the methylene Schiff base salt, which was characterized in the hydrated form.

Results and discussion

In contrast to the one-pot thermal Mannich condensation reaction in Scheme 1, our synthesis uses readily accessible aminals made from the condensation of formaldehyde with secondary amines at 0 °C (Scheme 2).[16,17] Böhme pioneered the quaternization of the aminal to generate the Schiff base (iminium) salt, and this procedure using acetyl chloride was followed.[17,18] There are numerous accounts of alkylation and nucleophilic addition onto methylene Schiff base salts,[16–28] including by non-vinylic amides.[27,28] The most utilised is commercial *N*,*N*-dimethylmethyleneiminium iodide or Eschenmoser's salt.[20,29] Inspired by the simplicity and low temperatures, acrylamides and methacrylamides were added onto *in situ* generated methylene Schiff salts to give the monomer hydrochloride salts of morpholine, pyrrolidine and piperidine.

The monomer hydrochloride salts **1a·HCl–3b·HCl** were precipitated upon the addition of diethyl ether to the reaction in acetonitrile, which allowed the separation of the soluble *N*-acetyl cycloamines (Scheme 2). The isolable **1a·HCl–3b·HCl** salts are themselves useful as monomeric building blocks in aqueous solution polymerizations.[14] Basification of the latter allowed the free *N*-[(cycloalkylamino)methyl]acrylamides **1a–3a** to be isolated on a 20–25 g scale in yields of 66–75% with the *N*-[(cycloalkylamino)methyl]methacrylamides **1b–3b** isolated in higher yields of 82–92% and on a ≥30 g scale.

Our *in situ* Schiff base salt approach was not applicable for larger cycloamines (azepane and azocane) and acyclic analogues. Isolation of the methylene Schiff base salts was deemed necessary in these cases due to the poor solubility of their aminals in acetonitrile. Seven and eight-membered heterocyclic base-containing monomers are useful for increased hydrophobicity in the ionisable block segment of amphiphilic copolymers promoting sharper pH-sensitivity of micelles.[11,12] In contrast, linear dialkyl amine-containing polyacrylamides generally have greater water solubility in comparison to heterocyclic amine-containing analogues affording higher LCSTs.[10] Treatment of the aminals with acetyl chloride in diethyl ether at 0 °C allowed access to both larger heterocyclic and acyclic methylene Schiff base salts **4a–4f**, which were more conveniently characterised as *N*-hydroxymethyl hydrochloride salt derivatives **5a–5f** (Scheme 3).

NMR spectra of iminium salts **4a–4f** showed mixtures with their respective hydrated derivatives **5a–5f**. For example, the ^{1}H-NMR spectrum in CD_2Cl_2 gave similar intensity signals for the *exo*-methylene of *N*-methylideneazocan-1-ium chloride (**4b**) at 8.87 ppm and its *N*-hydroxymethyl derivative **5b** *exo*-methylene at 4.74 ppm (Fig. 2a). Upon recrystallization from acetonitrile, the more stable *N*-(hydroxymethyl)azocan-1-ium chloride **5b** was obtained (Fig. 2b). It was thus more convenient to characterize the moisture sensitive methylene Schiff base salts **4a–4f** using NMR in D_2O, as **5a–5f** (Fig. 2c). An exception was *N*,*N*-dibutylmethaniminium chloride (**4f**), which appeared less hygroscopic. The NMR spectrum in CD_2Cl_2 contained only trace amounts of hydrated derivative **5f** (Fig. 3a). The *exo*-methylene at 8.58 ppm in CD_2Cl_2 for the methylene Schiff

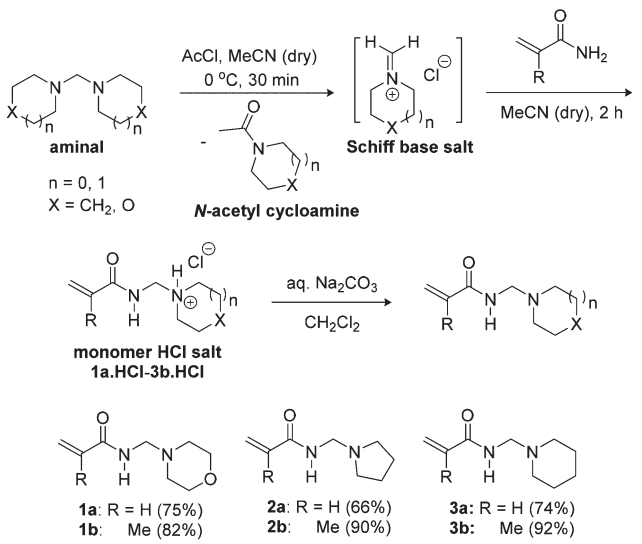

Scheme 2 Synthesis of *N*-[(cycloalkylamino)methyl]acrylamides **1a–3a**,[14] and *N*-[(cycloalkylamino)methyl]methacrylamides **1b–3b** using the *in situ* Schiff base salt approach.

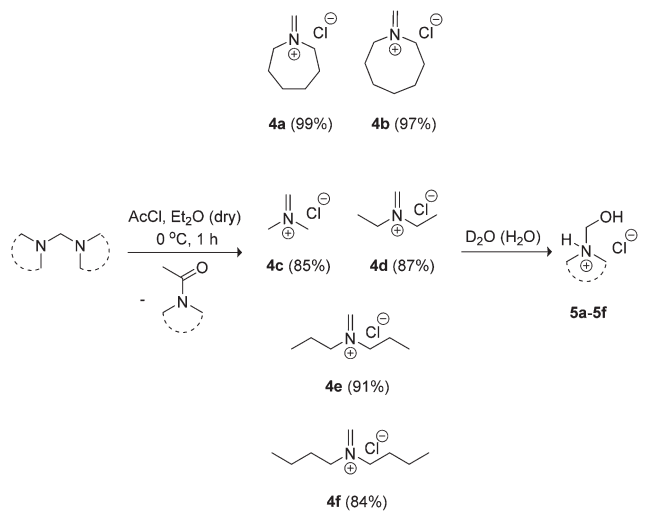

Scheme 3 Synthesis of methylene Schiff base salts **4a–4f** characterised by ^{1}H NMR as hydrated derivatives **5a–5f**.

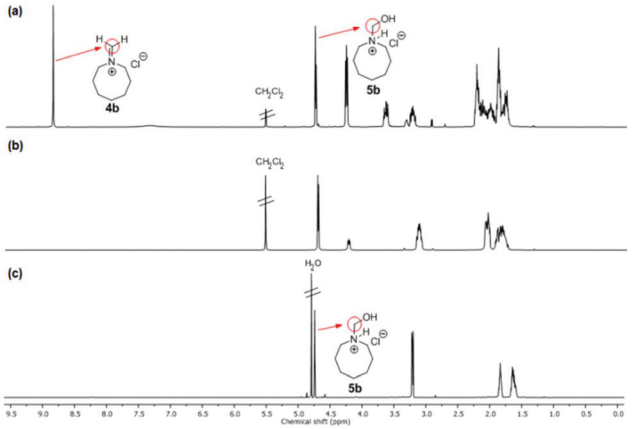

Fig. 2 ^{1}H-NMR spectrum: (a) of the initially isolated mixture containing *N*-methylideneazocan-1-ium chloride (**4b**) and *N*-(hydroxymethyl) azocan-1-ium chloride (**5b**) in CD_2Cl_2 and spectra after recrystallization from MeCN in (b) CD_2Cl_2, and (c) D_2O.

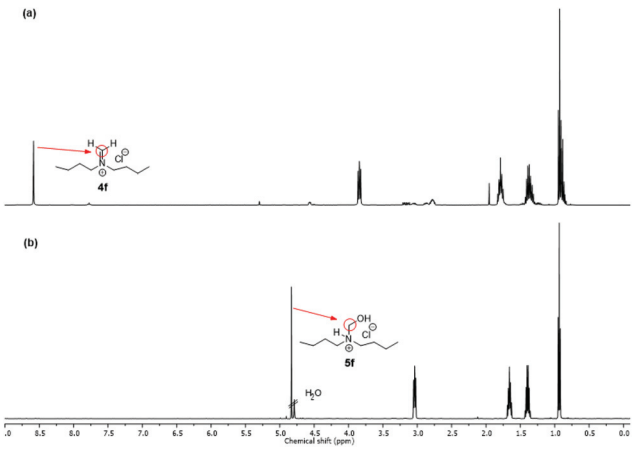

Fig. 3 ^{1}H-NMR spectrum: (a) of *N*,*N*-dibutylmethaniminium chloride (**4f**) in CD_2Cl_2 and (b) of *N*-butyl-*N*-(hydroxymethyl)butan-1-aminium chloride (**5f**) in D_2O.

base was replaced by the *exo*-methylene at 4.83 ppm in D_2O for *N*-butyl-*N*-(hydroxymethyl)butan-1-aminium chloride (**5f** in Fig. 3b).

The X-ray crystal structure of *N*-(hydroxymethyl)azocan-1-ium chloride (**5b**) was obtained (Fig. 4a, Table S1†). The large eight membered ring of **5b** was found to be disordered over two equally populated sites with both the N–H and O–H bonds found to be involved in H-bonding to the chloride counter ion (Fig. 4b). Interestingly, a search of the CCDC database for the R_2NH–CH_2–OH moiety gave only one hit, CSD code DIVDET, which was for a pyrimidine salt of tris(hydroxymethyl) ammonium chloride.[30] The hydroxymethyl hydrochlorides **5a–5f** were however difficult to isolate cleanly due to their susceptibility to decompose to formaldehyde.

Nucleophilic addition of acrylamides or methacrylamides onto the freshly prepared methylene Schiff base salts of azepane and azocane **4a** and **4b** gave the hydrochloride

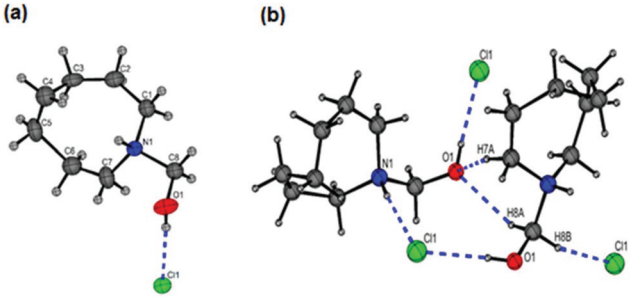

Fig. 4 The X-ray crystal structure of *N*-(hydroxymethyl)azocan-1-ium chloride (**5b**): (a) only one component of the ring disorder shown for clarity and (b) H-bonding interactions (Table S1†).

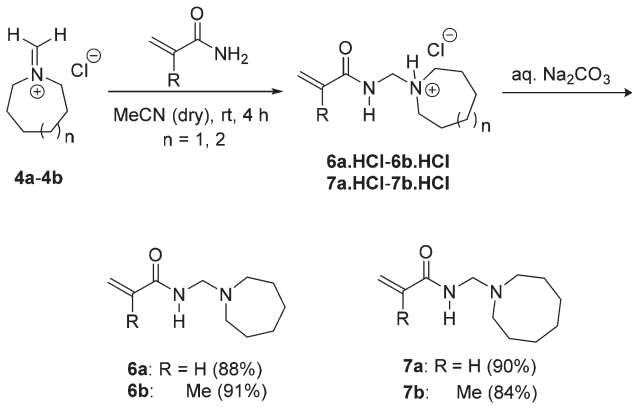

Scheme 4 Synthesis of seven and eight-membered *N*-[(cycloalkylamino)methyl]acrylamides **6a–7a** and *N*-[(cycloalkylamino)methyl] methacrylamides **6b–7b** from the freshly prepared methylene Schiff base salts.

monomer salts (**6a·HCl**, **6b·HCl**, **7a·HCl** and **7b·HCl**) after precipitation from diethyl ether (Scheme 4). The monomer HCl salts were suspended in dichloromethane and basified to give the monomers **6a–6b** and **7a–7b** in high yields of 84–91% (from **4a–4b**). Attempts to react acrylamide and methacrylamide with an analytically pure sample of *N*-(hydroxymethyl) azocan-1-ium chloride (**5b**) in dried acetonitrile resulted in the isolation of unreacted **5b** and some degradation with the release of formaldehyde. It follows that yields of the monomer from addition onto methylene Schiff base salts were determined by the extent of hydration of the latter substrate.

The X-ray crystal structure of *N*-[(azocan-1-yl)methyl]prop-2-enamide hydrochloride (**7a·HCl**) was obtained with very small fitting errors suggesting that the ring was in the optimal conformation (Fig. 5). The crystal structure showed N–H bonds forming H-bonding interactions with the chloride anions and the oxygen atoms resulting in intermolecular packing with some weaker C–H···Cl and C–H···O (see Fig. S1, S2 and Table S2†).

For the preparation of *N*-dialkyl amino substituted monomers, *N*-[(dialkylamino)methyl]acrylamides **8a–11a** and *N*-[(dialkylamino)methyl]methacrylamides **8b–11b**, freshly pre-

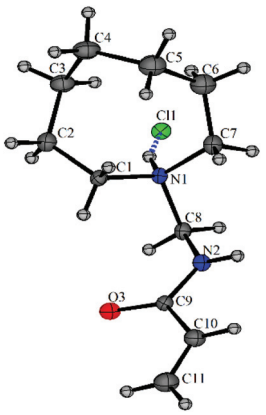

Fig. 5 The X-ray crystal structure of *N*-[(azocan-1-yl)methyl]prop-2-enamide hydrochloride (**7a·HCl**) with one molecule from the asymmetric unit shown.

pared acyclic Schiff base salts **4c–4f** were reacted with acrylamides and methacrylamides in acetonitrile at room temperature (Scheme 5). In this case, the isolation of the *N*-dialkyl amino substituted monomer hydrochloride salts proved difficult due to appreciable solubility in the reaction solvent and attempted precipitation solvents (including diethyl ether). Thus basification of the reaction mixture was preferred and the free monomer bases were isolated in multi-gram quantities (22–49 g) in yields of 69–90% without the isolation of the intermediate salts.

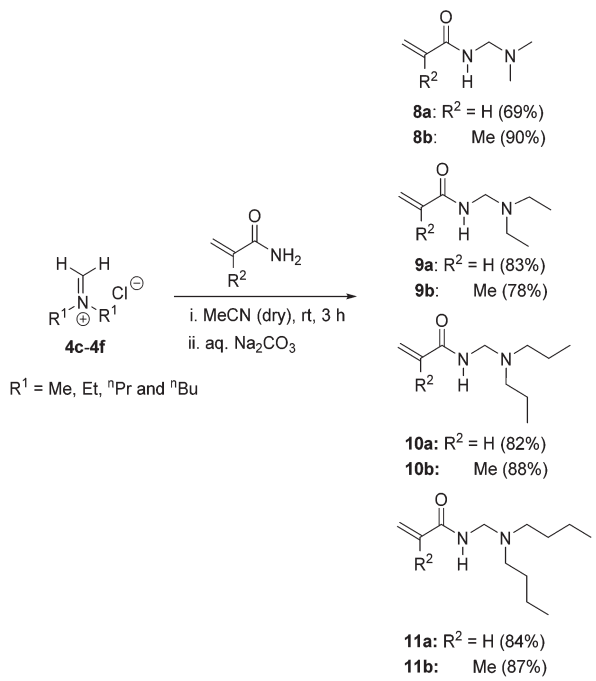

Scheme 5 Synthesis of *N*-[(dialkylamino)methyl]acrylamides **8a–11a** and *N*-[(dialkylamino)methyl]methacrylamides **8b–11b** from the freshly prepared Schiff base salts.

Conclusions

Readily accessible methylene Schiff base (iminium) salts have allowed the preparation of eighteen previously inaccessible acrylamides and methacrylamides containing methylene *N*-amino groups (both heterocyclic and acyclic). Heterocyclic substituted monomer syntheses have the added advantage of allowing the isolation of the monomer hydrochloride salt intermediate useful for polymerizations in water. For the preparation of monomers substituted with azepane, azocane, and acyclic derivatives, the iminium salts should be first isolated, prior to reactions with acrylamides and methacrylamides. Syntheses occur at low or ambient temperatures avoiding premature polymerization of vinyl compounds. Iminium salts are however hygroscopic and X-ray crystal structures of the hydrated eight-membered Schiff base salt, 1-(hydroxymethyl)azocan-1-ium chloride (**5b**), and the related monomer, *N*-[(azocan-1-yl)methyl]prop-2-enamide hydrochloride (**7a·HCl**) are described. Future research will involve controlled radical polymerizations of this new vinyl monomer class to give amphiphilic block copolymers for use as smart stimuli (temperature, pH, CO_2)-responsive materials.

Experimental

General information

Melting points were measured on a Stuart Scientific SMP1 melting point apparatus. Infrared spectra were recorded using a PerkinElmer Spec 1 with ATR attached. ^{1}H NMR spectra were recorded at 400 or 500 MHz and ^{13}C NMR were recorded at 101 or 125 MHz using a 400 MHz JEOL ECX and a 500 MHz Varian instrument respectively. The chemical shifts were recorded in ppm relative to Me_4Si. NMR assignments were supported by DEPT. Deuterated solvents were used for homonuclear lock, and the signals were referenced to the deuterated solvent peaks. 1,4-Dioxane was used as a reference for ^{13}C NMR in D_2O. High resolution mass spectra (HRMS) were recorded using an ESI time-of-flight mass spectrometer (TOFMS) in positive mode. The precision of all accurate mass measurements was better than 5 ppm. All reactions were performed under inert conditions.

Materials

All chemicals were obtained from commercial sources. Aminals, 1,1′-methylenedipyrrolidine,[16] 1,1′-methylenedipiperidine,[17] 1,1′-methylenebis(azepane),[31] *N*,*N*,*N*′,*N*′-tetramethylmethanediamine,[16] *N*,*N*,*N*′,*N*′-tetraethylmethanediamine,[16] and *N*,*N*,*N*′,*N*′-tetrapropyl-methanediamine[31] were readily prepared in high yields from the reaction of formaldehyde (Sigma-Aldrich, 37 wt% in H_2O) with the appropriate secondary amine according to the literature procedures. Distilled aminals were stored under vacuum and dry atmospheres in desiccators at room temperature. Heptamethyleneimine (Sigma-Aldrich, 98%), acetyl chloride (AcCl, Sigma-Aldrich, 98%), acrylamide (Sigma-Aldrich, 97%), and methacrylamide (Sigma-Aldrich, 98%) were

used as received. CH_2Cl_2 (Sigma-Aldrich, ≥99%), $CDCl_3$ (Sigma-Aldrich, 99.8 atom%), D_2O (Sigma-Aldrich, 99.9 atom%), KOH pellets (Sigma-Aldrich, ≥85%), Na_2CO_3 (Sigma-Aldrich, ≥99%), and $MgSO_4$ (Sigma-Aldrich, ≥99.99%) were used as received. The synthesis of *N*-[(morpholin-4-yl)methyl] prop-2-enamide **1a**, 2-methyl-*N*-[(morpholin-4-yl)methyl]prop-2-enamide **1b**, *N*-[(pyrrolidin-1-yl)methyl]prop-2-enamide **2a** and *N*-(piperidin-1-ylmethyl)prop-2-enamide **3a** is included in our recent communication.[14] For Schiff base salt and monomer synthesis all solvents were freshly distilled, and the reactions were carried out using anhydrous solvents using an inert nitrogen atmosphere. Acetonitrile (MeCN, Sigma-Aldrich, ≥99.9%) was freshly distilled over 3 Å molecular sieves and then CaH_2 (Sigma-Aldrich, 95%) and Et_2O (Et_2O, Sigma-Aldrich, ≥99.5%) were freshly distilled over Na wire and benzophenone (Sigma-Aldrich, 95%).

Synthesis of *N*-[(cycloalkylamino)methyl]methacrylamides using the *in situ* Schiff base salt approach

AcCl (14.30 mL, 0.20 mol) was added over 30 min to aminal (0.20 mol) in MeCN (40 mL) at *ca*. 0 °C. Methacrylamide (17.02 g, 0.20 mol) in MeCN (40 mL) was added, and stirred at *ca*. 20 °C for 2 h. Et_2O (200 mL) was added and the hydrochloride salt of the monomer was precipitated, filtered, and dried under vacuum. The hydrochloride salts (**1b·HCl–3b·HCl**) were recrystallized, dried, and characterized. An aqueous solution of Na_2CO_3 (100 mL, 3 M) was added to a suspension of the hydrochloride salt in CH_2Cl_2 (100 mL) and stirred for 30 min. The organic layer was separated, and the aqueous layer was washed with CH_2Cl_2 (4 × 250 mL). The combined organic extracts were dried ($MgSO_4$), filtered, and evaporated to dryness to give the monomer, which was recrystallized.

2-Methyl-*N*-[(pyrrolidin-1-yl)methyl]prop-2-enamide hydrochloride (2b·HCl). White solid; mp 131–133 °C (recryst. from MeCN); ^{1}H NMR (400 MHz, DMSO-d_6) δ 1.87–1.94 (m, 7H), 3.05–3.41 (m, 4H), 4.49 (d, *J* 6.7 Hz, 2H), 5.55–5.57 (m, 1H), 5.92–5.94 (m, 1H), 9.33–9.36 (t, *J* 6.7 Hz, 1H, NH), 10.61–10.94 (brs, 1H, NH); ^{13}C NMR (101 MHz, DMSO-d_6) δ 18.4 (Me), 22.9, 50.4, 56.4, 122.0 (all CH_2), 138.4 (C), 168.8 (C=O).

2-Methyl-*N*-[(pyrrolidin-1-yl)methyl]prop-2-enamide (2b). (30.29 g, 90%), white solid; mp 56–58 °C (recryst. from MeCN); ν_{max} (neat, cm^{-1}) 3215, 2962, 2819, 1655, 1619, 1521 (C=O), 1450, 1362, 1356, 1299, 1208, 1134, 1046; ^{1}H NMR (400 MHz, $CDCl_3$) δ 1.75–1.79 (m, 4H), 1.96 (s, 3H), 2.62 (t, *J* 6.4 Hz, 4H), 4.24 (dd, *J* 0.7, 6.2 Hz, 2H), 5.33–5.34 (m, 1H), 5.69–5.70 (m, 1H), 6.17–6.31 (brs, 1H, NH); ^{13}C NMR (101 MHz, $CDCl_3$) δ 18.8 (Me), 23.7, 51.0, 58.6, 119.8 (all CH_2), 140.1 (C), 168.7 (C=O); HRMS (ESI) *m*/*z* $[M + H]^+$, $C_9H_{17}N_2O$ calcd 169.1341 observed 169.1334.

2-Methyl-*N*-[(piperidin-1-yl)methyl]prop-2-enamide hydrochloride (3b·HCl). White solid; mp 143–145 °C (recryst. from MeCN); ^{1}H NMR (400 MHz, DMSO-d_6) δ 1.34–1.76 (m, 6H), 1.91 (s, 3H), 2.82–2.85 (m, 2H), 3.26–3.29 (m, 2H), 4.42 (d, *J* 6.6 Hz, 2H), 5.56 (s, 1H), 5.92 (s, 1H), 9.13 (t, *J* 6.6 Hz, 1H, NH), 10.12–10.32 (brs, 1H, NH); ^{13}C NMR (101 MHz, DMSO-d_6) δ 18.4 (Me), 21.2, 22.1, 49.7, 59.1, 121.9 (all CH_2), 138.4 (C), 168.7 (C=O).

2-Methyl-*N*-[(piperidin-1-yl)methyl]prop-2-enamide (3b). (33.54 g, 92%), white solid; mp 67–69 °C (recryst. from MeCN); ν_{max} (neat, cm^{-1}) 3353, 2934, 2852, 1671 (C=O), 1655, 1615, 1453, 1453, 1440, 1368, 1333, 1306, 1158, 1110, 1034; ^{1}H NMR (400 MHz, $CDCl_3$) δ 1.38–1.44 (m, 2H), 1.54–1.59 (m, 4H), 1.95 (s, 3H), 2.45–2.59 (m, 4H), 4.10 (d, *J* 6.4 Hz, 2H), 5.34 (s, 1H), 5.71 (s, 1H), 6.29–6.38 (brs, 1H, NH); ^{13}C NMR (101 MHz, $CDCl_3$) δ 18.8 (Me), 24.2, 25.9, 51.6, 62.4, 119.8 (all CH_2), 140.2 (C), 168.9 (C=O); HRMS (ESI) *m*/*z* $[M + H]^+$, $C_{10}H_{19}N_2O$ calcd 183.1497 observed 183.1493.

Synthesis of 1,1′-methylenebis(azocane)

Heptamethyleneimine (15.0 g, 0.13 mol) was added over 30 min to formaldehyde (37 wt% in H_2O, 6.2 mL, 0.07 mol) with stirring at *ca*. 0 °C. The solution was stirred overnight at *ca*. 20 °C, after which KOH pellets were added to form a saturated solution, and stirring was continued for 30 min. H_2O (40 mL) was added and the mixture was extracted with Et_2O (4 × 40 mL). The organic layers were combined and washed with H_2O (3 × 20 mL), dried ($MgSO_4$), and evaporated to dryness. Fractional distillation under reduced pressure gave the title compound as a colorless liquid (14.69 g, 88%); bp 138–140 °C (0.25 mmHg); ν_{max} (neat, cm^{-1}) 2915, 2846, 2779, 1657, 1472, 1448, 1358, 1250, 1158, 1094, 1046, 1017; ^{1}H NMR (400 MHz, $CDCl_3$) δ 1.51–1.68 (m, 20H), 2.53–2.60 (m, 8H), 3.02 (s, 2H); ^{13}C NMR (101 MHz, $CDCl_3$) δ 26.1, 27.9, 28.2, 52.9, 83.8 (all CH_2); HRMS (ESI) *m*/*z* $[M + H]^+$, $C_{15}H_{31}N_2$, calcd 239.2487, observed 239.2312.

Synthesis of *N*,*N*,*N*′,*N*′-tetrabutylmethanediamine

Dibutylamine (68.00 mL, 0.40 mol) was added over 30 min to formaldehyde (37 wt% in H_2O, 15.00 mL, 0.20 mol) with stirring at *ca*. 0 °C. The solution was stirred overnight at *ca*. 20 °C. KOH pellets were added to form a saturated solution, and the drying agent was removed by filtration. Fractional distillation under reduced pressure gave the title compound as a colorless liquid (45.98 g, containing about 10% of suspected (dibutylamino)methanol impurity by ^{1}H NMR); bp 112–114 °C (0.25 mmHg); ^{1}H NMR (400 MHz, $CDCl_3$) δ 0.89 (t, *J* 7.2 Hz, 12H), 1.28 (m, 8H), 1.33–1.41 (m, 8H), 2.42 (t, *J* 7.3 Hz, 8H), 2.98 (s, 2H); ^{13}C NMR (101 MHz, $CDCl_3$) δ 14.3 (Me), 20.9, 29.5, 52.0, 75.6 (all CH_2). HRMS (ESI) *m*/*z* $[M + H]^+$, $C_{17}H_{39}N_2$ calcd 271.3113 observed 271.3143. The title compound was used without further purification to prepare *N*,*N*-dibutylmethaniminium chloride (**4f**).

Synthesis of Schiff base salts

AcCl (21.33 mL, 0.3 mol) was added over 30 min to a stirred solution of aminal (0.3 mol) in Et_2O (150 mL) at *ca*. 0 °C, and the resulting white precipitate was stirred for an additional 30 min. Et_2O (200 mL) was added and the precipitate was filtered, and dried under vacuum to give the methylene Schiff-base salt (**4a–4f**). Iminium salts **4a–4f** were immediately used

in addition reactions with acrylamides and methacrylamides due to their hygroscopic nature.

1-Methylideneazepan-1-ium chloride (4a) (white solid, 43.85 g, 99%). 1-Methylideneazepan-1-ium chloride (**4a**) (white solid, 43.85 g, 99%) was characterized as *N*-(hydroxymethyl) azepan-1-ium chloride (**5a**)

^{1}H NMR (400 MHz, D_2O) δ 1.63–1.66 (m, 4H), 1.78–1.85 (brs, 4H), 3.17–3.21 (m, 4H), 4.77 (d, J 0.8 Hz, 2H); ^{13}C NMR (101 MHz, D_2O, 1,4-dioxane added) δ 25.2, 26.6, 46.8, 82.4 (all CH_2).

1-Methylideneazocan-1-ium chloride (4b) (white solid, 47.04 g, 97%). 1-Methylideneazocan-1-ium chloride (**4b**) (white solid, 47.04 g, 97%) was characterized as *N*-(hydroxymethyl) azocan-1-ium chloride (**5b**)

^{1}H NMR (500 MHz, D_2O) δ 1.57–1.67 (m, 6H), 1.81–1.86 (m, 4H), 3.21 (t, J 5.8 Hz, 4H), 4.74 (s, 2H); ^{13}C NMR (125 MHz, D_2O, 1,4-dioxane added) δ 23.9, 24.8, 25.2, 45.8, 82.4 (all CH_2).

***N*,*N*-Dimethylmethaniminium chloride (4c)[32] (white solid, 23.85 g, 85%).** *N*,*N*-Dimethylmethaniminium chloride (**4c**)[32] (white solid, 23.85 g, 85%) was characterized as hydroxy-*N*,*N*-dimethylmethanaminium chloride (**5c**)

^{1}H NMR (400 MHz, D_2O) δ 2.79 (s, 6H), 4.56 (s, 2H); ^{13}C NMR (101 MHz, D_2O, 1,4-dioxane added) δ 35.2 (Me), 82.4 (CH_2).

***N*,*N*-Diethylmethaniminium chloride (4d)[33] (white solid, 31.74 g, 87%).** *N*,*N*-Diethylmethaniminium chloride (**4d**)[33] (white solid, 31.74 g, 87%) was characterized as *N*-ethyl-*N*-(hydroxymethyl)ethanaminium chloride (**5d**)

^{1}H NMR (400 MHz, D_2O) δ 1.23 (t, J 7.3 Hz, 6H), 3.00–3.07 (m, 4H), 4.78 (s, 2H); ^{13}C NMR (101 MHz, D_2O, 1,4-dioxane added) δ 11.2 (Me), 42.9, 82.4 (both CH_2).

***N*,*N*-Dipropylmethaniminium chloride (4e)[34,35] (white solid, 40.85 g, 91%).** *N*,*N*-Dipropylmethaniminium chloride (**4e**)[34,35] (white solid, 40.85 g, 91%) was characterized as *N*-(hydroxymethyl)-*N*-propylpropan-1-aminium chloride (**5e**)

^{1}H NMR (400 MHz, D_2O) δ 0.92 (t, J 7.6 Hz, 6H), 1.65 (sext, J 7.6 Hz, 4H), 2.95 (t, J 7.6 Hz, 4H), 4.78 (s, 2H); ^{13}C NMR (101 MHz, D_2O, 1,4-dioxane added) δ 10.8 (Me), 19.7, 49.7, 82.4 (all CH_2).

***N*,*N*-Dibutylmethaniminium chloride (4f)[35] (white solid, 44.78 g, 84%).** *N*,*N*-Dibutylmethaniminium chloride (**4f**)[35] (white solid, 44.78 g, 84%) was characterized as *N*-butyl-*N*-(hydroxymethyl)butan-1-aminium chloride (**5f**)

^{1}H NMR (400 MHz, D_2O) δ 0.93 (t, J 6.0 Hz, 6H), 1.39 (sext, J 6.0 Hz, 4H), 1.66 (quint, J 6.0 Hz, 4H), 3.04 (t, J 6.0 Hz, 4H), 4.83 (s, 2H); ^{13}C NMR (101 MHz, D_2O, 1,4-dioxane added) δ 13.4 (Me), 19.8, 28.2, 47.9, 82.4 (all CH_2).

Synthesis of seven and eight-membered *N*-[(cycloalkylamino)-methyl]acrylamides and *N*-[(cycloalkylamino)methyl] methacrylamides

A solution of acrylamide or methacrylamide (0.03 mol) in MeCN (10 mL) was added to a solution of freshly prepared Schiff base salt **4a** or **4b** (0.04 mol) in MeCN (30 mL) and stirred at *ca*. 20 °C for 4 h. Et_2O (200 mL) was added and the hydrochloride salt of the monomer was precipitated, filtered, and dried under vacuum. The hydrochloride salts (**6a·HCl–6b·HCl** and **7a·HCl–7b·HCl**) were recrystallized, dried, and characterized. An aqueous solution of Na_2CO_3 (15 mL, 3 M) was added to a suspension of the hydrochloride salt in CH_2Cl_2 (20 mL) and left to stir for an additional 30 min and extracted with CH_2Cl_2 (4 × 50 mL). The organic layer was dried ($MgSO_4$), filtered and evaporated to dryness to give the corresponding monomers **6a–6b** and **7a–7b**.

***N*-[(Azepan-1-yl)methyl]prop-2-enamide hydrochloride (6a·HCl).** White solid; mp 136–138 °C (recryst. from MeCN); ^{1}H NMR (400 MHz, DMSO-d_6) δ 1.55–1.62 (m, 4H), 1.79–1.82 (m, 4H), 3.03–3.09 (m, 2H), 3.23–3.32 (m, 2H), 4.49 (d, J 6.8 Hz, 2H), 5.80 (dd, J 1.9, 10.2 Hz, 1H), 6.26 (dd, J 1.9, 17.2 Hz, 1H), 6.41 (dd, J 10.2, 17.2 Hz, 1H), 9.53 (t, J 6.8 Hz, 1H, NH), 10.46–10.63 (brs, 1H, NH); ^{13}C NMR (101 MHz, DMSO-d_6) δ 22.9, 26.1, 51.3, 59.2, 128.2 (all CH_2), 130.4 (CH), 166.2 (C=O).

***N*-[(Azepan-1-yl)methyl]prop-2-enamide (6a).** (4.81 g, 88%) colourless liquid; bp 134–136 °C (0.25 mmHg); ν_{max} (neat, cm^{-1}) 3278, 2922, 2852, 2852, 1656 (C=O), 1623, 1539, 1452, 1405, 1365, 1309, 1227, 1133, 1080; ^{1}H NMR (400 MHz, $CDCl_3$) δ 1.52–1.61 (m, 8H), 2.68 (t, J 5.6 Hz, 4H), 4.23 (d, J 6.2 Hz, 2H), 5.61 (dd, J 1.6, 10.2 Hz, 1H), 6.11 (dd, J 10.2, 17.0 Hz, 1H), 6.25 (dd, J 1.6, 17.0 Hz, 1H), 6.31–6.40 (brs, 1H, NH); ^{13}C NMR (101 MHz, $CDCl_3$) δ 26.9, 28.6, 53.1, 62.6, 126.7 (all CH_2), 131.1 (CH), 166.1 (C=O); HRMS (ESI) m/z $[M + H]^+$, $C_{10}H_{19}N_2O$ calcd 183.1497 observed 183.1516.

***N*-[(Azepan-1-yl)methyl]-2-methylprop-2-enamide hydrochloride (6b·HCl).** White solid; mp 88–90 °C (recryst. from THF); ^{1}H NMR (400 MHz, DMSO-d_6) δ 1.53–1.64 (m, 4H), 1.79–1.81 (m, 4H), 1.91 (s, 3H), 3.02–3.15 (m, 2H), 3.23–3.30 (m, 2H), 4.46 (d, J 4.3 Hz, 2H), 5.57 (s, 1H), 5.92 (s, 1H), 9.19 (m, 1H, NH), 10.28–10.44 (brs, 1H, NH); ^{13}C NMR (101 MHz, DMSO-d_6) δ 18.4 (Me), 22.8, 26.2, 51.4, 59.7, 122.0 (all CH_2), 138.4 (C), 168.7 (C=O).

***N*-[(Azepan-1-yl)methyl]-2-methylprop-2-enamide (6b).** (5.36 g, 91%) colourless liquid; bp 139–141 °C (0.25 mmHg); ν_{max} (neat, cm^{-1}) 3328, 2923, 2852, 1655, 1616 (C=O), 1526, 1373, 1313, 1201, 1133, 1088, 1020; ^{1}H NMR (400 MHz, $CDCl_3$) δ 1.56–1.68 (m, 8H), 1.96 (s, 3H), 2.72 (t, J 5.5 Hz, 4H), 4.24 (d, J 6.1 Hz, 2H), 5.33 (s, 1H), 5.69 (s, 1H), 6.12–6.22 (brs, 1H, NH); ^{13}C NMR (101 MHz, $CDCl_3$) δ 18.8 (Me), 27.0, 28.6, 53.2, 62.7, 119.6 (all CH_2), 140.3 (C), 168.8 (C=O); HRMS (ESI) m/z $[M + H]^+$, $C_{11}H_{21}N_2O$ calcd 197.1654 observed 197.1708.

***N*-[(Azocan-1-yl)methyl]prop-2-enamide hydrochloride (7a·HCl).** White solid; mp 87–89 °C (recryst. from EtOAc); ^{1}H NMR (400 MHz, DMSO-d_6) δ 1.43–1.70 (m, 6H), 1.76–1.96 (m, 4H), 3.10–3.16 (m, 2H), 3.22–3.32 (m, 2H), 4.48–4.68 (m, 2H), 5.69 (d, J 10.1 Hz, 1H), 6.25 (d, J 17.1 Hz, 1H), 6.43 (dd, J 10.1, 17.1 Hz, 1H), 9.58–9.67 (m, 1H, NH), 10.25–10.38 (brs, 1H, NH); ^{13}C NMR (101 MHz, DMSO-d_6) δ 22.1, 24.0, 25.1, 48.8, 59.2, 128.2 (all CH_2), 130.4 (CH), 166.2 (C=O).

***N*-[(Azocan-1-yl)methyl]prop-2-enamide (7a).** (5.30 g, 90%) colourless oil; ν_{max} (neat, cm^{-1}) 3328, 2917, 2850, 1657 (C=O), 1624, 1536, 1363, 1232, 1162, 1095, 1060; ^{1}H NMR (400 MHz, $CDCl_3$) δ 1.50–1.62 (m, 10H), 2.62–2.70 (m, 4H), 4.27 (d,

J 6.0 Hz, 2H), 5.65 (d, *J* 10.2 Hz, 1H), 5.91–6.02 (brs, 1H), 6.10 (dd, *J* 10.2, 17.0 Hz, 1H), 6.28 (d, *J* 17.0 Hz, 1H); ^{13}C NMR (101 MHz, $CDCl_3$) δ 26.1, 27.7, 28.0, 51.6, 62.6, 126.7 (all CH_2), 131.2 (CH), 166.0 (C=O); HRMS (ESI) *m*/*z* $[M + H]^+$, $C_{11}H_{21}N_2O$, calcd 197.1656, observed 197.1654.

***N*-[(Azocan-1-yl)methyl]-2-methylprop-2-enamide hydrochloride (7b·HCl).** White solid; mp 128–130 °C (recryst. from EtOAc); ^{1}H NMR (400 MHz, DMSO-d_6) δ 1.46–1.75 (m, 6H), 1.81–1.99 (m, 7H), 3.07–3.18 (m, 2H), 3.23–3.35 (m, 2H), 4.45–4.53 (m, 2H), 5.70 (s, 1H), 5.93 (s, 1H), 9.17–9.27 (brs, 1H, NH), 9.94–10.09 (brs, 1H, NH); ^{13}C NMR (101 MHz, DMSO-d_6) δ 18.4 (Me), 22.2, 24.0, 25.0, 48.9, 59.8, 122.0 (all CH_2), 138.4 (C), 168.6 (C=O).

***N*-[(Azocan-1-yl)methyl]-2-methylprop-2-enamide (7b).** (5.30 g, 84%) colourless oil; ν_{max} (neat, cm^{-1}) 3324, 2918, 2850, 1655, 1618 (C=O), 1523, 1452, 1363, 1201, 1162, 1095, 1060; ^{1}H NMR (400 MHz, $CDCl_3$) δ 1.49–1.59 (m, 10H), 1.93 (s, 3H), 2.61–2.66 (m, 4H), 4.21 (t, *J* 4.3 Hz, 2H), 5.28 (s, 1H), 5.64 (s, 1H), 6.12–6.26 (brs, 1H, NH); ^{13}C NMR (101 MHz, $CDCl_3$) δ 18.8 (Me), 26.0, 27.7, 28.0, 51.5, 62.7, 119.2 (all CH_2), 140.4 (C), 168.9 (C=O); HRMS (ESI) *m*/*z* $[M + H]^+$, $C_{12}H_{23}N_2O$, calcd 211.1838, observed 211.1810.

Synthesis of *N*-[(dialkylamino)methyl]acrylamides and *N*-[(dialkyl-amino)methyl]methacrylamides

A solution of acrylamide or methacrylamide (0.25 mol) in MeCN (50 mL) was added to a stirred solution of freshly prepared Schiff base salt **4c–4f** (0.25 mol) in MeCN (50 mL) and stirred at *ca*. 20 °C for 3 h. An aqueous solution of Na_2CO_3 (150 mL, 3 M) was added and the solution was stirred for an additional 30 min and extracted with CH_2CL_2 (4 × 250 mL). The organic layer was dried ($MgSO_4$), filtered and evaporated to give the corresponding acrylamides **8a–11a** and methacrylamides **8b–11b**.

***N*-[(Dimethylamino)methyl]prop-2-enamide (8a).** (22.11 g, 69%) colourless liquid; bp 64–66 °C (760 mmHg); ν_{max} (neat, cm^{-1}) 3281, 2942, 2827, 2780, 1659 (C=O), 1625, 1536, 1407, 1230, 1029; ^{1}H NMR (400 MHz, $CDCl_3$) δ 2.24 (s, 6H), 4.05 (d, *J* 6.4 Hz, 2H), 5.62 (dd, *J* 1.6, 10.2 Hz, 1H), 6.12 (dd, *J* 10.2, 17.0 Hz, 1H), 6.26 (dd, *J* 1.6, 17.0 Hz, 1H), 6.71–6.82 (brs, 1H); ^{13}C NMR (101 MHz, $CDCl_3$) δ 41.8 (Me), 61.5, 126.0 (both CH_2), 130.7 (CH), 166.2 (C=O); HRMS (ESI) *m*/*z* $[M + H]^+$, $C_6H_{13}N_2O$, calcd 129.1028, observed 129.1026.

***N*-[(Dimethylamino)methyl]-2-methylprop-2-enamide (8b).** (32.10 g, 90%) colourless liquid, bp 60–62 °C (0.25 mmHg); ν_{max} (neat, cm^{-1}) 3323, 2942, 2827, 1658 (C=O), 1619, 1523, 1453, 1311, 1196, 1049, 1033; ^{1}H NMR (400 MHz, $CDCl_3$) δ 1.92 (s, 3H), 2.23 (s, 6H), 4.03 (d, *J* 6.3 Hz, 2H), 5.30 (s, 1H), 5.66 (s, 1H), 6.31–6.45 (brs, 1H); ^{13}C NMR (101 MHz, $CDCl_3$) δ 18.7, 42.3 (both Me), 62.2, 119.5 (both CH_2), 140.1 (C), 169.0 (C=O); HRMS (ESI) *m*/*z* $[M + H]^+$, $C_7H_{15}N_2O$ calcd 143.1184, observed 143.1180.

***N*-[(Diethylamino)methyl]prop-2-enamide (9a).** (32.39 g, 83%) yellow oil; bp 65–67 °C (0.25 mmHg); ν_{max} (neat, cm^{-1}) 3289, 2969, 2828, 1657 (C=O), 1624, 1536, 1464, 1233, 1206, 1067; ^{1}H NMR (400 MHz, $CDCl_3$) δ 1.08 (t, *J* 7.2 Hz, 6H), 2.56 (q, *J* 7.2 Hz, 4H), 4.29 (d, *J* 6.1 Hz, 2H), 5.64 (dd, *J* 1.4, 10.2 Hz, 1H), 5.90–5.99 (brs, 1H), 6.09 (dd, *J* 10.2, 17.0 Hz, 1H), 6.28 (dd, *J* 1.4, 17.0 Hz, 1H); ^{13}C NMR (101 MHz, $CDCl_3$) δ 12.7 (Me), 45.4, 56.9, 126.6 (all CH_2), 131.0 (CH), 166.1 (C=O); HRMS (ESI) *m*/*z* $[M + H]^+$, $C_8H_{17}N_2O$, calcd 157.1341, observed 157.1337.

***N*-[(Diethylamino)methyl]-2-methylprop-2-enamide (9b).** (33.21 g, 78%) colourless liquid, bp 72–74 °C (0.25 mmHg); ν_{max} (neat, cm^{-1}) 3344, 2970, 2827, 1656 (C=O), 1617, 1522, 1455, 1375, 1197, 1066, 1046; ^{1}H NMR (400 MHz, $CDCl_3$) δ 1.03 (t, *J* 7.2 Hz, 6H), 1.90 (s, 3H), 2.52 (q, *J* 7.2 Hz, 4H), 4.22 (d, *J* 6.0 Hz, 2H), 5.27 (s, 1H), 5.63 (s, 1H), 6.11–6.21 (brs, 1H); ^{13}C NMR (101 MHz, $CDCl_3$) δ 12.7, 18.8 (both Me), 45.4, 57.3, 119.5 (all CH_2), 140.2 (C), 168.9 (C=O); HRMS (ESI) *m*/*z* $[M + H]^+$, $C_9H_{19}N_2O$ calcd 171.1497, observed 171.1789.

***N*-[(Dipropylamino)methyl]prop-2-enamide (10a).** (37.80 g, 82%) colourless plates, mp 25–26 °C; ν_{max} (neat, cm^{-1}) 3269, 2959, 2930, 1657 (C=O), 1623, 1550, 1457, 1246, 1185, 1069; ^{1}H NMR (500 MHz, $CDCl_3$) δ 0.82 (t, *J* 7.4 Hz, 6H), 1.44 (sext, *J* 7.4 Hz, 4H), 2.39 (t, *J* 7.4 Hz, 4H), 4.23 (d, *J* 6.0 Hz, 2H), 5.58 (dd, *J* 1.6, 10.2 Hz, 1H), 6.11 (dd, *J* 10.2, 17.0 Hz, 1H), 6.22 (dd, *J* 1.6, 17.0 Hz, 1H), 6.28–6.39 (brs, 1H); ^{13}C NMR (125 MHz, $CDCl_3$) δ 11.9 (Me), 20.9, 54.0, 58.1, 126.5 (all CH_2), 131.1 (CH), 166.1 (C=O); HRMS (ESI) *m*/*z* $[M + H]^+$, $C_{10}H_{21}N_2O$ calcd 185.1654, observed 185.1663.

***N*-[(Dipropylamino)methyl]-2-methylprop-2-enamide (10b).** (43.62 g, 88%) colourless liquid, bp 86–88 °C (0.25 mmHg); ν_{max} (neat, cm^{-1}) 3316, 2959, 2934, 2873, 1655 (C=O), 1619, 1524, 1456, 1374, 1183, 1075, 1052; ^{1}H NMR (400 MHz, $CDCl_3$) δ 0.85 (t, *J* 7.4 Hz, 6H), 1.46 (sext, *J* 7.4 Hz, 4H), 1.93 (s, 3H), 2.42 (t, *J* 7.4 Hz, 4H), 4.22 (d, *J* 6.0 Hz, 2H), 5.29 (s, 1H), 5.65 (s, 1H), 6.02–6.15 (brs, 1H); ^{13}C NMR (101 MHz, $CDCl_3$) δ 11.9, 18.8 (both Me), 20.9, 54.1, 58.5, 119.4 (all CH_2), 140.3 (C), 168.9 (C=O); HRMS (ESI) *m*/*z* $[M + H]^+$, $C_{11}H_{23}N_2O$ calcd 199.1810, observed 199.1800.

***N*-[(Dibutylamino)methyl]prop-2-enamide (11a).** (44.56 g, 84%) colourless liquid, bp 124–126 °C (0.25 mmHg); ν_{max} (neat, cm^{-1}) 3281, 3069, 2957, 2863, 1658 (C=O), 1625, 1542, 1456, 1459, 1366, 1180, 1071; ^{1}H NMR (400 MHz, $CDCl_3$) δ 0.89 (t, *J* 7.3 Hz, 6H), 1.24–1.33 (m, 4H), 1.40–1.47 (m, 4H), 2.45 (t, *J* 7.5 Hz, 4H), 4.26 (d, *J* 6.0 Hz, 2H), 5.63 (dd, *J* 1.5, 10.2 Hz, 1H), 5.88–6.00 (brs, 1H), 6.10 (dd, *J* 10.2, 17.0 Hz, 1H), 6.27 (dd, *J* 1.5, 17.0 Hz, 1H); ^{13}C NMR (101 MHz, $CDCl_3$) δ 14.1 (Me), 20.7, 30.0, 51.9, 58.3, 126.7 (all CH_2), 131.0 (CH), 166.0 (C=O); HRMS (ESI) *m*/*z* $[M + H]^+$, $C_{12}H_{25}N_2O$ calcd 213.1967, observed 213.1952.

***N*-[(Dibutylamino)methyl]-2-methylprop-2-enamide (11b).** (49.21 g, 87%) colourless liquid, bp 133–135 °C (0.25 mmHg); ν_{max} (neat, cm^{-1}) 3325, 2957, 2931, 2872, 1625 (C=O), 1525, 1456, 1374, 1296, 1179, 1083, 1034; ^{1}H NMR (400 MHz, $CDCl_3$) δ 0.89 (t, *J* 7.4 Hz, 6H), 1.25–1.34 (m, 4H), 1.40–1.47 (m, 4H), 1.95 (s, 3H), 2.46 (t, *J* 7.4 Hz, 4H), 4.24 (d, *J* 5.9 Hz, 2H), 5.32 (s, 1H), 5.66 (s, 1H), 5.98–6.06 (brs, 1H); ^{13}C NMR (101 MHz, $CDCl_3$) δ 14.1, 18.8 (both Me), 20.7, 30.0, 51.9, 58.6, 119.4 (all CH_2), 140.4 (C), 168.9 (C=O); HRMS (ESI) *m*/*z* $[M + H]^+$, $C_{13}H_{27}N_2O$ calcd 227.2123, observed 227.2129.

X-ray crystallographic studies

Single crystal X-ray diffraction data were collected using an Oxford Diffraction Xcalibur system operated using the CrysAlisPro software[36] and the data collection temperature was controlled at 150 K using a Cryojet system from Rigaku Oxford Diffraction. The crystals were hygroscopic and were first coated in cold paraffin oil before being transferred to the cold stream on the diffractometer. The crystal structures were solved using ShelxT version 2014/5,[37] and refined using ShelxL version 2017/1[38] both of which were operated within the Oscail software package.[39]

Crystal refinement data for 1-(hydroxymethyl)azocan-1-ium chloride (5b). Colourless crystals, $C_8H_{18}ClNO$, M = 179.68, monoclinic, space group $P2_1/c$, a = 11.3190(18), b = 10.9194(16), c = 7.7658(10) Å, α = 90, β = 90.269(13), γ = 90°, V = 959.8(2) Å^3, Z = 4, T = 150.0(1) K, ρ_{calcd} = 1.243 g cm^{-3}, refinement of 147 parameters on 2345 independent reflections out of 7528 measured reflections (R_{int} = 0.0709) led to R_1 = 0.0857 ($I > 2\sigma(I)$), wR_2 = 0.2182 (all data), and S = 1.119 with the largest difference peak and hole of 0.396 and −0.398 e Å^{-3}.

Crystal refinement data for *N*-[(azocan-1-yl)methyl]prop-2-enamide hydrochloride (7a·HCl). Colourless needle crystals, $C_{11}H_{21}ClN_2O$, M = 232.75, triclinic, space group $P\bar{1}$, a = 10.1121(7), b = 10.4420(6), c = 12.0205(14) Å, α = 95.695(8), β = 91.086(8), γ = 97.671(5)°, V = 1251.02(19) Å^3, Z = 4, T = 150.0(1) K, ρ_{calcd} = 1.236 g cm^{-3}, refinement of 271 parameters on 4487 independent reflections out of 7456 measured reflections (R_{int} = 0.0638) led to R_1 = 0.0684 ($I > 2\sigma(I)$), wR_2 = 0.2128 (all data), and S = 0.979 with the largest difference peak and hole of 0.852 and −0.705 e Å^{-3}.

Crystallographic data for compounds **5b** and **7a·HCl** have been deposited with the Cambridge Crystallographic Data Centre with deposition numbers CCDC 1819145 and 1819144 respectively.†

Conflicts of interest

There are no conflicts to declare.

Acknowledgements

We thank the Minstry of Education of the Kingdom of Saudi Arabia for supporting the PhD of Abdullah Alzahrani, and the Irish Research Council (IRC) for Goverment of Ireland Postdoctoral Fellowships for Styliana I. Mirallai and Benjamin A. Chalmers.

Notes and references

1 V. C. Mannich and W. Krösche, *Arch. Pharm.*, 1912, **250**, 647–667, DOI: 10.1002/ardp.19122500151.
2 F. F. Blicke, The Mannich Reaction, *Org. React.*, 2011, **1**(10), 303–341, DOI: 10.1002/0471264180.or001.10.
3 V. E. Müller, K. Dinges and W. Graulich, *Die Makromol. Chem.*, 1962, **57**, 27–51, DOI: 10.1002/macp.1962.020570103.
4 V. E. Müller and H. Thomas, *Angew. Makromol. Chem.*, 1973, **34**, 111–133, DOI: 10.1002/apmc.1973.050340108.
5 R. C. Baltieri, L. H. Innocentini-Mei, W. M. S. C. Tamashiro, L. Peres and E. Bittencourt, *Eur. Polym. J.*, 2002, **38**, 57–62, DOI: 10.1016/S0014-3057(01)00177-X.
6 M. L. Eritsyan, Z. B. Barsegyan, R. A. Karamyan, S. M. Manukyan, T. D. Karapetyan and K. A. Martirosyan, *Russ. J. Appl. Chem.*, 2011, **84**, 1257–1260, DOI: 10.1134/S1070427211070238.
7 E. C. Cho, J. Lee and K. Cho, *Macromolecules*, 2003, **36**, 9929–9934, DOI: 10.1021/ma034851d.
8 D. Roy, W. L. A. Brooks and B. S. Sumerlin, *Chem. Soc. Rev.*, 2013, **42**, 7214–7243, DOI: 10.1039/c3cs35499g.
9 Z. Song, K. Wang, C. Gao, S. Wang and W. Zhang, *Macromolecules*, 2015, **49**, 162–171, DOI: 10.1021/acs.macromol.5b02458.
10 K. Wang, Z. Song, C. Liu and W. Zhang, *Polym. Chem.*, 2016, **7**, 3423–3433, DOI: 10.1039/c6py00526h.
11 K. Zhou, Y. Wang, X. Huang, K. Luby-Phelps, B. D. Sumer and J. Gao, *Angew. Chem., Int. Ed.*, 2011, **50**, 6109–6114, DOI: 10.1002/anie.201100884.
12 H.-J. Li, J.-Z. Du, J. Liu, X.-J. Du, S. Shen, Y.-H. Zhu, X. Wang, X. Ye, S. Nie and J. Wang, *ACS Nano*, 2016, **10**, 6753–6761, DOI: 10.1021/acsnano.6b02326.
13 B. A. Chalmers, C. Magee, D. L. Cheung, P. B. Zetterlund and F. Aldabbagh, *Eur. Polym. J.*, 2017, **97**, 129–137, DOI: 10.1016/j.eurpolymj.2017.10.004.
14 B. A. Chalmers, A. Alzahrani, G. Hawkins and F. Aldabbagh, *J. Polym. Sci., Part A: Polym. Chem.*, 2017, **55**, 2123–2128, DOI: 10.1002/pola.28607.
15 X. Su, M. F. Cunningham and P. G. Jessop, *Polym. Chem.*, 2014, **5**, 940–944, DOI: 10.1039/c3py01382k.
16 H. Heaney, G. Papageorgiou and R. F. Wilkins, *Tetrahedron*, 1997, **53**, 2941–2958, DOI: 10.1016/S0040-4020(96)01174-X.
17 A. Porzelle and C. M. Williams, *Synthesis*, 2006, 3025–3030, DOI: 10.1055/s-2006-942539.
18 H. Böhme and K. Hartke, *Chem. Ber.*, 1960, **93**, 1305–1309, DOI: 10.1002/cber.19600930610.
19 H. Böhme and P. Backhaus, *Liebigs Ann. Chem.*, 1975, 1790–1796, DOI: 10.1002/jlac.197519751007.
20 J. Schreiber, H. Maag, N. Hashimoto and A. Eschenmoser, *Angew. Chem., Int. Ed. Engl.*, 1971, **10**, 330–331, DOI: 10.1002/anie.197103301.
21 G. Kinast and L.-F. Tietze, *Angew Chem., Int. Ed. Engl.*, 1976, **15**, 239–240, DOI: 10.1002/anie.197602391.
22 N. Abe, F. Fujisaki and K. Sumoto, *Chem. Pharm. Bull.*, 1998, **46**, 142–144, DOI: 10.1248/cpb.46.142.
23 N. Pemberton, V. Åberg, H. Almstedt, A. Westermark and F. Almqvist, *J. Org. Chem.*, 2004, **69**, 7830–7835, DOI: 10.1021/jo048554y.
24 Y.-Y. Ku, T. Grieme, Y.-M. Pu, A. V. Bhatia and S. A. King, *Tetrahedron Lett.*, 2005, **46**, 1471–1474, DOI: 10.1016/j.tetlet.2005.01.027.

25 B. R. Buckley, P. C. B. Page, H. Heaney, E. P. Sampler, S. Carley, C. Brocke and M. A. Brimble, *Tetrahedron*, 2005, **61**, 5876–5888, DOI: 10.1016/j.tet.2005.03.130.
26 V. Werner, M. Ellwart, A. J. Wagner and P. Knochel, *Org. Lett.*, 2015, **17**, 2026–2029, DOI: 10.1021/acs.orglett.5b00801.
27 D. Alker, L. M. Harwood and C. E. Williams, *Tetrahedron*, 1997, **53**, 12671–12678, DOI: 10.1016/S0040-4020(97)00788-6.
28 H. Möhrle and G. Keller, *Z. Naturforsch., B: J. Chem. Sci.*, 2003, **58**, 885–902, DOI: 10.1021/jo01291a032.
29 T. A. Bryson, G. H. Bonitz, C. J. Reichel and R. E. Dardis, *J. Org. Chem.*, 1980, **45**, 524–525, DOI: 10.1021/jo01291a032.
30 C. A. M. A. Huq, S. Fouzia and M. NizamMohideen, *Acta Crystallogr., Sect. E: Struct. Rep. Online*, 2013, **69**, 1766, DOI: 10.1107/S1600536813030559.
31 A. R. Bhat, A. I. Bhat, F. Athar and A. Azam, *Helv. Chim. Acta*, 2009, **92**, 1644–1656, DOI: 10.1002/hlca.200800461.
32 C. Karakus, L. H. Fischer, S. Schmeding, J. Hummel, N. Risch, M. Schäferling and Elisabeth Holder, *Dalton Trans.*, 2012, **41**, 9623–9632, DOI: 10.1039/C2DT30835E.
33 K. A. Jensen and L. Henriksen, *Acta Chem. Scand., Ser. B*, 1975, **29**, 877–883, DOI: 10.3891/acta.chem.scand.29b-0877.
34 C. Rochin, O. Babot, J. Dunoguès and F. Duboudin, *Synthesis*, 1986, 228–229, DOI: 10.1055/s-1986-31627.
35 H. Böhme and E. Raude, *Chem. Ber.*, 1981, **114**, 3421–3429, DOI: 10.1002/cber.19811141023.
36 *CrysAlisPro, 1.171.37.38*, Rigaku Corporation, Oxford, UK, 2015. http://journals.iucr.org/e/services/stdswrefs.html.
37 G. M. Sheldrick, *Acta Crystallogr., Sect. A: Found. Crystallogr.*, 2015, **71**, 3–8, DOI: 10.1107/S2053273314026370.
38 G. Sheldrick, *Acta Crystallogr., Sect. C: Cryst. Struct. Commun.*, 2015, **71**, 3–8, DOI: 10.1107/S2053229614024218.
39 P. McArdle, *J. Appl. Crystallogr.*, 2017, **50**, 320–326, DOI: 10.1107/S1600576716018446.